The phenotype and function of monocyte microparticles, and their characterisation in paediatric HIV infection

Natasha LUCKHURST

First Supervisor: Dr Francesca Arrigoni

Supervisory Team: Dr Nicholas Freestone and Professor Nigel Klein

A thesis submitted to partial fulfilment of the requirements of Kingston University for the award of Doctor of Philosophy

School of Life Science, Pharmacy and Chemistry

Kingston University London

October 2019

Declaration

I hereby declare that this thesis has been submitted exclusively for the degree of Doctor of Philosophy at Kingston University London and has not formed the foundation for any other award at any university or tertiary structure.

This thesis contains my original research and any contribution to this work by other individuals has been fully acknowledged. Where previously published work of others has been consulted or quoted, the authors of the work have been given full acknowledgement via referencing.

Natasha Luckhurst

Acknowledgements

First and foremost, a special thank you to my primary supervisor Dr Francesca Arrigoni, I am grateful for your continuous support and guidance throughout this journey. You have been an amazing mentor, pushing me out of my comfort zone and always challenging me to become a better scientist! To Dr Nick Freestone, you've had to put up with me many years now, from undergrad and now to PhD (sorry!), thank you for your support throughout, and always believing in me! No request has ever been too much, and he truly goes above and beyond the role of a supervisor and an educator. Lastly, Professor Nigel Klein, who has not only given me his support and guidance throughout this project but also welcomed me into his research group at the Institute of Child Health. He also provided me with access to patient samples, specialist equipment and a huge amount of resources without which would not have made this PhD possible.

A special mention to Dr Patricia Hunter, I cannot thank you enough! You have been a mentor and a true friend who continues to inspire me with your knowledge and enthusiasm! You have offered continued support, advice and guidance throughout this journey both in and outside the lab, which I am extremely grateful for. Without your generosity and knowledge, many of these experiments could not have been possible!

Thank you to Dr Dagmar Amber, who sat with me for many hours in the containment level 3 facility and Dr Mona Eliot who gave me emotional support when times were tough! I would also like to thank all my colleagues at ICH, with a special mention to James Bonner and Rijan Gurung who taught me the ropes of microparticle analysis!

To my colleagues in the IRTL both past and present, Sinead Holland, Lauren Mulcahy, The Great Dr Cowan, Sharan Asher, Katrina Viloria, Nico Lambri and Ronni Anderson. Thank you for the laughs, friendship and most importantly the alcohol - I love you all so dearly!

I am forever grateful for my partner in crime, Loryn Halliday, I really would not be at this stage right now if it wasn't for you. You have picked me up and kept me going so many times, you've always believed in me and been ready with tea, and a shoulder to cry on! Your strength and determination has inspired me, and I can't wait to see you crush your PhD – I'm so proud of you and what you have overcome!

Finally, I wouldn't be here without my friends, family and better half. To my girl gang, thank you for believing me in and being my personal cheerleaders - I'm in awe of you all and inspired daily by your strength and determination. A special mention to Nicholas Bennett who has been my rock throughout, always supporting me and pushing me, despite me neglecting him when I've been subsumed in work and in bed by 9 pm! Finally, thank you to my parents for their emotional support, and their attempted scientific advice! You have always been there to pick up the phone 24/7, and jumped in the car to see me when I've really needed you. You have been there to listen to me waffle on, complain and cry, but you've also been there every step to celebrate my achievements throughout! I hope I've made you proud!

Natasha Luckhurst, October 2019

Abstract

37 million people are currently living with HIV worldwide. With the development of Antiretroviral Therapy (ART) AIDS mortality has reduced, with cardiovascular disease (CVD) now the leading cause of HIV deaths. HIV associated CVD has been linked to chronic immune activation through the association of inflammatory biomarkers, clinical events and asymptomatic atherosclerosis; even from a young age. Microparticles (MPs), markers of cellular activation and injury, are also elevated in adults with HIV, and demonstrate the capacity to contribute to inflammation, endothelial dysfunction and coagulation. Monocytes play a key role in atherosclerosis initiation and display an activated, pro-inflammatory phenotype in paediatric HIV. Monocytic MPs (MMPS) are elevated in adults with HIV, thus the aim of this thesis was to quantify MMPS in HIV infected children and investigate their effects on monocytic function.

A novel negative isolation method was first optimised to enable the study of human monocyte function *ex vivo*. This isolation procedure allowed the negative enrichment of all three circulating monocyte subsets (Classical, Non-classical and Intermediate), with high purity and minimal activation. Extracted monocytes displayed minimal alterations in marker expression while retaining their phagocytic, migratory and cytokine secretion function *ex vivo*.

Using a monocytic cell line (THP-1), MP release under different stimulatory and apoptotic conditions was investigated. Under stimulatory conditions with cytokines and a calcium ionophore (A23187), MPs were released in a concentration-dependent manner, with endotoxin stimulation resulting in the highest quantity. Furthermore, MPs displayed a similar trend in surface marker expression in comparison to their parent cell. Next, we investigated the effects of THP-1 derived MMPS on human monocyte function employing the isolation method established. MMPS evoked the release of pro-inflammatory cytokines in addition to enhancing CD11b expression, adherence and transendothelial migration. This work demonstrates that MMPS activates monocytes and enhances endothelial migration, presenting a mechanism that contributes to atherosclerosis pathogenesis.

Finally, MMPS and MPs from an endothelial, platelet and T cell origin were enumerated in children with HIV infection pre/post ART initiation and healthy sex-age-matched controls. Plasma samples were collected during the CHAPAS-3 CV sub-study, from which we analysed 16 children receiving ART (≥2 years), 11 treatment-naïve children and 15 controls. Circulating MPs from an endothelial, platelet and T cell origin found in children with HIV infection normalised to levels found in healthy controls, following ART initiation and experience. MMPS were elevated within the treatment-naïve cohort and remained elevated despite treatment intervention; this elevation was also observed in the treatment-experienced cohort. The persistence of elevated MMPS indicates consistent monocyte activation despite successful viral suppression, supporting the activated phenotype reported in literature.

This data combined with the functional implications of MMPS on monocytic function described in this thesis elucidates a mechanism that contributes to elevated vascular inflammation reported within this population.

Keywords: Monocytes, MPs, HIV, CVD, Atherosclerosis

Presentations and abstracts

Oral Presentations

European Society for Pediatric Infectious Diseases, Malmo, Sweden, 2018. *'Alterations in cellular microparticle levels as a marker of cellular activation and injury in children with HIV infection'* **N. Luckhurst**, J. Kenny, P. Hunter, N. Freestone, N. Klein, F. Arrigoni

Science, Engineering and Computing conference, Kingston University, 2018. *'Identification of microparticle subsets in children with HIV infection, and their relation to increased cardiovascular disease risk within this population'* **N. Luckhurst**, J. Kenny, P. Hunter, N. Freestone, N. Klein, F. Arrigoni

Poster Presentations

British Society for Immunology Congress, Liverpool, December 2019. *'Circulating microparticle levels in children following the initiation of antiretroviral therapy'*

N. Luckhurst, J. Kenny, P. Hunter, N. Freestone, N. Klein, F. Arrigoni

British Society for Immunology Congress, Liverpool, December 2019. *'Monocyte-derived microparticles activate human monocytes and promote their transendothelial migration'* **N. Luckhurst**, P. Hunter, N. Freestone, N. Klein, F. Arrigoni

Table of contents

List of figures

List of tables

List of abbreviations

ACS	Acute Coronary Syndrome
AIDS	Acquired Immunodeficiency syndrome
ART	Combined highly active Antiretroviral Therapy
BBB	Blood Brain Barrier
CAC	Coronary Artery Calcium
CAD	Coronary Artery Disease
CCR	C-C chemokine receptor
CRP	C Reactive Protein
CVD	CVD
CV	CV
DAMPS	Damage Associated Molecular Patterns
DMSO	Dimethyl sulfoxide
EDTA	Ethylenediaminetetraacetic acid
ELISA	Enzyme-linked immunosorbent assay
EMP	Endothelial MP
FACS	Fluorescence-activated cell sorting
FBS	Foetal Bovine Serum
GIT	Gastrointestinal Tract
HIV	Human Immunodeficiency Virus
HDL	High Density Lipoprotein
HUVEC	Human Umbilical Vein Endothelial cells
ICAM-1	Intercellular Adhesion Molecule 1
IFN-Y	Interferon Gamma
IL	Interleukin
IMT	Intima-Media Thickness
LDL	Low-density lipoprotein

LMP	Leukocyte MP
LPS	Lipopolysaccharide
MCP-1	Monocyte chemotactic protein-1
MFI	Mean Fluorescent intensity
MI	Myocardial infarction
MMPs	Monocyte microparticles
MP	Microparticles
MSD	Mesoscale Discovery
NFKβ	Nucleoside reverse transcriptase inhibitor
NRTIs	Nuclear factor kappa-light-chain-enhancer of activated B cells
NNRTIs	Non-nucleoside reverse transcriptase inhibitor
NO	Nitric Oxide
NOS	Nitric Oxide Synthase
OxLDL	Oxidized low-density lipoprotein
PAMPS	Pathogen Associated Molecular Patterns
PBS	Phosphate-buffered saline
PBMC	Peripheral blood mononuclear cell
PI	Protease inhibitor
PMA	Phorbol 12-myristate-13-acetate
PMP	Platelet MPs
PPP	Platelet poor plasma
PS	Phosphatidylserine
PWV	Pulse Wave Velocity
RANTES	Chemokine Ligand 5
ROS	Reactive Oxygen Species
RPMI	Roswell Park Memorial Institute medium
SAA	Serum amyloid A

SMC	Smooth Muscle cell
TF	Tissue Factor
TLR	Toll-Like Receptor
TMP	T lymphocyte MP
TNF-α	Tumour necrosis factor-alpha
VCAM-1	Vascular cell adhesion protein 1

Chapter 1 - Introduction

1.1 HIV epidemic

Since its discovery in 1981, more than 75 million people have been infected with HIV (Human Immunodeficiency Virus); with approximately half of those dying as a result of the infection developing into Acquired immunodeficiency syndrome (AIDS) (del Rio, 2017). In 2018, World Health Organisation (WHO) estimates showed that 37.9 million people were living with HIV globally, with only 62% of those infected receiving combined highly active antiretroviral therapy (ART) (WHO, 2019).

In 2018, approximately 1.7 million people were newly infected with HIV, with 9.4% of these being in children below the age of 15 (WHO, 2019). HIV is most concentrated in Sub-Saharan Africa, accounting for 67% of the global HIV infection rate (WHO, 2019) however 101,600 people are also currently living with HIV in the United Kingdom (UK) (Nash S, Desai S, Croxford S, Guerra L, Lowndes C, Connor N, 2018) . There are multiple routes of transmission including injecting drug use, needle stick injuries and mother to child transmission (MTCT) however; sexual transmission among homosexual men remains the most common mode of transmission in the UK (Nash S, Desai S, Croxford S, Guerra L, Lowndes C, Connor N, 2018; WHO, 2019).

1.2 Pathogenesis of HIV-1

Following the identification of the epidemic, two forms of the virus have been discovered, HIV-1 and HIV-2. Despite similarities between the genetic structures of the two viruses, key differences lend HIV-2 to have a hindered ability to infect the immune system through its lower levels of viral replication, thus the progression to AIDS is much slower in comparison to HIV-1 (Nyamweya et al., 2013). As HIV-1 is most prevalent

globally and is the most predominant strain worldwide; this thesis will focus on this form of HIV infection (Campbell-Yesufu and Gandhi, 2011). The infection itself is characterised by the progressive depletion of CD4+ T helper cells eventually leading to immunosuppression and the progression to AIDS (McCune, 2001).

1.3 The course of HIV infection

Primary HIV infection usually occurs through the entry of the virus into the body across a mucosal surface (Royce et al., 1997). CD4+ T cells are the first immune cells to become infected due to their expression of CD4 (which is the primary receptor of HIV-1) and co-receptors CCR5, CXCR4 facilitating viral entry, and their large reservoirs in gut-associated lymphoid tissue (Alkhatib et al., 1996; Deng et al., 1996; Dragic et al., 1996; Feng et al., 1996). Once infected, viral replication takes place within these cells through the initial transcription of the single-stranded RNA, followed by the integration of viral DNA into the host genome. Once integrated, the transcription of mRNA encoding viral proteins takes place, along with the assembly of immature (non-infectious) HIV, eventually leading to shedding and virus maturation, allowing the infection surrounding cells (Freed, 2015) (Figure 1.1).

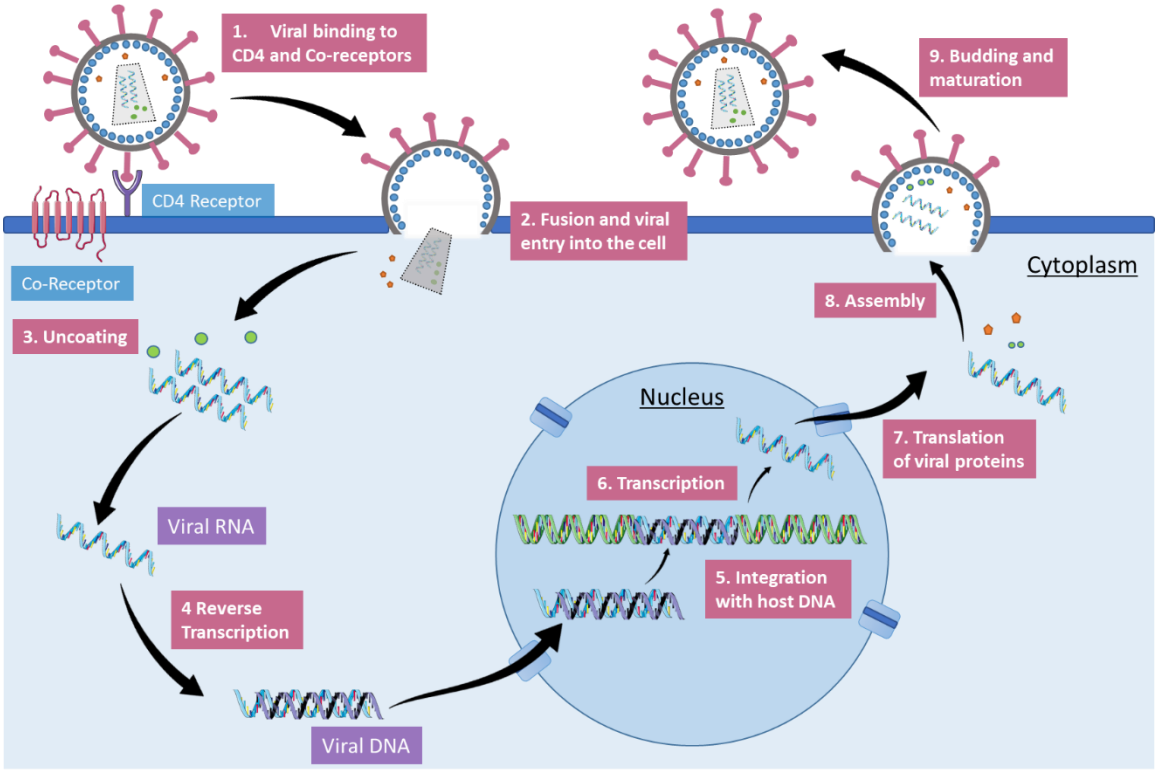

Figure 1.1: A schematic diagram demonstrating the HIV life cycle

The HIV virus can induce cell death in both HIV infected cells and uninfected 'bystander' cells through a number of mechanisms. With respect to the death of infected CD4+ cells, 3 pathways have been described: 1) Cell death following the viral activation of DNA dependent protein Kinase and sequential phosphorylation and activation of P53 dependent pathways (Cooper et al., 2013); 2) Caspase-1 mediated cell death following the accumulation of unintegrated reverse transcripts (Doitsh et al., 2010, 2014; Monroe et al., 2014); 3) The induction of pro-inflammatory cytokine release (IL-2, TNF-α and IL-1α) via NFKβ activation through the expression of Casp8p41 protein (Badley et al., 2008; Nie et al., 2002, 2007), following the transcription and translation of HIV protease (Taylor et al., 2010; Ventoso et al., 2005). The expression of this protein also leads to increased cell death by Caspase-9 mediated pathways (Badley et al., 2008; Sainski et al., 2011). The apoptosis of 'bystander' T cells is elevated through the direct interaction with soluble cytotoxic HIV proteins (Gp120, Tat, Nef and Vpr), the upregulation of death

ligands on the surface of immune cells, and through the overall heightened immune activation leading to activated cell death (Cummins and Badley, 2014).

Within 2 weeks of the primary infection, virus dissemination takes place by infected T cells migrating to lymph nodes and spreading the virus to neighbouring T cells by cell-cell contact; this provides a viral reservoir in the lymphoid tissues (Murooka et al., 2012). From here, the virus is able to further disseminate throughout the body through the release of viremia into the blood from replicating cells, leading to infection of T cells, monocytes, macrophages and dendritic cells (Février et al., 2011). In response to the virus, the host produces HIV specific CD8+ cells which cause the initial sharp decrease in viremia; this indicative of the individual's initial ability to control the virus (Borrow et al., 1994). This is described as the 'clinical latency' phase within which naïve CD4+ and HIV-1 specific CD8+ T cells recruited to lymph nodes and activated T cells become a target for viral replication, further enhancing the number of infected cells and increasing cell death (Grossman et al., 1998). The schematic diagram shown in figure 1.2 demonstrates the relationship between CD4+ T cell counts and HIV RNA viral copies over the time course of untreated HIV infection (Coffin and Swanstrom, 2013).

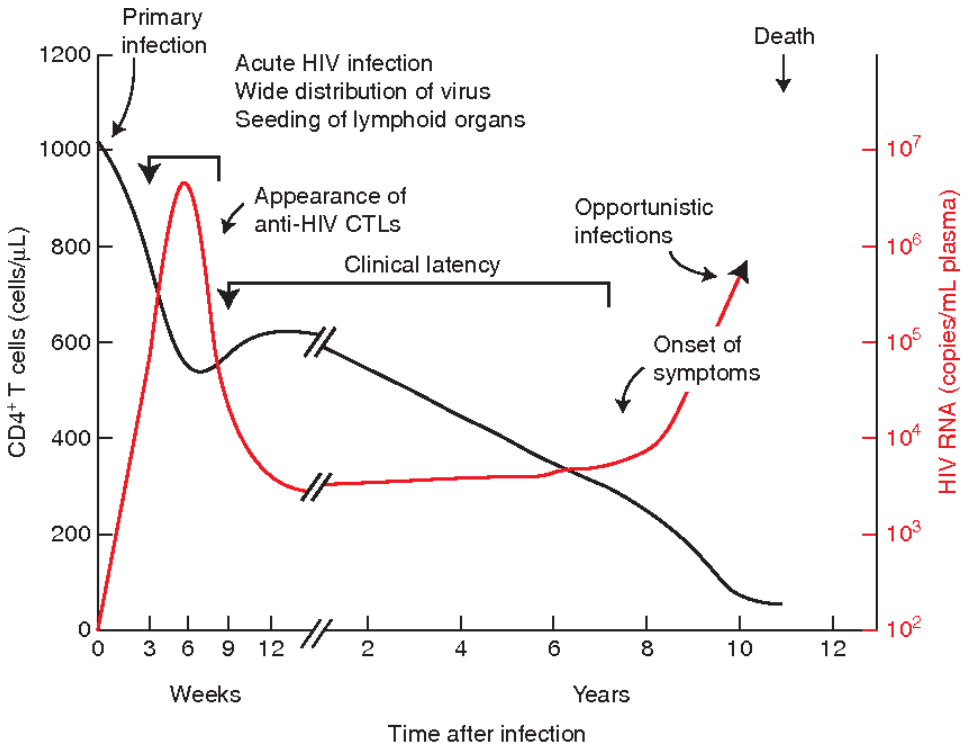

Figure 1.2: A schematic diagram displaying the relationship of CD4+ T cell numbers and HIV RNA copies/ml of plasma over the time course of uncontrolled HIV-1 infection (Coffin & Swanstrom, 2013).

The high viral replication rates and sequential CD4+ cell death that takes place in gut-associated, lymphoid tissue results in the increased translocation of bacterial production as the lining becomes more permeable. This elevated microbial translocation is one mechanism through which immune activation is increased in these patients (Brenchley et al., 2006), along with the induction of CD4+ and CD8+ T cell proliferation and activation (Deeks et al., 2004; Giorgi et al., 2002). These mechanisms ultimately result in the additional loss of these cells.

As the numbers of T cells gradually decline the infected individual loses the ability to control the virus and fight opportunistic infections. This leads to the development of

AIDS (defined as CD4+ T cell counts <200 cells/ml), as a result of innate and adaptive immune response impairment.

1.4 Management of HIV

Although there is currently no cure or vaccination for the treatment of HIV infection, Combined Highly active antiretroviral therapy (ART) has recently been developed to suppress viral replication, leading to an increased quality of life and lifespan of individuals living with HIV (Nakagawa et al., 2013; Samji et al., 2013). Since its discovery, AIDS mortality rates have dramatically reduced in people living with HIV, with patients expected to have a near-normal life expectancy (Nakagawa et al., 2013; Rodger et al., 2013). Additionally, more recent clinical studies have provided support for the Undetectable=Untransmittable (U=U) theory, whereby virally suppressed HIV infected individuals were unable to sexually transmit the virus (Cohen et al., 2016; Rodger et al., 2019).

Current antiretroviral drugs that have been approved for the use in adults and children are grouped into 5 different classes according to the stage of the viral life cycle it targets (Figure 1.3):

1) Nucleoside reverse transcriptase inhibitors (NRTIs) (for example Abacavir, Zidovudine) and 2) Non-Nucleoside reverse transcriptase inhibitors (NNRTIs) (for example Efavirenz, Nevirapine) both interfere with the initial transcription of the single-stranded viral RNA, leading to the termination of DNA synthesis.

3) Integrase inhibitors (for example Raltegravir) prevent the viral DNA from being integrated into the host genome, thus preventing the transcription of new viral RNA, and essential viral proteins that are needed for further replication. 4) Protease inhibitors

(for example Darunavir) inhibit the HIV enzyme protease which is required in the later stages of the HIV life cycle. This enzyme cleaves long peptide chains that are packaged into immature virions into functional proteins, maturing the virion. 5) Fusion and entry inhibitors (for example Maraviroc) prevent the entry of the virus into the cell.

Antiretroviral drugs are often given in combination, with two or more drugs from one or more classes to allow more effective maintenance of viral suppression.

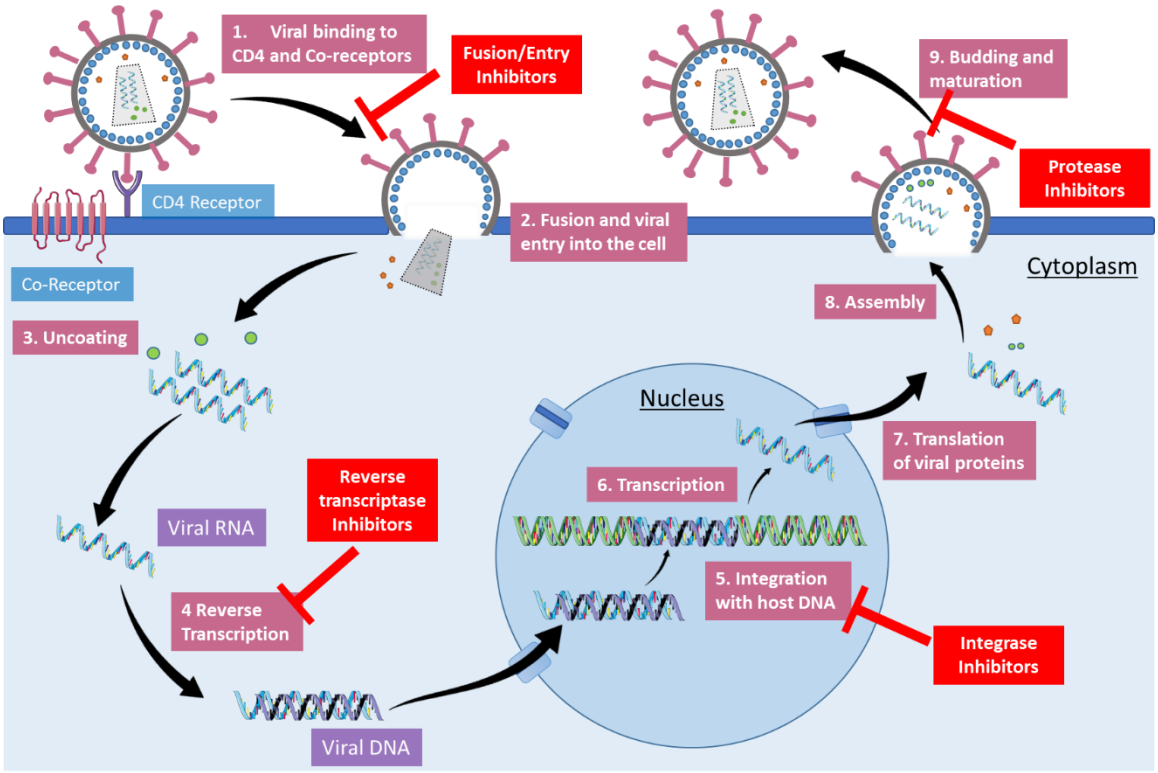

Figure 1.3: A schematic diagram demonstrating how combined antiretroviral therapies target different stages of the HIV life cycle

1.5 CVD morbidity in HIV infected individuals

Despite the increased quality and life expectancy of ART-treated HIV positive individuals (Palella et al., 1998), the number of non-AIDS co-morbidities has risen, with CVD accounting for approximately 11% of non-AIDS related deaths (Data Collection on Adverse Events of Anti-HIV drugs (D:A:D) Study Group et al., 2010; Feinstein et al., 2016; Palella et al., 2006). CVD risk is 1.5 to 2-fold greater in virally suppressed HIV infected

patients compared to uninfected individuals (Hsue and Waters, 2018; Shah et al., 2018). Furthermore, people living with controlled HIV have an increased risk of myocardial infarction (Drozd et al., 2017; Freiberg et al., 2013), ischemic stroke (Chow et al., 2012; Sico et al., 2015), heart failure (Butt et al., 2011; Freiberg et al., 2017), pulmonary hypertension (Barnett et al., 2008; Brittain et al., 2018) and coronary heart disease (Currier et al., 2003; Islam et al., 2012; Triant et al., 2007) compared to healthy adult populations.

To further support this relationship, people living with HIV also display higher rates of sub-clinical atherosclerosis as measured through physiological markers. Carotid Intima-Media Thickness (IMT) is currently the most reliable marker of sub-clinical atherosclerosis, and highly predictive of future cardiovascular (CV) events in the general population (Lorenz et al., 2012; O'Leary et al., 1999; Den Ruijter et al., 2012). IMT is measured by calculating the thickness between the intima and media of the coronary artery wall (Nezu et al., 2016).

Several longitudinal studies (Hanna et al., 2015; Hsue et al., 2012) and a large meta-analysis of over 5,000 HIV infected adults (Hulten et al., 2009) found increased IMT in HIV infected cohorts compared to negative control populations. Furthermore, the progression of intima-media thickening has been observed to increase faster in HIV positive patients over 1 year in comparison to non-infected adults (Hsue et al., 2004). This increase in IMT has also been shown to positively correlate with an increased risk of myocardial infarction and stroke, and coronary atherosclerosis (Ho and Hsue, 2009).

Through imaging of coronary artery calcium (CAC) by non-contrast computed tomography, HIV infected individuals showed higher risk and incidence of CAC (Kingsley

et al., 2015). In addition, the increased prevalence of non-calcified plaque (Fitch et al., 2013; Post et al., 2014; Zanni et al., 2014) and evidence of positive coronary arterial remodelling (Miller et al., 2015) have been observed within this population, making atherosclerotic plaque susceptible to rupture.

Despite the majority of evidence for CVD outcomes and risk associated with HIV being generated from adult studies, paediatric data has also shown supporting evidence, demonstrating a predisposition to CVD even from a young age (Idris et al., 2015; Miller et al., 2008; Werner et al., 2010). Significant increases in IMT compared to healthy age-matched controls have been observed in children and young adults (Bonnet et al., 2004; Charakida et al., 2005; Sainz et al., 2014), along with increases in arterial stiffness (assessed by Pulse wave velocity) (Charakida et al., 2009) and decreased flow-mediated dilation (a marker of endothelial function) (Bonnet et al., 2004). Using cardiac MRI and MR angiography, coronary artery abnormalities were observed in 14 of 27 CV asymptomatic HIV children and young adults (Mikhail et al., 2011).

In addition, coronary artery plaque prevalence in young HIV infected adults was positively associated with cytotoxic T cell activation and E-Selectin (a marker of endothelial activation), demonstrating the link between immune and endothelial activation in the early stages of atherosclerosis within this population (Mattingly et al., 2017). This is further supported by a small study performed by Ross et al., 2010, in which heightened hsCRP (high sensitivity C Reactive Protein, a plasma biomarker of inflammation) levels in HIV infected children was associated with IMT (Ross et al., 2010).

Other studies failed to show differences in IMT between HIV infected and uninfected children (Eckard et al., 2017; Hanna et al., 2016), or an initial increased IMT which

normalises after longitudinal follow up after ART initiation (Ross et al., 2010). The conflicting data reported in these studies are likely to attributable to small sample sizes, differences in patient demographics, study duration and study design.

With CVD now the leading cause of non-AIDS related death, and a HIV associated increased CV risk from a younger age, new challenges have emerged for the aging HIV population. With serious implications on morbidity, morality and quality of life within this patient group, there is a requirement to discover biomarkers to accurately predict CVD progression and events, in addition to developing successful intervention strategies specific to HIV positive individuals (Mcgettrick et al., 2018). With respect to interventions that reduce CV disease progression, careful consideration needs to be made for any potential interactions that these co-medications may have with current ART regimes, thus often requiring specialist care (Smit et al., 2015). The cause of this accelerated CVD progression is later discussed in more detail, however it involves the complex interplay between HIV associated factors including viremia, inflammation, immune dysfunction and ART use, along with general traditional risk factors (Ekong et al., 2020). By further understanding these mechanisms in relation to HIV specific factors, and how CVD progresses within this population, an effective prevention strategy can be developed in order to reduce the CVD related morbidity and mortality burden in people living with HIV and prolong lifespan equivalent to that of the general population.

1.6 Atherosclerosis pathogenesis

First described in the 19th century, atherosclerosis is characterised by an accumulation of lipids and fibrous elements in the lumen of the arteries, causing stiffening, swelling and damage to blood vessel walls. The disease is initiated by CV risk factors that cause the

endothelium to become activated, leading to leukocyte migration to sites of injury and endothelial dysfunction (Hansson, 2005).

1.6.2 Endothelial homeostasis and dysfunction

The normal homeostasis of the vascular endothelial lining demonstrates a balance between mechanisms of growth and repair to maintain a healthy functioning endothelial layer. Under these conditions, the endothelium regulates leukocyte adhesion, smooth muscle cell proliferation and vessel wall adhesion in response to surrounding physical and chemical signals (Kinlay et al., 2001; Maruyama, 1998). Cells respond to vasoactive molecules including nitric oxide (NO) in order to control the vasodilatation and vasoconstriction of the vessel wall (Deanfield et al., 2007). The ability for endothelial growth and repair relies on multiple angiogenic mechanisms, involving cell proliferation, migration and tube formation as well as factors from the surrounding microenvironment.

Repeated exposure to CV risk factors and chronic inflammatory conditions cause injury to the endothelium, switching cells from a quiescent state to one that is activated. This change in phenotype upregulates adhesion molecules (ICAM1, VCAM1, E-Selectin, P-Selectin), inflammatory cytokines (IL-8) and chemokines (MCP-1) to enhance leukocyte recruitment, promote pathological angiogenesis and cell senescence (Deanfield et al., 2007; Hansson, 2005; Woywodt, 2002). The imbalance of these mechanisms leads to an upregulation of pro-atherogenic events, giving rise to atherosclerosis. As endothelial dysfunction is one of the initiating factors of CVD, it is generally considered an early predictor of atherosclerosis (Maruyama, 1998).

1.6.3 Endothelial dysfunction leads to atherosclerosis from an early age

From childhood, exposure to CV risk factors causes this endothelial dysfunction, leading to the asymptomatic development of atherosclerosis. Symptoms primarily appear within the fourth decade when clinical events begin to occur, as depicted in figure 1.4 (Bentzon et al., 2014; Della Rocca and Pepine, 2010).

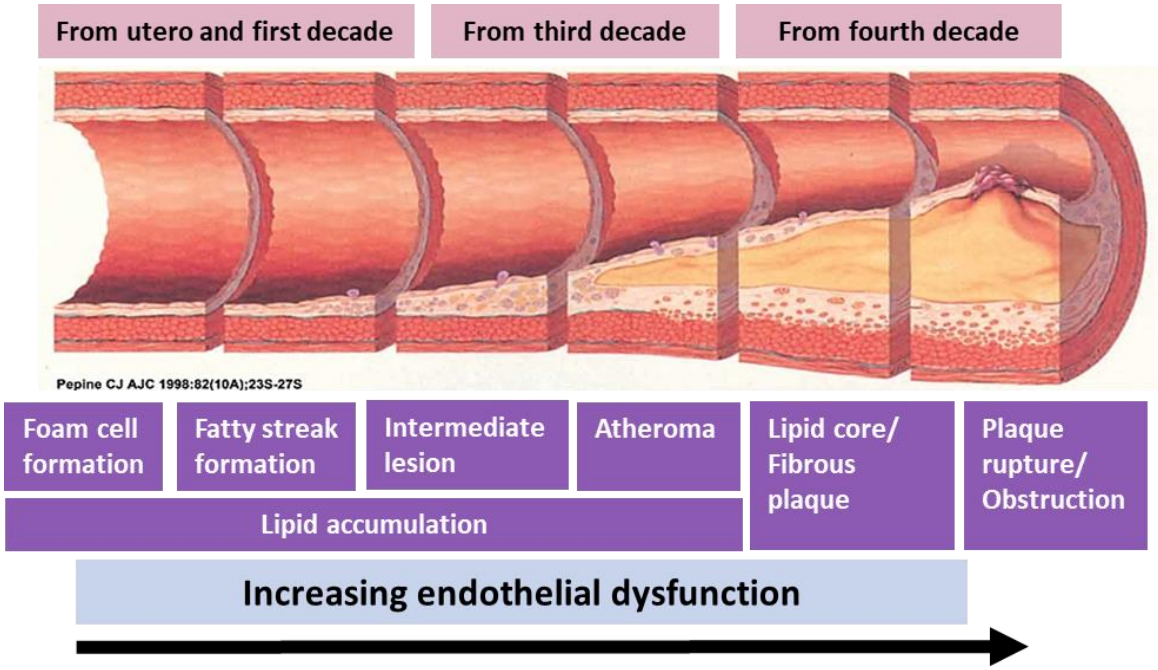

Figure 1.4: A diagram demonstrating the role of endothelial dysfunction in the progression of atherosclerosis over time, from the formation of foam cells in childhood to lesion formation and CV events in adulthood. (Adapted from the original print by Pepine 1998 and reprinted by Della Rocca & Pepine, 2010).

Although few children present with symptoms of atherosclerosis, alterations in the artery wall have been observed as early as the fetal development stage in utero, whereby the presence of fatty streak formation and intimal thickening has been reported (Milei et al., 2008; Napoli et al., 1997). Furthermore, previous studies have confirmed that endothelial dysfunction is present in children and progresses into

adulthood upon exposure to certain risk factors such as systemic inflammation (Fabbri-Arrigoni et al., 2012; Hingorani et al., 2000). Hypertension, diabetes, smoking and obesity have also been shown to induce endothelial dysfunction in children and young adults (Charakida et al., 2007). Moreover, evidence of structural changes to the arterial vascular bed and sub-clinical atherosclerosis (assessed by the measurement of IMT, Pulse Wave Velocity and Flow Mediated Dilation) has also been reported in children and adolescents living with HIV, as described previously (Bonnet et al., 2004; Chanthong et al., 2014; Charakida et al., 2005, 2009; Giuliano et al., 2008; McComsey et al., 2007; Ross et al., 2010).

1.6.4 Atherosclerosis disease progression

Atherosclerosis is initiated by the activation of the endothelium through inflammation, and LDL accumulation. LDLs within the intima (the artery wall) are oxidised by either NOS (Nitric Oxide Synthase), 15-LO (Lipoxygenase) or ROS (Reactive Oxygen species). The oxidized form of these lipids (oxidised LDL (OxLDL)) accumulates in the vascular wall, activating endothelial cells. As a result, the expression of ICAM-1, VCAM-1, P-selectin, E-selectin and integrins upregulated on the endothelial cell surface, in addition to the secretion of pro-inflammatory cytokines and chemokines (such as MCP-1) to attract circulating leukocytes (Collins et al., 2000; Dong et al., 1998; Shih et al., 1999; Skålén et al., 2002; Williams and Tabas, 1995).

Circulating monocytes respond to these signals and bind to the endothelium mediated through the interaction of adhesion molecules with β integrin receptors (CD11/CD18) on the monocyte surface (Meerschaert and Furie, 1995). Upon binding, these cells ‘roll’ along the endothelium, and infiltrate into the sub-endothelial intima space, where they

differentiate into macrophages (Cybulsky and Gimbrone, 1991; Nakashima et al., 1998). Macrophages engulf lipid molecules (such as OxLDL) via scavenger class A receptors and CD36 (Kunjathoor et al., 2002). This uptake leads to the development of foam cells that accumulate within the vessel wall, leading to the formation of a fatty streak.

The expression of adhesion molecules and the release of chemoattractants from the inflamed endothelium facilitate T cell recruitment to the site further enhancing the inflammatory response. Through T cell and macrophage signalling, the extracellular matrix is broken down, resulting in the migration and proliferation of smooth muscle cells from the media into the intima. These smooth muscle cells also restructure the vascular wall through the secretion of fibrin, collagen, and proteoglycans forming an extracellular matrix (Patel, 2014).

Following the continuous accumulation of lipids, apoptotic cells, foam cells and smooth muscle cells, the plaque increases in size and consequently causes the narrowing of the lumen. This process is called Intima-Media Thickening, which can be measured by imaging techniques to determine the severity of asymptomatic atherosclerosis including IMT, and non-contrast computed tomography. Clinical events such as myocardial infarction or stroke take place as the plaque enlarges and becomes unstable (Bentzon et al., 2014) (Figure 1.5).

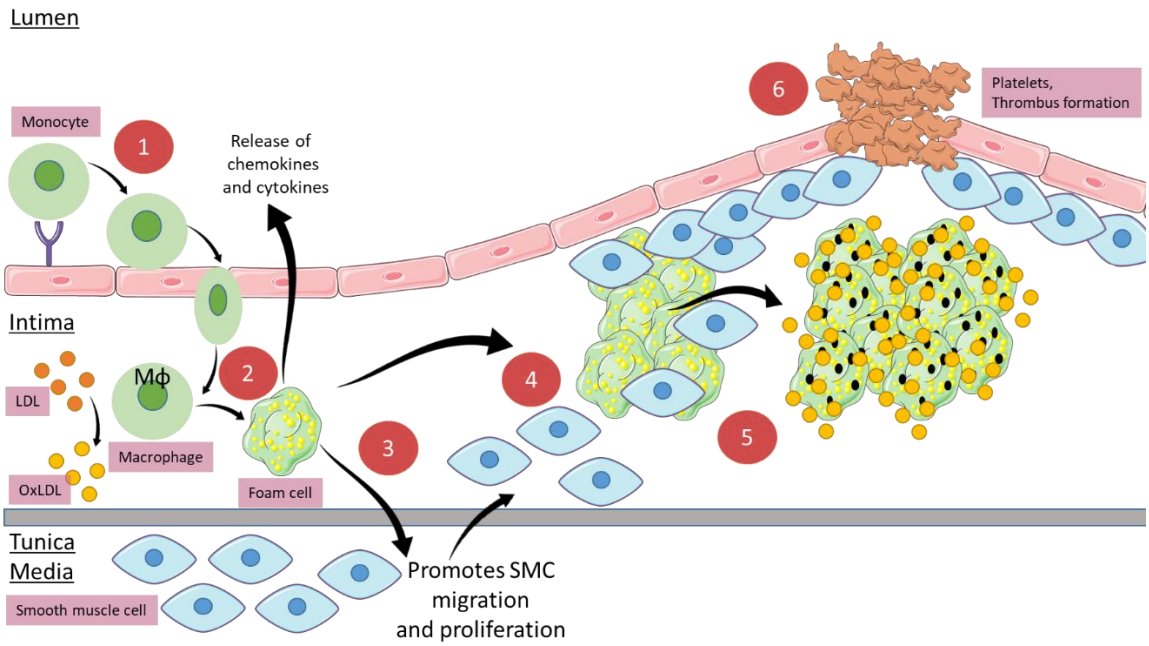

Figure 1.5: Schematic diagram of atherosclerosis pathogenesis

1) Endothelial dysfunction results in the increase of adhesion molecule expression on the endothelial cell surface. Monocytes bind to these receptors and transmigrate into the tunica intima. 2) Once in the intima they differentiate into macrophages and engulf OxLDL via scavenger receptors on their surface, this results in foam cell formation. Foam cells enhance monocyte and inflammatory cell recruitment by the release of chemokines and pro-inflammatory cytokines. 3) Foam cells also secrete growth factors that promote the proliferation of smooth muscle cells in the tunica media and their migration into the intima space. 4) The accumulation of foam cells and smooth muscle cells in the intima contributes to plaque progression. 5) These foam cells undergo apoptosis, forming a necrotic lipid core. In response, smooth muscle cells form a fibrous cap over this lipid core, resulting in the plaque size increasing further and narrowing the lumen. 6) As this grows, the plaque is venerable to rupture, leading to thrombosis formation. LDL: Low-Density Lipoprotein, OxLDL: Oxidised Low-Density Lipoprotein, Mφ: Macrophage, SMC: Smooth muscle cell.

1.7 Immune activation and CV risk associated with HIV

The link between abnormal chronic immune activation (Grund et al., 2016; Hunt et al., 2003, 2011; Kuller et al., 2008; Neuhaus et al., 2010) and CVD risk and mortality in HIV has been well established in a number of different HIV infected populations (Hsu et al., 2016; Hsue et al., 2012; Nordell et al., 2014; Smit et al., 2015). In the general population, biomarkers indicative of immune activation including CRP and IL-6 have been linked with increased risk of atherosclerosis and mortality (Danesh et al., 2004; Ridker, 2003; Sarwar et al., 2012; Swerdlow et al., 2012).

A similar association with these markers and CVD outcomes have also been reported in HIV positive populations. Both IL-6 and D-dimer have been associated with increased CVD risk, independent of CV risk factors (Duprez et al., 2012; Nordell et al., 2014) with a strong relation to all-cause mortality (Kuller et al., 2008). CRP, a soluble biomarker indicative of inflammation, has also been associated with CVD risk (Duprez et al., 2012; Triant et al., 2009).

Furthermore, markers of monocyte activation (sCD14 and sCD163) are elevated in HIV infected adults and correlate with plaque progression and carotid atherosclerosis (Burdo et al., 2011a; Fitch et al., 2013; Hanna et al., 2017; McKibben et al., 2015).

Most biomarker studies have focused on HIV infected adults, however paediatric biomarker data in children receiving ART has provided varying results (De Lima et al., 2018; Miller et al., 2010, 2012; Ross et al., 2010). Soluble markers of immune activation (MCP-1 and IL-6) and vascular dysfunction (sVCAM and sICAM) were both found to be elevated in 106 HIV infected youths compared to 55 healthy controls (Miller et al., 2010). These children also display an elevated inflammatory profile, with a higher CRP,

TNF-α levels, in addition to increased IMT (De Lima et al., 2018). In addition, levels of plasma CRP were associated with increased IMT, with a positive correlation between levels of sVCAM and ART duration (Ross et al., 2010). Since the relationship between immune activation and CVD rates has been well established within this population, the source of this immune activation is explored below.

1.8 Sources of immune activation

Currently, the mechanism for persistent inflammation in HIV infected individuals remains unclear, however a number of complex mechanisms are likely to contribute including; the HIV virus, ART side effects and immune activation (Christensen-Quick et al., 2017; d'Ettorre et al., 2016; Deeks, 2011; Gianella et al., 2014, 2016; Henrich et al., 2017; Maidji et al., 2017; Márquez et al., 2015). In addition, the increased prevalence of traditional CV risk factors within HIV populations, including; behavioural factors (Freiberg et al., 2010, 2013; Rasmussen et al., 2015), hypertension (Antonello et al., 2015), dyslipidaemia (Waters and Hsue, 2019), diabetes (Nix and Tien, 2014) and metabolic disturbances (Behrens et al., 2005; Nix and Tien, 2014) also contributes to the low-level inflammation immune activation observed in these patients.

1.8.1 Immune activation as a consequence of the HIV virus and its treatment

Perhaps the most obvious source of immune activation is the direct effect of the virus and the antigens it produces, on the innate and the adaptive immune system. Not only does it have the ability to activate T cells during virus fusion by co-receptor signalling (e.g. CCR5), but its viral RNA can also interact with pattern recognition receptors TLR-7 and TLR-9 cells directly in order to activate uninfected cells (Beignon et al., 2005). HIV also enhances pro-inflammatory cytokine release from monocytes and T cells (Birx DL,

Redfield RR, Tencer K, Fowler A, Burke DS & Tosato, 1990; Buonaguro et al., 1992; Cheung, Ravyn, Wang, Ptasznik, & Collman, 2008; Ji, Sahu, Braciale, & Cloyd, 2005; Molina, Scadden, Byrn, Dinarello, & Groopman, 1989), with these being upregulated directly from Tat and/or GP120 HIV protein interaction (Buonaguro et al., 1992; Cheung et al., 2008; Gibellini et al., 1994; Scala et al., 1994).

The treatment of the virus with ART has also been considered as a contributor to immune activation and CV risk, with a 26% increased risk of MI for every year of ART treatment (Friis-Møller et al., 2003).

In the SMART (Strategies for management of Anti-retroviral Therapy) trial, 5000 HIV positive patients were randomly assigned to two groups, either continuous ART or intermittent ART therapy (when CD4+ count rose above 350/µl ART was stopped and resumed when T cell numbers decreased to 250/µl or below). Results from this study demonstrated that within the drug intermittent group, risk of CV complications increased by 70% when compared to those on the continuous treatment arm, with CV events 5 times more prevalent in this treatment group (El-Sadr et al., 2006). Furthermore, patients in the treatment interruption cohort showed a greater risk of opportunistic infections and CV events, with biomarkers of inflammation (IL-6) and coagulation (D-dimer) displaying a strong relationship with all-cause mortality (Kuller et al., 2008). In 2006, 4 years after the study was initiated enrolment was terminated due to safety risks in patients recruited in the drug conservation group (episodic use of ART) (El-Sadr et al., 2006).

Protease inhibitors (PI) have been associated with an increased risk of MI as reported in the recent D:A:D study (data collection on adverse events of anti-HIV drugs), within

which each year of continuous PI use increased MI risk by 10% (Friis-Moller et al., 2007). Within the same study, the recent or current exposure rather the cumulative use to NRTIs, specifically abacavir also increased risk of MI (Sabin et al., 2008), with similar finding reported in other observational studies (Elion et al., 2018; Marcus et al., 2016).

It has been suggested that the treatment of HIV with these protease inhibitors induces endothelial dysfunction through: the impairment of vasorelaxation and increase of superoxide production, a reduction in NO production and its bioavailability and induction of endothelial cell senescence (Conklin et al., 2004; Lefèvre et al., 2010; Shankar et al., 2005). Furthermore, abacavir has been shown to increase platelet reactivity, promoting platelet aggregation thrombus formation. These therefore propose possible mechanisms through which these therapies contribute to CV risk (Satchell et al., 2011).

1.8.2 Monocyte activation as a consequence of increased microbial translocation

Gut microbial translocation is one of the major contributors to persistent immune activation (Brenchley et al., 2006; Monaco et al., 2017). During acute HIV infection, the gastrointestinal tract (GIT) becomes a prime target organ for HIV replication due to the large pool of T cells with a higher expression of co-receptors for viral entry (CD4+ CCR5+). During the initial acute infection, a rapid depletion in Th17 T cells (El Hed et al., 2011) from the GIT can be observed prior to peripheral T cell count becoming affected (Brenchley et al., 2004, 2006; Schuetz et al., 2014; Yukl et al., 2015). These cells play a key role in host defence against extracellular pathogens in the gut mucosa allowing alterations in the GIT immunity and structural damage to the intestinal mucosal barrier, increasing gut permeability, allowing microbial translocation further increasing immune

activation (Brenchley et al., 2004; Dillon et al., 2014; Dinh et al., 2015; Schuetz et al., 2014; Yukl et al., 2015).

The increase in gut permeability allows the entry of pro-inflammatory products from bacteria and fungi including which cause stimulation of both local and systemic innate immune cells (Dillon et al., 2014; Kawai and Akira, 2010; Monaco et al., 2017).

Monocytes as part of the innate immune system recognise structural components named Pathogen Associated Molecular Patterns (PAMPS) and Damage Associated Molecular Patterns (DAMPS) through the interaction with Toll-Like Receptors (TLR) on their surface (Janeway Jr. and Medzhitov, 2002; Zhang et al., 2010). These bacterial components also include circulating Lipopolysaccharide (LPS) and bacterial associated extracellular vesicles, which are elevated in people living with HIV (Ramendra et al., 2019; Tulkens et al., 2018). Upon TLR mediated recognition by monocytes, a signalling cascade is initiated leading to the production of pro-inflammatory cytokines (IL-6, TNF-α), chemokines and cell surface molecules commonly via the NF-κβ pathway (Mussbacher et al., 2019; Zhang and Ghosh, 2001), in addition to increased monocyte trafficking to the gut (Sankaran et al., 2008). As a consequence of this increased translocation of LPS, circulating monocytes become chronically activated (Brenchley et al., 2006).

CD14 is a co-receptor of LPS along with TLR4, which upon binding LPS causes the cleavage of CD14 from the cell surface allowing its release into the circulation in its soluble form (sCD14). Elevated plasma levels of sCD14 positively correlate with plasma levels of LPS (Brenchley et al., 2006), suggesting the use of sCD14 as an indirect measure of microbial translocation.

Even after ART initiation the numbers of gut mucosa T cells fail recover (Guadalupe et al., 2003, 2006; Jiang et al., 2009; Mavigner et al., 2012; Mehandru et al., 2006), in part attributing to the elevated levels of LPS and sCD14 in both HIV-infected adults and children. Indeed, it has been shown that these indirect markers of GIT barrier dysfunction predict mortality in ART-treated HIV positive patients (Hunt et al., 2014; Sandler et al., 2011).

1.8.3 Monocytes in HIV

Following the development of ART and the successful viral suppression of HIV, levels of monocyte activation and functional impairments are significantly reduced in comparison to treatment-naïve individuals however, these fail to normalise with healthy controls (Espíndola et al., 2018; Fischer-Smith et al., 2008). The constant low-level activation and dysfunction of these innate immune cells have been shown to contribute to CVD co-morbidity (Burdo et al., 2011a; Westhorpe et al., 2014) and all-cause mortality (Sandler et al., 2011) within this patient population.

1.8.3.1 Monocyte heterogeneity and function

Monocytes are phagocytic white blood cells of myeloid origin, (Serbina and Pamer, 2006; Tsou et al., 2007) accounting for approximately 6% of the leukocyte total population. These cells differentiate from pluripotent hematopoietic stem cells in the bone marrow (Saha and Geissmann, 2011) and enter into circulation via MCP-1 (Monocyte chemotactic protein-1 also known as CCL2) signalling (Tsou et al., 2007). Following this, these cells home into sites of injury and infection, infiltrate into tissues and differentiate into macrophages or dendritic cells (Auffray et al., 2009). Monocytes also have the ability to scavenge and eliminate viruses, bacteria, toxic substances and

apoptotic cells (Ziegler-Heitbrock et al., 2010), in addition to playing a crucial role in angiogenesis and tissue repair after injury (Nahrendorf et al., 2007; Ziegler-Heitbrock et al., 2010).

Until the 1980s monocytes were regarded as a single population, however in 1989 Passlick., *et al*, (Passlick et al., 1989) demonstrated that monocytes could be sub-divided into two phenotypically distinct populations based on their CD14 (is a lipopolysaccharide (LPS) co-receptor along with TLR4)) and CD16 (an FCγIII receptor) receptor expression (Clarkson and Ory, 1988; Wright et al., 1990). CD14++ CD16- monocytes were defined as classical whereas CD14+ CD16++ were labelled Non-classical and observed to be smaller in size in comparison to the classical subset (Passlick et al., 1989). More recently, a further CD16++ subset was discovered allowing this population to be sub-divided into the intermediate CD14+ CD16+ and non-classical CD14+ CD16++ (Ziegler-Heitbrock et al., 2010). Figure 1.6 shows the three distinct subsets visualised by flow cytometry after CD14 and CD16 staining (Wong et al., 2012).

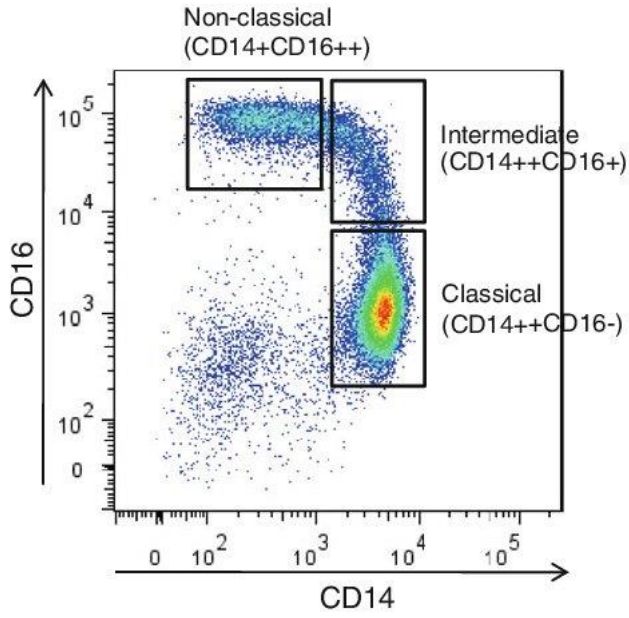

Figure 1.6: Flow cytometry dot plot demonstrating the gating strategy of the three monocyte populations based upon their expression of CD14 and CD16 (Wong et al., 2012).

Each subset is present in different abundances in the blood, and play specific roles in the immune response. In healthy adults, the total monocytic population is comprised of 90% with a classical phenotype, 5% with an intermediate phenotype and 5% with a non-classical phenotype (Ziegler-Heitbrock et al., 2010). They express multiple surface markers, with their phenotypic differences predicting their function as confirmed by a number of functional studies and genome analyses (Cros et al., 2010; Wong et al., 2011; Zawada et al., 2011).

1.8.3.2 Classical

Classical monocytes (CD14++ CD16-) are the most abundant subset in blood making up approximately 90% of total circulating monocyte population (Ziegler-Heitbrock et al., 2010). This population of monocytes has the ability to recognise PAMPs, micro-organisms, lipids and apoptotic cells through their expression of TLRs and scavenger receptors. They express a number of CD markers and genes that are linked with phagocytosis confirming their high phagocytic activity (Cros et al., 2010), as well high levels of CCR2 (MCP-1 receptor) on their surface allowing their emigration from the bone marrow and homing to site of infection and inflammation (Ancuta et al., 2003; Cros et al., 2010; Tacke et al., 2007; Weber et al., 2000; Wong et al., 2011). Stimulation of classical monocytes with LPS induces the release of a number of pro-inflammatory cytokines and chemokines including TNF-α, MCP-1, IL-6, IL-8 and IL-1β; as well as the anti-inflammatory cytokine IL-10 (Cros et al., 2010; Smedman et al., 2012; Wong et al., 2011). The importance of this subset in tissue repair has recently been demonstrated by gene profiling, showing their preferential expression of genes associated with angiogenesis, wound healing and coagulation (Cros et al., 2010; Wong et al., 2011; Zawada et al., 2011). In comparison to CD16+ monocytes, classical monocytes are

considered less mature (Xu et al., 2008; Zawada et al., 2011; Ziegler-Heitbrock et al., 2010).

1.8.3.3 Intermediate

The intermediate population is often regarded as the transition population from classical to non-classical, sharing both phenotypic and functional similarities for each of these subsets. Similar to classical monocytes, intermediate monocytes selectively migrate towards sites of inflammation. However, they produce higher levels of inflammatory cytokines and express pro-antigenic markers on their surface in comparison to the other monocyte populations. In response to LPS, intermediate monocytes produce more IL-1β, TNF-α compared to other subsets, with IL-6, IL-8 and IL-10 production equivalent to the classical population (Cros et al., 2010; Wong et al., 2011).

With respect to surface marker expression, intermediate monocytes display the highest expression of HLA-DR (Major histocompatibility complex) class II (Quinn et al., 1987; Wong et al., 2011; Zawada et al., 2011) compared to classical and non-classical subtypes for antigen presentation, promoting T cell proliferation. They express a number of chemokine receptors including CCR2 and CCR5, which allows tissue invasion, leukocyte attachment and trans-endothelial migration via the interaction with CCL2 and CCL5 (Tacke et al., 2007; Tsou et al., 2007). CCR2 expression is most abundant on this monocytic population (Hijdra et al., 2013), to aid their recruitment to the lymph nodes in response to inflammation and infection (Lund et al., 2016). It has been suggested that this population utilises these chemokine receptors to home into atherosclerotic plaques and accelerate plaque formation, as both MCP-1 and CCL5 have previously been

associated with atherosclerosis disease progression (González et al., 2001; Muntinghe et al., 2009).

Intermediate monocytes and a small proportion of non-classical monocytes express Tie-2 (Tyrosine Kinase 2) on their surface (Murdoch et al., 2007; Venneri et al., 2007), allowing them to exhibit pro-angiogenic behaviour (Zawanda 2011, Coffelt 2010). Tie-2 is an angiopoietin receptor predominantly expressed on endothelial cells and a small proportion of monocytes (Murdoch et al., 2007). Tie-2 has two extracellular ligands. Angiopoietin 1 (ANG-1) autophosphorylates Tie-2 upon binding, leading to the activation of intracellular pathways promoting cell survival and stabilisation, and angiopoietin 2 (ANG-2) that acts as an antagonist of ANG-1, inhibiting Tie-2 mediated cell activation, inducing their sensitivity to inflammatory mediators (Teichert-Kuliszewska et al., 2001). Endothelial cell survival and migration has been shown to be regulated via this pathway and plays an essential role in vessel formation in angiogenesis (Sato et al., 1995). Circulating Tie-2 expressing monocytes migrate towards ANG-2, and display and altered cytokine release in response, suggesting an important role their recruitment to sites of inflammation, and their involvement in cytokine mediated inflammatory processes (Murdoch et al., 2007).

In addition, Tie-2 expressing monocytes (TEMs) demonstrate pro-angiogenic properties in vitro and in vivo, using a mouse tumour model within which ANG-2 was overexpressed in endothelial cells. This study demonstrated that TEM activated endothelial cells and promoted their angiogenesis evaluated using sprouting and tube formation assays. Using the in vivo mouse model, the authors also reported greater infiltration of Tie-2+ monocytes into tumours supporting the chemotactic effect of ANG-

2 (Coffelt et al., 2010). These studies support the role these TEMs may play in accelerating angiogenesis in vivo in patient populations where this subset of monocytes is expanded.

1.8.3.4 Non-classical

The third subset, non-classical monocytes (CD14+ CD16++), displays a crawling behaviour along the endothelium, allowing their detection and elimination of infected or damaged cells and debris along the endothelial-blood interface (Auffray et al., 2007; Carlin et al., 2013). CD14+ CD16++ monocytes express low levels of CCR2 and no CD62L (Ancuta et al., 2003; Tallone et al., 2011) reflecting their maturity in comparison to classical and intermediate monocytes (Merino et al., 2011; Sunderkötter et al., 2004; Ziegler-Heitbrock et al., 1993). This population express the highest levels of CX3CR1 (a chemokine receptor involved in leukocyte adhesion and migration), and upregulation of genes linked with cytoskeleton mobility (Auffray et al., 2007; Randolph et al., 2002; Wong et al., 2011; Zawada et al., 2011); facilitating their patrolling function along the blood vessel wall *in vivo*. Stimulation of non-classical monocytes with LPS causes a limited secretion of pro-inflammatory cytokines, with IL-1β and TNF-α being predominantly secreted upon interaction with viruses and nucleic acids (Cros et al., 2010).

In humans, it is generally accepted that classical monocytes (CD14++ CD16-) migrate from the bone marrow into the circulation, where they mature into intermediate monocytes (CD14+ CD16+), and sequentially into non-classical monocytes (CD14+ CD16++) (Zawada et al., 2011). This hypothesis supports the functional and phenotypic overlap observed within the subsets (Ziegler-Heitbrock et al., 2010), and is supported by

genetic profiling which has shown an increase in genes associated with maturation from classical to non-classical via the intermediate subset (Wong et al., 2011; Zawada et al., 2011), and through mathematical modelling (Tak et al., 2017). This has been further supported in a number of *in vitro* and *in vivo* studies. Cultures of CD34+ hematopoietic stem cells initially differentiate into classical monocytes, with an increased expression of CD16 over time with subsequent culture (Stec et al., 2007). *In vivo* studies have demonstrated that after hematopoietic stem cell transplantation (HSCT), patients initially increased their classical population cell number, followed by the appearance of the intermediate and non-classical population expansion (Rogacev et al., 2015).

1.8.4 Altered monocyte activation and phenotype in HIV infection

During uncontrolled HIV infection, monocytes become chronically activated though the direct infection with the virus itself and by increased microbial translocation. This leads to the secretion of pro-inflammatory cytokines and their aberrant movement contributing to immune activation (Amirayan-Chevillard et al., 2000; Ancuta et al., 2008).

As a result of the CD4 T cell depletion from the gut and increased microbial translocation, an expansion of the CD14+ CD16+ intermediate subset with a decrease in the classical CD14++ population is observed within the first 2 weeks of HIV infection (Kim et al., 2010).

The expansion of this CD16+ monocytic population (Amirayan-Chevillard et al., 2000; Ellery et al., 2007; Pulliam et al., 1997; Thieblemont et al., 1995) also provides an additional mechanism for viral dissemination as this subset permissive to HIV infection. The expansion of CD16+ monocytes correlates with high viral loads, despite low CD4+ T cell counts in treatment-naïve individuals (Han et al., 2009). Moreover, this subset ‘shift’

to a more pro-inflammatory phenotype and through the direct interaction with the virus results in impaired phagocytosis, intracellular killing, chemotaxis, antigen presentation and cytokine production (Sassé et al., 2012).

Following the initial initiation of ART, this activated phenotype is reduced, evidenced through a decrease in CD163 expression, and absolute numbers of inflammatory monocytes (Burdo et al., 2011a). A reduction in cytokine production by inflammatory monocytes is also observed (Amirayan-Chevillard et al., 2000) however, not all of these phenotypic and functional changes are reversed following treatment intervention.

The presence of viral DNA has also been found within the circulating monocytic population following successful viral suppression, therefore providing a source of viral persistence in patients on ART (Calcaterra et al., 2001; Lambotte et al., 2000; Sonza et al., 2001; Zhu et al., 2002). The intermediate population is most permissive to HIV infection *in vivo* and harbours the virus despite treatment intervention providing further implications for this subset expansion *in vivo* (Ellery et al., 2007).

Furthermore, these impairments in monocyte function remain, through an inflammatory shift in the monocytic populations, resulting in a decrease in the classical subset and expansion of intermediates and non-classical cells (Chen et al., 2017; Han et al., 2009; Jaworowski et al., 2007).

This 'shift' in monocytic populations results in the reduction of the highly phagocytic population and hinders the ability of T cell antigen presentation, further contributing to immune dysfunction. This impairment in phagocytic ability has also been observed in both viraemic and virally suppressed patients (Hearps et al., 2012; Michailidis et al., 2012).

The alteration of monocyte phenotypic markers also continues in virally suppressed individuals, with a decrease in CD62L and CD115 expression, and an increase in CD11b, along with innate immune activation markers sCD163, neopterin and CXCL10. These functional and phenotypic changes mimic those observed in elderly patients suggestive of HIV induced immune ageing in monocytes (Hearps et al., 2012). Moreover, increased expression of CD11a and CD11b facilitates their recruitment to inflammatory sites and promotes their involvement in inflammation (Leite Pereira et al., 2019).

Ex vivo experiments using monocytes isolated from HIV infected patients receiving ART have also provided insight into functional impairments that may also contribute to accelerated atherosclerosis disease progression.

Circulating monocytes isolated from HIV infected individuals, displayed a higher tendency to form foam cells following transendothelial migration in comparison to uninfected controls, with their serum also increasing foam cell formation. These monocytes also display an impaired cholesterol efflux from the cells *in vitro*, and limited movement following transendothelial migration, potentiating foam cell formation (Maisa et al., 2015).

1.8.5 Biomarkers associated with monocyte activation

Biomarkers of monocyte activation support their relationship with CVD progression in HIV infected individuals. The expansion of the intermediate monocyte subset as previously described positively correlates with serum biomarkers of monocyte activation and inflammation, IL-6, sCD14 and hsCRP (Wilson et al., 2014). In a longitudinal 2 year study following HIV positive individuals on first-line ART, biomarkers of monocyte activation (IL-6, IP-10, MIG (Monokine induced gamma interferon) and sCD14) were all

elevated prior to treatment intervention, with sCD14 remaining higher compared to healthy controls following therapy initiation (Hattab et al., 2015).

IL-6 is a primary inflammatory cytokine secreted by monocytes following their activation. Therefore, in the instance of HIV infection monocytic derived IL-6 is likely to contribute to the increased plasma levels of IL-6 observed in both untreated and ART-treated HIV positive patients. These elevations in plasma IL-6 have been strongly associated with CVD mortality and death within this population (Kuller et al., 2008).

sCD14 plasma levels are also elevated in HIV infected individuals independent of ART treatment compared to healthy age-matched controls (Lien et al., 1998; Méndez-Lagares et al., 2013; Merlini et al., 2012), and correlate with sub-clinical atherosclerosis prevalence (Kelesidis et al., 2012; Longenecker et al., 2014). Furthermore, sCD14 is positively associated with plasma levels of pro-inflammatory molecules including IL-6, CRP, SAA and D-dimer, and has been shown to independently predict mortality in HIV infected persons (Sandler et al., 2011).

sCD163 has also been proposed as a more specific marker for monocyte/macrophage activation. CD163 is a haemoglobin scavenger receptor expressed exclusively on the surface of mononuclear phagocytes and shed along with other inflammatory signals upon LPS binding to TRL4 (Møller, 2012). sCD163 has been shown to increase in untreated HIV patients before ART therapy, which declines after the initiation of therapy however, these still remain higher than uninfected controls (O'Halloran et al., 2015; Satchell et al., 2011; Ticona et al., 2015). Furthermore, increases in sCD14 and sCD163 in HIV infected males receiving ART is associated with coronary artery calcium levels, indicative of sub-clinical atherosclerosis, and arterial inflammation (McKibben et al.,

2015). Indeed, sCD163 has been independently associated with non-calcified coronary plaque percentage in 102 asymptomatic young infected males (Burdo et al., 2011b). Moreover, higher levels of plasma sCD163 in HIV positive females with non-calcified coronary plaques highlight the predictive potential of these markers of subclinical atherosclerosis within these patients (Fitch et al., 2013).

The elevation of both monocyte activation markers and inflammation in HIV has shown a strong association with coronary artery calcium (Baker et al., 2014; Longenecker et al., 2014), IMT (Dirajlal-Fargo et al., 2017) and predictive of CV morbidity and mortality (Duprez et al., 2012; Grund et al., 2016; De Luca et al., 2013; Nordell et al., 2014). The association of these biomarkers indicative of monocyte activation with clinical and sub-clinical CVD rates provides evidence to support the mechanistic role of these cells in atherosclerosis disease progression. This additionally demonstrates the importance of understanding the drivers of monocyte activation in long term ART, to further elucidate their role in HIV associated CVD.

1.9 Microparticles as markers of cellular activation and injury

Microparticles (MPs) (also referred to as microvesicles) are increasingly being considered as clinical biomarkers of vascular injury, inflammation and thrombosis. These particles are small membrane small lipid-rich particles released from the plasma membrane of cells upon cellular activation, stress, injury and senescence (Gasser and Schifferli, 2004; Koifman et al., 2017).

MPs can be distinguished from other cell-derived vesicles including exosomes by their size (ranging from 100nm to 1µm) and their expression of Phosphatidylserine (PS). This allows their discrimination and detection in plasma by flow cytometry.

MPs are a distinct population of extracellular vesicles in comparison to apoptotic bodies, despite their similarity in PS expression. Apoptotic bodies are formed during the late stages of apoptosis following cell collapse, leading to the formation of larger membrane covered fragments (1-5µm). In contrast to this, MPs are released in the early stages of programmed cell death, leading to the generation of much smaller membrane bound vesicles (0.1-1µm) (Distler et al., 2005a). This size differences allows their isolation by different centrifugation-based protocols (Crescitelli et al., 2013), and discrimination by flow cytometry using the combination of PS expression and a size gate of <1µm. Furthermore, apoptotic body content includes cell organelles, DNA fragments and histones that are indicative of cell death, whereas MPs are composed of membrane, cytoplasmic and nuclear contents of the parent cells, including mRNA, RNA, proteins and lipids (Povero and Feldstein, 2016) (currently, no interactions between apoptotic bodies and MPs have been reported in the literature at the time of writing this thesis). In addition, MPs also express cell specific markers on their surface, thus indicating the characteristics of the plasma membrane during MP production (Del Conde et al., 2005). This marker expression further allows the characterisation of MPs according to parent cell origin by flow cytometry.

These circulating particles also contain chemokines, cytokines, proteins, and nucleic acids (miRNA, mRNA and DNA) from their secreting cells. Their composition allows them to influence their surrounding environment and makes them integral in modulating intercellular communications. Through cell signalling induction, MPs influence a number of cellular processes including invasion, migration, proliferation and apoptosis, allowing their functional role in inflammation, (Batool et al., 2013), thrombosis (Iii and Mackman, 2012) and angiogenesis (Martinez and Andriantsitohaina, 2011).

Through a highly regulated process, MPs are released from a number of cell types and have been measured in; peripheral blood, saliva, urine and cerebrospinal fluid (Berckmans et al., 2011; Jayachandran et al., 2012; Patz et al., 2013; Rood et al., 2010).

MPs are released constitutively into the circulation in low numbers under normal conditions, where they play a key role in several biological functions through their ability to communicate with other cells types, transfer cell surface receptors and initiate cell signalling. These physiological processes include hemostasis, thrombosis, inflammation, and angiogenesis. However, in disease where their release is aggravated, circulating MP numbers become elevated causing them to contribute to pathophysiological processes through the upregulation of their activity, and consequently accelerating disease progression (Simak and Gelderman, 2006). Elevated MP phenotypes have been reported in a number of inflammatory disease states including diabetes (Sabatier et al., 2002a; Salem et al., 2015; Zahran et al., 2019), pulmonary hypertension (Amabile et al., 2008; Narin et al., 2014; Preston et al., 2003), heart failure (Berezin et al., 2016; Montoro-García et al., 2015) and atherosclerotic disease (Koga et al., 2005; Leroyer et al., 2007; Philippova et al., 2011).

1.9.1 MP formation

MP release occurs as a consequence of the rearrangement of the cells cytoskeletal structure, and the alterations in the plasma membrane phospholipid order resulting in PS being externalised. The translocation of PS from the inner membrane to the outer membrane is the initial event that leads to MP shedding from the cell, thus MPs act as reliable markers of cell injury and activation. In resting cells, phospholipids adopt an asymmetric distribution in the cell membrane whereby the outer membrane is enriched

with neutral phospholipids (phosphatidylcholine, phosphatidylethanolamine), and the inner face of the membrane contains aminophospholipids (PS, phosphatidylinositol) (Zachowski et al., 1984).

Within the cell membrane, there are 3 main proteins that modulate the asymmetric distribution of these phospholipids; these are floppase, flippase and scramblase. Flippase is an ATP-dependent protein that modulates the transportation of aminophospholipids from the outer surface of the membrane to the inner surface of the membrane (Seigneuret and Devauxt, 1984). This protein is responsible for maintaining the distribution of membrane phospholipids under resting conditions, however with high concentrations of intracellular Ca^{2+}, this protein is inhibited allowing alterations in the phospholipid distribution (Bitbol et al., 1987). Floppase is also an ATP-dependent protein; it facilitates the transportation of PS from the inner face to the outer face of the membrane (Daleke, 2003). Lastly, scramblase is a protein that becomes activated by a high intracellular concentration of Ca^{2+}, it functions as a non-specific lipid transporter allowing the randomisation of phospholipids inside the cell (Zhao et al., 1998).

Under normal resting conditions, the intracellular concentrations of Ca^{2+} remain low leading to the activation of flippase alone; allowing normal phospholipid membrane distribution. When cells become activated by an external stimulus or calcium ionophore, there is a sustained release of cytosolic Ca^{2+} into the cytoplasm which inhibits this protein, in turn activating scramblase (Bitbol et al., 1987; Suzuki et al., 2013). The consequence of this activation causes a disruption in the phospholipid membrane distribution and its asymmetry, allowing the movement of PS from the inner to the outer face of the cell membrane. Additionally, the high intracellular Ca^{2+} also activates kinases

and calpain responsible for the breakdown of actin-binding proteins, leading to cytoskeleton disruption (Fox et al., 1991). The changes to the plasma membrane initiated by Ca^{2+} influx induce cell membrane blebbing and the release of MPs from the parent cell into the extracellular space surrounding it.

During apoptosis, MP formation is attributed to the activation of caspase-3 and ROCK-1 kinase, which leads to phosphorylation of myosin light chain kinase. The activation of this kinase allows the movement of actin and myosin, resulting in the formation of MPs through cytoskeleton detachment from the plasma membrane (Coleman et al., 2001).

1.9.2 MP uptake and communication with target cells

One way in which MPs are thought to mediate communication, influencing phenotype and function of surrounding cells is through the interaction and transfer of biological information (receptors, enzymes, proteins, transcription factors, mRNA, nucleic acids) (Théry et al., 2009). It is suggested that the interaction of MPs with recipient cells is though a number of different mechanisms, although these processes are not fully understood. Numerous putative mechanisms have been suggested that include:

1) The direct activation of receptors on the target cell surface by MPs
2) The transfer of bioactive components including proteins, genetic material and lipids from the MP
3) Membrane fusion between the MPs and recipient cell allowing the expression of surface markers on target cells, and finally
4) Phagocytosis or endocytosis mechanisms leading to the internalisation of the MPs (Benameur et al., 2019). Through the interaction with MPs, target cell function can be influenced by the activation of specific pathways or by the

induction of phenotypic changes (Del Conde et al., 2005; Obregon et al., 2006; Whale, 2006).

1.9.10 MPs as biomarkers of CVD

The initial damage to the endothelium and its consequential dysfunction leads to the release of endothelial MPs into the circulation (Dignat-George and Boulanger, 2011), which are elevated in the plasma of patients with high CV risk (Amabile et al., 2014; Lee et al., 2012) and sub-clinical atherosclerosis (Chironi et al., 2006).

Circulating levels of endothelial (EMP), leukocyte (LMP) and platelet-derived MPs (PMP) increase in patients with an elevated risk of developing CVD, including diabetes mellitus (Diamant et al., 2002; Koga et al., 2005; Sabatier et al., 2002b) hypertension (Preston et al., 2003), and hypercholesterolemia (Pirro et al., 2006). Individuals with high CV risk display higher numbers of PMP and Tissue Factor (TF) MP that demonstrate pro-coagulant activity, associated with subclinical atherosclerotic plaque burden (Suades et al., 2015).

Furthermore, MPs from a leukocyte, platelet and endothelial origin display a biomarker potential, as these phenotypes are elevated in asymptomatic individuals with sub-clinical atherosclerosis (Amabile et al., 2005; Chironi et al., 2006). This suggests a possible use of these MP sub-types as predictors of atherosclerotic alterations, thus allowing earlier clinical diagnosis and treatment initiation.

These elevated sub-types are also altered with advanced stage CVD, with PMP and EMPs elevated in the plasma of patients with coronary calcification and stable CAD (Christersson et al., 2016; Jayachandran et al., 2008). Furthermore, PMP and EMPs are

also higher in patients diagnosed with acute coronary syndrome (ACS) when compared to the general public (Bernal-Mizrachi et al., 2004; Mallat et al., 2000; Morel et al., 2009).

Moreover, treatments used to improve CV outcomes have also been shown to decrease levels of MPs for example, patients receiving stains show a reduced number of circulating, platelet, leukocyte and endothelial MPs (Suades et al., 2013). However in this instance, it is unclear if this is a consequence of the drug itself, or from its role in decreasing cholesterol levels, inflammation and a reduction in CV risk.

1.9.11 MPs and their role in CVD disease progression

In addition to their potential value as predictive biomarkers of vascular dysfunction, their role as intracellular communicators has gained interest as a possible contributing mechanism to CVD progression (Dignat-George and Boulanger, 2011). Atherosclerosis is an inflammatory disease characterised by the attachment, rolling and migration of leukocytes to the endothelium, in response to the release of inflammatory mediators following endothelial dysfunction and lipid peroxidation. This inflammatory response leads to the accumulation of lipids, platelets, vascular smooth muscle cells, and further inflammatory cell infiltration into the intimal layer; narrowing the blood vessel lumen.

Several studies have demonstrated the various roles MP subtypes play in plaque initiation, formation and instability both *in vitro* and *in vivo* however their exact mechanism in disease pathogenesis remains unknown.

1.9.11.1 Endothelial-derived MPs

In vitro, endothelial cells produce MPs in response to: TNF-α (Brown et al., 2011), LPS in the presence of fatty acids (Del Turco et al., 2007), IL-1α (Abid Hussein et al., 2007) and CRP (Devaraj et al., 2011; Wang et al., 2007). The expression of surface markers on EMP is determined by their stimulus during activation or apoptosis. MPs formed as a result of endothelial cell activation have a high expression of E-Selectin, I-CAM and V-CAM, whereas increased VE-Cadherin, P-CAM and endoglin are expressed on apoptotic derived EMPs (Jimenez et al., 2003).

These phenotypes demonstrate the ability to disturb vascular endothelial homeostasis *in vitro* in both rat and bovine endothelial cells by stimulating the formation of free radicals, thus reducing the bioavailability of eNOS (Brodsky et al., 2004; Densmore et al., 2006). An autocrine effect has also been reported from EMPs derived from stimulated endothelial cells, whereby the interaction of these MPs with quiescent endothelial cells results in an upregulation of ICAM-1 mRNA expression, and sICAM shedding; an effect not observed with quiescent MPs (Curtis et al., 2009).

Elevated EMP levels in hypercholesteraemic mice induced eNOS dysfunction and inhibited angiogenesis (assessed by endothelial cell tube formation), in isolated heart endothelial cells (Ou et al., 2011). This was similarly observed *in vitro* whereby pathological concentrations of EMPs observed in CVD ($1x10^5$ EMPs/ml) induced oxidative stress in HUVECs assed by superoxide production (Brodsky et al., 2004) and impaired angiogenesis measured by tube formation on matrigel substrate. These effects again were not observed at physiological concentrations ($1x10^3$-$1x10^4$ EMPs/ml) (Mezentsev et al., 2005).

In addition to their role in inflammation and angiogenesis, they also display protective properties. Upon exposure of endothelial cells to activated protein C (coagulation factor XIV), EMPs are released that retain the Endothelial Protein Receptor C (EPCR-APC) complex as shown through RNA sequencing. This complex has an anti-coagulant and anti-inflammatory effect by reducing the production of both IL-1 and TNFα, thrombin production and TF thus displaying a potential protective mechanism *in vivo* (Kreutter et al., 2017; Pérez-Casal et al., 2009). This protective role is further supported by the blockage of EMP release in HUVECs with Y-27632 and calpeptin increasing endothelial cell detachment and apoptosis *in vitro* (Abid Hussein et al., 2007).

1.9.11.2 Monocyte-derived MPs

Monocytic MPs are generated *in vitro* in response to a number of stimuli including TNFα (Eyre et al., 2011), LPS (Ben-Hadj-Khalifa-Kechiche et al., 2010), Fas ligand (Terrisse et al., 2010), etoposide (Mastronardi et al., 2011) and calcium ionophore A23187 (Bardelli et al., 2012; Cerri et al., 2006).

Monocyte-derived MPs influence apoptosis and cell proliferation, stimulate coagulation pathways, and have a pro-inflammatory effect on a variety of cell types (Aharon et al., 2008; Cerri et al., 2006; Eyre et al., 2011; Mastronardi et al., 2011; Neri et al., 2011; Wang et al., 2011). Furthermore, MPs from a monocyte origin also display an autocrine effect, as previously demonstrated by an increase in IL-6 and TNF-α cytokine release, oxygen radical production and NF-κβ activation in human monocytes (Bardelli et al., 2012).

1.9.11.3 Platelet-derived MPs

PMPs that form the largest proportion of circulating MPs are elevated in a number of CVD disease conditions (Arraud et al., 2014). Their release is triggered by endotoxin (Ståhl et al., 2011), thrombin (Terrisse et al., 2010), sheer stress (Holme et al., 1998; Miyazaki et al., 1996), hypoxia (Gemmell et al., 1993), and low temperatures (Bode and Knupp, 1994).

PMP have high pro-coagulant properties by interacting with activated coagulation factors IXa, Va, Xa and VIII through a high-affinity binding site on their surface (Chou et al., 2004; Gilbert et al., 1991; Hoffman et al., 1992).

Experiments have also demonstrated their potential role in inflammatory processes associated with atherosclerosis. Stimulation of endothelial cells by platelet-derived MPs results in the increase of I-CAM, V-CAM and E-selectin expression and pro-inflammatory mediators (IL-6 and IL-8) (Nomura et al., 2001). This is supported by further *in vitro* studies whereby ICAM expression was increased on HUVECS, and subsequent adhesion of U937 cells (a monocytic cell line) was enhanced (Barry et al., 1998).

Furthermore, platelet-derived MPs have demonstrated the ability to deliver chemokine CCL5 to the endothelium, promoting leukocyte recruitment to atherosclerotic plaques observed in mice (Mause et al., 2005). Their exposure of GP1β (platelet ligand for leukocyte integrin Mac1 (CD11b/CD18, αMβ2)) on their surface, provides the ability to facilitate the binding of monocytes to the activated endothelium (Barry et al., 1997, 1998; Mause et al., 2005). MPs from a platelet origin positive for P-selectin can also interact directly with monocytic cells, via P-selectin glycoprotein-1, a mechanism by which leukocytes may also tether to activated endothelial cells (Forlow et al., 2000).

1.9.11.4 T lymphocyte-derived MPs

Fewer studies have investigated the involvement of T cell-derived MPs (TMPs) in the context of atherosclerosis pathogenesis, and inflammation in comparison to EMPs, MMPS and PMP. TMPs are derived from activated and apoptotic T cells *in vitro* through their treatment with TNF-α (Distler et al., 2005b), etoposide (Distler et al., 2005b), actinomycin D (Distler et al., 2005b; Martin et al., 2004), staurosporine (Distler et al., 2005b; Ullal and Pisetsky, 2010), phytohemagglutinin and PMA (Martin et al., 2004; Scanu et al., 2008; Shefler et al., 2010).

MPs from apoptotic T cells reduce eNOS activity, leading to a decrease in NO production, and increasing oxidative stress in endothelial cells *in vitro* (Mostefai et al., 2008). This decrease in eNOS activity was associated with the impairment of PI3k, ERK1/2 and NF-kβ pathways, and also increased ROS production leading to lower NO bioavailability (Mostefai et al., 2008). Similarly, TMPs derived from T lymphocyte cell lines induced vascular dysfunction by causing alteration in the NO pathway (Tesse et al., 2005); where similar effects were also observed in TMPs derived from diabetic patients T cells, and *in vivo* circulating MPs from diabetic and HIV positive patients (Martin et al., 2004).

1.9.12 MPs in inflammatory diseases

It is evident that both the origin and the environment under which MPs are generated influence their function and potential role in immune activation and atherosclerosis pathogenesis. MP levels are elevated in patients with chronic inflammatory diseases, with an associated increased CVD risk. These include type-2 diabetes (Li et al., 2016), multiple sclerosis (Marcos-Ramiro et al., 2014; Sáenz-Cuesta et al., 2014), vasculitis (Clarke et al., 2010; Nakaoka et al., 2018) pre-eclampsia (Zhang et al., 2018),

inflammatory bowel disease (Leonetti et al., 2013; Voudoukis et al., 2016), rheumatoid arthritis (Viñuela-Berni et al., 2015) and systemic lupus erythematosus (Nielsen et al., 2011); in addition to HIV.

In adults living with HIV infection, elevations in MPs from an endothelial, platelet and monocytic origin have been reported compared to uninfected healthy controls (Corrales-Medina et al., 2010; Hijmans et al., 2019; Kelly, 2016; Mayne et al., 2012; Da Silva et al., 2011). Furthermore, total circulating MPs isolated from controlled HIV individuals induced greater endothelial dysfunction of endothelial cells *in vitro* in comparison to MPs isolated from healthy controls (Hijmans et al., 2019); thus providing an additional mechanistic role of MPs in CVD pathogenesis.

1.10 Research focus

To summarise, several complex mechanisms underlie the accelerated atherosclerotic disease progression observed in HIV infected populations (as depicted in figure 1.7, (Vachiat et al., 2017)), with many of these contributing factors present from childhood.

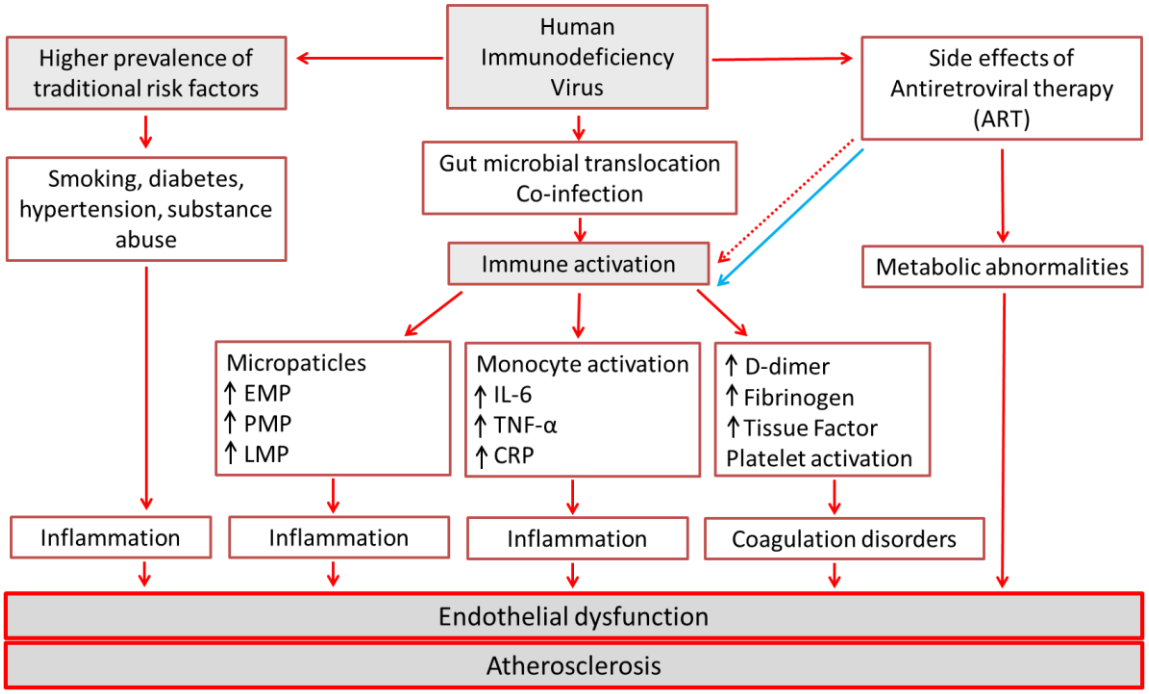

Figure 1.7: A schematic diagram summarising the complex mechanisms underlying chronic inflammation observed in patients with HIV infection, and their contribution to endothelial dysfunction and atherosclerotic disease progression (Image adapted from Vachiat., et al 2017). *The blue line represents the reduction of immune activation following ART initiation, whereas the dotted red line represents the pro-inflammatory effects observed with ART. IL: Interleukin, TNF: Tumour Necrosis Factor, CRP: C - reactive protein, EMP: Endothelial MPs, PMP: Platelet MPs, LMP: Leukocyte MPs*

It is suggested that activated monocytes play a key mechanistic role in atherosclerosis disease progression in these patients. One mechanism by which monocytes may contribute to the atherogenic process is via the release of MPs and their autocrine function, influencing monocytic interaction with the endothelium however, this has been largely unexplored.

With respect to number of MPs in HIV infection, at present there in no information quantifying the levels and phenotypes of MPs in plasma from a HIV-infected paediatric cohort, nor what the effect of ART treatment initiation on these circulating MPs may be. It is important to study these factors in paediatric HIV infection because atherosclerosis begins to develop in early childhood, with evidence that this may accelerated within the context of HIV infection. Therefore, by investigating MPs in HIV-infected children, we can examine the possible mechanisms that may contribute CVD pathogenesis from an early age, in addition to highlighting the importance to develop preventative measures. This setting also provides an additional advantage of studying HIV associated mechanisms with limited influence from traditional risk factors that may present in adulthood.

1.11 Hypothesis and aims

To help to expand our current understanding of MPs, this thesis focused on the following hypotheses:

Hypothesis 1: Stimulated and apoptotic monocytes release quantitatively different MPs, which mimic the phenotype of the parent cell.

To address this hypothesis, the following aims were investigated:

- To assess the suitability of a novel negative isolation method, allowing the isolation of un-activated monocytes directly from whole blood without; altering subset distribution.
- Using a monocytic cell line to investigate the conditions under which MPs are released.

Hypothesis 2: MPs derived from monocytes have the ability to activate quiescent monocytes, switching them to a pro-inflammatory phenotype and function.

To address this hypothesis, the following aims were investigated:

- Using the novel separation method to isolate monocytes from whole blood and investigate the functional effects of their MMPS by assessing;
- Influence on cytokine secretion, migratory and chemotaxis functionality.

Hypothesis 3: MPs from a monocytic origin are elevated in children with HIV infection, compared to healthy controls, and remain altered following ART initiation. Moreover, endothelial MPs, indicative of endothelial activation and dysfunction, are likely to be altered in children with HIV infection and following treatment intervention.

To address these hypotheses, the following aims were investigated:

- To Identify and quantify circulating MP populations (EMP, MMPS, TMP and PMP) isolated from the plasma of 2 pediatric HIV infected cohorts: treatment-naïve, treatment-experienced (ART duration ≥2 years) in comparison to healthy control children.
- To measure changes in these MP populations following ART initiation for 48 weeks.

Chapter 2 – General methods

This chapter outlines the general methods used in more than one results chapter. Details of methodologies that have been adapted or specific to a single results chapter are discussed in detail in the relevant chapter.

2.1 Cell lines and cell culture

2.1.1 THP-1 cells

The human monocytic leukaemia cell line, THP-1 were a kind gift from Dr Mona Bajaj-Elliott at the Institute of Child Health, characterised by their round, single cell morphology. These suspension cells were cultured in Roswell Park Memorial Institute medium-1640 (RPMI 1640) (Sigma Aldrich, UK), supplemented with 100U/ml penicillin (Sigma Aldrich, UK), 2mM L-Glutamine (Sigma Aldrich, UK) and 100µg/ml streptomycin (Sigma Aldrich, UK), and supplemented with 10% Foetal Bovine Serum (FBS) (Sigma Aldrich, UK). Cells were cultured at a seeding density of 2 x 10^5 viable cells/ml (cell viability was determined using trypan blue (Sigma Aldrich, UK)), at 5% CO_2, at 37^{o}C. For experiments, only cell cultures with cell viability greater than 95% were used as defined by trypan blue staining, and cells below passage 11.

2.1.2 Human Umbilical Vein Endothelial Cells

Human umbilical vein endothelial cells (HUVECS), (neonatal, pooled) were purchased from Sigma-Aldrich, UK. HUVECs were cultured in endothelial cell growth medium (EGM) (Sigma Aldrich, UK) supplemented with 10% FCS (Sigma Aldrich, UK). To passage HUVECs, 80% confluent flasks were washed 3 times with pre-warmed PBS to remove any non-adherent cells and remaining FCS. A 1x trypsin solution (Sigma Aldrich, UK) was then added to the flask and incubated at 37^{o}C for 1 minute, after this period cells were

viewed under the microscope to ensure the detachment of adherent cells; in some cases, detachment was aided by gently tapping the flask against the benchtop. 1ml of pre-warmed FBS was then added to the flask to deactivate the trypsin and transferred into a 50ml sterile flacon tube and centrifuged, to determine cell viability and cell number. For all experiments, HUVECs were only used between passages 2-6.

2.1.3 Cell freezing

HUVECs and THP-1 cells were frozen at a seeding density of $0.5x10^6$/ml in a freezing medium composed of 90% FBS, 10% Dimethyl sulfoxide (DMSO) (Sigma Aldrich, UK).

Cells were frozen using a freezing container at -80^{o}C for 24 hours, then transferred to liquid nitrogen for long term storage.

2.1.4 Flow cytometry of THP-1 cells

Flow cytometry was used to determine the effect of various treatments on THP-1 cell phenotype. After treatment, cells were washed once in PBS and re-suspended in FACS buffer at a volume of 200µl per number of antibody panels (Details of antibody panels and corresponding isotype controls can be found in the relevant results section). Samples were transferred into a 96 well U-bottom plate for staining and spun at 500g for 4 minutes. Primary conjugated fluorescent antibodies were diluted in 50µl FACS buffer at an optimised concentration, added to the cell pellet and incubated in the dark for 30 minutes at 2-8°C. After this period, 150µl of FACS buffer was added and centrifuged at 500g for 4 minutes. The supernatants were discarded, and the remaining cell pellets were washed a further 3 times following the same protocol to remove any unbound antibody. The cell pellets were re-suspended in 200µl 1x BD Cell Fix (BD Biosciences) and left at 2-8°C in the dark until flow cytometry analysis.

Samples were acquired on a BD-LSRII (BD Biosciences, UK) at the Flow Cytometry Core Facility within the Camelia Botnar Laboratories at the Institute of Child Health, Great Ormond Street Hospital, University College London. Analyses were performed using the Flow-Jo Software (Flow Jo, USA).

2.2 Patient samples

2.2.1 Ethical approval

Ethical approval to take blood from healthy volunteers was granted by Kingston University (SEC REC 1516/005). All participants were given the necessary information about the study and were required to provide written informed consent. Participants had the right to withdraw from the study at any time, including the withdrawal of data already obtained.

All HIV plasma samples previously collected as part of the CHAPAS-3 clinical trial and the subsequent CV sub-study set up by Dr Julia Kenny (full ethical approval was given from University College London (1665/002), Baylor College of Medicine, Uganda (H-27028), Joint Clinical Research Centre, Uganda, National Drug Authority, Uganda (293/ESR/NDA/DID-12/2010), Uganda National Council for Science and Technology (HS 774), University of Cape Town (143/2010), Pharmaceutical Regulatory Authority, Zambia (DMS/105/1/112) and The University of Zambia (012-01-09)). Samples were processed and analysed in the containment level three laboratories in the Infection, Inflammation and Rheumatology (IIR) department, 6th floor, UCL Great Ormond Street Institute of Child Health, 30 Guilford Street, London WC1N 1EH.

2.2.2 Immunophenotyping of monocytes in whole blood

Surface marker expression and phenotypic analysis of monocytes from whole blood were determined by flow cytometry. Blood was collected in EDTA tubes (BD Biosciences, UK) and stored at room temperature prior to analysis; all samples were analysed within 4 hours of collection.

5µl of the directly labelled flow cytometry antibody corresponding to the marker of interest was added to 100µl of whole blood and incubated at room temperature for 30 minutes in the dark. 2ml of 1x BD FACS lysing solution (Catalogue No. 349202, BD Biosciences, UK) was added, vortexed, and further incubated at room temperature in the dark for 20 minutes. Following this, 2ml of cold FACS buffer (PBS containing 1% FBS) was added, and lysed samples were centrifuged at 400g for 5 minutes. Samples were then further washed with 4ml cold FACS buffer and re-centrifuged at the same speed and duration. The lysed blood samples were re-suspended in 200µl FACS buffer and left at 2-8°C in the dark until flow cytometry analysis. All samples were acquired within 24 hours of preparation.

Samples were acquired on a BD-LSRII (BD Biosciences, UK) at the Flow Cytometry Core Facility within the Camelia Botnar Laboratories at the Institute of Child Health, Great Ormond Street Hospital, University College London. Analyses were performed using the Flow-Jo Software (Flow Jo, USA).

Details of specific antibody panels for each experiment are outlined in the Methods section in individual results chapters.

2.2.3 Isolation of monocytes from whole blood

As monocytes were required to be isolated from whole blood to carry out functional assays, a custom monocyte negative selection isolation kit (EasySep Direct Monocyte without CD16 Depletion) was created by StemCell Technologies (StemCell Technologies, CA). An MTA Agreement was arranged with StemCell Technologies in order to explore and define optimal isolation conditions using this new product (The unsigned MTA agreement can be found in Appendix 1, as the signed copy is held by the company themselves). Findings from these experiments were presented to the company's R&D specialists for product development and reported in Chapter 3 of this thesis.

The negative selection technique removes unwanted cells from whole blood leaving a final suspension of untouched inactivated target cells.

2.2.3.1 StemCell monocyte Isolation

Monocytes were isolated directly from whole blood using the StemCell™ custom monocyte isolation kit following the manufacturer's protocol. Briefly, 3ml of whole blood was transferred into 14ml FACS polystyrene tubes, to which 50µl/ml (150µl) of the isolation cocktail and 50µl/ml (150µl) of the RapidSpheres™ were added. These were incubated at room temperature for 5 minutes.

After this time, 4ml of medium (Ca^{2+} and Mg^{2+} free phosphate-buffered saline (PBS) + 1mM EDTA), was added to the sample and placed in the EasySep BigEasy™ magnet for 5 minutes. The enriched cell fraction was poured off into a new FACS tube (without removing from the magnet), to which 50µl/ml (150µl) of the RapidSpheres™ was further added and incubated for an additional 5 minutes. The cell suspension was again poured off into a new FACS tube before the final addition and incubation with the

RapidSpheres™ (50µl/ml (150µl)), then placed back into the BigEasy™ magnet for 5 minutes. The enriched monocyte suspension was placed back into the BigEasy™ magnet for 5 minutes to remove any remaining spheres and contaminating cells, then poured off ready for use in future experiments and for purity and activation analysis by flow cytometry as previously described.

For *in vitro* experiments, the monocyte fraction was centrifuged at 500g for 5 minutes, with cell number and viability being determined by trypan blue exclusion dye. Purity was determined by flow cytometry, with only preparations above 85% used for experiments. These cells were cultured in RPMI-1640 cell culture media supplemented with 10% FBS, L-glutamine, penicillin and streptomycin (Sigma Aldrich, UK). All monocytes were used in experiments immediately after isolation.

In some experiments an alternative magnet and temperature was used, in these cases, any deviations from the standard protocol have been highlighted in the methods section of the results chapter.

2.3 MP analysis by flow cytometry

2.3.1 Isolation of MPs following cell culture

MPs were isolated from cell culture by centrifuging cell supernatants at 5000g for 5 minutes, after which the supernatant was removed and centrifuged again. The resulting sample was then stored in 200µl aliquots and either used immediately for analysis or stored at -80^{o}C.

2.3.2 Isolation of MPs from whole blood

In addition to analysing MP release from monocytes, MP phenotypes were characterised in patient samples collected from healthy adults and children, in addition to children with HIV infection as part of the CHAPAS-3 clinical trial.

Whole blood was collected in 3.2% trisodium citrate tubes (BD Biosciences, UK) and left at room temperature prior to processing. Samples were processed within 4 hours of collection.

Blood samples were divided into 1.5ml aliquots, and centrifuged at 5000g for 5 minutes, after which the supernatant was decanted and centrifuged again. The platelet-poor plasma (PPP) was then stored in 200µl aliquots and either used immediately for analysis or stored at -80^{o}C for later analysis.

2.3.3 Detection of cellular MPs

If previously frozen, 200µl PPP samples/cell supernatants were quickly thawed in a water bath set to 37^{o}C and centrifuged at 17000g at 4^{o}C for 60 minutes as previously described (Eleftheriou et al., 2012). The supernatant was carefully decanted leaving 20µl, to which annexin V buffer (BD Biosciences, UK) was added equal to the volume (200µl) of the original sample.

An antibody mix was made containing the directly labelled antibodies for the corresponding markers of interest along with FITC conjugated Annexin V (BD Biosciences, UK). Annexin V buffer was added to make a final volume of 10µl. To the antibody mix 40µl of the re-suspended MPs were added and incubated at room temperature in the dark for 20 minutes with continuous shaking. After the incubation,

150µl of annexin V buffer was added to each well and fixed using BD CellFix (BD Biosciences, UK). Samples were stored at 4°C in the dark until analysis. All samples were acquired by flow cytometry within 4 hours of preparation.

Details of the staining panels and individual antibody and isotype control details will be described in the relevant methods sections in each results chapter.

2.3.4 Preparation of latex beads for analysis

Latex beads were used in flow cytometry to create an appropriately sized gate and to enumerate MP numbers accurately. To do this, two different bead sizes were required for each analysis; these were prepared immediately before each experiment.

1.1µm beads (Sigma Aldrich, UK) were used to set the gate for the MPs for particle sizes <1µm. Particles above this size were most likely to be cell debris, apoptotic bodies or platelets rather than MPs. Beads were prepared by adding 6µl to 2ml sterile filtered H_2O, 5µl of this was then further diluted by 200µl of sterile-filtered H_2O.

3.0µm beads (Sigma Aldrich, UK) were used to enable effective enumeration of MPs. Beads were prepared by adding 6µl to 2ml of sterile-filtered H_2O, 10µl of this was then further diluted by 190µl of sterile-filtered H_2O.

2.3.5 Flow cytometry instrument settings for MP detection

All MP samples were acquired on a BD LSR II Flow Cytometer (BD Biosciences, UK) at the Flow Cytometry Core Facility within the Camelia Botnar Laboratories at the Institute of Child Health. Using previously validated instrument settings (Bonner, 2017; Clarke et al., 2010), samples were analysed using a logarithmic scale with the FSC threshold lowered

to 500; instrument settings were checked between acquisitions by running 1.1 µM and 3µM latex beads.

Samples were acquired for 1 minute on a low flow rate and gated based upon their size and presence of Annexin V as previously described (Combes et al., 1997).

2.3.6 Gating strategy for MP detection

As previously mentioned MPs are defined as being less than 1µm and Annexin V positive, therefore an initial gate was set in order to gate out any contaminating cells or particles larger than 1µm. To define these populations, 1.1µm beads were first acquired allowing the determination of the <1 µm gate. Figure 2.1 shows a representative histogram showing how this gate is set.

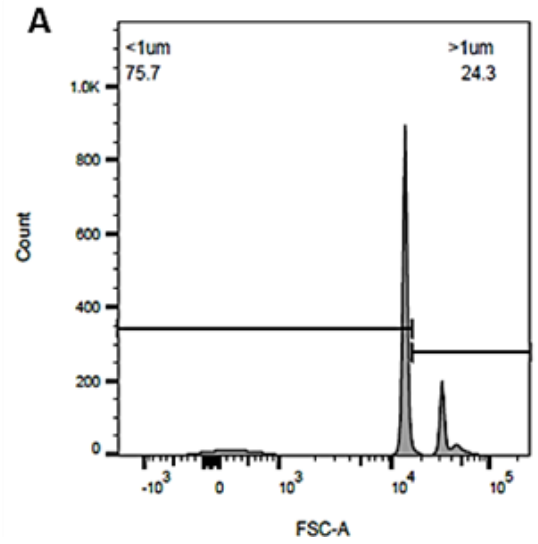

Figure 2.1: Flow cytometry histogram demonstrating how the MP size gate was defined

A Forward scatter Vs count histogram of the 1.1 µm beads. The sharp peak observed just after 1x10^4 are the beads, therefore the bisector is lined up with the end of the peak thus setting the <1µm gate.

From this, MPs were gated on upon their Annexin V positivity. As Annexin V is a protein that relies on the presence of calcium to bind, a negative control containing the Annexin V antibody re-suspended in calcium-free PBS was used to define a positivity cut off. By comparing the calcium-free sample to a positive stained sample it is evident where the Annexin V positive events occur (figure 2.2), thus the Annexin V positive gate can easily be defined. This gate was applied to all samples for analysis.

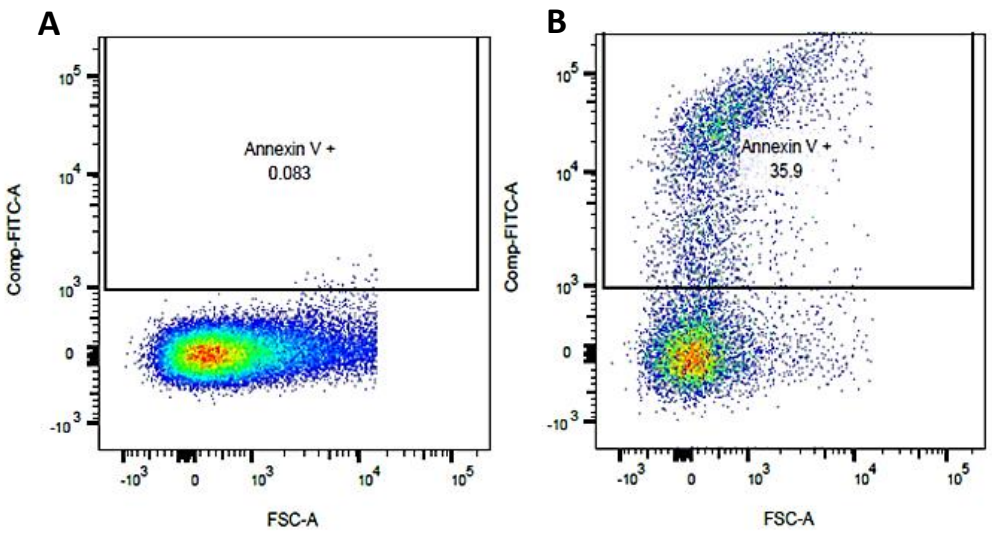

Figure 2.2: Flow cytometry dot plot of MPs demonstrating how the Annexin V positive gate was defined

A representative dot plot of the calcium free Annexin V sample showing Side scatter Vs FL1-H (Annexin V) (A) alongside a representative dot plot of a positive stained sample showing Side scatter Vs FL1-H (Annexin V) (B), demonstrating how the Annexin V positive gate was defined within the MP size gate.

Within the Annexin V positive gate, MPs were phenotyped according to surface marker expression and enumerated using Flow-Jo software (Flow Jo, USA). Figure 2.3 demonstrates the gating strategy used to define microparticle populations.

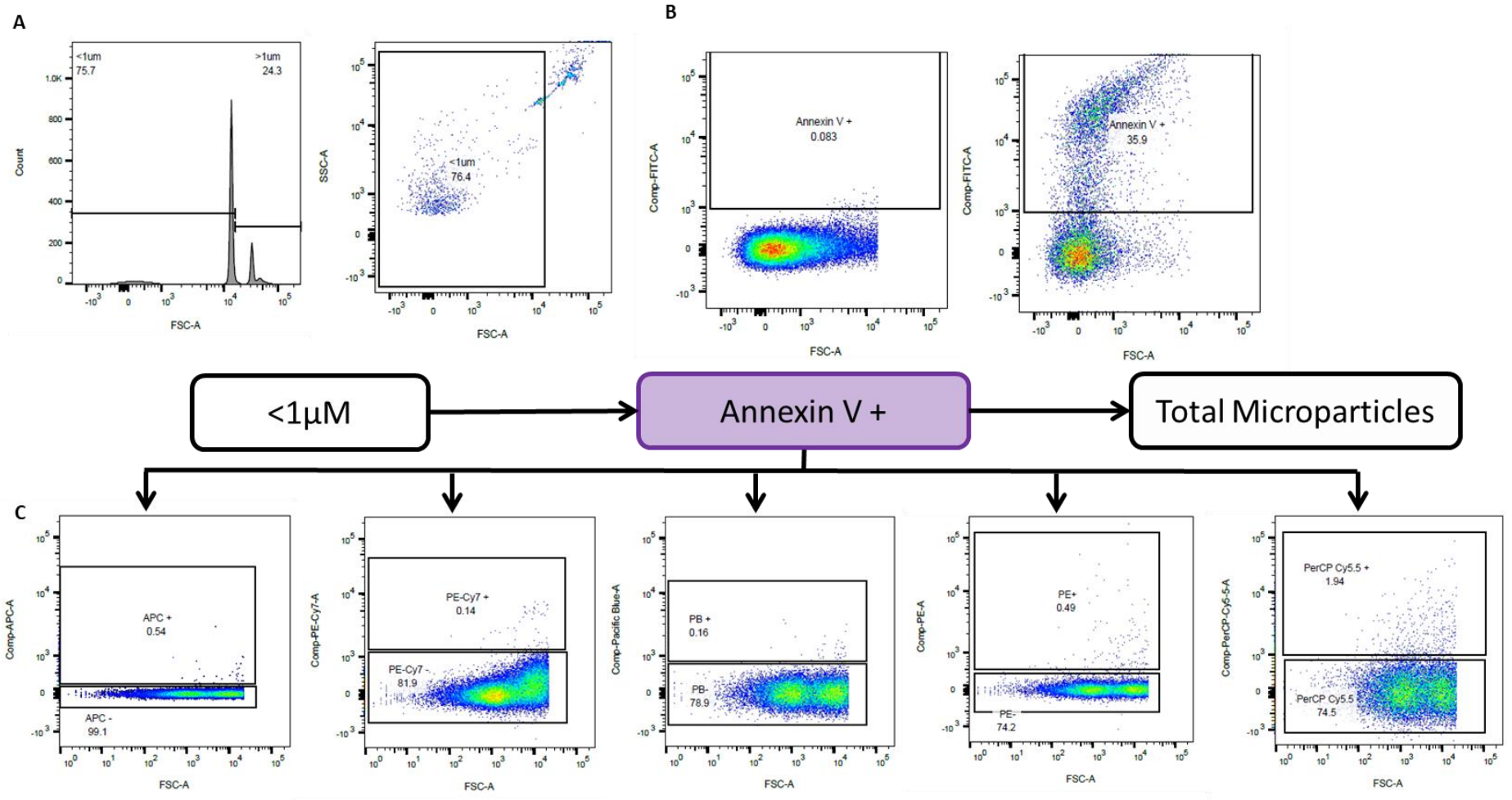

Figure 2.3: MP gates set for 6-marker panel staining

MPs from plasma of healthy adults were analysed by flow cytometry to set MP gates. A) MPs are defined as being <1µM in diameter, thus a size gate was determined using 1.1µM beads. B) Within this size gate, MPs were defined by their expression of Annexin V. A MP gate was set using a 'negative control' whereby Annexin V was incubated with MPs in Ca^{2+} free conditions (PBS –Mg, $CaCl_2$) preventing its binding to PS. Only events within the <1µM and Annexin V gate were classed as MPs. C) Following this, MP gates for each fluorochrome were set using isotype controls.

2.3.7 MP quantification

To calculate the absolute number of MPs in each sample, a known number of 3 µM latex beads (200,000) were acquired for the same duration and flow rate (1 minute on a low flow rate) as MP samples. With the number of latex beads acquired during this period, the number of Annexin V positive events in each sample and the original volume of supernatant used; the absolute number of MPs per ml of plasma was calculated using the following equation:

$$MP\ number/ml\ of\ plasma = \frac{(200{,}000 \div no.\ of\ beads\ counted) \times no.of\ Annexin\ v\ positive\ events \times no.\ of\ tubes\ used\ for\ the\ sample}{Volume\ of\ plasma\ (ml)}$$

2.4 Functional assays

To assess monocyte functionality following isolation and treatment with monocytic MP, the following assays were developed.

2.4.1 Monocyte MP release

To induce MP release from monocytes, 1x10^6 THP-1 cells were either treated with LPS (O111:B4, Sigma Aldrich, UK) (10ng/ml, 50ng/ml, 100ng/ml, 1000ng/ml), TNF-α (R&D systems, UK) (10ng/ml, 50ng/ml, 100ng/ml, 1000ng/ml), INF-γ (R&D systems, UK) (100 units/ml, 250 units/ml, 500 units/ml) or A23187 (Sigma Aldrich, UK) (2µM, 6µM, 12µM, 18µM, 24µM) for 4 hours (or 10 minutes for A23187). In addition, MPs were also released via apoptosis, using serum starvation conditions for; 48, 72 and 96 hours. After this time, cell supernatants were centrifuged twice at 5000g for 5 minutes and stored at -80^{o}C. The number of MPs released, and phenotype was analysed in these samples by flow cytometry.

2.4.2 Live/dead staining of THP-1 cells

$1x10^6$ serum starved THP-1 cells were stained with a combination of Annexin V and PI (propidium iodide) in order to determine apoptotic cell number. Unfixed THP-1 cells were re-suspended in 500µl of 1x Annexin V binding buffer containing 5µl of Annexin V-FITC (1:100 dilution) and incubated at room temperature for 20 minutes in the dark. After this, 50µl of PI (50µg/ml) was added to the sample prior to FACS analysis. All samples were acquired immediately after staining on a BD FACSCalibur at a low flow rate until 10,000 events had been recorded within the monocyte gate.

2.4.3 Phagocytosis assay

To determine the phagocytic ability of isolated monocytes and THP-1s, a phagocytosis assay kit (Cambridge Bioscience, UK) was used that utilises latex beads coated in FITC-labelled rabbit IgG for monocytes to engulf. $1x10^5$ isolated monocytes or THP-1 cells were pre-treated with LPS 10ng/ml for 4 hours or culture media, after which cells were washed, and the IgG labelled beads were added at a dilution of 1:100 in RPMI. Cells were incubated at 37°C for 2 hours to allow phagocytosis and were centrifuged at 400g for 5 minutes. To remove any beads bound to the surface of the cells rather than those engulfed, monocytes were incubated for 1 minute in a trypan blue solution (1:10) to quench surface FITC fluorescence, thus allowing the detection of an internalised FITC signal only. Cells were then washed and re-suspended in assay buffer.

Samples were analysed by flow cytometry using either the BD LSRII or the BD FACSCalibur. Phagocytosing cells were defined as the percentage of FITC positive cells within the monocytic gate.

2.4.4 Chemotaxis

Monocyte chemotaxis was assessed by measuring the migration of cells towards a chemoattractant through a porous 5.0 µM Transwell membrane. Isolated monocytes were pre-treated with a variety of reagents for 2 hours. To the top of a 5.0µM polycarbonate transwell (Corning, ThermoFisher, UK) $5x10^4$ pre-treated monocytes were added, with MCP-1 (R&D Systems, UK) (See individual chapters for concentrations) added to the lower chamber. Transwells were left for 4 hours at 37^{o}C to allow the free migration of monocytes to the lower chamber, as this was found to be the optimum time for monocyte migration based on preliminary experiments (data presented in Appendix 3). After 4 hours the membrane insert was removed, and migrated cells were imaged at 100x magnification in 5 random fields using a phase-contrast microscope (Leica Microsystems, DE).

2.4.5 Transendothelial migration

The transendothelial migration of isolated monocytes was also assessed using this transwell method. $1x10^4$ HUVECs were seeded onto the upper chamber of a 5.0µM transwell and cultured for 2-3 days to form a monolayer. To ensure a fully confluent monolayer had formed on in the transwell insert, a single membrane was removed and stained with crystal violet. After removal, the insert was fixed using 3.7% paraformaldehyde for 10 minutes and washed in PBS. A cotton swab was used to gently remove cells on the lower side of the transwell, and stained with 0.2% crystal violet (Sigma Aldrich, UK) for 15 minutes, this step ensures that only cells on the upper side of the membrane are stained with crystal violet. Finally, the insert was washed with distilled water 3 times, left to dry and visualised using the phase-contrast microscope.

Once a fully confluent layer of HUVECs was established and confirmed using this method, $5x10^4$ Monocytes that had been pre-treated for 4 hours with monocyte-derived MPs or MP supernatants were added to the top chamber, with the chemoattractant added to the lower chamber. Monocytes were left to freely migrate through the endothelial monolayer to the lower chamber for 4 hours. Migrated cells were imaged at 100x magnification at 5 random fields using a phase-contrast microscope (Leica Microsystems, DE).

2.4.6 Adherence to an endothelial monolayer

The ability of isolated monocytes to adhere to an endothelial monolayer was also assessed under static conditions. Isolated human monocytes ($5x10^4$) were challenged with MMPS, MP supernatant or LPS 10ng/ml for 4 hours and washed with PBS. These monocytes were then co-incubated on endothelial monolayers for 1 hour and subsequently washed 3 times with warmed PBS to remove any non-adherent cells. Adhered monocytes were stained by Diff-Quick staining (Sigma-Aldrich, UK), and images were taken at 200x in three random fields using a phase-contrast microscope (Lecia Microsystems, DE). Only monocytes that had adhered and were associated with an endothelial cells counted.

2.4.7 Cytokine secretion analysis

2.4.7.1 IL-6 ELISA

IL-6 cytokine release was quantified in cell culture supernatants following the manufacturer's instructions (ThermoFisher, UK). Corning™ Costar™ ELISA plates were coated overnight at 4°C with 100µl/well coating buffer. Wells were washed 3 times with wash buffer and blocked for 1 hour at room temperature with 200µl ELISA/ELISASPOT

diluent, followed by a final wash before samples and standards were added. 100µl of each sample (1:2 dilution) and standards (200pg/ml, 100pg/ml, 50pg/ml, 25pg/ml, 12.5pg/ml, 6.25 pg/ml, 3.125 pg/ml and 0 pg/ml) were plated in duplicate and left overnight at 4°C for maximum sensitivity. Following this overnight incubation, all wells were washed 5 times with wash buffer and 100µl/well of detection antibody for 1 hour at room temperature. After this time, wells were washed again with wash buffer and each well was incubated with 100µl of Streptavidin-HRP for 30 minutes at room temperature. A final wash was performed, followed by the addition of 100µl/ml TMB solution for 15 minutes at room temperature, to which 50µl/well of stop solution was added after this time. The plate was read immediately on a microplate reader at both 450nm and 570nm, of which readings at 570nm were subtracted from those recorded at 450nm to minus any background interference.

2.4.7.2 MSD

Cytokines were analysed in cell culture supernatants using the V-PLEX Cytokine Panel 1 Human Kit purchased from MSD (MesoScale Discovery, USA). This kit quantifies levels of IL-1β, IL-6, IL-8, IL10, IFN-γ and TNF-α. Samples were analysed according to the manufacturer's instructions. Briefly, the MSD plate was washed 3 times using the wash buffer, after which 50µl of supernatants (diluted 2-fold for using the assay diluent), assay calibrators and controls were added and incubated at room temperature for 2 hours.

After this, the MSD plate was washed 3 times with wash buffer, and 25µl of the detection antibody was added and left at room temperature for 2 hours on a plate shaker. The plate was washed a further 3 times using the wash buffer, and 150µl of 2x

read buffer was added to each well and analysed on the MSD instrument (MesoScale Discovery, USA).

2.4.8 Influence of monocyte-derived MPs on human monocyte phenotype

To investigate the influence of monocytic MPs on cell phenotypes, $1x10^5$ isolated human monocytes were treated with monocytic MPs or MP supernatants for 2, 4 and 24 hours. 50µl of an antibody cocktail was added to the cell pellets of these cultures and incubated at 4°C for 30 minutes. Details of antibody cocktail panels are outlined in the methods sections in subsequent results chapters. After 30 minutes cell pellets were washed twice with a FACS buffer, and fixed with BD cell fix for storage at 4°C until flow cytometry acquisition.

2.5 Statistics

One-Way ANOVA (Analysis of Variance) followed by a Tukey's post hoc test or Two-Way ANOVA followed by a Sidak's post hoc test were performed determined by the number of independent variables in each experiment, and the number of data sets. In addition, student's *t-test* were also performed to determine the significance between 2 groups, these analyses were performed using GraphPad Prism software (USA). SPSS (UK) was used to analyse patient demographics and MP counts in the CHAPAS-3 cohort, where statistical differences were determined using Wilcoxon matched-pairs signed rank and Mann-Whitney-U non-parametric tests. Details of individual statistical analyses are described in the subsequent results chapters.

Chapter 3 - Monocyte isolation from whole blood: Method validation and optimisation

3.1 Introduction

As monocytes play a key role in atherosclerotic disease pathogenesis, their isolation from whole blood allows the study of inflammation pathogenesis, provides information on how these contribute to disease progression, and highlights potential therapeutic targets. For isolated monocytes to reflect their *in vivo* state, a separation technique should be used that requires minimal sample handling to preserve target cell phenotype and functionality, with minimal activation and few contaminating cell populations. Isolation methods that have been established are based on three key principles: adhesion, density centrifugation and antibody binding (Tomlinson et al., 2013). This introduction highlights limitations for the current isolation methods available, and considerations to be made when extracting monocytes to study their functionality in active disease states.

3.1.1 Isolation by adherence

Monocyte isolation by adhesion relies on cells sticking to plastic or glass via β_2 integrin interaction. This technique is quick, easy and inexpensive; requiring initial PBMC isolation by density centrifugation, followed by subsequent cell culture and multiple washes to remove contaminating cells. Surface expression of CD11b, CD18 and CD54 are elevated on monocytes isolated via this technique (Stent and Crowe, 1997) indicative of monocyte activation. Furthermore, Zhou., *et al* (2012) reported that despite reasonable monocyte yields, similar to immunomagnetic separations ($1.9\pm0.6x10^5$/ml Peripheral

Blood), purity was low in isolated monocyte cultures (67.3±3.6%), with most contaminants from lymphocytes and platelets (Zhou et al., 2012).

3.1.2 Isolation by density centrifugation

An alternative method of isolation is by density centrifugation. Monocytes can be isolated directly from whole blood using a combination of density centrifugation and negative selection. A cocktail of tetrameric antibody complexes (TAC) targeting unwanted cells for removal (CD2, CD3, CD8, CD19, CD56, CD66b, CD123 and glycophorin A) is added to whole blood. When this is centrifuged over a density medium such as Ficoll, the unwanted cells bind to their corresponding TACs and form a pellet with red blood cells. A purified monocytic population can be isolated from the buffy coat layer between the medium and plasma. Monocyte yield has been reported to be substantially higher using this method ($4.2\pm0.6x10^5$/ml peripheral blood) in comparison to immunomagnetic selection and isolation by adherence, however in this case purity was compromised. Similar to separation by adherence, this technique shows large contaminants of lymphocytes, platelets and non-specific cellular aggregates in the final isolated fraction, with low monocyte purity (percentage purity: 64.2±4.3%) (Zhou et al., 2012). It is important to note that although monocytes isolated using this method were observed to actively phagocytose *E.coli*, contaminating platelets were also phagocytosed (Zhou et al., 2012); suggestive of a competing effect. This demonstrates one way in which isolation contaminants may interfere with further downstream functional assays.

Density centrifugation is also employed as an initial step prior to immunomagnetic selection. Ficoll-Plaque density gradient media separates PBMCs (Peripheral Blood Mononuclear Cells) from contaminating red blood cells and granulocytes. Although this

method displays clear advantages in a clinical setting, as samples can be stored and processed in the future, this preparation has been shown to alter monocyte subset proportions and CD14+, CD16+ surface marker expression. Flow cytometry analysis of whole blood compared to PBMCs has shown a significant decrease of 20% in the classical monocyte subset, with a corresponding increase of the non-classical population and intermediate monocytes (Mukherjee et al., 2015). Furthermore, the same study highlights how density gradient separation causes changes to CD14+, CD16+ surface marker expression within each of the monocyte populations themselves (Mukherjee et al., 2015).

In addition to this, alterations in CD163 and chemokine surface marker expression on each of the monocyte subsets have also been observed after density centrifugation in comparison to whole blood (Nieto et al., 2012; Tippett et al., 2011). Furthermore, Ficoll-isolated monocytes demonstrated a reduced chemotactic response to MCP-1 (CCL2) compared whole blood monocytes, which may be attributed to the significant loss of CCR2 expression on these cells (Nieto et al., 2012). This data provides evidence that subset distribution and phenotypes can be altered after PBMC purification from whole blood, which may lead to inconsistent functional observations in isolated monocytes *in vitro.*

3.1.3 Isolation by antibody binding

3.1.3.1 Fluorescence-activated cell sorting

Fluorescence-activated cell sorting (FACS) uses antibody stains against a specific cell surface marker, for detection and sorting by flow cytometry. FACS sorting allows the isolation of multiple cell types from a single sample, with the isolated fraction having

few contaminating populations (Basu et al., 2010). Although isolated fractions have a high purity, it has been reported that this method of separation results in particularly low yields of monocytes, with concerns that antibody binding to CD14+ may induce activation (Beliakova-Bethell et al., 2014).

3.1.3.2 Immunomagnetic separation

Immunomagnetic separation relies on the attachment of antibodies conjugated to microbeads against a surface antigen specific to the target cell, the cocktail is then passed through a strong magnetic field to isolate target cells. This separation method is the most common technique used as a cheaper alternative to FACS sorting, and does not require specialist equipment. The target cell population is isolated by either positive or negative selection as described.

3.1.3.3 Positive isolation

This isolation procedure relies on the attachment of the antibody conjugate directly to the target cell. Positive monocyte isolation utilizes the binding of antibody conjugates to CD14+, highly expressed by monocytes ensuring their high purity.

Positive isolation gives rise to a highly pure monocyte fraction (Beliakova-Bethell et al., 2014; Kho et al., 2017; Zhou et al., 2012), with limited contamination from T cells, B cells and unidentified cells (1.3%, 0.3% and 15% respectively) (Beliakova-Bethell et al., 2014). Furthermore, this method produces the highest yield of isolated monocytes compared to alternative isolation techniques (negative and FACS sorting) (Beliakova-Bethell et al., 2014), however, this method fails to isolate non-classical populations due to their lower expression of CD14+ (Kho et al., 2017).

Through the binding of microbeads to co-receptors on the cell surface, it has been suggested that cellular activation may be triggered (Dixon et al., 1989; Stanciu et al., 1996), or cause receptor blocking inhibiting LPS stimulation functional effects (Elkord et al., 2005). This will be further discussed in section 3.3.2.3.

3.1.3.4 Negative isolation

With these issues surrounding other isolation techniques, a negative selection method may be employed, minimising interference of the magnetic beads with the target cell population. This technique uses antibody conjugates to bind to CD markers on contaminating non-target cells, thus resulting in an enriched, 'untouched' target cell population.

Most common negative selection methods require PBMC isolation prior to separation, with enriched monocyte fractions displaying similar yields to positive isolation methods (Beliakova-Bethell et al., 2014). However, enriched suspensions showed more contaminating populations (Beliakova-Bethell et al., 2014; Kho et al., 2017), with higher proportions of contaminating platelets and unidentified cells found (Beliakova-Bethell et al., 2014; Kho et al., 2017; Zhou et al., 2012). Following negative isolation from PBMCs, high yields of all three monocyte sub-populations were present in the negatively isolated fraction however, alterations in CD14+ expression were reported (Kho et al., 2017).

Current isolation kits that utilize negative selection methods to isolate monocytes from whole blood causes the loss of CD16+ monocyte populations, due to antibody targets for this CD marker used to deplete contaminating granulocytes.

3.1.3.5 Influence of immunomagnetic separation on monocyte function in vitro

Despite reports that microbeads are biodegradable, do not induce cellular activation or trigger any downstream pathways; some studies have demonstrated functional impairments following isolation (Bhattacharjee et al., 2017; Kho et al., 2017; Lynn et al., 1993).

Alterations in pro-inflammatory and anti-inflammatory cytokine secretion have been observed to be dependent on the isolation method used. IL-8 production from negatively sorted monocytes stimulated with LPS, was six times higher compared to positively isolated monocytes, with RANTES and TGF-β1 secretion also being elevated from this population (Bhattacharjee et al., 2017). Furthermore, positively sorted monocytes displayed a delayed inflammatory response to LPS (Bhattacharjee et al., 2017) suggesting that this impairment is due to CD14+ microbeads blocking LPS mediated stimulation as previously indicated (Lynn et al., 1993). Lastly, the same study showed that antibody microbeads remain bound to positively isolated monocytes for up to 6 days in standard culture conditions (Bhattacharjee et al., 2017).

Functional studies investigating the influence of monocytes on the blood-brain barrier (BBB) integrity found that the method of monocyte enrichment influenced functional capacity. Positively isolated monocytes had a larger effect on BBB disruption (Measured by Electric Cell Substrate Impedance Sensing) compared to negative selection methods (Kho et al., 2017). They reported that this observation may have been due to direct activation from the conjugation of CD14+ microbeads influencing their behaviour, or due to contaminating cell populations in the enriched fractions of isolated monocytes influencing the functionality of both monocytes and endothelial cells (Kho et al., 2017).

This study demonstrates the importance of purity in the enriched monocyte fraction specifically with regards to functional studies.

In contrast to this, the observation that CD14+ can still be detected by immunofluorescence after positive isolation, suggests that this receptor remains functional after separation (Zhou et al., 2012). In addition, monocytes had the ability to phagocytose *E. coli*, irrespective of the immunomagnetic separation procedure used (Zhou et al., 2012).

With clear advantages and disadvantages of each isolation technique (as summarised in Table 3.1) each should be considered when selecting the appropriate method for further downstream experiments.

Isolation method	Advantages	Disadvantages
Adherence	-Rapid procedure -Inexpensive -Good monocyte yield	-Requires initial PBMC isolation which may cause alterations in surface marker expression -Low purity (≈67%) -Leads to monocyte activation -Upregulation of adhesion molecules
Density centrifugation	-High yield - Rapid procedure -Inexpensive	-Low purity (≈64%) -Alteration in monocyte subset distribution -Alteration in surface marker expression
Fluorescence-activated cell sorting	-Isolation of multiple cell types from a single sample -High purity -Rapid procedure -High throughput -Rare populations can be isolated, thus individual monocyte subsets can be isolated -All three monocyte subsets recovered	-Expensive -Requires antibody binding to CD14, potentially leading to monocyte activation -Requires training, and specialist equipment
Positive isolation	-Rapid procedure -Inexpensive -High yield -High purity (≈83%)	-Relies on antibody binding directly to CD14, potentially leading to monocyte activation Loss of CD14 low populations (Intermediate and non-classical) -May require prior PBMC isolation -Impairments in cytokine secretion in response to LPS have been reported
Negative isolation	-Rapid procedure -Inexpensive -High yield -High purity (≈86%) -Monocytes are 'untouched' -Monocytes are inactivated -All three monocyte subsets can be recovered	-Some negative isolation methods may require prior PBMC isolation -Direct negative isolation from whole blood results in the loss of CD14 low populations (Intermediate and non-classical) -Alterations in CD14 surface marker expression have been reported

Table 3.1: Advantages and disadvantages of current monocyte isolation methods

Negative selection methods display a clear advantage in avoiding interference with the target cell; however most commercially available kits require PBMC isolation prior to negative selection which could introduce initial phenotypic changes.

Currently, only one commercial kit is available to negatively select monocytes from whole blood which utilises CD16+ antibodies to deplete granulocytes; also eliminating the non-classical and intermediate subsets. Despite the low percentage of this population, it has been suggested that the inclusion of this subset following isolation may give rise to varying functional responses *in vivo* (Kho et al., 2017). In addition, this also leads to isolated monocyte functionally being more reflective of their behaviour *in* vivo; an aspect which is particularly important when studying monocytes in disease.

Taking these findings into consideration, these studies highlight the importance of monocyte yield, purity, activation stasis and individual subset presence when assessing a new enrichment method.

3.2 Aims and objectives

In order to carry out experiments on isolated monocytes, assessing monocyte functionality *ex vivo*, a novel negative selection method was developed and optimised as part of an MTA agreement with StemCell™ Technologies (Appendix 1). This method is unique as isolation can be performed directly from whole blood without the need for PBMC purification.

This chapter assesses the suitability of this novel method of monocyte selection and addresses the following aims:

1) To optimise the isolation conditions of a novel method of negative selection directly from whole blood, to determine the ideal conditions for:
    a. Purity
    b. Monocyte activation
    c. Subset recovery
    d. Yield
2) To assess the impact of this selection method on monocyte phenotype and surface marker expression in comparison to whole blood.
3) To assess the impact of this selection method on monocyte function.

3.3 Methodology

3.3.1 Patient recruitment

3.3.1.1 Ethical approval

Ethical approval for this study was granted by Kingston University (SEC REC 1516/005). All participants were fully informed about the study and were required to provide written informed consent prior to blood samples being taken. Prior to the blood draw, participants were required to complete a brief medical history questionnaire to ensure that volunteers meet the inclusion criteria. Participants were excluded from the study if they had a higher CV risk (smoker, hypertension, diabetic or high cholesterol), or a family history of CVD. Volunteers had the right to withdraw from the study at any time, including the withdrawal of data already obtained.

3.3.2 Whole blood Flow cytometry analysis

To phenotype monocytes in whole blood, antibodies corresponding to markers of interest were first added directly to whole blood followed by red blood cell lysis. Antibody cocktails (See section 3.6.2.1 for details of staining panels, and appendix 2 for details of isotype controls) were added to 100µl of whole blood and incubated at room temperature for 30 minutes in the dark. After staining, 2ml of 1x BD FACS lysing solution (Catalogue No. 349202, BD Biosciences) was added, vortexed, and further incubated at room temperature in the dark for 20 minutes. Following this, 2ml of cold FACS buffer (PBS containing 1% FBS) was added, and lysed samples were centrifuged at 400g for 5 minutes. Samples were then further washed with 4ml cold FACS buffer and re-centrifuged at the same speed and duration. The lysed blood samples were re-

suspended in 200µl FACS buffer and left at 2-8°C in the dark until flow cytometry analysis. All samples were acquired within 24 hours of preparation.

Tables 3.2 outlines the antibody panel that was designed to phenotype monocytes in whole blood.

Panel 1					
Target	**Fluorochrome conjugate**	**Clone**	**Isotype**	**Source**	**Dilution (Volume/100µl Whole Blood)**
CD14	AF700	63D3	IgG1, κ	Biolegend	5µl
CD16	PerCp-Cy5.5	3G8	IgG1, κ	BD Biosciences	5µl
HLA-DR	BV510	L234	IgG2a, κ	Biolegend	5µl
DUMP: CD3 CD20 CD56 CD66b	PE-Cy7	UHT1 2H7 MEM-188 G10F5	IgG1, κ IgG2b, κ IgG2a, κ IgM, κ	Biolegend	2.5µl
CD11b	APC	CBRM1/5	IgG1, κ	Biolegend	5µl

Table 3.2: Monocyte phenotyping antibody panel

3.3.3 Isolation of monocytes from whole blood using StemCell™ Custom Kit

To isolate monocytes directly from whole blood, a negative selection kit was developed by StemCell™ Technologies. To find the optimal enrichment conditions, antibody cocktail beads were added to whole blood either on ice (labelled as 8°C) and at room temperature (labelled as 25°C) as suggested through correspondence with R&D team members at StemCell™ Technologies. 50µl of the antibody cocktail was added to 1ml of whole blood, along with 50µl of the RapidSpheres™ and incubated at the required temperature (8°C/25°C) for 5 minutes in a 14ml FACS tube. To this, EasySep medium

(PBS containing 2% FBS and 1 mM EDTA) was added to 4x the volume, and the FACS tube was placed in the required magnet (Big Easy™/Easy Eights™) for 5 minutes.

The purified fraction was then removed from the suspension by leaving the FACS tube inside the magnet and either pouring off the supernatant into a new FACS tube for the Big Easy™ magnet or using a pipette to transfer the purified fraction to a new FACS tube. To this, an additional 50µl of the RapidSpheres™ were added and incubated for a further 5 minutes (at 8°C/25°C) before placing the tube back into the magnet to allow separation for extra 5 minutes. This purification step was repeated for a third time, after which the enriched fraction was placed back into the magnet for a final 5-minute incubation to remove any remaining RapidSpheres™.

The remaining enriched monocytes were re-suspended in either FACS buffer for flow cytometry analysis or RPMI 1640 10% FBS for downstream functional experiments. Cell viability was determined >98% by trypan blue exclusion after each isolation.

3.3.4 Antibody staining of isolated monocytes

To phenotype isolated cells, cell pellets were stained with antibodies corresponding to markers of interest. Cells were plated in a 96 U-bottom well plate at a seeding density of $5x10^5$/200µl and washed with cold FACS buffer. Cell pellets were stained with 50µl of antibody cocktail and incubated in the dark at 2-8°C for 30 minutes. After this period, 150µl of FACS buffer was added and centrifuged at 350g for 4 minutes. The supernatants were discarded, and the remaining cell pellets were washed a further 3 times following the same protocol to remove any unbound antibody. The cell pellets were re-suspended in 200µl 1x BD Cell Fix (BD Biosciences) and left at 2-8°C in the dark until flow cytometry analysis.

The antibody panel detailed in table 3.2 was also used to phenotype isolated monocytes, the antibody panel described in table 3.3 was used to assess isolated fraction purity.

Purity panel					
Target	**Fluorochrome conjugate**	**Clone**	**Isotype**	**Source**	**Dilution**
CD14	AF700	63D3	IgG1, κ	Biolegend	1:50
CD3	PE-Cy7	UHT1	IgG1, κ	Biolegend	1:50
CD235a	PE	HI264	IgG2a, κ	Biolegend	1:50
CD19	PerCp-Cy5.5	HIB19	IgG1, κ	BD Bioscience	1:50
CD66b	FITC	G10F5	IgM, κ	Biolegend	1:50

Table 3.3: Monocyte purity antibody panel

3.3.5 Sample acquisition

All samples were acquired within 24 hours of sample preparation on a low flow rate for 120 seconds. Samples were run on a BD LSRII flow cytometer located within the Flow Cytometry Core Facility, Camelia Botnar Laboratories, University College London, Great Ormond Street Hospital, 85 Lamb's Conduit, London WC1N 3JH.

3.3.6 Flow cytometry gating strategy

After flow cytometry acquisition, monocyte phenotype was analysed using Flow-Jo Software (Flow Jo, USA). Compensation was applied to samples post-flow cytometry acquisition within the FlowJo software, using latex compensation beads (BD Biosciences) as a control. A representative gating strategy shown below was used to determine phenotype and marker expression, this was applied to all whole blood and isolated samples (In isolated samples the monocyte population was gated directly).

Figure 3.1 shows the forward scatter Vs side scatter graph produced by analysing whole blood.

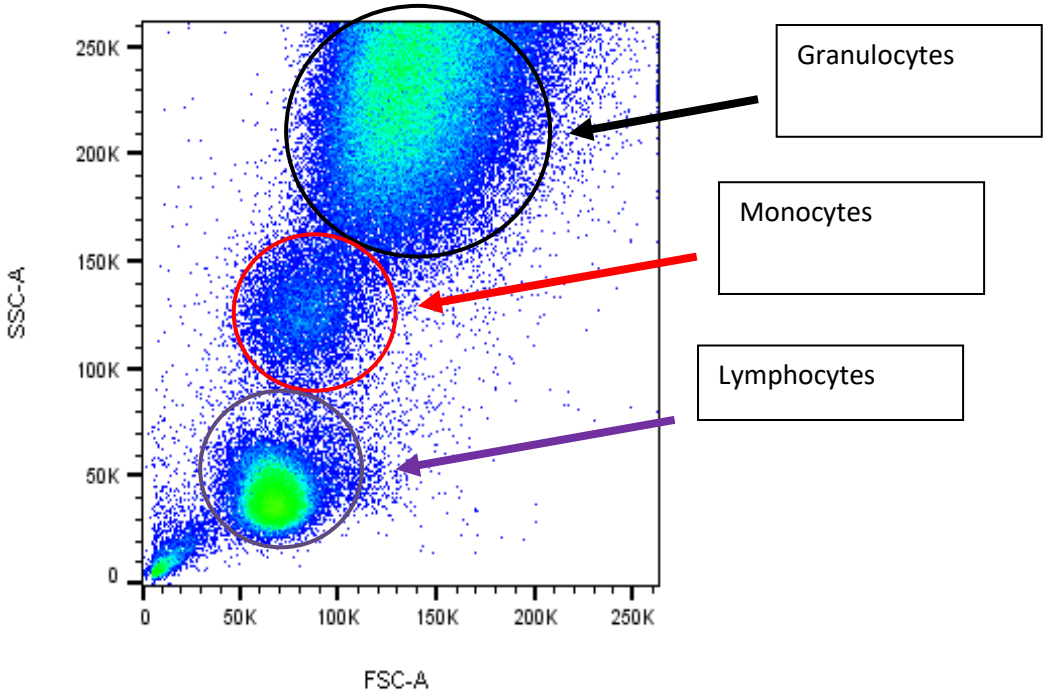

Figure 3.1: FSC Vs SSC dot plot of lysed whole blood, highlighting the granulocyte, monocyte and lymphocyte populations

however further gating was used to ensure that the monocyte population was correctly identified (Figure 3.2). Initially, a 'dump' channel was used to gate out unwanted cells, staining CD3+, CD20+, CD56+ and CD66b+ cells on T cells, B cells, natural killer cells and granulocytes respectively. These antibodies were all directly conjugated to a PE-Cy7 fluorochrome, allowing the negative population to be selected (Figure 3.2A). Monocytes were then gated based on their positive HLA-DR expression (Figure 3.2B), with individual subsets being identified based upon their CD14 and CD16 surface marker expression (Figure 3.2C).

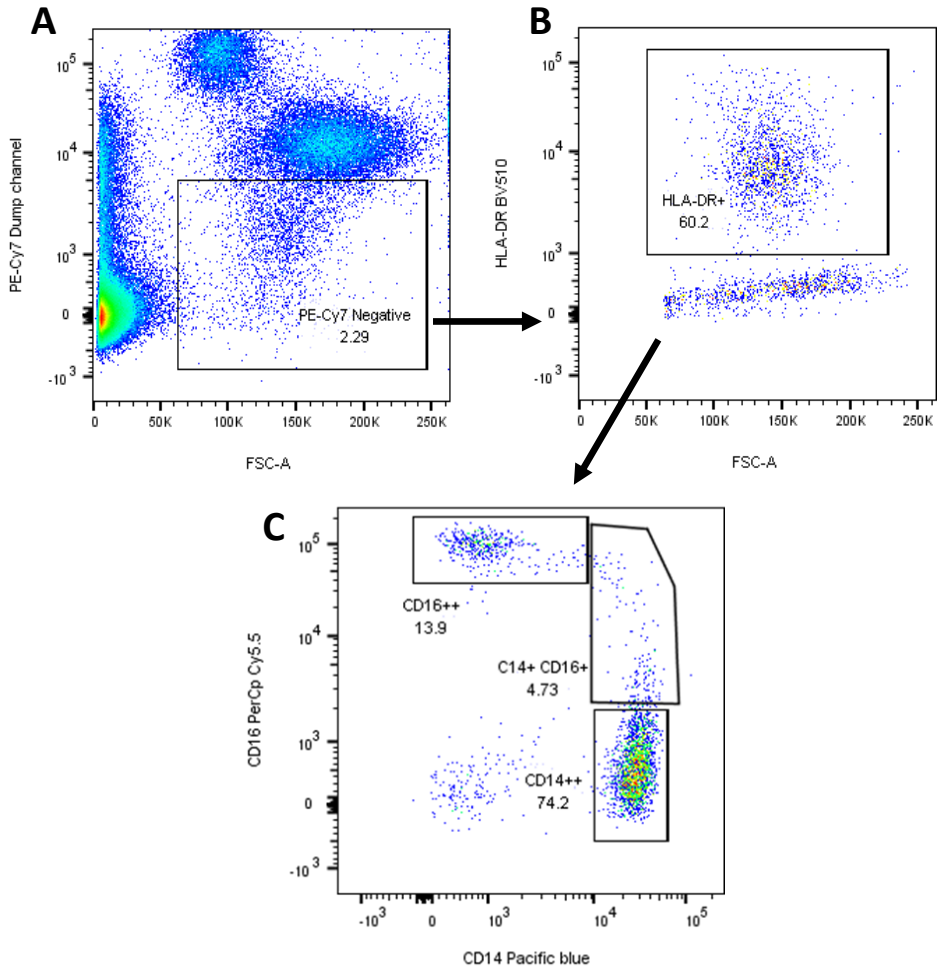

Figure 3.2: Flow cytometry dot plots demonstrating how the monocytic population was gated on in whole blood, and the identification of the corresponding monocyte subsets

Whole blood was stained with primary conjugated antibodies against CD3, CD20, CD56, CD66b- PE-Cy7, CD14-Pacific blue and CD16-PerCp-Cy5.5. The antibodies all conjugated to PE-Cy7 were used as a 'dump' channel in order to gate out unwanted cells, allowing the negative population to be selected (A). Monocytes were then gated based on their positive HLA-DR expression (B), with individual subsets being identified based upon their CD14 and CD16 surface marker expression (C).

Following this, specific surface marker expression was assessed based upon percentage expression, and mean fluorescence intensity (MFI).

3.3.7 Assessment of monocyte function

Phagocytic ability, migratory function and cytokine secretion of isolated monocytes and THP-1 cells were assessed as described in Chapter 2, General methods, Section 2.4.2, 2.4.3 and 2.4.6 respectively.

3.3.8 Statistics

All statistical analysis was performed using GraphPad Prism software, with the statistical test used detailed in the relevant results section.

3.4 Results

3.4.1 Human monocytes can be negatively isolated from whole blood with minimal contamination

Monocytes were isolated using immunomagnetic techniques from whole blood using two different magnet strengths in parallel (Big Easy™ and Easy Eights™) at two temperature conditions (8˚C and 25˚C) as previously described in section 3.3. Isolated fractions were stained and analysed by flow cytometry.

The Big Easy™ magnet proved to be a superior magnet for separation compared to the Easy Eights™ magnet, with monocytes consisting of >90% of the isolated populations (91.58%±0.77% and 91.10%±0.78%, 25˚C and 8˚C respectively), whereas the Easy Eights™ magnet had a purity of <32% (31.16%±4.61% and 22.61%±4.87%, 25˚C and 8˚C respectively). The purity of the fractions under each of the four conditions are shown in the pie charts in Figure 3.3 and Table 3.4). Red blood cells were the largest contaminating cell type in the Easy Eights™ isolated fraction, forming around 50% of the cell populations (54.70%±8.08% and 54.73±8.63%, 25˚C and 8˚C respectively) compared to just 0.70% using the Big Easy™ magnet (0.63%±0.20% and 0.65%±0.15%, 25˚C and 8˚C respectively); likely to be attributed to the supernatant aspiration steps required in the Easy Eights™ methodology.

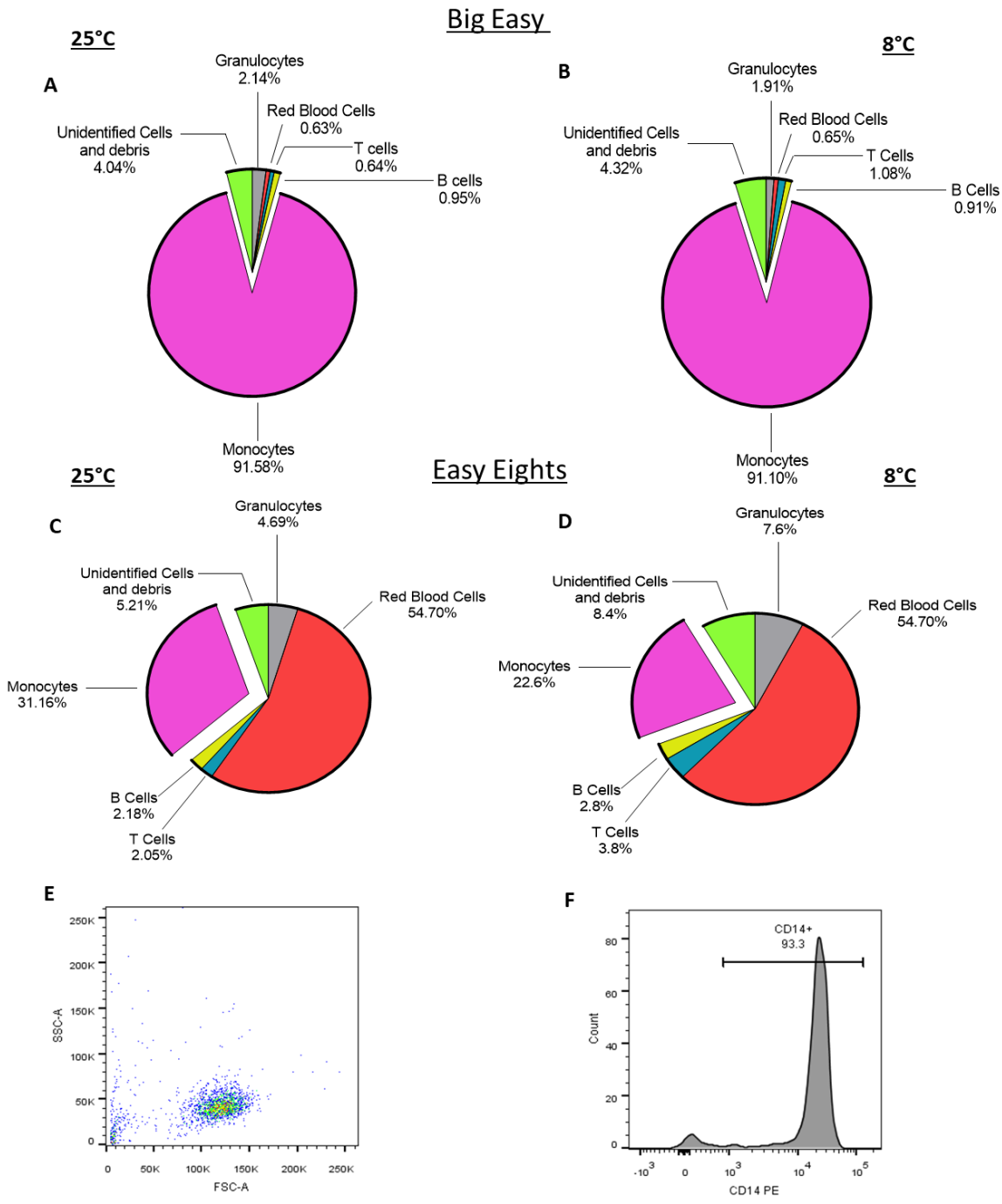

Figure 3.3**: **Purity of enriched monocyte fractions following negative isolation using four different conditions

Monocytes were negatively isolated from whole blood using two different magnets at two temperatures: A) Big Easy™ 25˚C (n=8 biological replicates), B) Big Easy™ 8˚C (n=9 biological replicates), C) Easy Eights™ 25˚C (n=8 biological replicates) D) Easy Eights™ 8˚C (n=8 biological replicates).Purities of the enriched supernatants were determined by flow cytometry, by staining isolated fractions with CD14 (monocytes), CD66b (Granulocytes), CD235a (Red Blood cells), CD4+ (T cells) and CD19 (B cells). Pie charts represent the mean percentage of each cell type, shown as a percentage of a whole. E) Representative FSC vs SSC flow cytometry plots showing the purified monocyte population using the Big Easy™ magnet at 8˚C, along with a representative histogram (F) demonstrating the purified CD14+ population.

Differences in contaminating granulocytes, T cells, B cells and unidentified cells also occurred between isolation conditions, dependent upon the magnet strength, and the temperature at which the isolation was performed. As before, the Easy Eights™ magnet showed a higher percentage of contaminating cells at both incubation temperatures when compared to the Big Easy™ magnet. Within the enriched monocyte fraction, granulocytes formed the largest contaminating population (4.69%±1.45% and 7.65%±2.19%, 25˚C and 8˚C respectively), followed by CD3+ T cells (2.05%±0.73% and 3.84%±2.22%, 25˚C and 8˚C respectively) and B cells (2.18%±0.86% and 2.81%±1.33%, 25˚C and 8˚C respectively).

The Big Easy™ magnet displayed a similar percentage purity of monocytes between the two temperatures; where low contaminations of CD3+ T cells (0.64%±0.17% and 1.08%±0.24%, 25˚C and 8˚C respectively) and CD19+ B cells were observed (0.95%±0.25% and 0.91%±0.26%, 25˚C and 8˚C respectively), with largest identified contaminants being granulocytes as expected (2.14%±0.84% and 1.91%±0.75%, 25˚C and 8˚C respectively).

As the Big Easy™ magnet obtained a higher purity of monocytes in the enriched fraction at both temperatures compared to the Easy Eights™, only this magnet was used in future experiments.

	Big Easy™ 25˚C Mean ± SEM (Range)	**Big Easy™ 8˚C** Mean ± SEM (Range)	**Easy Eights™ 25˚C** Mean ± SEM (Range)	**Easy Eights™ 8˚C** Mean ± SEM (Range)
Monocytes	**91.58%** ± 0.77% (88.45%-95.10%)	**91.10%** ± 0.78% (88.5%-95.55%)	**31.16%** ± 4.61% (17.90%-50.30%)	**22.61%** ± 4.87% (5.30%-38.30%)
Granulocytes	**2.14%** ± 0.84% (0.10%-7.36%)	**1.91%** ± 0.75% (0.69%-7.55%)	**4.69%** ± 1.45% (0.74%-10.30%)	**7.65%** ± 2.19% (1.34%-15.60%)
Red Blood cells	**0.63%** ± 0.20% (0.14%-2.00%)	**0.65%** ± 0.15% (0.20%-1.57%)	**54.70%** ± 8.08% (18.70%-75.30%)	**54.73%** ± 8.63% (18.20%-79.40%)
T cells	**0.64%** ± 0.17% (0.11%-1.27%)	**1.08%** ± 0.24% (0.25%-2.16%)	**2.05%** ± 0.73% (0.29%-5.55%)	**3.84%** ± 2.22% (0.60%-16.90%)
B cells	**0.95%** ± 0.25% (0.26%-2.45%)	**0.91%** ± 0.26% (0.12%-2.52%)	**2.18%** ± 0.86% (0.15%-6.25%)	**2.81%** ± 1.33% (0.23%-10.40%)
Unidentified, Cell debris	**4.04%** ± 1.10% (0.34%-9.95%)	**4.32%** ± 0.79% (0.21%-6.83%)	**5.21%** ± 2.00% (1.12%-15.49%)	**8.36%** ± 2.80% (1.57%-17.14%)

Table 3.4: Cell populations found in isolated fractions under different conditions. Data displayed as mean±SEM (Range)

3.4.2 Negative isolation from whole blood allows the recovery of all three monocyte subsets

The presence of the three monocyte populations was then assessed in the enriched monocyte fraction. As before, monocytes were isolated in parallel using the Big Easy™ magnet at 8˚C and 25˚C from healthy donors and analysed by flow cytometry.

From the results, there was no clear advantage to using the Big Easy™ magnet at either temperature, no significant difference was observed in either monocyte subsets under each condition. Performing the isolation at 8˚C demonstrated an enhanced percentage recovery for both the intermediate and non-classical populations (25˚C: 50.14 % ±9.63% vs 8˚C: 69.57 % ±7.66%, p=0.1404; 25˚C: 35 .14%±8.02% vs 8˚C 53.71 % ± 9.93, p=0.1714 intermediate and non-classical groups respectively) in comparison to 25˚C, however these were not statistically significant (Figure 3.4).

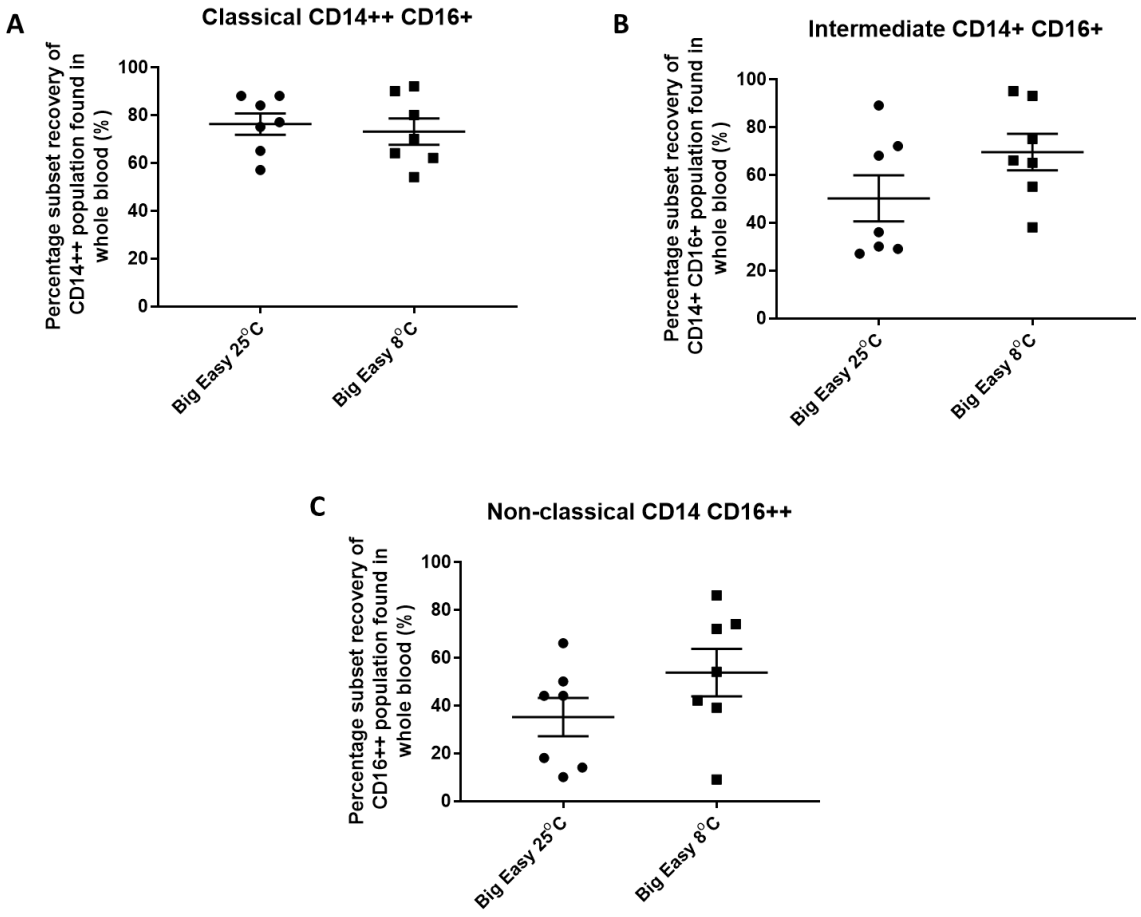

Figure 3.4: Percentage recovery of each monocyte sub-population following isolation using the Big Easy magnet at 25˚C and 8˚C

Subset recovery was determined by flow cytometry analysis following negative isolation from whole blood, using the Big Easy magnet at 25˚C and 8˚C. All three monocyte populations were gated on, following the gating strategy outlined in figure 3.2 for the monocytic population in whole blood, and in isolated fractions. Subset recovery is displayed as the percentage of each subset found in whole blood. Results are indicative of n=7 donors, circles and squares show each individual data point, with bars representing mean ±SEM p=ns, un-paired students t-test.

3.4.3 Isolated monocytes display a low change in CD11b expression

Another important consideration to make when optimising a novel method is to determine if the isolation process induces any non-specific activation, if this occurs the activation may influence downstream functional assays performed using the isolated cells. To investigate this possibility, the expression of CD11b, a marker of leukocyte activation (Macey 1994) was examined in the total monocyte population and individual subsets. CD11b expression at each temperature was determined by flow cytometry. Monocyte isolations and red blood cell lysis were performed in parallel for each sample, thus results are displayed as a change in CD11b expression from monocyte expression in whole blood (figure 3.5).

At each temperature, the change in CD11b median fluorescence intensity (MFI) expression was not statistically different between conditions for the total population and the individual subsets (p=0.4432, p=0.5446, p=0.3318, p=0.2788; Big Easy 8˚C versus 25˚C, total monocyte population, classical, intermediate and non-classical respectively). The non-classical and intermediate subsets demonstrated the largest increase in expression (25˚C: 305.4± 116.5 and 243.5± 30.55; 8˚C: 156.7± 60.17 and 216.9± 93.12, non-classical and intermediate respectively).

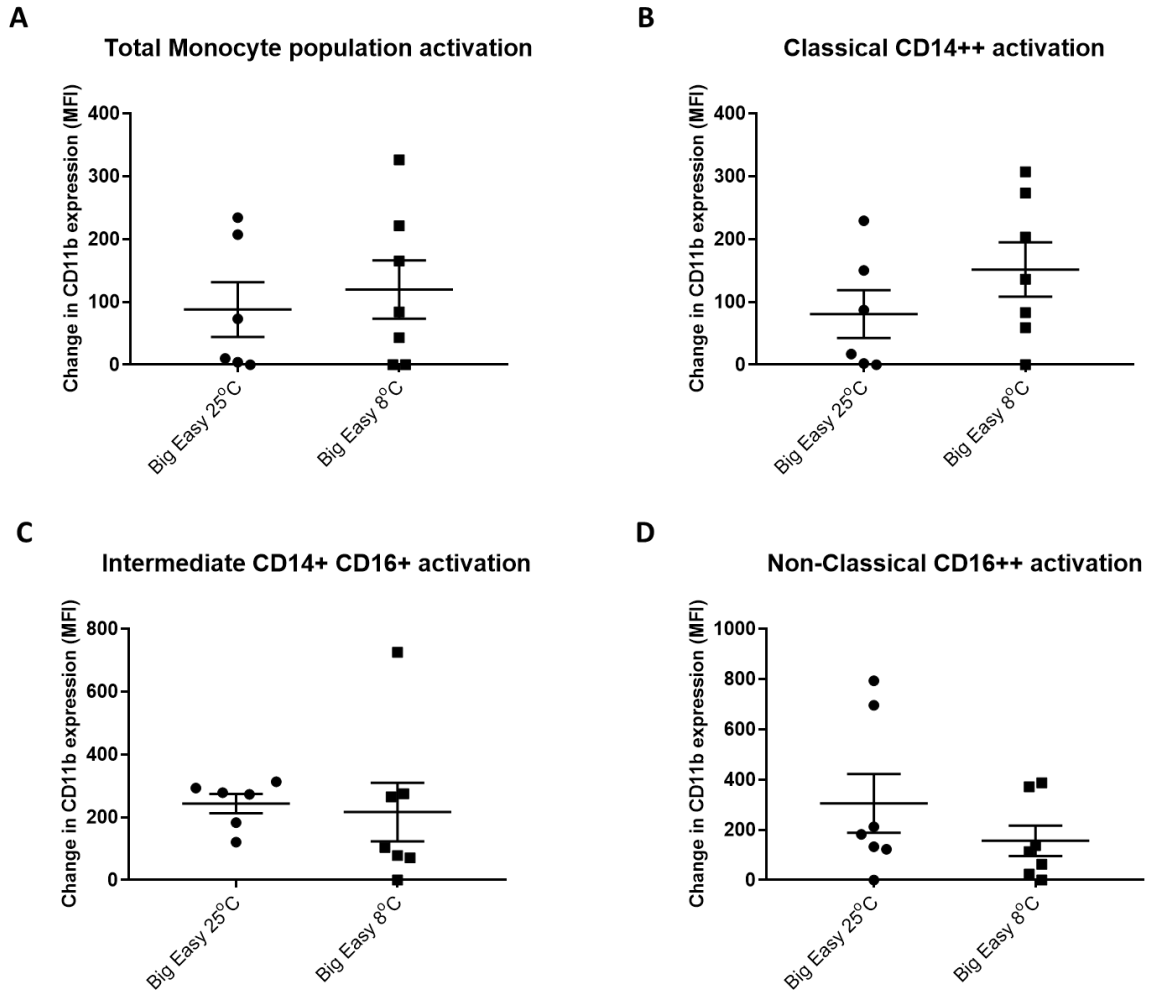

Figure 3.5: Change in CD11b expression on the total monocyte, and sub-populations following isolation using the Big Easy magnet at 25˚C and 8˚C

Levels of monocyte activation was calculated for the total monocyte population and subsets by determining the change in CD11b MFI after isolation compared to whole blood. All three monocyte populations were gated on, following the gating strategy outlined in figure 3.2 for the monocytic population in whole blood, and in isolated fractions. Following this, the MFI of CD11b was calculated for each individual monocyte subset and the total monocytic population in both whole blood and isolated fractions. Results are indicative of n=6 donors at 25°C, and n=7 at 8°C, circles and squares show each individual data point, with bars representing mean ±SEM p=ns un-paired students t-test.

3.4.4 Big Easy isolation at each temperature displayed similar yields

The yield of monocytes in the enriched fraction was calculated following isolation using the Big Easy™ at 8˚C and 25˚C. Performing the isolation at 8˚C resulted in a higher yield of isolated monocytes in the enriched fraction ($2.01x10^5 \pm 1.10x10^4$ /ml of peripheral blood, n=33) when compared to isolation conditions at 25˚C ($1.84x10^5 \pm 2.22x10^4$ /ml of peripheral blood, n=8), however this difference was not statistically significant (*p*=0.21, unpaired *t-test* assuming unequal variances, the sample size for 8˚C is higher than 25˚C due to this being the chosen condition for further experiments beyond these optimisation steps).

With little non-specific activation occurring at each of the temperatures, and little difference between purities, future experiments were carried out using the Big Easy™ magnet at 8˚C, due to its trend towards higher recovery and yield of all three populations.

3.4.5 Monocyte isolation does induce changes in surface marker expression

After isolation procedures had been defined, the extent of alteration in subset distribution and surface marker expression was investigated. Distribution and phenotypic markers in each of the monocyte subsets was examined following monocyte isolation using the Big Easy™ magnet at 8˚C by flow cytometry; surface marker expression was quantified by MFI.

Classical and intermediate populations were not altered significantly in comparison to whole blood (Classical: WB: 87.73%±0.85% vs Isolated monocytes: 90.20%±1.05%, Intermediate: WB: 5.43%±0.69% vs Isolated monocytes: 5.02%±0.09%). However a

significant decrease in the non-classical population was observed (WB: 5.7%±0.28% vs isolated monocytes: 4.56%±0.17%, p=0.0024).

In the classical monocyte population, no statistical differences were seen between whole blood and isolated monocytes in CD14, CD16 and HLA-DR surface marker expression. Intermediate populations showed no significant difference between CD14 and CD16 expression in each of the conditions however, HLA-DR displayed a significant decrease in expression from 25,832±3,729 MFI to 14,049±1,677 MFI in the isolated monocytic fraction (p=0.0163). CD16 expression in the non-classical subset significantly increased from 2,9491±1,928 MFI to 47906±1763 MFI (p<0.0001) however, changes in CD14 and HLA-DR expression remained non-significant (Figure 3.6).

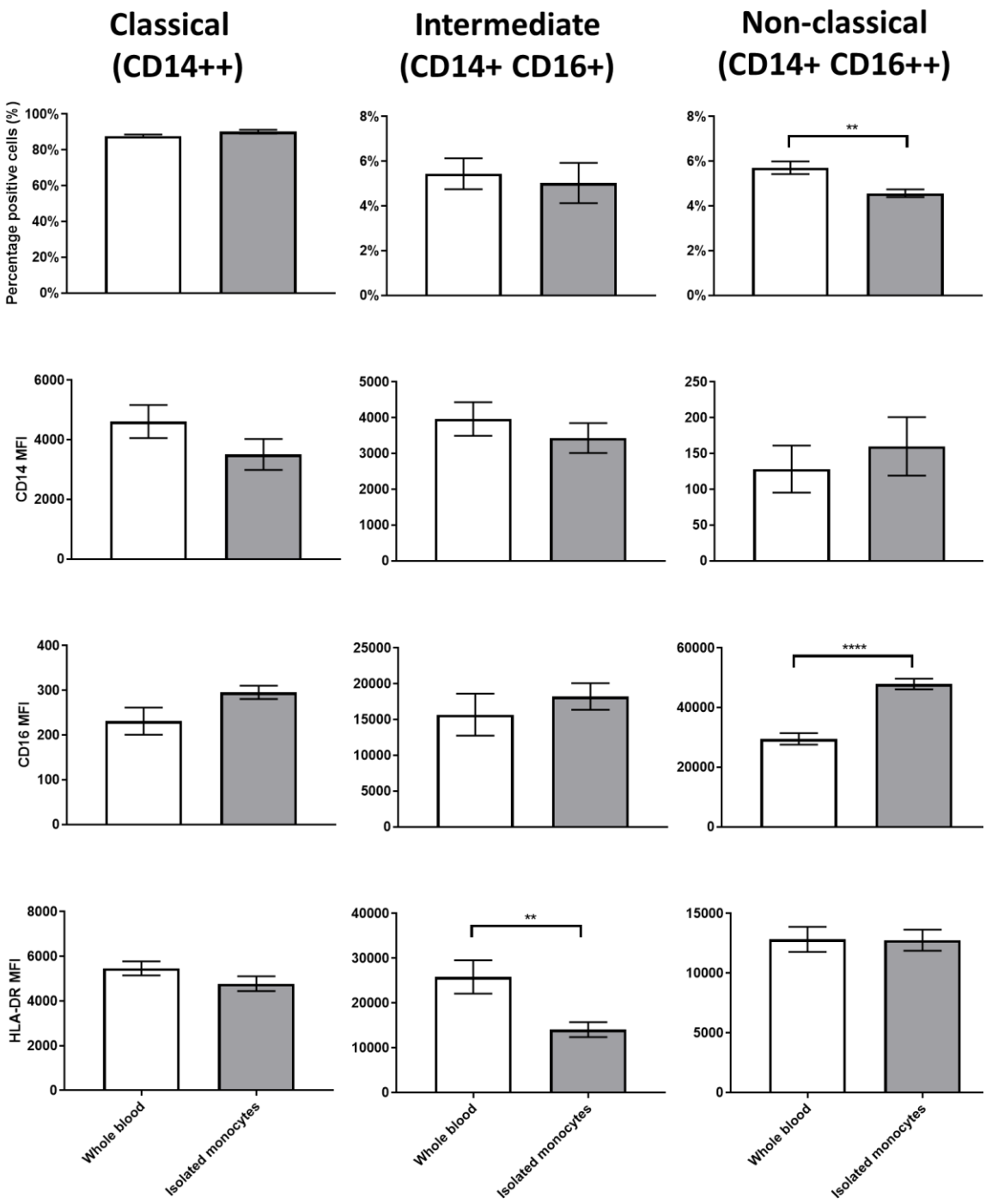

Figure 3.6: Change in monocyte population percentage and CD14, CD16 and HLA-DR surface marker expression on each of the monocyte subsets following red blood cell lysis and isolation

*Percentage and surface marker expression of CD14, CD16 and HLA-DR in each of the monocyte subsets was determined by flow cytometry, of lysed whole blood (n=3 biological replicates) and isolated monocytes using the Big Easy magnet at 8˚C (n=3 biological replicates) in parallel. All three monocyte populations were gated on, following the gating strategy outlined in figure 3.2 for the monocytic population in whole blood, and in isolated fractions. Following this, the MFI of CD14, CD16 and HLA-DR was calculated for each individual monocyte subset and the total monocytic population in both whole blood and isolated fractions. Results are displayed as percentage and median fluorescent intensity (MFI), with error bars representing SEM. Significance was determined using a paired students t-test, ** denotes p<0.05, **** denotes p<0.0001.*

3.4.6 Functionality of isolated monocytes compared to a monocytic cell line

For these experiments, the function of isolated monocytes was compared to a THP-1 cell line, as these cells are accepted as a monocytic model and widely used in literature (Qin, 2012). The following key functions were examined: cytokine secretion, phagocytosis and migration.

3.4.6.1 Isolated monocytes produce cytokines in response to increasing concentrations of Lipopolysaccharide

Human monocytes have to ability to release a number of pro-inflammatory and anti-inflammatory cytokines, which influence disease progression, pathogen engulfment, and adaptive immune regulation. Positive isolation methods have previously demonstrated impairment in cytokine release following LPS stimulation. Therefore, cytokine release was analysed in the isolated monocyte fraction following stimulation with increasing concentrations of LPS.

For each of the cytokines detected, increasing concentrations of LPS failed to induce significant cytokine secretion in THP-1 cells, with IL-1β and IL-6 being below the limit of detection (0.05pg/ml and 0.06pg/ml respectively) (Figure 3.7).

Conversely, in isolated monocytes, secretion was significantly increased following LPS stimulation with each of the cytokines analysed (IL-1β, IL-6, IL-8, IL-10 and TNF-α), which remained statistically significant when compared to controls and THP-1 cells (figure 3.7).

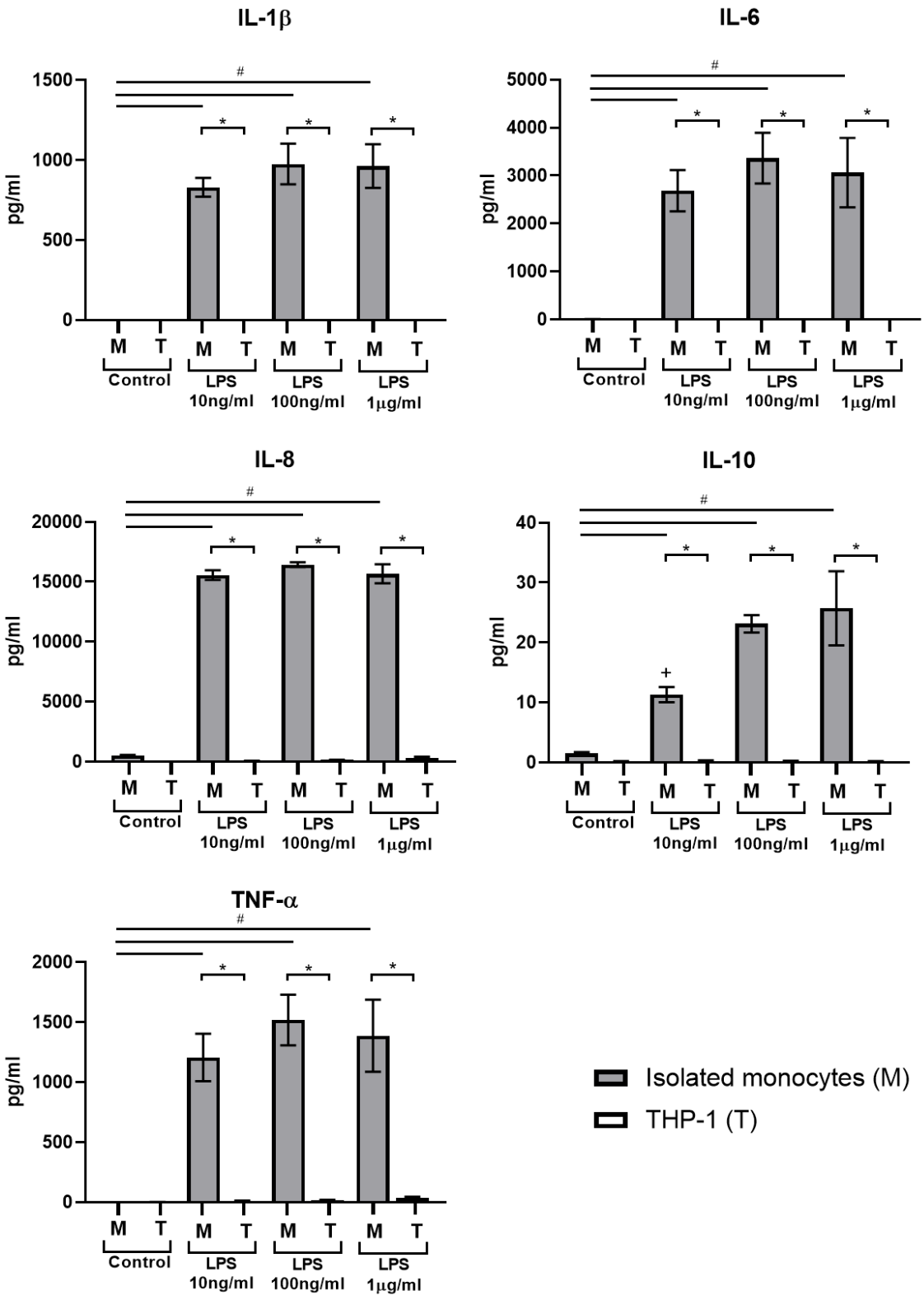

Figure 3.7: Isolated monocytes secrete pro-inflammatory and anti-inflammatory cytokines in response to increasing concentrations of Lipopolysaccharide

*To assess cytokine release, 1x10^5 isolated monocytes (M) using the Big Easy magnet at 8˚C (n=3 biological replicates) and THP-1 cells (T) (n=3 biological replicates) were exposed to increasing concentrations of LPS for 6 hours. Supernatants were collected, and cytokine secretion was analysed by MSD. Results are displayed as the concentration/ml, with error bars representing SEM. Significance was determined by TWO-WAY ANOVA with a Sidak's multiple comparison test, * denotes p<0.0001 Isolated monocytes versus THP-1, # p<0.0001 control monocytes versus stimulated cells, and + p<0.05 LPS 10ng/ml versus 100ng/ml and 1000ng/ml.*

3.4.6.2 Human monocyte phagocytic ability is not impaired after isolation

One of the primary functions of monocytes *in vivo* is the phagocytosis of foreign particles, thus this was investigated in monocytes extracted using this novel method of isolation. Although this assay uses latex beads rather than a pathogen, this is a well-documented model for the study of phagocytosis *in- vitro*, enabling the analysis on a single-cell level and within whole populations (Brabazon et al., 2018; Martinez-Skinner et al., 2013).

The percentage uptake of phagocytosed FITC beads was lower within the primary monocyte population isolated directly from whole blood (figure 3.8), in comparison to unstimulated THP-1 cells (45.43%±2.63% vs 58.27±2.80%; p=<0.05, isolated monocytes and THP-1 cells respectively). With LPS stimulation, phagocytic activity increased in both THP-1 and isolated monocytic populations, however these both failed to reach significance between in comparison to unstimulated cells (54.80%±2.50% versus 45.43%±2.63%; p=0.09 and 58.27±2.80% versus 61.20%±2.46%; p=0.4759, isolated monocytes and THP-1 cells respectively).

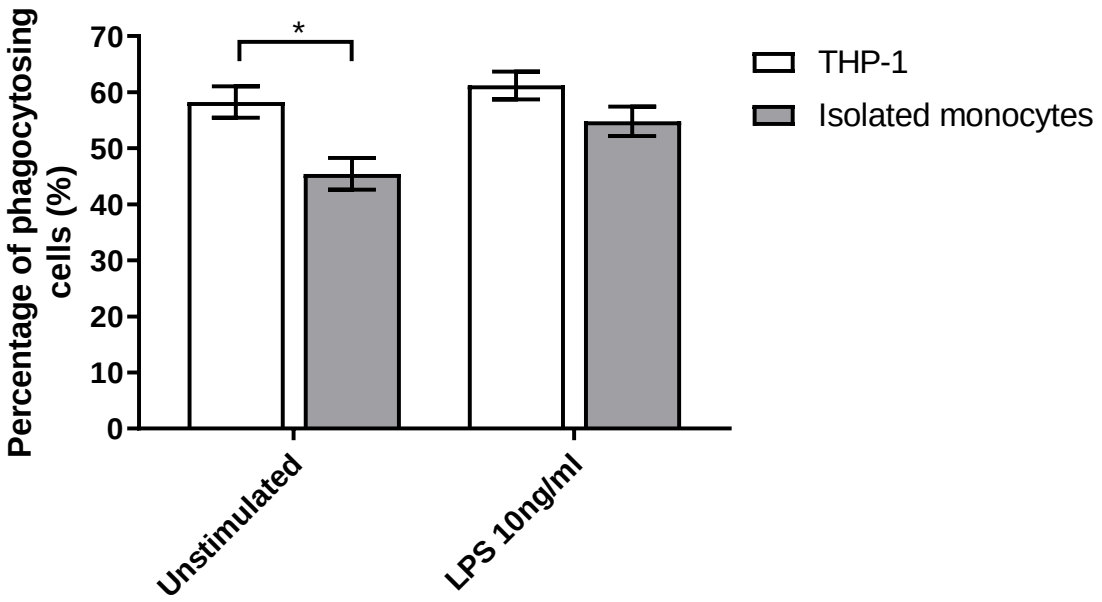

Figure 3.8: The effect of monocyte isolation on phagocytic ability

*Isolated monocytes, using the Big Easy magnet at 8˚C (n=3 biological replicates, grey bars) and THP-1 cells (n=3 biological replicates , white bars) (1x10^5) were either pre-treated with LPS 10ng/ml 4 hours or with media alone, after which FITC IgG latex beads (1:100) were added for 1 hour. After this period monocytes were fixed, and samples were acquired by flow cytometry. Results are displayed as a percentage of phagocytosing cells of the gated parent population (%), with error bars representing SEM. Significance was determined using a students unpaired t-test for comparisons between THP-1 cells and human monocytes, and a paired students t-test to compare unstimulated and LPS treatment conditions. * denotes p<0.05.*

3.4.6.3 Isolated human monocytes migrate towards MCP-1

Another primary function of monocytes *in vivo* is to migrate towards sites of tissue injury and inflammation in response to MCP-1 secreted by a number of cells including endothelial and smooth muscle cells (Cushing et al., 1990).

After the 4 hour incubation period, MCP-1 (5ng/ml) induced migration of isolated monocytes and THP-1 through the micro-porous membrane, in comparison to RPMI-1640 alone. As the concentration of MCP-1 increased, the number of THP-1 cells migrated through the barrier also increased (5ng/ml: 131.92%±55.99%, 15ng/ml: 202.15%±53.27%, 25ng/ml: 227.27%±39.79%, 50ng/ml: 269.02%±28.88%) (Figure 3.9).

In contrast, a greater percentage of monocytes isolated from whole blood migrated towards 5ng/ml MCP-1 compared THP-1 cells (201.64%±15.12% vs 131.92%±55.99%). Following the increase in chemoattractant concentration, the migration percentage remained consistent within the isolated human monocyte population (15ng/ml: 216.42%±30.40%, 25ng/ml: 206.80%±20.06%, 50ng/ml: 222.60%±32.65%) (Figure 3.9). As MCP-1 at a concentration of 5ng/ml induced a significant increase in monocyte migration from the upper to the lower chamber compared to media alone, this concentration of chemoattractant was selected for future migration experiments (See Chapter 4).

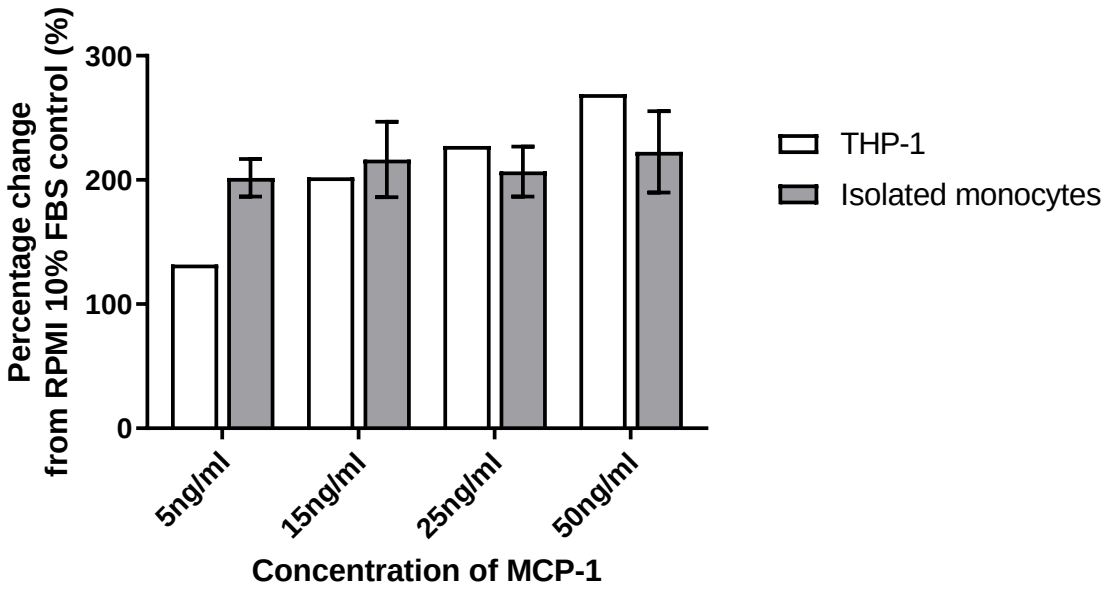

Figure 3.9: The effect of increasing concentrations of MCP-1 on monocyte migration after 4 hours

Isolated monocytes, using the Big Easy magnet at 8˚C (grey bars, n=3 biological replicates) and THP-1 (white bars, n=1) ($5x10^4$) were added to the top chamber of the 5.0µm pore inserts, and left to freely migrate to the lower compartment of the well containing increasing concentrations of Monocyte chemoattractant protein -1 (MCP-1) (5ng/ml, 15ng/ml, 25ng/ml and 50ng/ml) for 4 hours. Images were taken at 5 random fields at 100x magnification, and the number of cells per field were counted. Results are displayed as a percentage change of migrated cells compared to an RPMI 1640 10% FBS control; bars represent the mean percentage change in migrated cells ± SEM. p=ns determined by a ONE-WAY ANOVA with a Tukey's post hoc test.

3.5 Discussion

Monocytes play a key role in several pathogenic diseases, including HIV and CVD, with their subset distribution often shifted to a more pro-inflammatory phenotype in many instances (e.g. an expansion of CD16+ populations). As these cells contribute to the acceleration of disease, it is often desirable to study their function *ex vivo*.

Commercially available isolation procedures either rely on binding to the CD14 receptor (FACS sorting and positive isolation) providing potential impairments in functionality, requires prior PBMC purification that demonstrates alterations in surface marker expression (Mukherjee et al., 2015; Nieto et al., 2012; Tippett et al., 2011), or depletes CD16+ populations (negative selection).

The novel isolation method described here negatively isolates human monocytes directly from whole blood, without the loss of the CD16+ monocytic populations. Initial experiments optimised this isolation method, adjusting magnet strength and temperature to optimise purity, sub-population isolation and extraction of un-activated cells.

The two magnets used in these experiments were the Big Easy™ magnet and the Easy Eights™ magnet manufactured by StemCell™ Technologies; these magnets differ in their magnetic field strength due to their design. The Easy Eights™ magnet has a lower magnetic strength due to a smaller area of the tube in contact with the magnet itself, in comparison to the Big Easy™ in which the tube is inserted directly in the middle of the magnet. The differences observed in the purities of the isolated monocyte fraction between the two magnets is reflective of these variances of the magnetic field, and the

protocol associated with them (e.g. pouring off isolated fractions versus pipetting off the isolated fractions).

The Easy Eights™ isolation resulted in a much lower purity of enriched monocytes, as it was more difficult to remove the purified fraction without disturbing the bound antibody cocktail beads. Purity may be improved with this magnet by performing an additional round of separation, or by isolating monocytes from a smaller volume of blood (<4ml as used in these experiments). The Big Easy™ magnet gave a high purity of isolated monocytes at both temperatures with the largest contaminating population being granulocytes.

To further optimise isolation conditions, the protocols were performed at room temperature (25˚C) and on ice (2-8˚C). These two temperatures were selected, as StemCell's protocols for other isolation kits are optimised to be performed at 25˚C, however it was suggested by StemCell's technical team that carrying out the isolation at 2-8˚C may yield a higher purity and recovery. This lower temperature causes the cell surface to become less fluid, and helps prevents antibody capping; facilitating their capture on the magnet by increasing antibody binding. Indeed, performing the isolation on ice using the Big Easy™ magnet in comparison to room temperature conditions resulted in a higher recovery of all three populations, although these were not found to be statistically significant.

Finally, activation status was determined for each of the cell populations as a way of measuring cell activation, as previously described (Macey et al., 1995). CD11b is an adhesion molecule found on the surface of monocytes, which is upregulated following activation. Previous studies have demonstrated that rapid temperature changes alter

adhesion molecule expression (Forsyth and Levinsky, 1990; Macey et al., 1995) in addition to density centrifugation, and dextran sedimentation (Macey et al., 1995).

These results demonstrated that using colder isolation conditions resulted in lower CD11b surface marker expression in comparison to 25˚C for each of the populations aside from the classical subset however, these also failed to reach statistical significance.

Furthermore, with respect to monocyte yields in the enriched fraction, these did not significantly alter with isolation conditions however, the yield was higher when the isolation was performed on ice. The yields calculated from this enrichment procedure remain consistent with those reported in literature following positive and negative selection ($2.2\pm0.3\times10^5$/ml of peripheral blood; (Zhou et al., 2012)).

Taking all these results into consideration, the Big Easy™ magnet was used at 2-8˚C, as it yielded a higher purity when compared to the Easy Eights™ at both temperatures, and displayed a higher subset recovery, and increased yields when compared to the Big Easy™ magnet at 25˚C.

The type of monocyte isolation method has previously been shown to affect phenotype, cytokine production and phagocytosis of isolated cells (Elkord et al., 2005; Zhou et al., 2012) thus, this functionality was assessed using these optimised isolation conditions.

Monocyte phenotype was analysed by flow cytometry to look for alterations in surface marker expression as a consequence of the isolation procedure. Both the percentage distribution and surface maker expression of CD14, CD16 and HLA-DR on classical monocytes were not significantly altered following extraction compared to whole blood. HLA-DR expression was however decreased within the intermediate subset, whereas a

decrease in the percentage distribution of the non-classical subset and increase in CD16 expression was observed compared to whole blood. These alterations in distribution and surface marker expression are likely to be a phenomenon associated with isolation procedures, previously reported in monocytes (Mukherjee et al., 2015) and other immune cells (Zhou et al., 2012). In addition, changes in temperature or cell culture have been observed to induce the internalisation of chemokine receptors, with monocytes appearing negative (Nieto et al., 2012).

Although this provides a potential disadvantage to this isolation method, it is unlikely that *any* separation procedure prevents alterations in expression due to the sensitive nature of monocytes, therefore an ideal method should induce minimal changes. In each population, the CD14 co-receptor for LPS shows no significant alteration compared to whole blood, thus suggesting that functional responses to LPS would remain.

In addition to phenotypic changes, previous studies have demonstrated that some isolation procedures impair monocyte function therefore, following isolation using this enrichment method, functionality was investigated. For these experiments, isolated monocytes were compared to a monocytic cell line, THP-1 cells. Cytokine secretion upon activation is a primary function of monocytes *in vivo*, therefore this was analysed following the stimulation of monocytes and THP-1 cells with increasing concentrations of LPS. The monocytic cell line showed little cytokine release when challenged with LPS, consistent with previous reports (Schildberger et al., 2013), likely to be attributable to their low CD14 expression as confirmed by flow cytometry (Aldo et al., 2013; Bosshart and Heinzelmann, 2004). On the other hand, enriched monocytes displayed dose-dependent increases of pro and anti-inflammatory cytokine secretion in response to LPS,

thus demonstrating that isolated cells were able to respond to stimulation and thus more relevant monocytic functionality *in vivo*.

Isolated monocytes displayed the ability to phagocytose IgG covered latex beads, which increased following LPS stimulation. In each case however, a lower percentage of uptake was observed compared to THP-1 cells. This decrease in phagocytosis observed may be attributed to contaminating cells in the enriched population, in addition to the heterogeneous monocyte populations, thus is more clinically relevant to functionality *in vivo*. As an alternative to this assay, methods have recently been developed to study phagocytic activity directly in whole blood by flow cytometry (Bicker et al., 2008; Gupta-Wright et al., 2017; Meaney et al., 2016), which provides the advantage of being able to fluorescently detect individual monocyte sub-populations.

A further key function of monocytes *in vivo* is to migrate to sites of inflammation and injury in response to the secretion of chemokines from various cell types. To mimic this *in vitro,* migration was assessed using the transwell chambers as previously described. Both human monocytes and THP-1 cells showed a significant increase in migration towards MCP-1 in comparison to control, at a concentration as low as 5ng/ml. Previous studies have demonstrated an impairment in migration towards MCP-1 and fMLP after Ficoll isolation due to a decrease in the expression of chemokine receptors (Nieto et al., 2012). Data presented in this chapter demonstrates no significant differences between responses to MCP-1 at all concentrations between isolated monocytes and THP-1 cells. In addition, this novel method of isolation does not require PBMC isolation by Ficoll prior to negative selection, therefore avoids these issues. This data therefore provides evidence to suggest that migratory function remains unaltered after purification.

In summary, data presented in this chapter provides optimal isolation conditions to separate monocytes directly from whole blood, with minimal contamination or activation and high percentage subset recovery. In addition, this isolation method yields monocytes competent to perform phagocytosis, migration and to release cytokines while displaying functional responses to LPS.

Our data was compared with the most commonly used monocytic-like cell line to study monocyte function and regulation in the CV system (Qin, 2012). THP-1 cells are an immortalized cell line established from the peripheral blood taken from a paediatric case of acute monocytic leukaemia (Tsuchiya et al., 1980). Although widely used, this homogeneous population displays alterations in gene expression, CD marker expression and chemotaxis, in comparison to positively isolated CD14+ monocytes (Riddy et al., 2018). Therefore the use of primary cells, when possible, provides an advantage over cell lines as marker expression and functionality is maintained. This is particularly relevant when studying monocytes in disease, whereby changes in subset distribution, function and phenotype often occur. This leads to their function being more reflective of that in the *in vivo* setting, and more relevant to study the role of monocytes and their subsets in disease pathogenesis.

Despite this, the value of THP-1 cells as a monocytic model *in vitro* should not be ignored, as these cells are easy to obtain, highly proliferative, and highly uniform, preventing the influence of donor variation and contamination. Furthermore, these cell lines provide an experimental model when primary cells are unobtainable or limited in the case of paediatric populations. Other commercially available isolation methods were

not compared in this study due to their inability to either; isolate all three monocyte populations or the requirement of density separation.

This isolation technique purifies monocytes directly from whole blood with limited interference also avoiding the need for prior PBMC isolation. Although this is preferable and suitable in this case, often other clinical samples may be collected with delay or may come from multiple locations or have already undergone PBMC isolation. Future experiments may be designed to optimise isolation conditions after PBMC purification or investigate the effect of long-term culture on functionality and phenotype of isolated monocytes.

This method provides an advantage over current techniques, as monocytes are not directly targeted in the isolation process, and all three populations are recovered. This optimised isolation procedure can therefore be used to investigate monocytic activity in several disease settings, in which subset distribution may influence function thus, providing a more accurate picture of functionality *in vivo*.

The experimental conditions optimised and validated in this chapter provided the experimental design strategies for the following chapters. Through the isolation of inactivated monocytes that were functionally viable, we could investigate MP influence on monocytic function and phenotype.

Chapter 4 - Monocytic MP generation, characterisation and influence on monocyte function

4.1 Introduction

Monocytes display an activated phenotype in a number of diseases, with the expansion of the pro-inflammatory subset reported in CVD and HIV (Wong et al., 2012). As a consequence of this heightened activation status, elevated (monocyte microparticle) MMP levels have been reported in several disease states (Berezin et al., 2016; Hijmans et al., 2019; Narin et al., 2014; Philippova et al., 2011; Sabatier et al., 2002b). The ability for MMPS to influence monocyte behaviour has been largely unexplored, thus this chapter investigates the potential for these circulating particles to further enhance monocyte activation; and its consequential effects on disease pathogenesis in the context of CVD.

4.1.1 Phenotype and composition of Monocyte MPs

MMPS are released *in vivo* upon cellular activation and apoptosis. *In vitro,* MPs have been derived from human monocytes and monocytic cell lines following treatment with TNFα (Eyre et al., 2011), LPS (Ben-Hadj-Khalifa-Kechiche et al., 2010), Fas ligand (Terrisse et al., 2010), etoposide (Mastronardi et al., 2011) and calcium ionophore (A23187) (Bardelli et al., 2012; Cerri et al., 2006).

Upon formation, the phenotype, protein patterns and composition of MPs are influenced by their mechanism of formation via apoptosis or activation and the type of stimulus (Jimenez et al., 2003; Miguet et al., 2006). Monocytic MPs released from THP-1 cells in response to LPS, soluble P-selectin and IgG stimulation displayed an altered phenotype when compared to spontaneously produced MPs in control conditions

(Bernimoulin et al., 2009; Wen et al., 2014), in addition to an enhanced expression of pro-inflammatory mRNA including IL-8, IL-6 and TNF-α which mirrored a similar increase in the corresponding parent cells (Wen et al., 2014). Furthermore, monocytic MPs have demonstrated the ability to harbour active Tissue Factor (TF) on their surface allowing their participation in the coagulation cascade (Khaspekova et al., 2016).

Moreover, MPs derived from THP-1 cells upon stimulation with soluble P-selectin were found to be approximately 40% PS positive, whereas those derived from LPS stimulation were higher at approximately 60% (Bernimoulin et al., 2009). In addition, proteomic profiling revealed 100 common proteins found in P-Selectin and LPS generate MPs with 408 unique proteins associated with LPS stimulation predominantly comprised of mitochondrial and nuclear proteins, and 52 unique to P-selectin MPs involved in signal transduction and cell communication (Bernimoulin et al., 2009). These differences in composition and receptor expression demonstrate how MPs derived from one cell type under different conditions may have the ability to induce various effects on target cell behaviour.

4.1.2 The influence of monocyte-derived MPs on cellular function

Monocytic MPs have been shown to exert both pro-inflammatory and anti-inflammatory effects on a number of different cell types including endothelial cells, epithelial cells, smooth muscle cells and monocytes (Aharon et al., 2008; Bardelli et al., 2012; Cerri et al., 2006; Essayagh et al., 2007; Neri et al., 2011; Sarkar et al., 2009; Wang et al., 2011).

MMPS induce the expression of the inflammatory cytokines IL-8 and MCP-1 in airway epithelial cells through the induction of NF-κB translocation (Cerri et al., 2006; Neri et al., 2011). Similar effects have been observed in human podocytes whereby a dose-

dependent release of IL-6 and MCP-1 was observed in response to increasing concentrations of MMPS (Eyre et al., 2011). Moreover, the adhesion molecules ICAM-1, VCAM-1 and E-selectin are up-regulated in epithelial and endothelial cells following MMPS treatment (Cerri et al., 2006; Wang et al., 2011; Wen et al., 2014), via ERK1/2 and NF-κB pathways through IL-1 receptor signalling in the latter case (Wang et al., 2011). A mechanism by which these MPs may enhance inflammation is by aiding the recruitment of leukocytes to the endothelium.

Furthermore, MPs have demonstrated the ability to alter target cell phenotype by receptor transfer. Surface marker expression of TF is elevated in endothelial cells in response to prolonged exposure to both apoptotic and LPS stimulated MPs, through MP adherence to the target cell membrane and by directly increasing TF production (Aharon et al., 2008). Furthermore, peripheral blood mononuclear cells display the ability to transfer CCR5 (a co-receptor for HIV entry) to CCR5- monocytes and CD4+ T cells which allowed their infection with M-tropic HIV-1 *in vitro*. This chemokine receptor was further transferred to endothelial cells following the transendothelial migration of PBMCs (Mack et al., 2000), thus providing a possible mechanism through which MPs may play a role in HIV disease progression.

With respect to endothelial function, apoptotic MMPS enhances NO production from endothelial cells (Mastronardi et al., 2011), and induce apoptosis (Aharon et al., 2008). Similar observations were made in co-cultures of vascular smooth muscle cells and supernatants from LPS stimulated monocytes, within which significant cell death was reported (Sarkar et al., 2009).

Finally, the potential autocrine effect of monocytic MPs has also been documented. A23187 derived MPs from THP-1 cells induced pro-inflammatory (IL-6 and TNF-α) cytokine secretion, oxygen radical production, and NF-κB activation in both human monocytes and macrophages, in addition to anti-inflammatory effects through the upregulation of PPARγ protein expression (Bardelli et al., 2012). PPARγ is a protein that can interact with the p65 subunit of NF-κB; preventing its nuclear translocation (Chen et al., 2003).

Anti-inflammatory properties of MMPS have also been reported in a brain endothelial cell line (hCMEC/D3), whereby MMPS treatment reduced endothelial permeability and increased impedance resulting in monolayer tightness and hindrance of leukocyte extravasation (Wen et al., 2014). However, the authors report that the uptake of MMPS by endothelial cells promoted endothelial vascularisation, thus this effect may be attributed to a negative feedback effect of endothelial MPs as a consequence of MMPS treatment rather than the monocytic particles themselves (Wen et al., 2014).

4.2 Aims and Objectives

The aim of this chapter is to investigate the conditions under which MMPS are released, and the functional influence of MMPS on monocytic behaviour *ex vivo* further.

To do this, the following primary objectives were:

1) To assess the impact of different apoptotic and stimulatory treatment conditions on THP-1 cell MP release
2) To determine how the method of MP release influences both parent cell and MP phenotype

Following this, human monocytes were isolated from whole blood using the optimised method, as described in chapter 3, to address the following:

3) To investigate the potential role that these MMPS isolated from THP-1 cells may play in altering monocytic function, using the isolation method previously optimised, by looking at:
    a. Pro-inflammatory cytokine release
    b. Influence on monocyte phenotype
    c. Chemotaxis
    d. Adhesion
    e. Transendothelial migration

4.3 Methods

4.3.1 Cell culture

THP-1 cells, HUVECs, and primary monocytes were isolated and cultured as described in Chapter 2, General methods, Section 2.1.1, 2.1.2 and 2.2.3 respectively.

4.3.2 Phenotyping of cells by flow cytometry

Flow cytometry was used to determine the effect of various treatments on cell phenotype. The staining of both THP-1 cells and isolated monocytes was carried out using the following method. After treatment, cells were washed once in PBS and re-suspended in FACS buffer at a volume of 200µl per antibody panel. Samples were transferred into a 96 well U-bottom plate for staining and spun at 500g for 4 minutes. Fluorescent antibodies were diluted in 50µl FACS buffer at an optimised concentration, added to the cell pellet and incubated in the dark for 30 minutes at 2-8°C. Table 4.1 and 4.2 detail the antibody panels used within this chapter. Details of isotype controls are listed in appendix 2.

THP-1 phenotyping panel					
Target	**Fluorochrome conjugate**	**Clone**	**Isotype**	**Source**	**Dilution**
Panel 1					
CD14	AF700	63D3	IgG1, κ	Biolegend	1:50
CD11b	APC	CBRM1/5	IgG1, κ	Biolegend	1:50
CD142	PE	HTF-1	IgG1, κ	eBioscience	1:25
CD54	FITC	HA58	IgG1, κ	Biolegend	1:50

Table 4.1: THP-1 phenotyping panels

Isolated monocytes phenotyping panel					
Target	**Fluorochrome conjugate**	**Clone**	**Isotype**	**Source**	**Dilution**
Panel 1					
CD14	PE	M5E2	IgG2a, κ	Biolegend	1:50
CD11c	PE-Cy7	3.9	IgG1, κ	Biolegend	1:50
CD11b	APC	CBRM1/5	IgG1, κ	Biolegend	1:50
Panel 2					
CD14	PE	M5E2	IgG2a, κ	Biolegend	1:50
CCR2 (CD192)	PerCp Cy5.5	K036C2	IgG2a, κ	Biolegend	1:50
CD204	APC	7C9C20	IgG2a, κ	Biolegend	1:50
CD36	FITC	CB38	IgM, κ	BD Biosciences	1:50

Table 4.2: Isolated monocytes phenotyping panels

After staining, cells were washed twice in 200µl FACS buffer, and re-suspended in 200µl 1x cell fix (BD Biosciences), covered and left at 2-8°C until flow cytometry acquisition. All samples were acquired on the BD LSRII, with all events recorded for 60 seconds at a medium flow rate. Compensation was applied to samples post-flow cytometry acquisition within the FlowJo software, using latex compensation beads (BD Biosciences) as a control.

4.3.3 MP generation

To investigate the conditions under which MPs are released from monocytes and their influence on monocyte function, THP-1 cells were used to generate MPs using the following conditions. THP-1 cells were used as an alternative to human monocytes in initial experiments, due to their ease of access and highly proliferative nature. This allowed high cell numbers to be subjected to activation or apoptosis conditions to produce large quantities of uniform MMPS populations for phenotyping and functional assessment.

4.3.3.1 Stimulating MPs

To isolate and quantify MPs released under inflammatory conditions, $1x10^6$ THP-1 cells/ml were stimulated with increasing concentrations of LPS (10ng/ml, 50ng/ml, 100ng/ml, 1000ng/ml), TNF-α (10ng/ml, 50ng/ml, 100ng/ml), and IFN-Y (100U/ml, 250U/ml, 500U/ml) for 4 hours in RPMI-1640 cell culture media supplemented with 10% FBS, 2mM L-glutamine, 100U/ml penicillin and 100µg/ml streptomycin. The calcium ionophore A23187, was also used to stimulate MP release from THP-1 cells at various concentrations (2µM, 6µM, 12µM, 18µM, 24µM) as previously described (Bardelli et al., 2012; Cerri et al., 2006; Neri et al., 2011), for 10 minutes in RPMI-1640 cell culture media supplemented with 2mM L-glutamine, 100U/ml penicillin and 100µg/ml streptomycin, without FBS. For all treatments, concentrations above the highest reported induced >5% cell death thus MP release was not evaluated.

Cell cultures were centrifuged at 500g for 5 minutes to remove all cells, with resulting supernatants centrifuged at 1500g for 15 minutes to remove cell debris. Supernatants were stored at -80°C for quantification and phenotyping at a later date.

Although calcium ionophores such as A23187 do not physiologically activate cells and are not found *in vivo*, unlike compounds such as LPS, there is rapid MP release and no potential for endotoxin carryover.

For functional experiments, MPs were generated from THP-1 cells by calcium ionophore stimulation. $2x10^6$ cells/ml were incubated with 12µM for 10 minutes in serum-free RPMI-1640 cell culture media. Cell cultures were centrifuged at 500g for 5 minutes to pellet all cells, and supernatants were centrifuged for a further 15 minutes at 1500g to remove any cell debris. The resulting supernatant was diluted 1:2 in PBS and centrifuged at 20,000g for 45 minutes at 4°C to pellet MPs. The resulting MP pellets were then washed by re-suspending in 1000µl PBS, and centrifuged again at 20,000g for 45 minutes at 4°C. The final MP pellet was stored at -80°C, and quantified by flow cytometry prior to functional experiments.

4.3.3.2 Generating apoptotic MPs

Apoptotic conditions were generated by starvation of THP-1 cells as previously described in the literature (Aharon et al., 2008; Koifman et al., 2017). Briefly, $1x10^6$ THP-1 cells/ml were cultured in RPMI-1640 culture media in serum-free conditions for; 48, 72 and 96 hours, after this time cell cultures were centrifuged at 500g for 5 minutes and cell-free supernatants were collected. These resulting supernatants were centrifuged at 1500g for 15 minutes to remove further cell debris and then stored at -80°C for quantification and phenotyping.

For MP analysis, the collected supernatants were centrifuged at 20,000g for 45 minutes at 4°C to pellet MPs. The final MP pellet was stored at -80°C, Prior to functional

experiments MPs were quantified by flow cytometry along with the cells with the MPs had originated from.

Cells were immediately stained with Annexin V and PI for flow cytometry analysis to determine the percentage of cell death.

4.3.4 Annexin V/PI staining of cells by flow cytometry

In order for cells to be associated with their MP number, apoptotic cells were detected by flow cytometry using a combination of Annexin V and PI staining. As outlined in section 2.4.2, unfixed $1x10^6$ THP-1 cells that had been serum-starved for different time periods (as described previously), were re-suspended in 500µl of 1x Annexin V binding buffer containing 5µl of Annexin V-FITC (1:100 dilution) and incubated at room temperature for 20 minutes in the dark. After this, 50µl of PI (50µg/ml) was added to the sample prior to FACS analysis. All samples were acquired immediately after staining on a BD FACSCalibur at a low flow rate until 10,000 events had been recorded within the monocyte gate.

4.3.4.1 Gating stratergy

Following acquisition, compensation and analysis was performed using FlowJo software. Annexin V was used in conjunction with PI staining in these experiments in order to identify both early and late apoptotic/dead cells from viable cells or those undergoing necrosis. Figure 4.1 demonstrates the gating strategy used, highlighting how these cell types were distinguished.

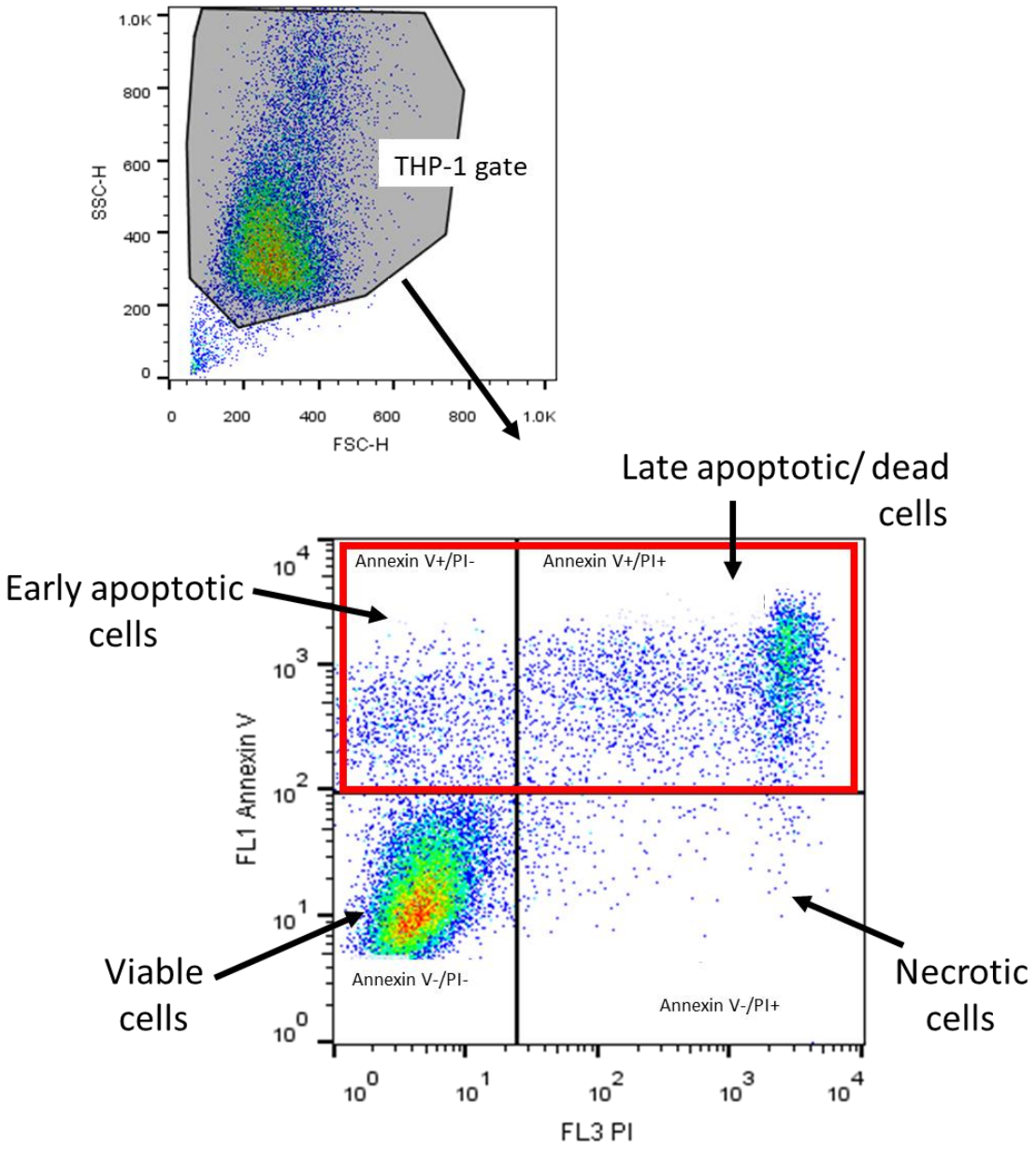

Figure 4.1: Flow cytometry plots demonstrating the gating strategy used to identify apoptotic THP-1 cells following serum starvation

Serum starved THP-1 cells were stained with Annexin v and PI, and analysed by flow cytometry. Following acquisition, the population of THP-1 cells were identified and gated on based on their FSC and SSC. Within this population, a quadrant was used to identify viable cells (Annexin V-/PI-), early apoptotic cells (Annexin V+/PI-), late apoptotic/dead cells (Annexin V+/PI+) and necrotic cells (Annexin V-/PI+) as shown. In order to determine the number of apoptotic cells over the duration of the experiment, the percentage of early apoptotic and late apoptotic/dead cells were combined using the gate highlighted in red.

The aim of this experiment was to determine the number of apoptotic cells, and their relation to apoptotic MP release, thus to determine the number of early apoptotic and late apoptotic cells, the percentage of Annexin V+/PI- and Annexin V+/PI+ were combined as shown in the red box highlighted in figure 4.1. Furthermore, PI was used to ensure that cells were undergoing apoptosis rather than necrosis throughout this experiment, and thus generated MPs were derived from an apoptotic origin.

4.3.5 MP quantification and phenotyping by flow cytometry

MPs were analysed by flow cytometry to determine both their phenotype and number when subjected to certain laboratory conditions. Briefly, as described above, collected supernatants were centrifuged at 17,000g for 60 minutes at 4^{o}C, and MP pellets re-suspended into a volume of 1x Annexin V buffer equivalent to the original starting supernatant volume. 40µl of this suspension was then added to 10µl of each antibody panel (appropriately titrated) for phenotyping or to Annexin V (1:50 dilution) for quantification. Table 4.3 details the specific antibodies used for these experiments.

MP phenotyping panel					
Target	**Fluorochrome conjugate**	**Clone**	**Isotype**	**Source**	**Dilution**
Panel 1					
Annexin V	FITC	-	-	BD Bioscience	1:50
CD14	PE	M5E2	IgG2a, κ	Biolegend	1:50
CD11b	APC	CBRM1/5	IgG1, κ	Biolegend	1:50
Panel 2					
Annexin V	PE	-	-	BD Bioscience	1:50
CD142	APC	HTF-1	IgG1, κ	eBioscience	1:25
CD54	FITC	HA58	IgG1, κ	Biolegend	1:50

Table 4.3: Monocytic MPs phenotyping panels

MPs were incubated in the dark, on a shaker at room temperature for 20 minutes. 150µl of 1x Annexin V binding buffer was added and the sample then stored at 4^{o}C until flow

cytometry acquisition. All samples were acquired on a BD LSRII for 60 seconds on a low flow rate and quantified as previously described in Chapter 2 – General Methods.

MPs released from apoptotic and activated endothelial cells was also investigated, with data presented in Appendix 6 and 7.

4.3.6 Influence of Monocyte MPs on human monocyte function

Following the generation and isolation of MMPS, their influence on cell behaviour was analysed.

4.3.6.1 Stimulation of human monocytes by monocyte-derived MPs

To assess the influence of MMPS on human monocyte functionality and phenotype, MPs derived from A23187 stimulated THP-1 cells were incubated with isolated monocytes at a 1:1, 1:5 and 1:10 ratio (Cells: MPs) for various time periods depending on the assay performed. For each concentration of MPs added to monocytes, a supernatant control was run in parallel to ensure the effects observed were due to the MPs, rather than any residual A2187 in the MP supernatant.

In these functionality experiments to assess the supernatant independently of MPs, the RPMI-1640 cell culture media (10% FBS) was sterile filtered through a 0.22µM filter. The same batch of sterile-filtered media and FBS was used for all experiments and replicates.

4.3.6.2 Influence of Monocyte MPs on human monocyte phenotype

To investigate the influence of MMPS on monocytic surface marker expression, isolated human monocytes were treated with A23187 derived MMPS from THP-1 cells (1:10) for 2, 4 and 24 hours along with the corresponding supernatant control and culture media

alone. After this time, monocytes were centrifuged and stained for phenotyping by flow cytometry as outlined in 4.3.2, using the antibodies listed in Table 4.2.

4.3.6.3 Cytokine release

4.3.6.3.1 IL-6 ELISA

IL-6 cytokine release was quantified in cell culture supernatants by ELISA following 6, 18 and 24-hour incubations with apoptotic and stimulated monocyte-derived MPs. Quantification was performed following the manufacturer's instructions, which are detailed in General methods Chapter 2

4.3.6.3.2 MSD (Mesoscale discovery)

Cytokines were analysed in cell culture supernatants from MP treated monocytes using the V-PLEX Cytokine Panel 1 Human Kit purchased from MSD (mesoscale discovery). This kit quantifies levels of IL-1β, IL-8, IL10, IFN-γ and TNF-α in cell culture supernatants. Samples were analysed according to the manufacturer's instructions, detailed in general methods chapter 2.

4.3.6.4 Chemotaxis

Monocyte chemotaxis was assessed by measuring the migration of cells towards a chemoattractant through a porous transwell membrane. Isolated monocytes were pre-treated with MMPS, MP supernatants or RPMI-1640 for 2 hours. To the top of a 5.0µM polycarbonate transwell (Corning, Fisher, UK) $5x10^4$ monocytes pre-treated with either 1:10 MPs, MP pellet supernatant or media alone were added, with 5ng/ml MCP-1 added to the lower chamber. Transwells were left for 4 hours at 37^oC to allow the free migration of monocytes to the lower chamber. After 4 hours the membrane insert was

removed, and migrated cells were imaged at 100x magnification at 5 random fields using a phase-contrast microscope.

4.3.6.5 Monocyte adhesion to endothelial cells under static conditions

In order to assess the influence of MMPS on the ability of monocytes to adhere to an endothelial monolayer (HUVEC), a static adhesion assay was performed. For this, $5x10^4$ isolated human monocytes were pre-treated with MMPS at a 1:10 ratio (Monocytes: MPs), MP supernatant or LPS 10ng/ml for 4 hours. After this time monocytes were washed in PBS and incubated at 37^oC with HUVECs that had been cultured to confluence; an additional positive control was used whereby endothelial cells were pre-treated with TNF-α 10ng/ml for 24 hours. After 1 hour, non-adherent monocytes were removed by washing three times with warm PBS, and adhered monocytes were stained by Diff-Quick stains (Sigma Aldrich, UK) Images were taken at 200x in three random fields, with only monocytes that had adhered and were associated with an endothelial cells counted. Monocytes were easily distinguished from endothelial cells based on their small darker size and lack of observable cytoplasm as depicted in figure 4.2.

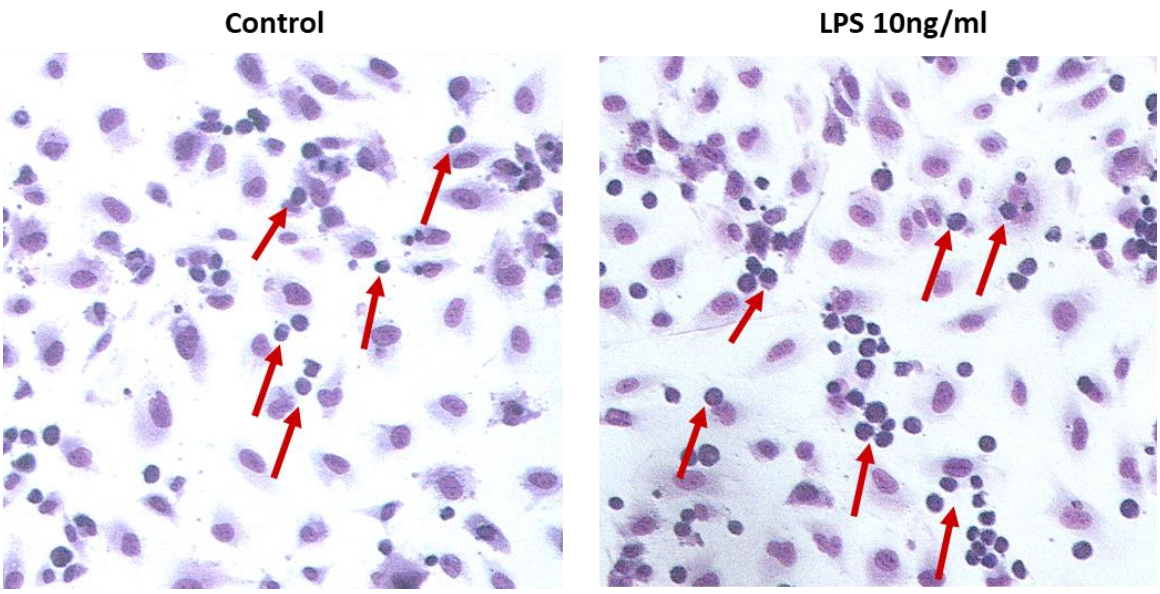

Figure 4.2: Diff-Quick staining of control and LPS pre-treated monocytes to endothelial cells after 1 hour

Adhered monocytes were distinguished from endothelial cells based on their size and morphology as indicated by the red arrows. Images taken at 100x magnification.

4.3.6.6 Transendothelial migration

Migration of monocytes across an endothelial layer was also assessed using transwell membranes coated in a confluent endothelial monolayer. $1x10^4$ HUVECs were seeded onto the upper chamber of a gelatine coated 5.0µM transwell and cultured for 2-3 days to confluence. To ensure a fully confluent monolayer had formed, one insert from the plate was removed and stained with crystal violet. The insert was fixed using 3.7% paraformaldehyde for 10 minutes and washed in PBS. A cotton swab was used to gently remove cells on the lower side of the transwell, and stained with 0.2% crystal violet for 15 minutes, this step ensured that only cells on the upper side of the membrane were stained with crystal violet. Finally, the insert was washed with distilled water 3 times, left to dry and visualised using the phase-contrast microscope. Figure 4.3 shows crystal

violet staining of the endothelial monolayer on the upper side of the transwell after 24 and 72 hours after which a confluent monolayer had formed.

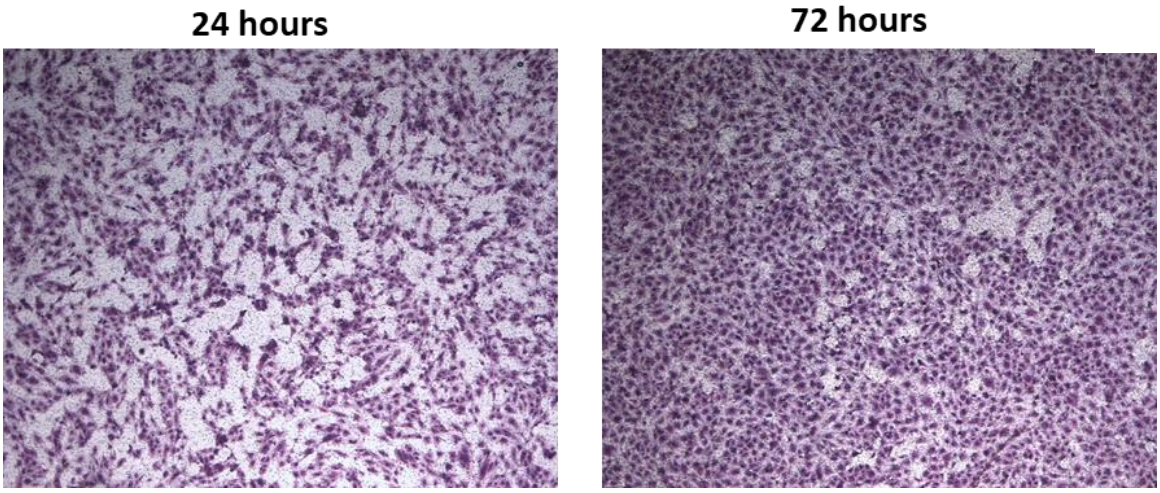

Figure 4.3: Crystal violet staining of an endothelial monolayer, cultured on the upper side of 0.2% gelatine coated Transwell inserts after 24 and 72 hours.

Following the confirmation of a fully confluent monolayer using this method, 5x 10^4 Monocytes pre-treated for 4 hours with either MMPS or MP supernatants were added to the top chamber (200µl), with the 5ng/ml MCP-1 chemoattractant added to the lower chamber (700µl). Monocytes were left to migrate through the endothelial monolayer to the lower chamber for 4 hours, and migrated cells were imaged at 100x magnification at 5 random fields using an inverted phase-contrast light microscope (Lecia, UK).

4.4 Results

4.4.1 Apoptotic MPs are released from monocytic cells in serum starvation conditions

MPs are released from both activated cells and apoptotic cells. Experiments were initially performed to discover the optimal time for apoptotic MP generation from serum-starved THP-1 monocytes for 48-96 hours, as previously described (Aharon et al., 2008; Koifman et al., 2017).

THP-1 cells undergoing apoptosis generated a significantly increased number of monocytic MPs at 72 (p=0.012) and 96 hours (p=0.0001) than when compared to quiescent cells under control conditions (0% FBS 1,031,157±128,117; 10% FBS 508,784±129,017; 0% FBS 1,442,677±41,564 vs 10% FBS 535,276±99,862, mean MP number ± SEM at 72 and 96 hours respectively) (Figure 4.4A).

At each time point, the numbers of apoptotic derived MPs correlated with the number of apoptotic THP-1 cells as determined by Annexin V and PI staining (p=0.0134, R^2= 0.3254, Pearson R value = 0.574) (Figure 4.4B).

From these experiments the 72 hour time point was selected as the optimum for apoptotic MP generation as this provided the earliest significant increase in MPs released compared to control, thus was used for further experiments.

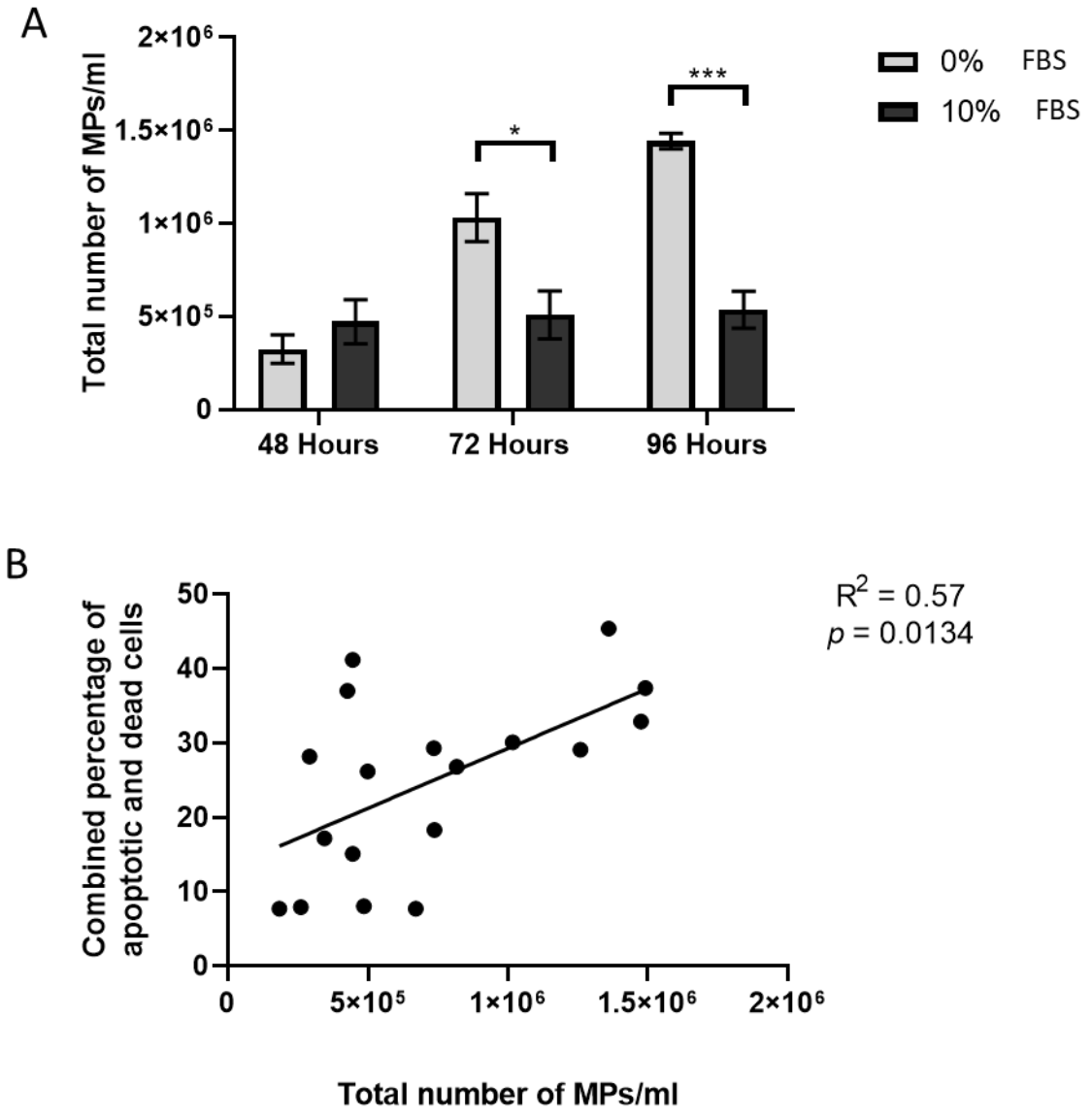

Figure 4.4: THP-1 cells release MPs in serum-starvation conditions

*1x10⁶ THP-1 cells/ml were cultured in RPMI-1640 in either 10% FBS (n=3 biological replicates, black bars) or serum free conditions (n=3 biological replicates, grey bars) for 48, 72 and 96 hours. Annexin V+ MPs (<1µm) were enumerated by flow cytometry (A). A positive association was found between the number of MPs/ml and the combined percentage of early apoptotic and late apoptotic/dead cells (Annexin V+/PI- and Annexin V+/PI+) (B), Pearson's correlation coefficient R=0.57, p=0.0134. Data is displayed as mean ±SEM, with differences assessed by TWO-WAY ANOVA, with a Sidak's post hoc test * p<0.05, *** p<0.001.*

4.4.2 THP-1 cells release different quantities of MPs following activation with different stimuli

In addition to apoptosis, THP-1 cells were also challenged with 4 different types of inflammatory stimuli at incremental concentrations to measure the responses of monocytes to produce MPs and to see if they varied from apoptotic stimuli. These experiments would also allow validation of the concentration of calcium ionophore A23187 and LPS to use in phenotyping and functional experiments.

MPs were derived from THP-1 cells challenged with increasing concentrations of A23187, LPS, TNF-α and IFN-γ. THP-1 cells stimulated with the calcium ionophore A23187 released MPs in a dose-dependent manner, however quantitatively these were only statistically significant with concentrations above 12μM (12μM 760,641±101,244 vs control 373,569±78,342 p= 0.039; 18μM 859,231±121,630 vs control 373,569±78,342 p=0.028; 24μM 975,905±121,391 vs control 373,569±78,342 p=0.0062) (Figure 4.5).

A similar trend was observed with LPS stimulation, whereby all concentrations of LPS were able to induce an increase in MP number compared to control conditions, however only concentrations above 50ng/ml generated a statistical increase in MPs compared to control (50ng 3,125,579±225,704 vs control 1,239,750±174,928 p=0.0027; 100ng/ml 4,050,800±471,309 vs control 1,239,750±174,928 p=0.005; 1000ng/ml 5,962,358±1,194,487 vs control 1,239,750±174,928 p=0.0051) (Figure 4.5).

Stimulation with TNF-α also induced MP release however, a higher concentration was required to significantly increase MP number to control in comparison to LPS (100ng/ml 3,734,767±874,736 vs control 1,239,750±174,928 p=0.049).

The number of MPs released from THP-1 cells challenged with IFN-γ also increased with stimulus concentration, reaching a plateau at 250 units/ml, whereby MP release became significant compared with control (250 units/ml 3,330,463±344,217 vs control 1,239,750±174,928 *p*=0.0056; 500 units/ml 3,691,858±213,277 vs control 1,239,750±174,928 *p*=0.0009) (figure 4.5).

From these dose-response experiments, A23187 at 12µM and LPS at 100ng/ml were used in further experiments, as these concentrations both elicited an MP release within the EC_{70}-EC_{80} (Effective concentration) range, and also as previously described (Bardelli et al., 2012; Cerri et al., 2006; Wen et al., 2014) (See Appendix 4 and 5).

Neither TNF-α or IFN- γ were chosen as an activating stimulus in any experiments beyond this point as these were both analysed in cytokine secretion experiments described in section 4.4.4.

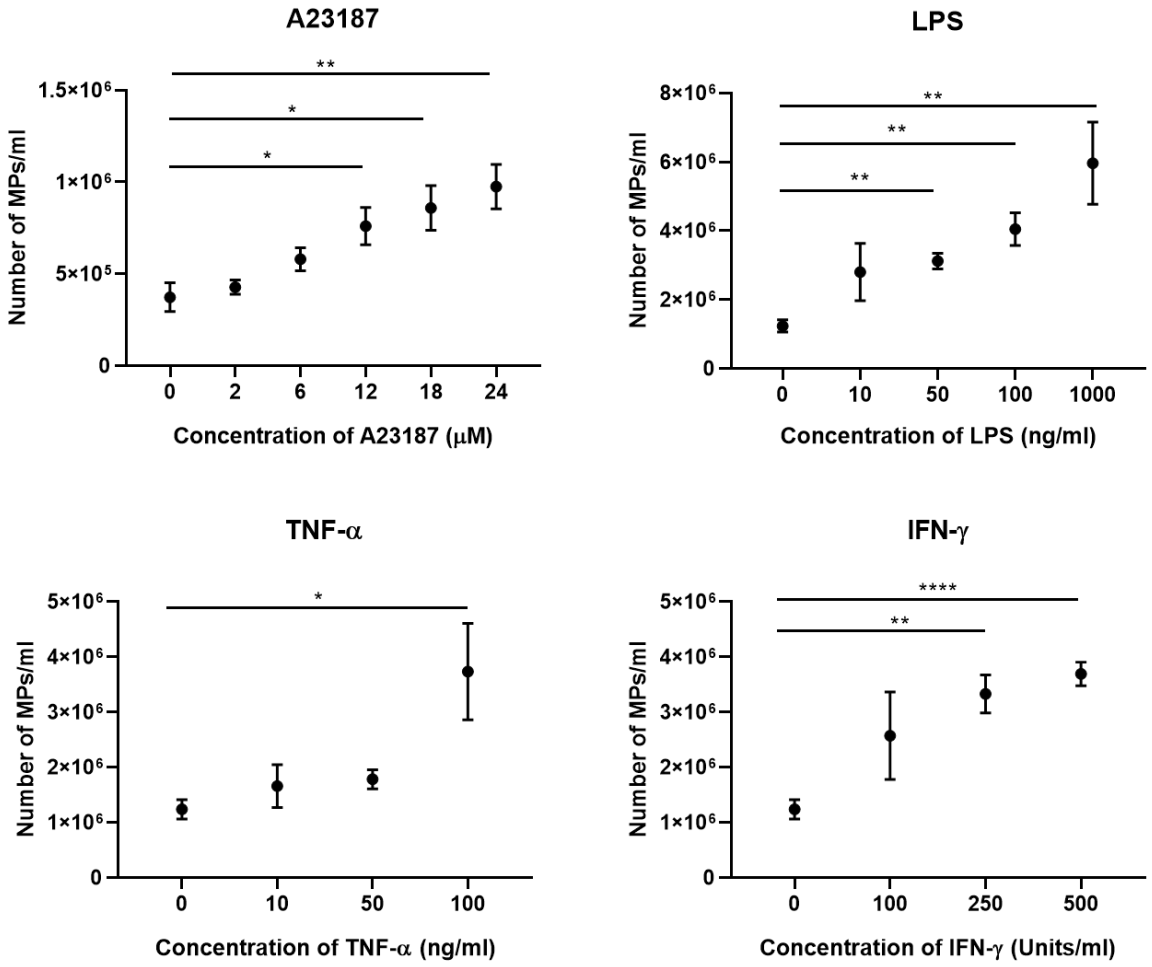

Figure 4.5: THP-1 cells release quantitatively different MPs following stimulation

*1x10^6 THP-1 cells/ml challenged with increasing concentrations of LPS (n=3 biological replicates), TNF-α (n=3 biological replicates) and IFN-γ (n=3 biological replicates) for 4 hours or 10 minutes for A23187 stimulation (n=3 biological replicates) in accordance with literature (Cerri., et al 2006, Neri., et al 2011, Bardelli., et al 2011). Annexin V+ MPs (<1μm) were enumerated by flow cytometry, with data displayed as mean ±SEM. Differences for each treatment determined by ONE-WAY ANOVA, with a Tukey's post hoc test * p<0.05, ** p<0.01, *** p<0.001, **** p<0.0001.*

4.4.3 THP-1 cells release phenotypically different MPs depending on treatment conditions

To determine if MMPS from apoptotic cells displayed distinct phenotypes from activated cells, MMPS were derived from THP-1 cells following treatment with either; LPS, A23187 or serum starvation. The phenotypes of these MPs (defined by their size <1µm and expression of Annexin V) and their relation to parent cell marker expression were characterised by surface antigen presentation measured by flow cytometry (data presented in table 4.4 and figure 4.6).

Stimulation by; LPS, calcium ionophore, and starvation conditions did not influence the expression of CD142 and CD11b in both THP-1 cells and their derived MPs (Table 4.4).

A significant increase in CD14 expression was only observed after treatment with LPS when compared with A23187 (33.76%±2.26% vs 17.87%±0.44% p=0.0063) however, LPS CD14 expression was not significantly altered with any other treatment. In contrast, CD14 expression on MMPS was not significantly upregulated in any experimental condition (Figure 4.6).

LPS stimulation and starvation conditions were also able to significantly upregulate percentage CD54 antigen expression on monocytes when compared to control and A23187 stimulation (for LPS stimulation 67%±1.76% vs control 9.7%±0.36% p<0.0001, 67%±1.76% vs A23187 14.28%±0.68% p<0.0001 and 67%±1.76% vs starvation 28.27%±7.93% p<0.0001. For Starvation 28.27%±7.93% vs control 9.7%±0.36% p=0.0013, 28.27%±7.93% vs A23187 14.28%±0.68% p=0.019). This upregulation was also observed in the resulting MMPS population from apoptotic and LPS derived MMPS (for LPS stimulation 28.7%±0.90% vs control 12.98%±2.37% p<0.0001, for A23187

21.83%±1.22% vs control 12.98%±2.37% p=0.007. For starvation 29.03%±1.91% vs control 12.98%±2.37% p<0.0001, 29.03%±1.91% vs A23187 21.83%±1.22% p=0.03).

Percentage expression THP-1 cells					
CD Marker	**Control (RPMI 1640)**	**Serum starved**	**LPS 100ng/ml**	**A23187 12µM**	**Sig. between groups**
CD142	2.05%±1.23%	3.42%±0.97%	3.9%±0.35%	0.57%±0.12%	ns
CD11b	1.52%±0.06%	2.81%±1.18%	4.81%±0.36%	2.18%±0.12%	ns
Percentage expression MPs					
CD142	8.50%±0.35%	9.23%±0.20%	12.05%±0.57%	8.29%±0.50%	ns
CD11b	13.9%±0.21%	14.20%±0.17%	15.47%±1.40%	13.9%±0.91%	ns

Table 4.4: Percentage expression of CD142 and CD11b on THP-1 cells and their corresponding MPs following stimulation with; LPS and A23187 or by starvation. *ns= non-significant between groups.*

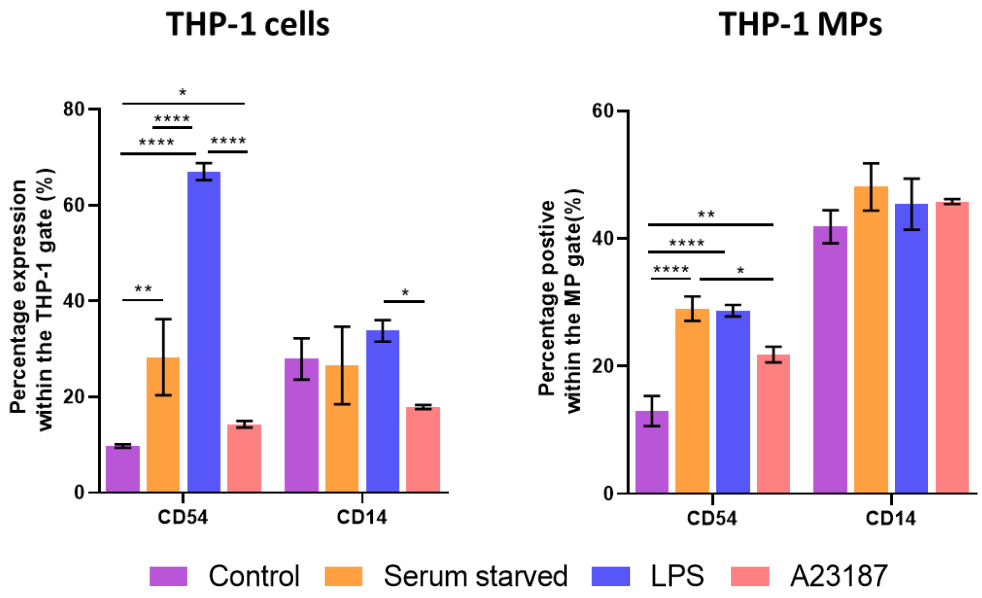

Figure 4.6: Serum starved and activated THP-1 cells release MPs with different CD marker profiles (percentage positive) depending upon the type of stimulus

*1x10^6 THP-1 cells/ml were challenged with either: 12µM A23187 (n=3 biological replicates, pink bars), 100ng/ml LPS (n=3 biological replicates, blue bars), starved of serum for 72 hours (n=3 biological replicates, orange bars) or serum (control) conditions 10% FBS (n=3 biological replicates, purple bars). Percentage expression of the surface markers FITC-CD54 and PE-CD14 was measured on parent cells and Annexin V+ MPs (<1µm) by flow cytometry. Data is displayed as mean percentage expression within the monocytic or Annexin V+ MP gate ±SEM. Differences for each treatment determined by a ONE-WAY ANOVA, with a Tukey's post hoc test. * p<0.05, ** p<0.01, *** p<0.001, ****

A similar trend was observed when comparing the mean fluorescence intensity of surface antigens on THP-1 cells and the MPs they released (defined by their size <1µm and expression of Annexin V). Stimulation by; LPS, calcium ionophore, and starvation conditions did not influence the expression of CD142, CD14 and CD11b in both THP-1 cells and their derived MPs (data presented in table 4.5 and figure 4.7).

MFI THP-1 cells					
CD Marker	**Control (RPMI 1640)**	**Serum starved**	**LPS 100ng/ml**	**A23187 12µM**	**Sig. between groups**
CD142	901±61	973±39	1,057±155	941±55	ns
CD11b	842±10	786±33	864±31	746±93	ns
CD14	429±29	594±68	500±36	651±16	ns
MFI expression MPs					
CD142	365±7	365±9.64	355±1.33	353±2.8	ns
CD11b	789±4	802±7	804±16	789±9	ns
CD14	813±17	908±37	837±43	830±7	ns

Table 4.5: MFI of CD142, CD14 and CD11b on THP-1 cells and their corresponding MPs following stimulation with; LPS and A23187 or by starvation. *ns= non-significant between groups.*

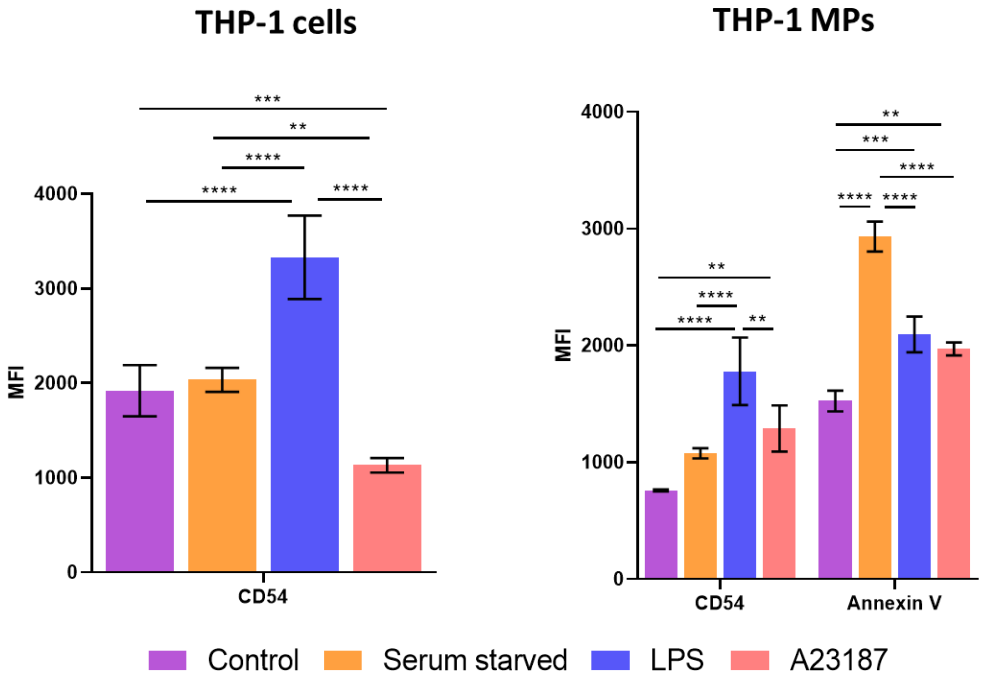

Figure 4.7: Serum starved and activated THP-1 cells release phenotypically different MPs depending upon type of stimulus

*1x10^6 THP-1 cells/ml were challenged with 12µM A23187 (n=3 biological replicates, pink bars), 100ng/ml LPS (n=3 biological replicates, blue bars), serum starved for 72 hours (n=3 biological replicates, orange bars) or control conditions 10% FBS (n=3 biological replicates, purple bars). Surface marker expression was characterised on both parent cells and Annexin V+ MPs (<1µm) by flow cytometry by staining with FITC-CD54. Data is displayed as mean MFI within the monocytic or Annexin V+ MP gate ±SEM. Differences for each treatment determined by a ONE WAY-ANOVA with a Tukey's post hoc test. * p<0.05, ** p<0.01, *** p<0.001, **** p<0.0001.*

With respect to CD54 MFI, only 100ng/ml LPS stimulation for 4 hours was able to significantly upregulate surface antigen expression (3,330±441 vs control 1,920±271 $p<0.0001$, 3,330±441 vs A23187 1,131±76 $p<0.0001$ and 3,330±441 vs starvation 2,034±126 $p<0.0001$) (Figure 4.7), which was also mirrored in the MPs derived from these cells (LPS 1,779±288 vs control 759±7 $p<0.0001$, LPS 1,779±288 vs A23187 1,290±198 $p=0.0041$ and LPS 1,779±288 vs starvation 1,078±44 $p<0.0001$). CD54 expression on cells was downregulated with calcium ionophore treatment when compared to control, starvation and LPS (1,131±76 vs control 1,920±271 $p=0.003$, 1,131±76 vs starvation 2,034±126 $p=0.0007$ and 1,131±76 vs LPS 3,330±441 $p<0.0001$) however, an upregulation of this CD54 antigen on the MP surface was observed following A23187 when compared to control (1,290±198 vs control 759±7 $p=0.0097$).

The expression of PS was also quantified by MFI on the surface of MPs generated under each of the treatment conditions. Apoptotic MPs expressed the highest amount of PS on their surface which was significantly increased when compared with control, LPS and A23187 derived MPs (2,932±129 vs control 1,524±88 $p<0.0001$, 2932±129 vs LPS 2,096±153 $p<0.0001$ and 2,932±129 vs A23187 1,971±55 $p<0.0001$). Furthermore, LPS and A23187 treatment also increased MP PS surface expression when compared to control (LPS 2,096±153 vs control 1,524±88 $p=0.0007$ and A23187 1,971±55 vs control 1,524±88 $p=0.009$).

4.4.4 Monocytic MPs induce the release of pro-inflammatory cytokines from isolated human monocytes

Following the validation of MP release from THP-1 cells, MMPS were cultured with human monocytes isolated using the methodology outlined in the previous chapter. For these experiments, MMPS were derived from THP-1 cells due to their highly proliferative nature allowing the generation of large quantities of MPs to be used in multiple functional assays. IL-6 was chosen as a marker for monocyte activation as previously described (Schildberger et al., 2013), thus its secretion following MMPS treatment from human monocytes was first analysed. Monocytes were challenged with increasing concentrations of MMPS, derived from A32187 stimulated THP-1 cells, or from the corresponding MP supernatant concentration with cytokine secretion measured at 6, 18 and 24 hours (figure 4.8).

Although LPS generated MPs provide the most biologically relevant model of MP release, A23187 stimulation was chosen as the preferred method, as endotoxin was detectable in the MP pellet despite thorough washing cycles; determined by a positive pierce LAL assay result.

Increases in IL-6 secretion with the highest MP concentration when compared to the corresponding supernatant controls were statistically significant (18 hours: 1:10 MP 67pg/ml±28 vs supernatant 1:10 1.98pg/ml±0.82 $p<0.0001$; 24 hours: 1:10 MP 98.48pg/ml±19.99 vs supernatant 1:10 9.46pg/ml±1.40 $p<0.0001$), demonstrating that these effects were attributable to the MPs themselves rather than small molecules or contaminating A23187 carried over in the MP supernatant.

IL-6 release from isolated monocytes was only significantly increased after 18 and 24 hours of treatment with the highest concentration of MMPS at a ratio of 1:10 (Cell: MPs). (Figure 4.8). This increase in IL-6 secretion was significant when compared to control, and increasing concentrations of MPs at 1:1 and 1:5 at both 18 and 24 hours.

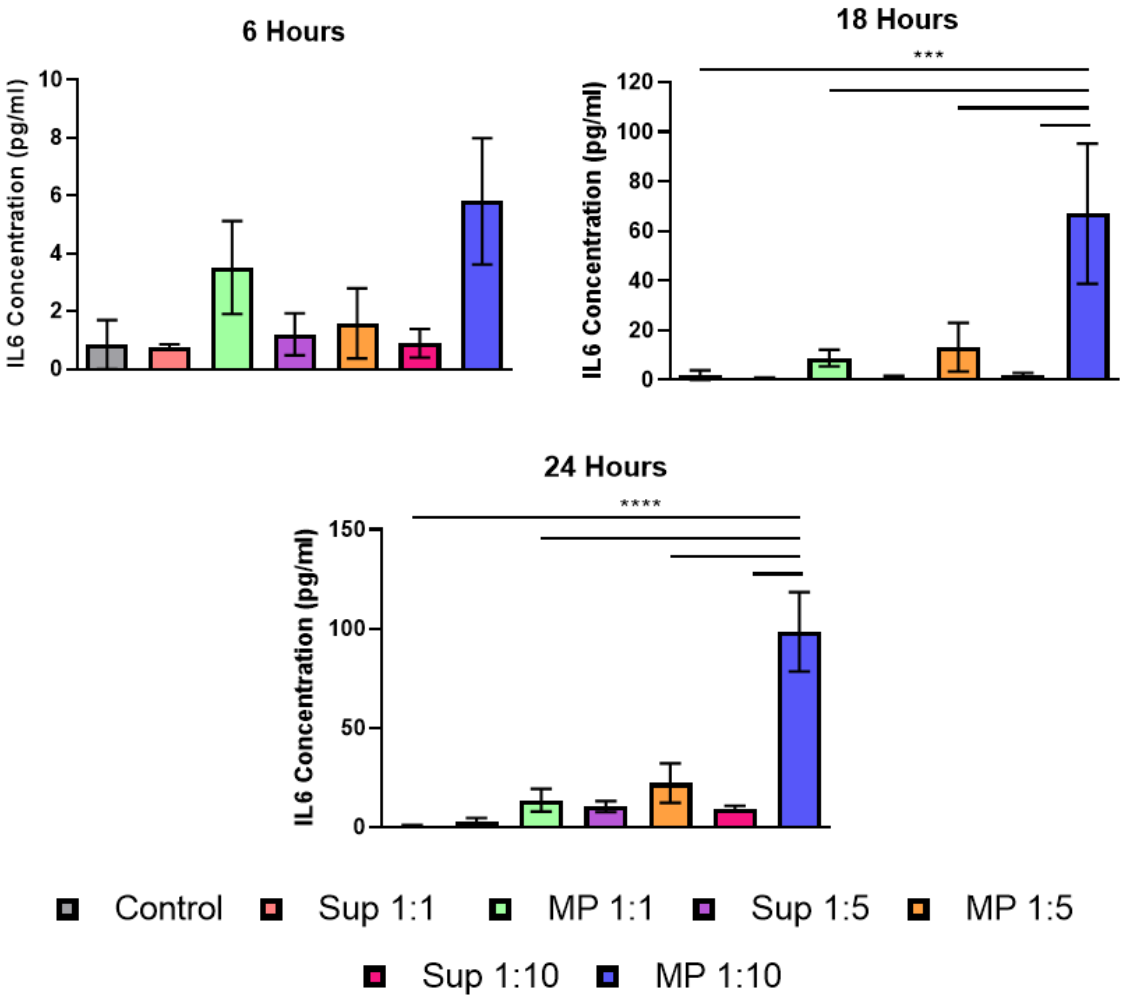

Figure 4.8: Monocytic MPs induce the secretion of IL-6 from isolated human monocytes

*IL-6 secretion from 2x10^4 Human monocytes (n=3 biological replicates) was analysed by ELISA following the treatment with increasing concentrations of MMPS (1:1, 1:5, 1:10) and the corresponding supernatant controls (1:1, 1:5, 1:10) for 6,18 and 24 hours. Data is displayed as mean cytokine secretion ±SEM. Differences for each treatment determined by a ONE-WAY ANOVA, with a Tukey's post hoc test. *** p<0.001, **** p<0.0001.*

In order to investigate the influence of MMPS on the release of other monocytic cytokines (IL-1β, IL-8, IL-10, IFN-γ and TNF-α), 24 hours was selected as the optimum time point (Figure 4.9).

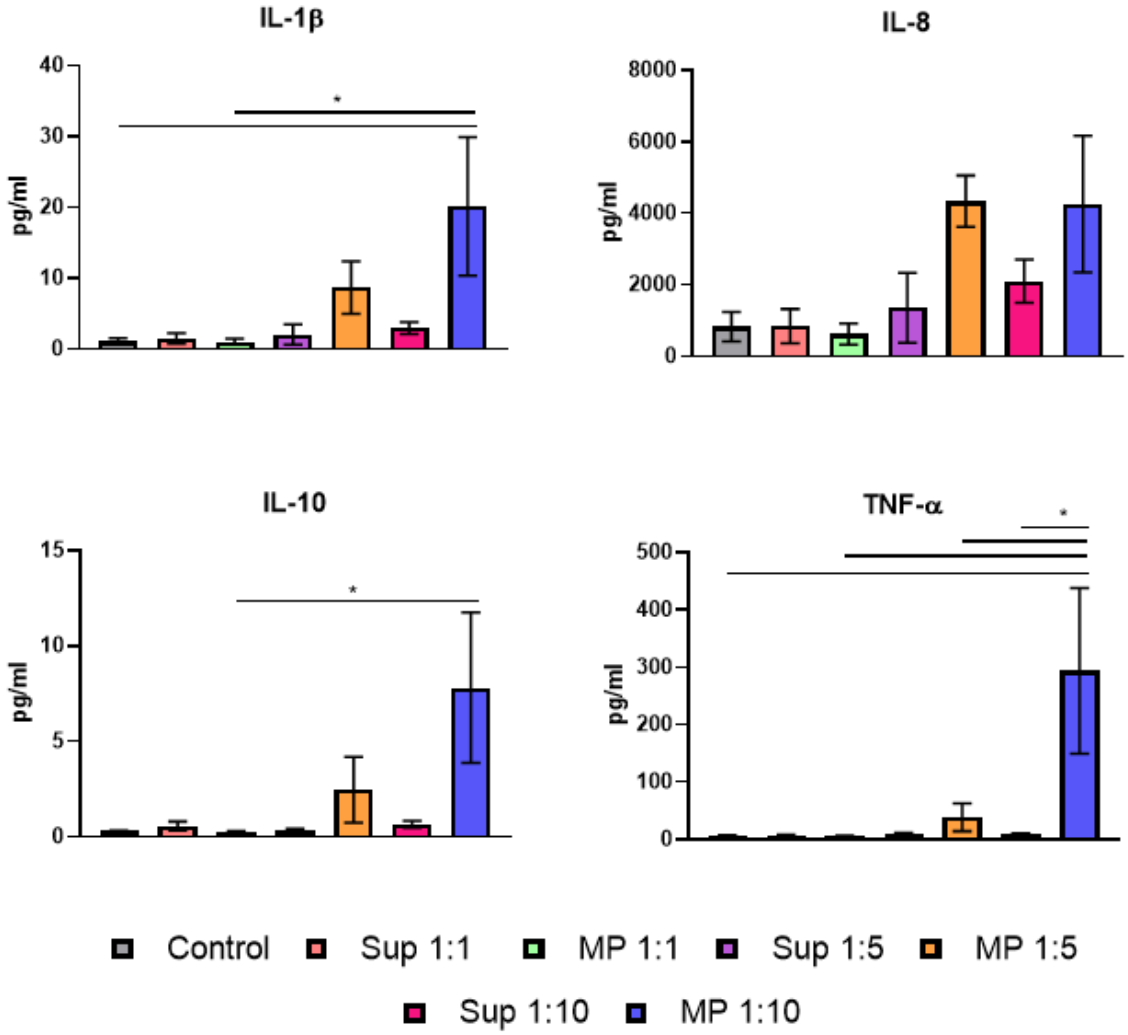

Figure 4.9: Monocytic MPs induce the secretion of TNF-α from isolated human monocytes

*IL-1β, IL-8, IL-10 and TNF-α secretion from 2x10^4 Human monocytes (n=3 biological replicates) was analysed by MSD following the treatment with increasing concentrations of MMPS (1:1, 1:5, 1:10) and the corresponding supernatant controls (1:1, 1:5, 1:10) for 24 hours. Data is displayed as mean cytokine secretion ±SEM. Differences for each treatment determined by a ONE WAY-ANOVA, with a Tukey's post hoc test. * denotes significance at p<0.05*

Monocyte derived MPs significantly increased IL-1β cytokine secretion from human monocytes at the highest concentration (1:10) when compared with control conditions (MMPS 20.13pg/ml±9.74pg/ml; control 1.12pg/ml±0.41pg/ml, p=0.0447) and MMPS at

the lowest concentration (1:1) (MMPS 1:10 20.13pg/ml±9.74pg/ml; MMPS 1:1 1.06pg/ml±0.41pg/ml, *p*=0.0435). Despite the increase in IL-1β from 2.96pg/ml±0.84 to 20.13pg/ml±9.75pg/ml in the 1:10 MP supernatant condition compared to the equivalent MMPS treatment, this difference failed to reach statistical significance *p*=0.087.

This was similarly observed with IL-10 anti-inflammatory secretion whereby the maximum MMP concentration increased cytokine release however, this was only statistically significant when compared to the lowest MMP condition (MP 1:10 7.81pg/ml±3.94pg/ml; versus MP 1:1 0.23pg/ml±0.059pg/ml, *p*=0.048). Furthermore, despite the increase in IL-8 secretion with MMP treatment at 1:5 and 1:10 ratios in each case, these failed to reach significance when compared to control and corresponding MP pellet supernatant.

Finally, human monocytes challenged with the highest concentration of MMPS (1:10) released an elevated amount of TNF-α in comparison to all other treatment conditions (MMPS 1:10 293pg/ml±144pg/ml versus control 6.31pg/ml±1.36pg/ml, *p*=0.014; versus MMPS 1:1 5.39pg/ml±1.40pg/ml *p*=0.0135; versus MMPS 1:5 38.37pg/ml±24.19pg/ml *p*=0.0354). In addition, this remained statistically significant when compared to the corresponding supernatant control (MMPS 1:10 293pg/ml±144pg/ml versus sup 1:10 8.59pg/ml±2.20 *p*=0.0149). For all treatment conditions IFN-γ was below the limit of detection (7.47pg/ml).

MMPS at the highest ratio/concentration 1:10 elicited the largest pro-inflammatory cytokine release and was therefore used in future experiments.

4.4.5 Monocytic MPs influence the expression of surface molecules on human monocytes

Once concentrations of monocyte MPs had been validated and appropriate time points optimised, the influence of monocyte-derived MPs on extracted human monocyte functionality and surface marker expression was investigated.

Initial experiments that analysed the changes in adhesion molecules (CD11b, CD11c), chemokine receptors (CCR2) and surface markers associated with lipid uptake (CD36, CD204) were analysed on the surface of isolated monocytes at 2, 4 and 24 hours following treatment with MMPS or corresponding MP pellet supernatants (figure 4.10).

For all treatment conditions, CD11c was expressed on >95% of cells within the monocytic gate and was not significantly altered over the 24-hour time course due to its high expression on the monocytic gate; thus MFI was quantified for this marker. With respect to CD11c MFI, surface marker expression was not significantly increased with MMPS treatment at any time point when compared to control conditions and MP supernatant. CD11c expression did however peak at 4 hours when compared to control (MMPS 1:10; 8,236±454 vs control; 5,489±181 p=0.06) and MP supernatant (MMPS 1:10; 8,236±454 vs supernatant 1:10; 5,543±179 p=0.066) however, these were not significant. The percentage of monocytes that were CD11b positive increased following MMP treatment at each time point however, this increase was only statistically significant when compared to control (70.9%±6% vs 34%±7.8% p=0.017) and MP supernatant (70.9%±6% vs 36.9%±9.61% p=0.0257) after a 4 hour incubation period.

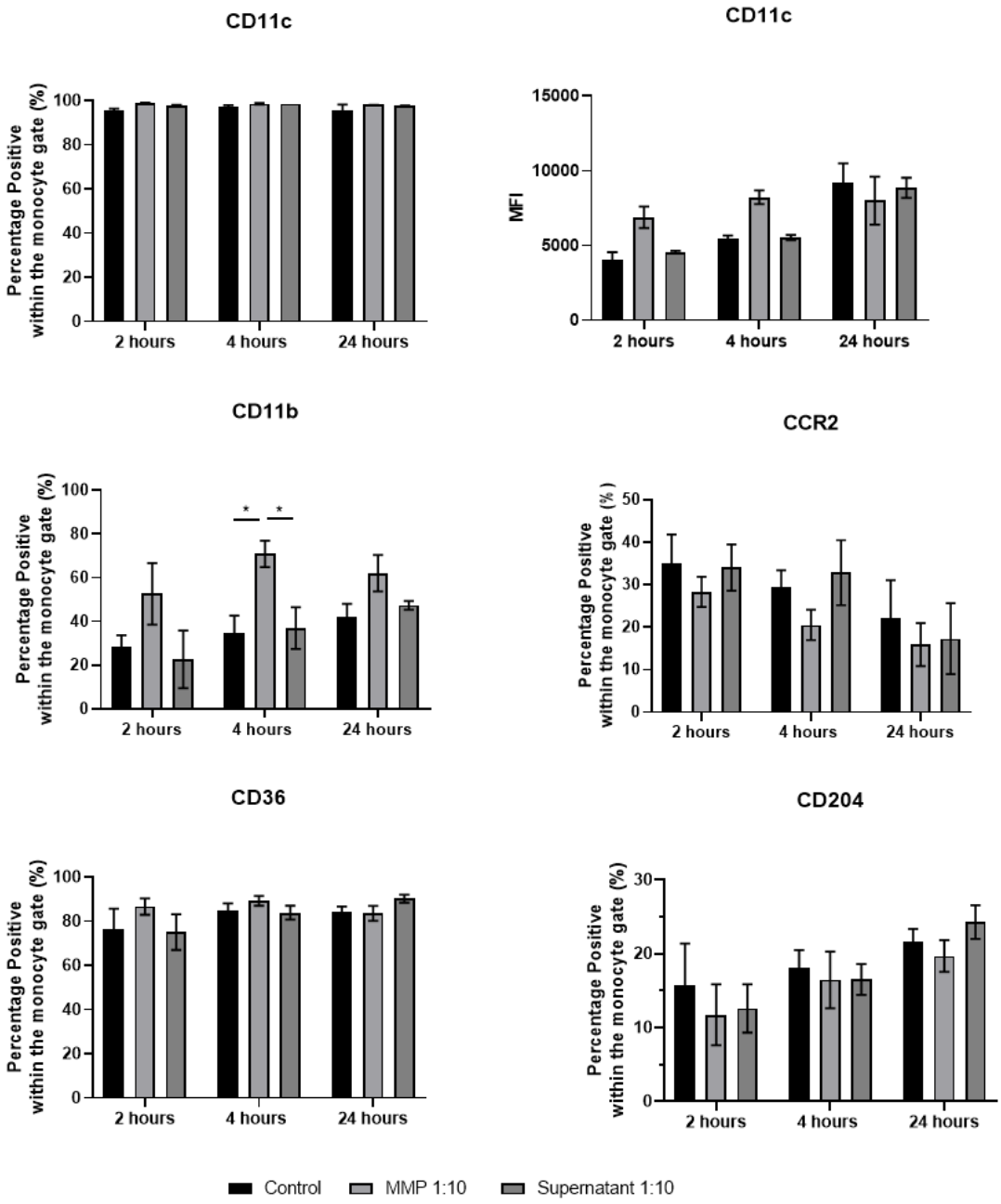

Figure 4.10: A23187 derived monocytic MPs alter monocyte phenotype

*$1x10^5$ Human monocytes were challenged with MMPS 1:10, supernatant 1:10 or control conditions 10% FBS (n=3 biological replicates) for 2, 4 and 24 hours. Surface marker expression was characterised using flow cytometry by staining with FITC-CD36, APC-CD11b, PECy7-CD11c, PerCp-Cy5.5 CCR2 and APC CD204. Data is displayed as mean percentage positive within the monocytic gate ±SEM, in the case of CD11c, surface expression is also displayed as MFI±SEM. Differences for each treatment determined by a TWO-WAY ANOVA, with a Tukey's post hoc test. * denotes significance at p<0.05.*

With respect to CCR2, the percentage of monocytes positive for this surface antigen was highest across all treatments after 2 hours, with MMP reducing receptor expression however this failed to reach significance when compared to control and the corresponding MP supernatant (28.30%±3.53% vs 35.10%±6.75% p=0.72 and 28.30%±3.53% vs 34.03%±5.46% respectively). Furthermore, CCR2 surface expression continued to decrease with all treatment conditions over the 24-hour time course, however in each case percentage expression remained lower in the MMP treatment condition compared to control and supernatant.

Finally, the percentage expression of lipid uptake receptors CD36 and CD204 were quantified in the monocytic gate. No significant differences were observed between treatments at all three time points for CD36, with little change in receptor expression throughout the time course. A similar trend was observed with CD204 however, this surface antigen was upregulated in all treatment conditions over the total 24 hour time period.

As the 4 hour time point was optimum to increase CD11b adhesion molecule expression, this was selected as the incubation period for adhesion and transmigration functionality assays. CCR2 percentage expression was highest at the 2 hour time point across all conditions, thus this was selected for the treatment period for chemotaxis and migration experiments to MCP-1 (CCL2). Due to limited changes in lipid uptake receptor expression with no visible increasing trends after any incubation period, the decision was taken not to investigate the influence of MMP on lipid uptake in this thesis.

4.4.6 Monocytic MPs do not affect human monocyte chemotaxis towards MCP-1

Having demonstrated no change in surface expression of CCR2 following treatment with MMPS, the chemotactic response of monocytes following MMPS treatment was therefore investigated (figure 4.11).

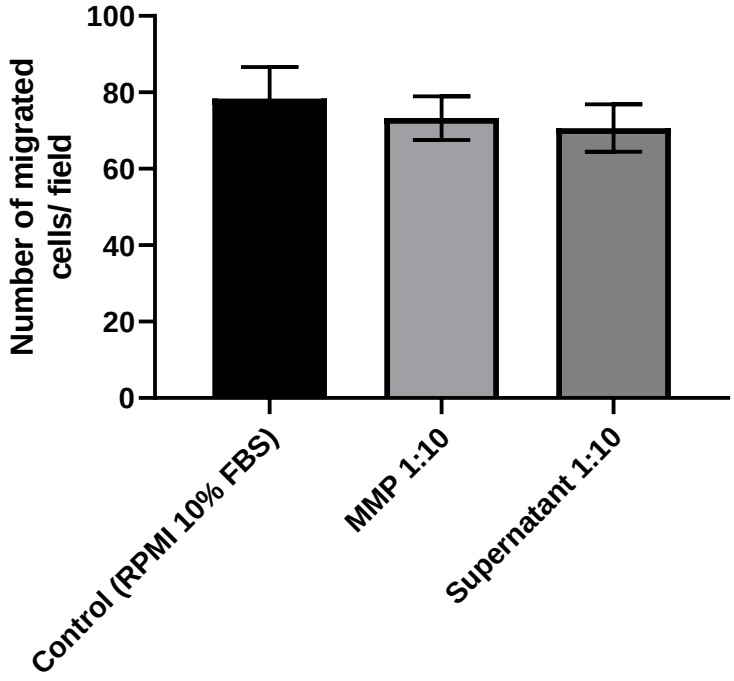

Figure 4.11: The effect of MMPS pre-treatment on the migration of human monocytes to MCP-1

$5x10^4$ isolated monocytes were pre-treated with MMPS (1:10), supernatant (1:10) or control conditions for 2 hours (n=3 biological replicates). After this time cells were added to the top of a 5.0μM pore transwell insert and left to freely migrate towards 5ng/ml MCP-1 for 4 hours. Images were taken at 5 random fields, at 100x magnification. Results are displayed as number of cells migrated/field±SEM. Differences for each treatment determined by a ONE-WAY ANOVA, with a Tukey's post hoc test.

Following the pre-treatment of isolated monocytes with MMPS and the MP pellet supernatant, fewer cells migrated through the Transwell towards MCP-1 (73.25±15.670 monocytes migrated/field and 70.64±6.20 monocytes migrated/field respectively) compared to control conditions (78.4±8.20 monocytes migrated/field), however the difference in cell migration in each condition did not reach significance (Control Versus MMPS p=0.85; control versus MP pellet supernatant p=0.70; MMPS versus MP pellet supernatant p=0.96).

4.4.7 Monocytic MPs enhance human monocyte adhesion to endothelial cells

The influence of MPs on monocyte adhesion to endothelial cells was investigated, comparing the influence of LPS and the inflammatory cytokine TNF-α on adhesion (figure 4.12).

The highest increase in the number of monocytes bound to endothelial cells was observed following the pre-treatment of endothelial cells with 10ng/ml TNF-α for 24 hours (89%±14%).

MMPS significantly enhanced the adhesion of monocytes to the endothelial monolayer when compared to control (27%±3% percentage of endothelial cells with monocytes bound and 14%±2% percentage of endothelial cells with monocytes bound respectively p=0.0307), which was also significant when compared to the corresponding supernatant control (27%±3% percentage of endothelial cells with monocytes bound and 12%±3% percentage of endothelial cells with monocytes bound respectively p=0.0240). Adhesion of monocytes to the endothelial monolayer was further increased following 10ng/ml LPS treatment (in this case used as a positive control), which was significant when compared to control (34.7%±5% percentage of endothelial cells with monocytes bound and 14%±2% percentage of endothelial cells with monocytes bound respectively p=0.0193) and supernatant treatment (34.7%±5% percentage of endothelial cells with monocytes bound and 12%±3% percentage of endothelial cells with monocytes bound respectively p=0.0208).

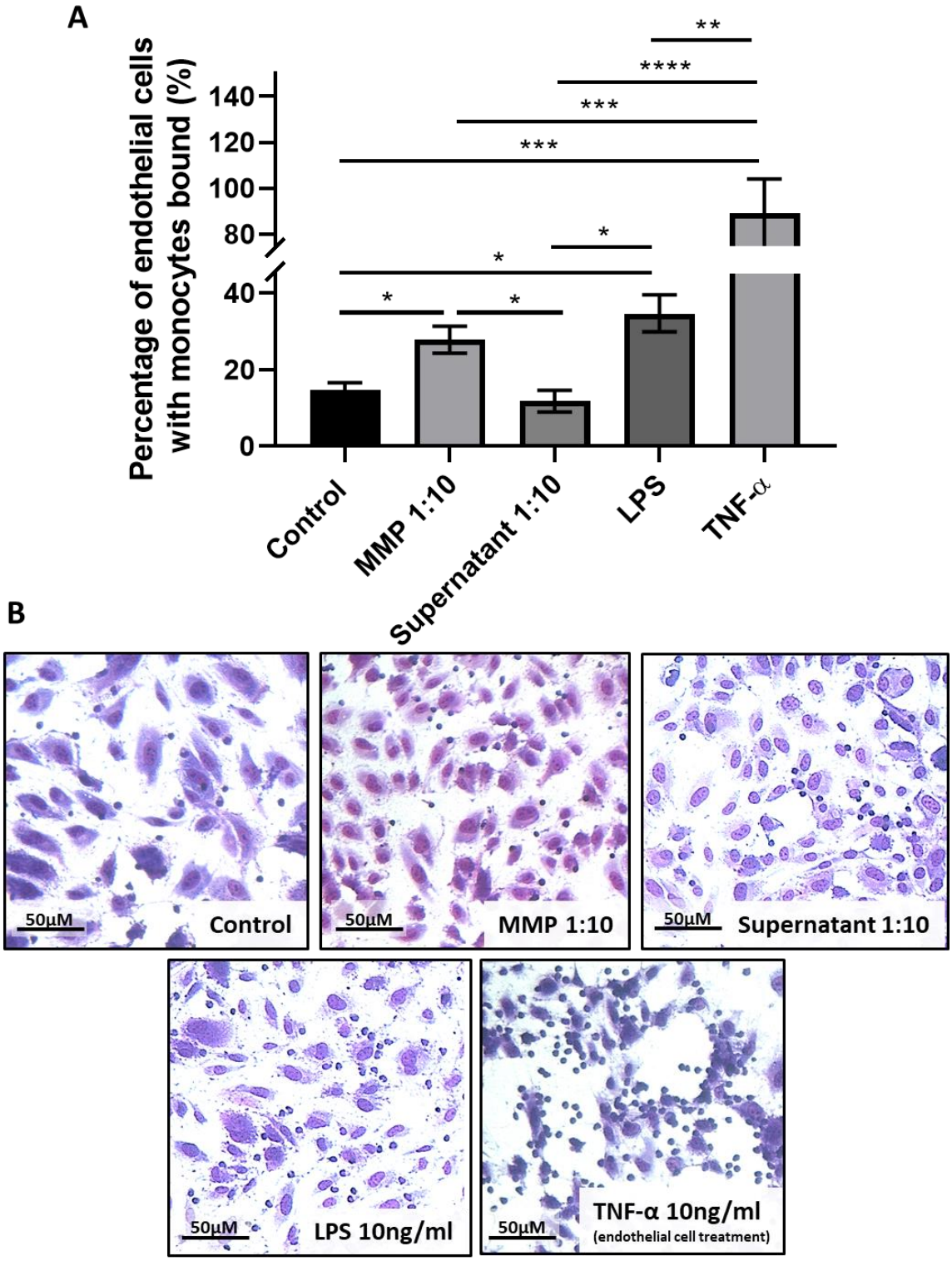

Figure 4.12: The effect of MMPS pre-treatment on the adhesion of human monocytes to HUEVCs

*(A) 5x10^4 isolated monocytes were pre-treated with MMPS (1:10), supernatant (1:10), 10ng/ml LPS or control conditions (RPMI 1640, 10% FBS) for 4 hours (n=3 biological replicates for each treatment). After this time, human monocytes were added to a fully confluent monolayer of HUVECs (One well was pre-treated for 24 hours with TNF-α to act as an additional positive control), and left to adhere for 1 hour. Adhered monocytes were washed with PBS, and stained with Diff-Quick staining. Results are displayed as the percentage of endothelial cells with monocytes bound±SEM. Differences for each treatment determined by a ONE-WAY ANOVA, with a Tukey's post hoc test. * p<0.05, ** p<0.01, *** p<0.001, **** p<0.0001. (B) Representative images of adhered human monocytes to endothelial cells following the pre-treatment of monocytes with MMPS 1:10, supernatant 1:10, LPS 10ng/ml or HUVEC pre-treatment with 10ng/ml TNF-α. Images taken at 200x magnification, Scale bar = 50µM.*

4.4.8 Monocytic MPs enhance monocytic transendothelial migration

Having demonstrated an enhanced monocyte adhesion to endothelial cells, but not migration to MCP-1 alone following incubation with MMPS, it was investigated whether MMPS could influence transendothelial migration using a transwell coated with endothelial cells (Figure 4.13). To ensure that a fully confluent monolayer had formed, crystal violet staining of one transwell insert was performed prior to the addition of monocytes to confirm this as shown in figure 4.3.

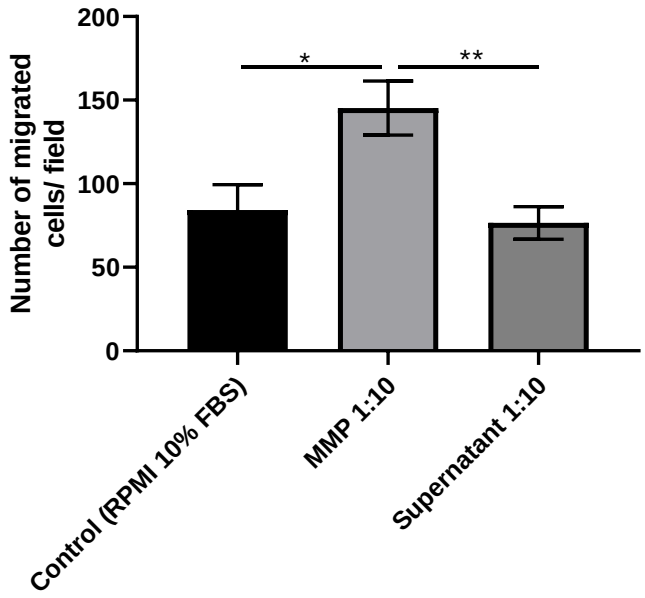

Figure 4.13: The effect of MMPS pre-treatment on the transendothelial migration of monocytes

*$5x10^4$ isolated monocytes were pre-treated with MMPS (1:10), supernatant (1:10) or control conditions for 4 hours (n=3 biological replicates). After this time cells were added a confluent HUVEC monolayer grown on the top of a 5.0μM pore transwell insert (as confirmed by crystal violet staining), and left to freely migrate towards 5ng/ml MCP-1 for 4 hours. Images were taken at 5 random fields, at 100x magnification. Results are displayed as number of cells migrated/field±SEM. Differences for each treatment determined by a ONE-WAY ANOVA with a Tukey's post hoc test. * p<0.05, ** p<0.01.*

MMPS (1:10) significantly increased the number of monocytes migrated through the endothelial monolayer compared to control (145±16 monocytes migrated/field and 78±8 monocytes migrated/field respectively p=0.013). Similarly, this increase was also significant when compared to the corresponding supernatant control (145±16 monocytes migrated/field and 76±10 monocytes migrated/field respectively p=0.008). This suggests that this effect is attributed to MMPS rather than any small molecules remaining in the supernatant. No differences were observed between control treatment and pre-treatment with the MP pellet supernatant.

4.5 Discussion

To investigate the conditions under which monocytic MPs are released and their phenotypic characterisation. THP-1 cells were used initially as they provided an advantage of high cell numbers and a pure cell population, leading to large MP numbers and homogenous MP populations generated. Cryo SEM imaging of MMPS from apoptotic THP-1 cells (serum-starved) showed that MP protrusions from the cell membrane occurs after a minimum of 48 hours, with little MP formation within the first 24 hours (Koifman et al., 2017). Therefore, in these experiments, a time course of 48-96 hours was performed to induce cell death. Our data showed that after 72 hours MP number was increased when compared to control conditions, correlating positively with the percentage of apoptotic cells, supporting the link between apoptosis and MP generation. This link between cell death and MP release was also found in endothelial cells (HUVEC) (data presented in Appendix 6), in addition to endothelial MP release following TNF-α stimulation (data presented in Appendix 7).

A larger quantity of MPs from THP-1 cells were generated following stimulation with LPS compared to apoptosis in agreement with the observations made by Koifman., *et al* (2017), with the addition of pro-inflammatory cytokines TNF-α and IFN-γ (Koifman et al., 2017). THP-1 cells were also activated with a calcium ionophore, A23187. A23187 is a carrier ionophore that stimulates MP release in a similar fashion activating stimuli by increasing cytosolic calcium levels, however this bypasses receptor binding. This increase in intracellular calcium therefore disrupts the cell membrane asymmetry and leads to MP budding (Koshiar et al., 2014). All treatment conditions evoked a concentration-

dependent MP release compared to controls, with LPS the most potent stimulator evident from the largest increase in MP production.

As MPs are derived by plasma membrane budding they carry proteins and lipids found within the parent cell therefore different MP phenotypes reflect their parent cell origin depending on the type of stimulus. MP analysis has demonstrated that different stimuli produce unique proteomic and phenotypic profiles from THP-1 and MM6 (Mac-Mono 6, a monocytic cell line) cell lines (Bernimoulin et al., 2009; Wen et al., 2014).

Data in this chapter has supported this, demonstrating that MP surface antigen expression varies depending on whether the stimulus is an activating or apoptotic one compared to quiescent MPs. ICAM-1 (CD54+) is a pro-inflammatory surface marker that was most influenced by LPS stimulation, upregulating both numbers of CD54+ MPs and the MFI. This is in accordance with previous observations whereby LPS stimulated MM6 cells increased cellular and MP expression of this surface antigen, along with a pro-inflammatory RNA profile that mirrored parent cells (Wen et al., 2014).

Unexpectedly, we did not observe an elevated expression, or proportion, of tissue factor (TF, CD142) on the surface of either MPs or parent cells under stimulatory conditions. *In vitro* and *in vivo* LPS stimulation has been reported to upregulate TF on the surface of human monocytes (Brand et al., 1991; Brekke et al., 2013; Egorina et al., 2005), with LPS monocytic derived MPs *in vitro* similarly expressing CD142 and exhibiting thrombotic activity (Khaspekova et al., 2016). However, our experiments using 100ng/ml LPS failed to induce an increase in TF antigen expression on THP-1 cells or their corresponding MP populations. An increased surface expression of CD142 has previously been described in THP-1 cells following the incubation with higher LPS concentrations (10µg/ml-

100µg/ml), thus the inability of LPS to induce TF expression in this case may be attributable to the lower concentration of LPS used (100ng/ml) (Sabbione et al., 2018).

Apoptotic MMPS expressed more PS on their surface compared to all other conditions, with both stimulated conditions also displaying an increased MFI of PS when compared to quiescent MPs. This is likely to be representative of surface expression on the outer membrane of the parent cell, as PS exposure occurs due to activation, apoptosis and necrosis (Bevers et al., 1982, 1983; Fadok et al., 1992). This phenotyping data demonstrates similar trends in cell surface marker expression on parent cells and MP populations supporting the concept that MMPS mirror their parent cells, in addition to demonstrating one of the ways in which they may exert varying biological functions *in vivo* (Wen et al., 2014).

MPs from different cellular origins also have the ability to induce monocyte/macrophage activation (Baj-Krzyworzeka et al., 2007; Barry et al., 1998; Carpintero et al., 2010; Distler et al., 2005b; Jy et al., 2004; Scanu et al., 2008), in addition to an autocrine effect observed from MMPS themselves (Bardelli et al., 2012).

One primary action of monocytes *in vivo* is to release various cytokines upon activation. In accordance with the literature, we found that IL-6 pro-inflammatory cytokine secretion was only significantly elevated after 18 and 24-hour stimulation following treatment with the highest MMPS concentration (monocyte: MMPS ratio (1:10)) (Amoruso et al., 2010; Bardelli et al., 2005, 2012). Since the largest increase was observed after 24 hours, this was selected as the optimum time point, whereby IL-1β, IL-8, TNF-α, IFN-γ and IL-10 cytokine secretion were also quantified.

The pro-inflammatory cytokines TNF-α and IL-6 displayed a similar trend, whereby secretion was significantly increased upon treatment with the highest concentration of MMPS. This data supports observations made by Bardelli., *et al* (2012), whereby MMPS derived from A23187 stimulated human monocytes increased IL-6 and TNF-α secretion with maximal effects observed at 10μg/ml MMPS (Bardelli et al., 2012). This elevation in cytokine secretion is likely to be as a result of NF-κβ activation, as previously described by Bardelli *et al.,* (2012).

Alongside the increase in inflammatory mediators, MMPS also induced the expression of activation markers. In this study, MMPS upregulated the percentage of monocytes expressing CD11b, which has also been reported in U937 cells following treatment with platelet-derived MPs (Barry et al., 1998), and endothelial-derived MPs (Jy et al., 2004). CD11b is an integrin that regulates the adhesion of monocytes to the endothelium through the interaction of ICAM-1, facilitating their migration and inflammatory response (Muller, 2013). Similar to the effects of platelet MPs, CD11c expression was not statistically significantly altered following MMPS treatment, however an increase was observed in this study supporting the concept that MPs from different cellular origins display varying biological functions (Barry et al., 1998). These differences may also be attributable to the use of a monocytic cell line rather than human monocytes in the latter study.

Despite MMPS treatment failing to induce any significant changes in CCR2, CD36 and CD204 expression over the 24-hour time course, CCR2 expression was downregulated compared to control, and the MP pellet supernatant conditions at all three time points. The downregulation of this chemokine receptor on human monocytes has previously

been reported following the treatment with LPS and pro-inflammatory cytokines (IFN-γ, TNF-α and IL-1β) (Penton-Rol et al., 1998; Sica et al., 1997), as a mechanism for activated monocytes to inhibit reverse endothelial transmigration (Randolph and Furie, 1996) and further monocyte recruitment. Thus, we speculate this downregulation of CCR2 may be a consequence of MMPS enhancing monocyte activation, supported by the increase in activation marker expression and inflammatory mediators as described.

It was then determined if these changes in phenotype would lead to alterations of chemotactic, adherence and migratory function. With respect to monocyte chemotaxis, MMPS treatment failed to induce any significant changes in migration towards MCP-1 (a chemokine that modulates monocyte chemotaxis); an effect potentially observed due to non-significant changes in CCR2 (MCP-1 receptor) expression previously shown.

MMP pre-treatment enhanced monocyte adhesion to an endothelial monolayer; an effected potentially mediated by the increased CD11b expression on these cells. The ability for monocyte-derived MPs to induce adhesion molecule expression has previously been reported in epithelial and endothelial cells, whereby expression of ICAM-1, VCAM-1 and E-selection is upregulated (Cerri et al., 2006; Wang et al., 2011; Wen et al., 2014).

This evidence strongly suggests that the increased chemotactic function and adherence to endothelial cells induced by MPs would also influence the transmigration through the endothelium. Our work shows that transendothelial migration was upregulated following the incubation of monocytes with MMPS for 4 hours compared with MP pellet supernatant controls and media alone. This work supports previous observations (by Barry., *et al* (1998) and Jy., *et al* (2004)) whereby pre-treatment of U937 cells with PMP

and EMP upregulated adhesion marker expression, which led to enhanced adhesion (with respect to PMP) and transmigration (Barry et al., 1998; Jy et al., 2004).

In summary, data in this chapter has demonstrated that MPs derived from monocytic cells under different conditions vary quantitatively and phenotypically, mimicking their parent cell phenotype. This work supports previously reported autocrine effects of MMPS, whereby pro-inflammatory cytokine secretion is upregulated, in addition to also presenting novel findings that MMPS can alter monocyte activation status and upregulate adherence and transendothelial migratory functions. At present the mechanism through which these MMPS exert their function is not yet fully understood, however further evaluating MP effects on target cells and their composition may help to elucidate these mechanisms.

In inflammatory diseases, having increased circulating MMPS may therefore contribute to the promotion of monocyte adhesion and transmigration to endothelial cells; propagating atherogenesis. Our next aim was to therefore characterise alterations in the monocyte MP population found in individuals exposed to chronic inflammatory disease, namely HIV.

Chapter 5 - MP subsets in paediatric HIV infection

5.1 Introduction

The previous chapter describes the pro-inflammatory effects of MMPS on human monocyte function, promoting cytokine release, endothelial adherence and transendothelial migration. As these are the initiating steps in endothelial inflammation and vascular dysfunction, in disease states where MMPS are elevated, this provides a possible further mechanism through which atherosclerosis pathogenesis is accelerated in these patients.

In addition to MMPS, MPs from other cellular origins have also been shown to play a role in CVD progression including; platelets, T cells and endothelial cells. Thus, this chapter aims to characterise levels of these circulating MP phenotypes as well as MMPS in the setting of paediatric HIV infection, whereby atherosclerotic disease is accelerated.

5.1.1 MPs in HIV infection

In patients with HIV infection treated with ART, HIV associated mortality and morbidity is reduced, however the incidence of non-AIDS related co-morbidities has increased. The most common comorbidity is CVD, linked to elevated levels of systemic inflammation that is observed within these patients (Nou et al., 2016). As MPs are usually released in response to cellular activation, it is likely that MP levels in these patients are reflective of this ongoing immune activation. Indeed, increased numbers of endothelial, monocytic and platelet MPs have been reported in adults with HIV infection (Corrales-Medina et al., 2010; Hijmans et al., 2019; Kelly, 2016; Mayne et al., 2012; Da Silva et al., 2011).

HIV virally suppressed adults receiving ART, express higher numbers of platelet MPs (CD31+/CD42b+) compared to healthy controls. No differences in PMP numbers were found within the HIV infected cohort with respect to ART type, duration of ART or time with undetectable viral load (Corrales-Medina et al., 2010).

Furthermore, the percentage of PMPs positive for P-selectin and TF, indicative of their activation, were elevated in HIV infected adults receiving ART when compared to healthy age-matched controls (Mayne et al., 2012). The expression of TF on monocytes and platelets correlated with this MP TF expression in both HIV infected individuals and healthy controls but failed to show any relationship between viral load or T cell counts (Mayne et al., 2012). Within the same cohort, PMP expression of P-selectin and TF displayed a positive association with sCD14, suggesting a link between monocyte activation and TF expression on platelets (Mayne et al., 2012). In addition, MP TF activity was 39% lower in ART-treated patients compared to treatment-naïve HIV infected individuals; a potential mechanism that leads to coagulation pathway activation contributing to the risk of non-AIDs complications (Baker et al., 2013).

Endothelial MPs (EMPs) have also been shown to be elevated in plasma from ART-treated HIV patients compared to an age-matched healthy control population (Kelly, 2016; Da Silva et al., 2011). Total MP number from a monocytic, endothelial (PCAM+, E-selectin+) and platelet (CD42a+) origin correlated with Pulse Wave Velocity (PWV) in HIV infected adults from Malawi, with total MP number and EMPs elevated in comparison to healthy controls (Kelly, 2016).

Likewise, HIV infected men with controlled viremia receiving ART showed markedly higher circulating levels of endothelial, platelet, monocytic and leukocyte derived MPs

compared to age-matched controls (Hijmans et al., 2019). These isolated MPs induced greater inflammation, oxidative stress, senescence and apoptosis of HUVECs *in vitro*, compared to healthy control MPs, demonstrating their ability to contribute to endothelial activation and damage (Hijmans et al., 2019).

The quantity and phenotypes of specific MPs circulating in the plasma of children with HIV infection are currently unknown. With an aim to understand this, MPs were analysed in plasma samples taken from HIV infected children, and controls recruited into the CHAPAS-3 clinical trial and subsequent cardiovascular sub-study.

5.1.2 CHAPAS-3 clinical trial and cardiovascular sub-study

The "**C**hildren with **H**IV in **A**frica **P**harmacokinetics and **A**cceptability/Adherence of **S**imple Antiretroviral Regimens (CHAPAS) 3" trial was an open-label randomised phase II/III clinical trial conducted between 2010 and 2013. Throughout this period a total of 478 children between the age of 1 month and 13 years were recruited across 3 sites in Uganda and one in Zambia (Mulenga et al., 2016).

The aim of the study was to evaluate the toxicity and efficacy of NRTI-containing first-line ARTs in treatment-naïve children and ART-experienced children that had been taking stavudine-containing first-line therapy for more than 2 years. Upon recruitment, both treatment-naïve and treatment-experienced children were randomised to a treatment arm, within which they were prescribed abacavir, zidovudine or stavudine, with either Nevirapine or Efavirenz and Lamivudine. Patients were followed up over 96 weeks, with CD4+ T cell counts analysed at weeks 6, 12, 24, 48, 72 and 96 weeks, and viral load measured at weeks 48 and 96. The study reported no major differences in clinical outcomes, viral suppression and CD4 percentage recovery with the different

NRTI regimes, with similar low toxicity levels reported in each treatment group (Mulenga et al., 2016).

As part of the CHAPAS-3 clinical trial, 208 ART naïve and 74 treatment-experienced children were additionally recruited into a CV sub-study. 284 sex and age-matched healthy control children were also recruited into the study from the community, well-child clinics, surgical outpatient clinics and siblings of CHAPAS-3 patients.

This study aimed to determine the influence of both controlled and uncontrolled HIV infection on measurements of vascular function: IMT, PWV, and biomarkers of inflammation, vascular injury and disordered thrombogenesis. In addition, longitudinal changes in these measurements were also assessed over 96 weeks within both HIV infected cohorts. As with the main CHAPAS-3 trial, at baseline, treatment-naïve and treatment-experienced children were randomised to an NRTI-containing ART treatment arm.

The CHAPAS CV sub-study showed that children with untreated HIV infection display evidence of asymptomatic atherosclerosis, through an increase in IMT and PWV compared to uninfected children. ART-experienced children displayed similar IMT and PWV to healthy control children, with IMT continuing to improve over the 96 week follow up. These improvements in vascular function were also observed within the treatment-naïve cohort, following the initiation of ART strongly suggestive that structural changes can be reversed following successful viral suppression.

Biomarkers indicative of CV injury, inflammation and thrombogenesis were elevated within the treatment-naïve population in this trial compared to controls. Following

treatment intervention within this group, levels of these biomarkers significantly decreased but did not normalise to healthy control levels. Similar observations were made within the treatment-experienced cohort, with biomarkers remaining elevated despite effective ART for a median of 3.5 years. Although these were reduced, they remained outside the healthy control range. These results support literature demonstrating that although ART intervention reduces inflammatory biomarkers, these levels fail to normalise with healthy controls.

This work by Dr Kenny demonstrates that despite improvements in vascular function following ART initiation, abnormalities in inflammatory biomarkers remain (Kenny, 2016).

5.2 Aims and Objectives

In children with HIV infection the dynamics of circulating MPs, and how these are altered in response to ART initiation are currently unknown. Therefore, MPs were quantified and phenotyped in 2 HIV infected paediatric cohorts recruited within the CV sub-study of the CHAPAS-3 clinical trial.

To do this, the following objectives were:

1) Multi-colour flow cytometry panels were designed in order to phenotype MPs from endothelial, monocytic, platelet and T cell origins in plasma from adult healthy controls.

2) The impact of different fixation methods on MP number in the plasma from adult healthy controls was assessed, facilitating method optimisation of HIV patient samples allowing them to be removed from containment level 3 laboratories.

3) This method was applied to stored patient samples from HIV infected treatment-naïve individuals, HIV infected treatment-experienced and healthy controls recruited in the CV CHAPAS-3 sub-study; allowing the analysis of circulating MP phenotypes and numbers.

5.3 Methodology

5.3.1 Longitudinal study population

Blood collection for MP assessment was taken upon recruitment into the CV sub-study of the CHAPAS-3 trial between 2010 and 2013. Samples were collected at baseline, from 2 HIV infected cohorts, and age-matched healthy controls, with an additional sample collected at the 48-week follow-up assessment for the 2 HIV infected populations. Healthy control children were recruited into the study from the community, well-child clinics, surgical outpatient clinics and siblings of CHAPAS-3 patients in South Africa. Patient medical and family history was obtained during the initial visit, with clinical measurements (weight, height, blood pressure, lipids, CD4+ counts) being recorded with each routine visit to the clinic.

Blood was collected in sodium citrate tubes and depleted of platelets through centrifugation at 500g for 5 minutes, with the plasma removed and re-centrifuged at the same speed and duration. A minimum of 500µl of platelet-poor plasma from each patient was stored at -80°C. For MP analysis, 42 patient samples across all three patient cohorts were included in the study.

5.3.2 MP quantification

The enumeration of MPs derived from endothelial cells, T lymphocyte, monocytes and platelets was performed as previously described in Chapter 2. Briefly, after quickly thawing 250µl of plasma, samples were centrifuged for 5 minutes at 5000g twice in order to remove any remaining platelet contamination. Following this, supernatants were centrifuged for 60 minutes at 17,000g, 4^{o}C to pellet MPs.

MP pellets were then re-suspended in 250µl of 1x Annexin V binding buffer, and divided equally across 6 antibody panels allowing their characterisation; table 5.1 details the specific antibodies and dilutions used in these experiments (details of isotype controls can be found in appendix 2).

Surface marker	MP origin	Isotype	Fluorochrome conjugate	Dilution
Annexin V	All	N/A	FITC	1:50
CD3	T Lymphocyte	IgG2a, κ	PerCp Cy5.5	1:50
CD4	T Lymphocyte	IgG1, κ	APC	1:50
CD8	T Lymphocyte	IgG1, κ	PE Cy7	1:50
CD62p	Platelet/ Endothelial	IgG1, κ	PerCp Cy5.5	1:50
CD142	Platelet/ Monocytic	IgG1, κ	APC	1:20
CD31	Platelet/ Endothelial	IgG1, κ	PE Cy7	1:50
CD14	Monocytic	IgG2a, κ	Pacific Blue	1:50
CD42a	Platelet	IgG1, κ	PE	1:50
CD144	Endothelial	IgG1, κ	APC	1:20
CD106	Endothelial	IgG1, κ	PerCp Cy5.5	1:50
CD54	Endothelial	IgG1, κ	Pacific Blue	1:50
CD105	Endothelial	IgG1, κ	PE	1:50
CD62e	Endothelial	IgG1, κ	PE	1:50

Table 5.1: List of phenotypic markers used for MP detection in patient samples

Following a 20-minute incubation with each antibody cocktail at room temperature with continuous shaking, samples were further diluted with 150µl Annexin V buffer and stored at 4°C until flow cytometry acquisition (acquisition details are defined in Chapter 2). Prior to flow cytometry analysis, samples were fixed in order to inactivate any remaining HIV viral particles using 1x BD cell fix.

This method of fixation was validated using plasma samples from healthy controls, to ensure there was no interference from the fixation method with MP quantification. This method optimisation step is described in the results section 5.3.1 within this Chapter.

Latex beads were run to determine size-exclusion gates and absolute enumeration as described in Chapter 2.

5.3.3 Gating strategy for MP enumeration

The MP population was initially gated based on their size being less than 1.0µm, and Annexin V positivity using FlowJo software (USA). Compensation was applied to samples post-flow cytometry acquisition within the FlowJo software, using latex compensation beads (BD Biosciences) as a control, and confirmed using single-stained MP populations found in plasma from healthy controls. Within the Annexin V positive population of MPs, positive gates for each marker were set based upon isotype control staining and applied to each panel.

Following this, MP phenotypes derived from endothelial cells, T lymphocyte, monocytes and platelets were characterised according to the gating flow diagram in figure 5.1.

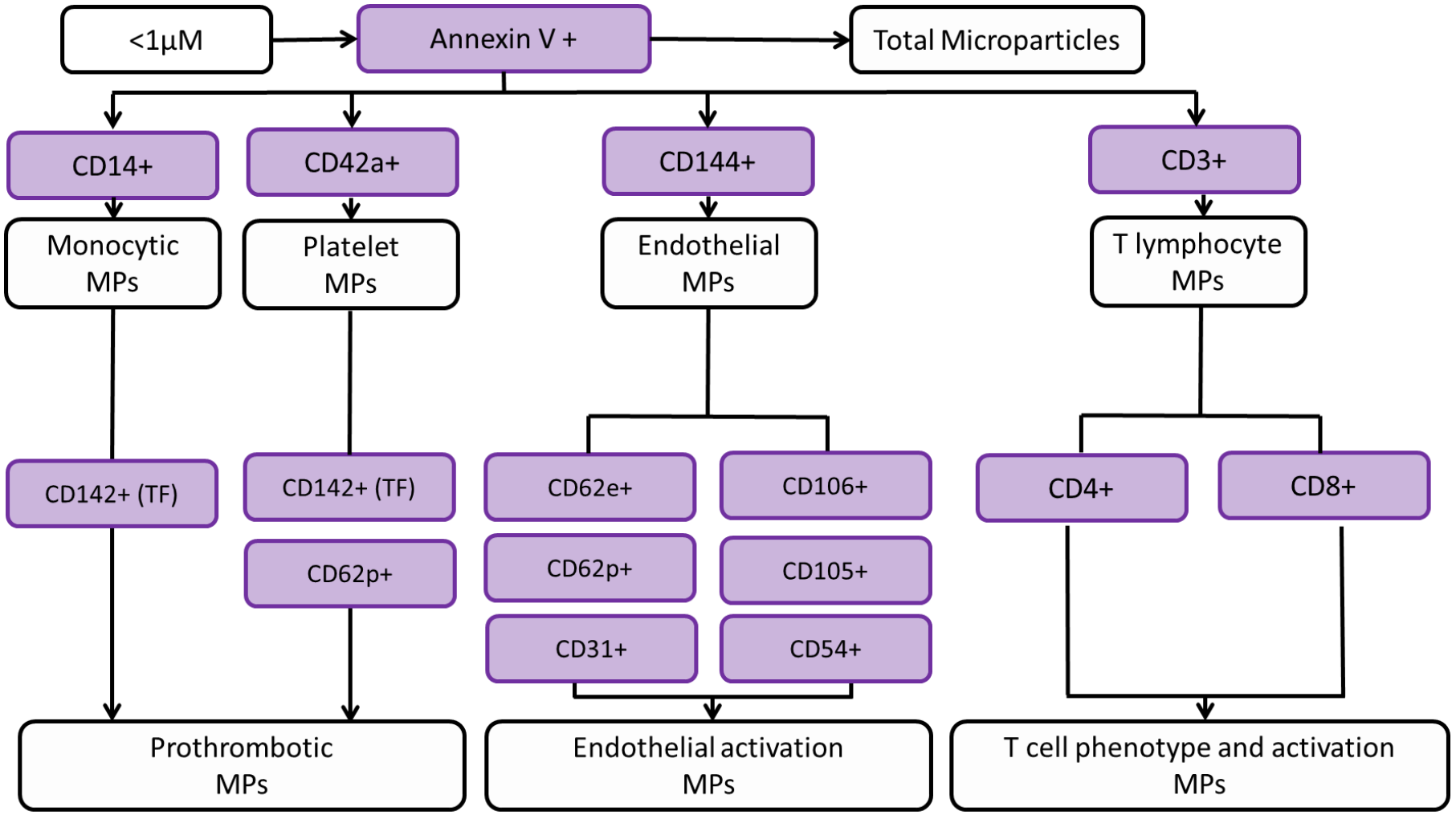

Figure 5.1: MP characterisation flow diagram

A flow diagram detailing the gating strategy used to characterise MP populations within patient samples. All MPs were defined as being <1μM size, and positive for phosphatidylserine expression (positive for Annexin V). MPs were subsequently divided based upon antibody binding to surface markers, predicting cellular origin.

5.3.4 Statistical analysis

Statistical analysis was performed using either GraphPad or SPSS software. Differences between patient groups for clinical and laboratory measurements were determined using a Student's *t*-test. To highlight any significant differences in MP counts between groups, a non-parametric Mann-Whitney *U*-test was used. To assess the significance of the change in MP number between week 0 and week 48 within the treatment-naïve group and the ART-experienced, a paired Wilcoxon rank test was performed. Differences were considered significant when $p \leq 0.05$.

5.4 Results

5.4.1 MP fixation

In order to allow any material that has the potential to contain any HIV viral particles to be removed from containment level 3 laboratories, stained MP containing patient samples were first fixed to inactivate any viral particles present. This allowed their analysis in communal containment level 2 laboratories. As this fixation step provided the potential to interfere with MP quantification, a range of paraformaldehyde (PFA) concentrations (1%, 2%, 4%) and BD Cell fix were tested using MPs isolated from the plasma of healthy adult to assess their impact on total MP number and phenotypes (Figure 5.2).

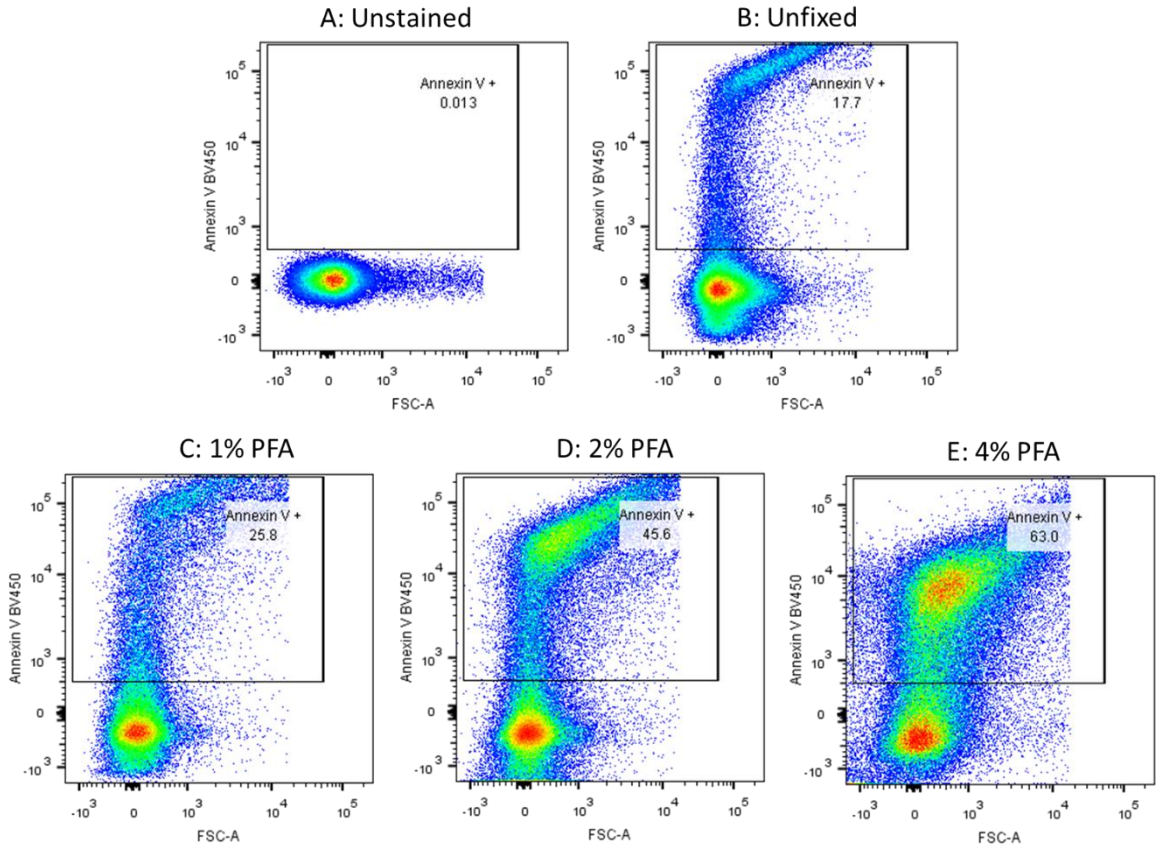

Figure 5.2: Representative flow cytometry dot plots of MPs isolated from the plasma of healthy adults, where samples were left unfixed (B) or fixed 1% (C), 2% (D) and 4% (E) paraformaldehyde (PFA) prior to acquisition.

Following PFA fixation (1%, 2% and 4%) MP counts increased with concentration compared to unfixed controls (Figure 5.2). BD Cell fix was therefore tested as an alternative fixation method (Figure 5.3), again using the plasma of healthy adults to assess their impact on total MP number and phenotypes.

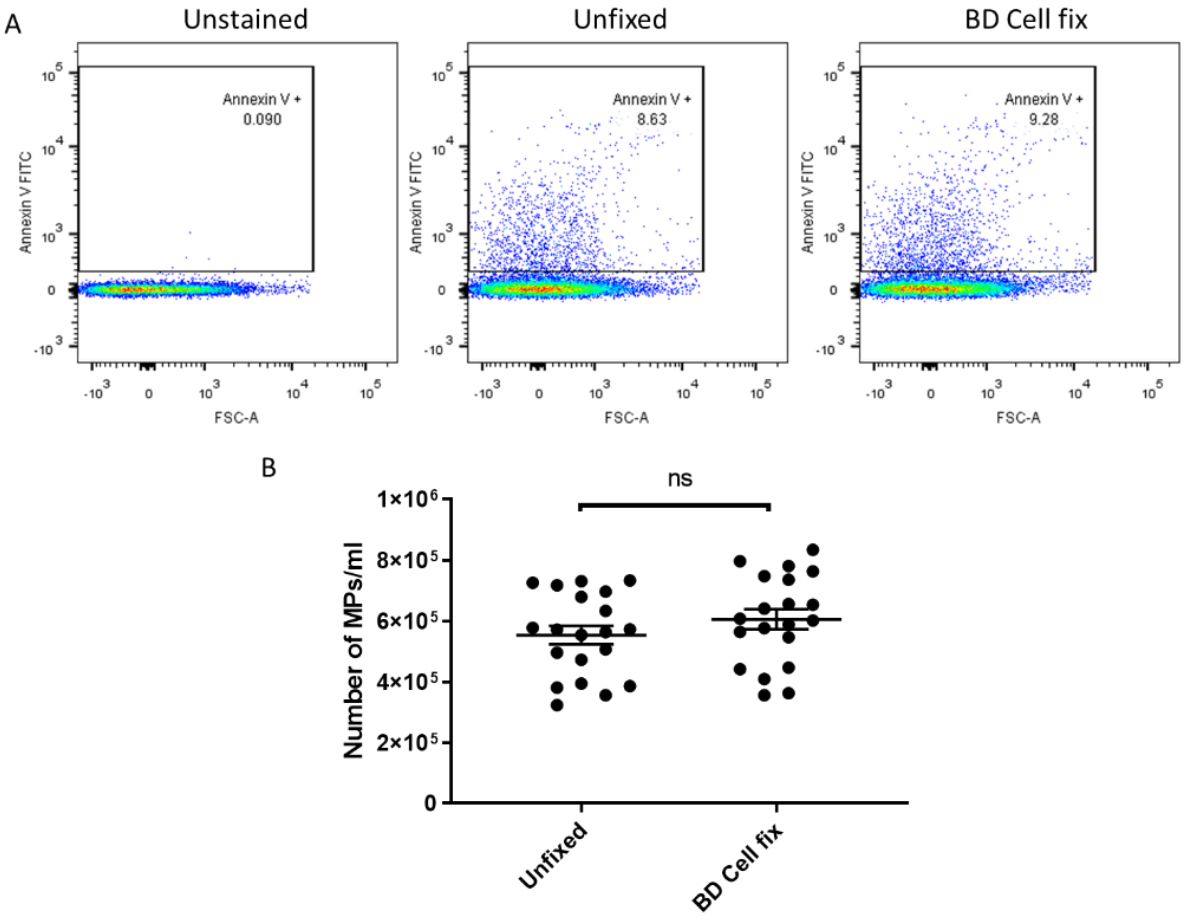

Figure 5.3: The impact of 0.5x BD Cell fixation on total MP number

A) Representative flow cytometry dot plots showing the percentage of MPs isolated from the plasma of healthy adults, where samples were left unfixed or fixed with 0.5x BD cell fix prior to acquisition. B) Total circulating MP number (<1µm, Annexin V+) were characterised in the plasma of healthy control adults by (n=4 biological replicates, 5 technical replicates). Results displayed as mean±SEM, with statistical differences determined by a paired students t-test, ns= Non-significant,

Analysis of the total circulating MPs in the plasma of healthy adults showed that number of Annexin V positive events, within the <1µm size gate, did not significantly alter following fixation (553,000±30,434 versus 604,900±32,689, unfixed and BD Cell fix respectively; *p*=0.2525).

This was also observed within Annexin V+ CD42a+ platelet MP populations (Figure 5.4A) and Annexin V+ CD14+ monocytic MP populations (Figure 5.4B).

Upon fixation, PMP number increased from 108,675±12,775 MPs/ml to 112,875±11,951 MPs/ml along with TF positive PMPs from 1,397±280 MPs/ml to 1,827±507 MPs/ml however, in each case these differences were non-significant (0.5122 and 0.1613 respectively). Similarly, MMP numbers increased from 25,800±1,849 MPs/ml to 26,725±1,040 MPs/ml along with TF positive MMPS from 1,520±604 MPs/ml to 2,500±743 MPs/ml however, these differences were also non-significant (0.7675 and 0.0598 respectively).

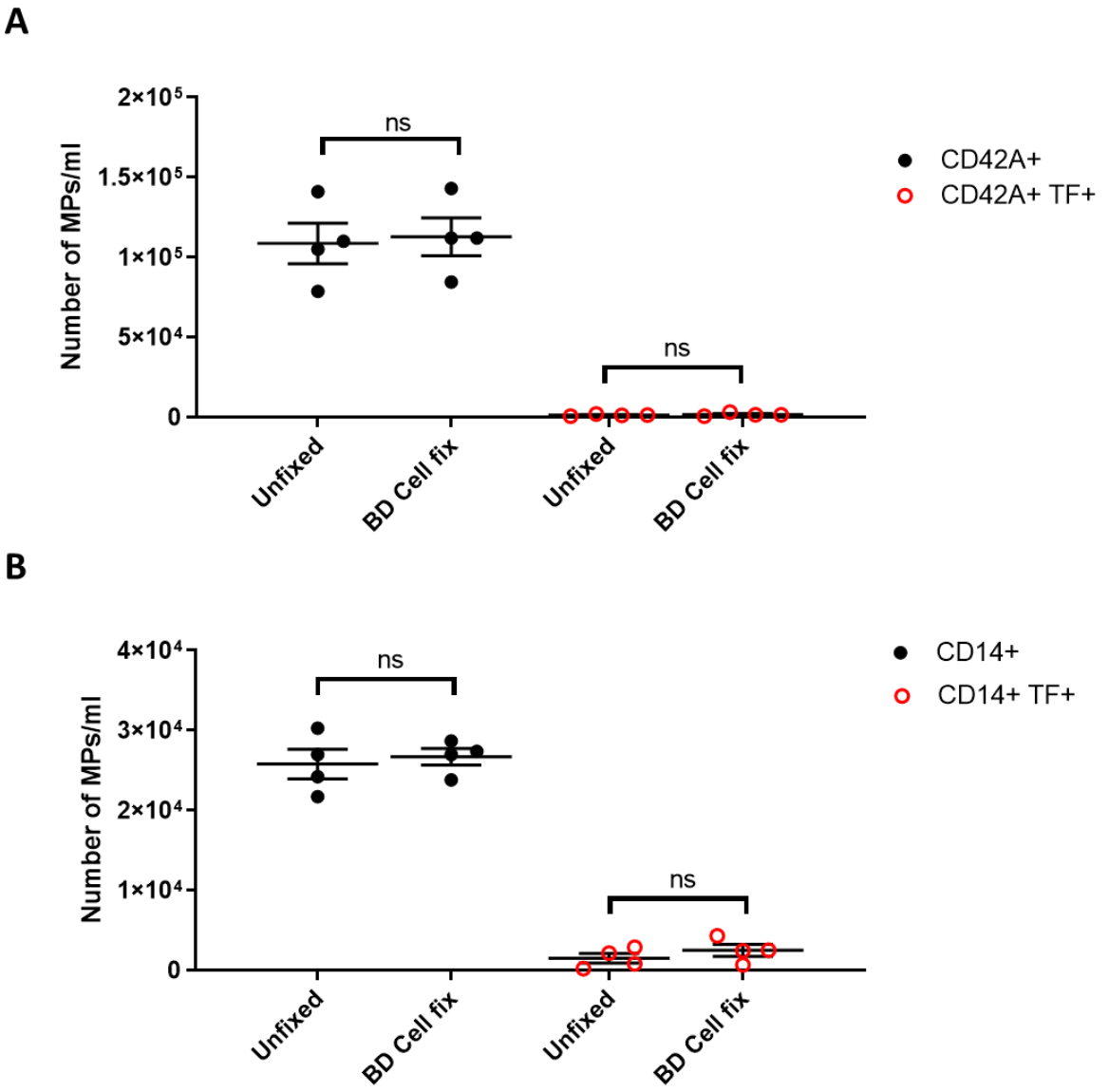

Figure 5.4: The impact of 0.5x BD Cell fixation on platelet and monocytic MP number

Platelet and monocytic MPs were characterised in the plasma of healthy control adults (n=4 biological replicates) by flow cytometry, where samples were left unfixed, or fixed with 0.5x BD Cell fix prior to acquisition. Total platelet MP number were characterised as <1µm Annexin V+ and CD42a+ (A), in addition to Tissue factor+ PMPs (CD42a+ CD142+). In addition to Total monocytic MP number, characterised as <1µm Annexin V+ and CD14+ (B) and Tissue factor+ MMPS (CD14+ CD142+). Results displayed as mean±SEM, with statistical differences determined by a paired students t-test, ns= Non-

The impact of fixation on T cell MPs were also analysed (Figure 5.5). MPs from a T cell origin were defined by their expression of Annexin V and CD3. These MPs increased from 32,433±13,275 MPs/ml to 34,966±14,077 MPs/ml following fixation, however this increase failed to reach significance (p=0.1626). Furthermore, CD3+ CD4+ and CD3+ CD8+ MP counts remained similar between both conditions (CD3+ CD4+: 3,206±1,040 versus 3,130±830, unfixed and fixed respectively; p=0.9103 and CD3+ CD8+: 5,543±1,986 versus 6,123±1,749, unfixed and fixed respectively; p=0.0798).

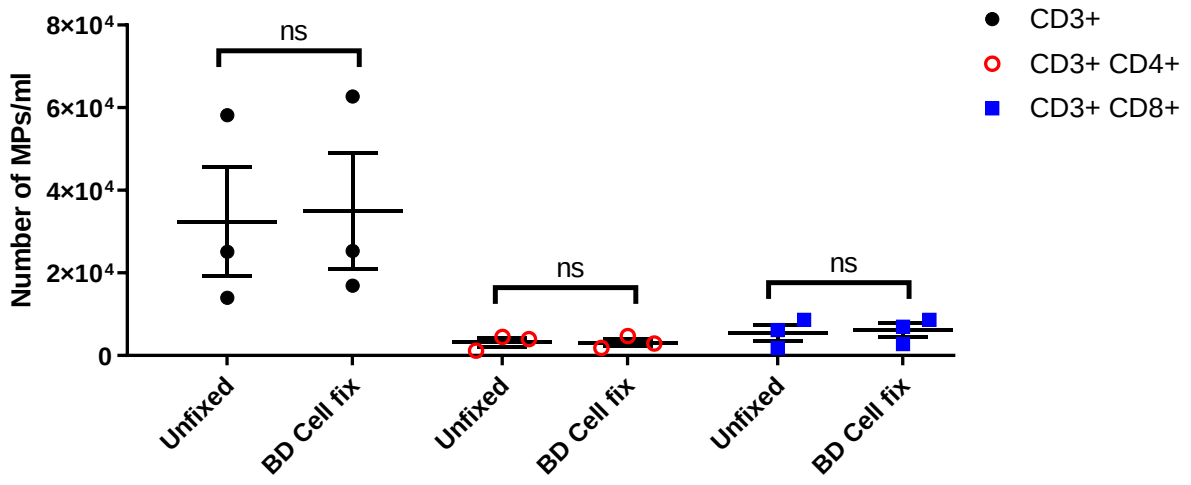

Figure 5.5: The impact of 0.5x BD Cell fixation on T cell MP Number

T Cell MPs were characterised in the plasma of healthy control adults (n=3 biological replicates) by flow cytometry, where samples were left unfixed, or fixed with 0.5x BD Cell fix prior to acquisition. Total T Cell MP Number were characterised as <1µm Annexin V+ and CD3+, in addition to T cell population phenotypes (CD3+ CD4+, CD3+ CD8+). Results displayed as mean±SEM, with statistical differences determined by a paired students t-test, ns= Non-significant, p=>0.05.

Finally, CD144+ endothelial MPs were also characterised following fixation (Figure 5.6A), along with activated phenotypes (Figure 5.6B).

Following fixation, MPs from an endothelial origin remained unaltered (20,080±5,736 versus 20,932±4,907, unfixed and fixed respectively; p=0.5759), along with each sub-population: CD62e+ (25,373±3,456 versus 30,750±3,817, unfixed and fixed respectively; p=0.0566), CD144+ CD62e+ (3,150±1,039 versus 4,822±1,184, unfixed and fixed respectively; p=0.2566), CD144+ CD105+ (3,727±2,324 versus 3,640±1,986, unfixed and fixed respectively; p=0.2057), CD144+ CD31+ (525±132 versus 722±218, unfixed and fixed respectively; p=0.1821) and CD144+ CD54+ (877±93 versus 1,060±94, unfixed and fixed respectively; p=0.2083).

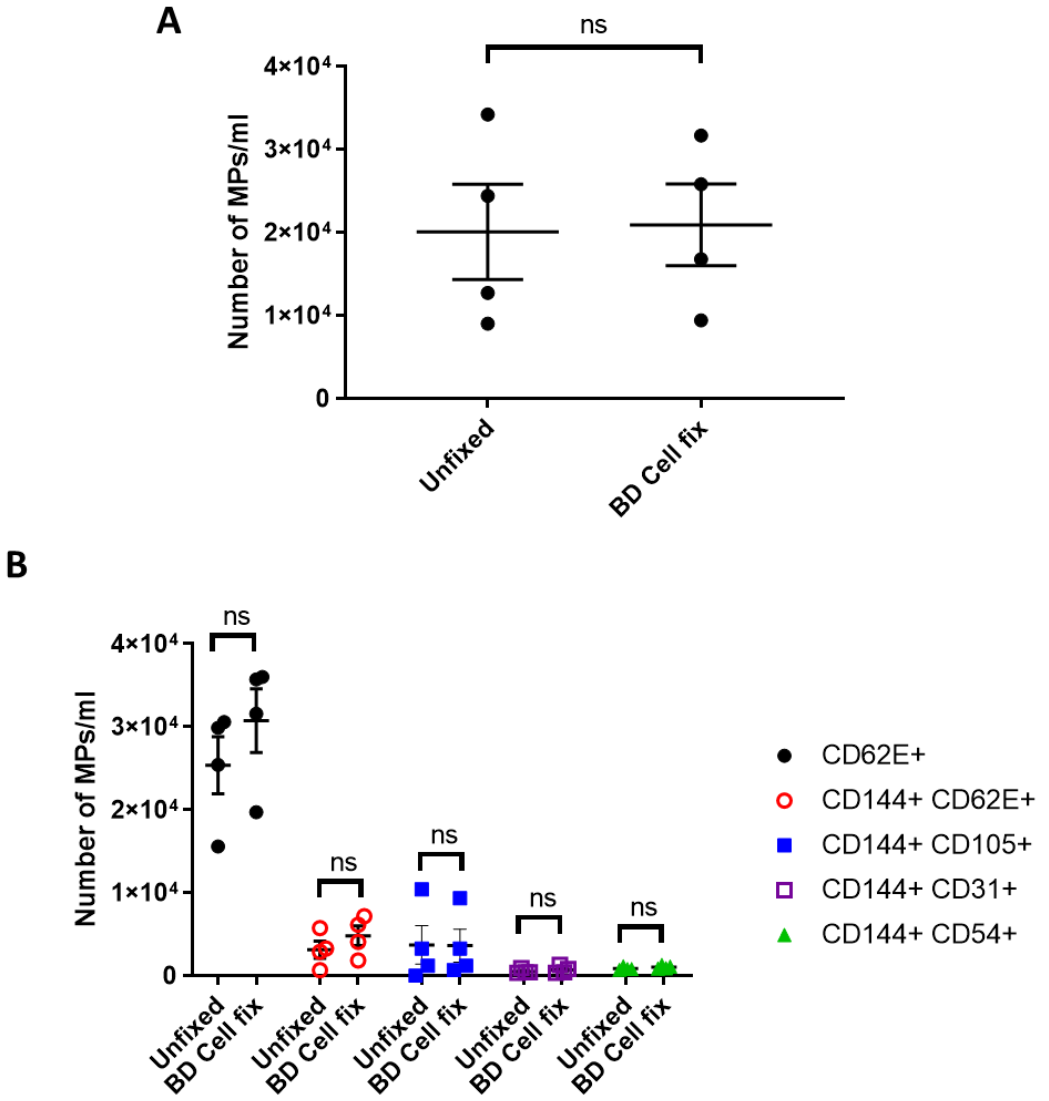

Figure 5.6: The impact of 0.5x BD Cell fixation on endothelial MP number

Endothelial MPs were characterised in the plasma of healthy control adults (n=4 biological replicates) by flow cytometry, where samples were left unfixed, or fixed with 0.5x BD Cell fix prior to acquisition. Total endothelial MP number were characterised as <1µm Annexin V+ and CD144+ (A), in addition to activated phenotypes (CD62e, CD144+ CD62e+, CD144+ CD105+, CD144+ CD31+, CD144+ CD54+) (B). Results displayed as mean±SEM, with statistical differences determined by a paired students t-test, ns= Non-significant, p=>0.05.

BD Cell fix (0.5x) was the selected method for subsequent analyses as all MP markers measured were calculated to be within 95% confidence limits, with no significant differences between unfixed and fixed samples.

5.4.2 MPs in HIV: Demographic description of patients at baseline

Plasma samples from 11 HIV infected patients who were antiretroviral treatment-naïve (mean age (range) 8.06 years (4.38-12.67)) and 16 HIV infected patients that were antiretroviral experienced (on treatment for >2 years; mean age (range) 8.66 years (5.24-12.25)) were included in the sub-study, and matched to plasma from 15 healthy control patients (mean age (range) 9.12 years (5.01-12.82); Table 5.2 outlines patient clinical and laboratory measurements at the time of recruitment into the CHAPAS-3 study.

Patients in the treatment-naïve group started on ART at an older age compared to those who were treatment-experienced (mean 8.06 years vs 5.02 years p = 0.0041). As expected, viral load was significantly higher in treatment-naïve compared to treatment-experienced (183636 vs <100 (defined as undetectable) viral load, copies/ml naïve vs treated respectively; p = <0.001). CD4 cell counts were lower in the treatment-naïve patient group compared to treatment-experienced (mean 336.4 vs 1205 cell number/ml naïve versus treated respectively; p = 0.001) and the healthy control population (mean 336.4 vs 957.4 p = <0.001).

High-density lipoprotein (HDL) levels were lower in the HIV treatment-naïve patient group compared to those on ART (0.89 vs 1.448 mmol/L, naïve versus treated respectively p = 0.003) and healthy controls (0.89 vs 1.447 mmol/L, naïve versus treated respectively p = 0.02). Total triglyceride levels were also higher in the treatment-naïve group compared to the healthy control cohort (1.198 vs 0.796 mmol/L, naïve versus treated respectively p = 0.04), but within ranges recorded for the ART-experienced children. No differences were observed between all patient groups with other clinical and laboratory measurements collected.

	HIV + Treatment-naïve at enrolment (TN)	**HIV + Treatment-experienced (ART>2years) at enrolment** (TE)	**HIV - Healthy controls** (HC)	***P*-value**
Sample size	n=11	n=16	n=15	
Age (years; range)	8.06 (4.380-12.67)	8.66 (5.240-12.25)	9.12 (5.01-12.82)	TN vs TE: 0.5505 TN vs HC: 0.3269 TE vs HC: 0.6092
Gender; Male (%) Female (%)	 5 (45%) 6 (54%)	 9 (56%) 7 (43%)	 7 (46%) 8 (53%)	-
Age ART was initiated (years; range)	8.06 (4.38-12.67)	5.02 (2.25-9.85)	-	**TN vs TE: 0.0041**
Duration on ART (Years; range)	-	3.77 (2.26-7.06)	-	-
Treatment Arm; D4T ZDV ABC	 1 (9%) 3 (27%) 7 (63%)	 3 (18%) 4 (25%) 9 (56%)	-	-
NNRTI; EFV NVP	 9 (81%) 2 (18%)	 3 (18%) 13 (81%)	-	-
BMI; (range)	15.35 (13.70-17.22)	15.36 (13.62-18.24)	15.97 (13.88-17.78)	TN vs TE: 0.9784 TN vs HC: 0.2015 TE vs HC: 0.1977
Laboratory measurements				
CD4+ count Week 0; (range)	336.4 (105-654)	1205 (365-2600)	957.4 (474-1329)	**TN vs TE: 0.001** **TN vs HC: <0.001** TE vs HC: 0.155
Viral Load Week 0 (Copies/ml)	183636 (9275-682105)	<100	-	**TN vs TE: <0.001**
Total cholesterol (mmol/L); (range)	3.57 (2.18-4.62)	4.10 (2.86-5.25)	3.80 (2.26-7.03)	TN vs TE: 0.0772 TN vs HC: 0.6212 TE vs HC: 0.4353
HDL; (mmol/L); (range)	0.89 (0.47-1.31)	1.448 (0.99-1.36)	1.447 (0.26-2.29)	**TN vs TE: 0.003** **TN vs HC: 0.0203** TE vs HC: 0.8950
LDL; (mmol/L); (range)	1.967 (0.96-2.72)	1.918 (1.36-2.55)	1.974 (0.59-3.98)	TN vs TE: 0.8296 TN vs HC: 0.9817 TE vs HC: 0.8481
Triglycerides; (mmol/L); (range)	1.198 (0.69-1.91)	0.8367 (0.33-2.08)	0.786 (0.24-1.81)	TN vs TE: 0.0874 **TN vs HC: 0.0393** TE vs HC: 0.7861

Table 5.2: Demographic and laboratory data from HIV infected children and healthy controls at week 0

Stavudine (D4T), Zidovudine (ZDV), Abacavir (ABC), Non-nucleoside reverse-transcriptase inhibitors (NNRTI), Efavirenz (EFV), Nevirapine (NVP), Body Mass Index (BMI), high-density lipoprotein (HDL), low-density lipoprotein (LDL), Treatment-naïve (TN), Treatment-experienced (TE), Healthy controls (HC). Data expressed as mean (range). Differences between treatment groups were determined using an unpaired student's t-test.

5.4.3 Longitudinal effects of antiretroviral therapy on MP number

MP analysis was carried out at the time of recruitment, t=0, and 48 weeks following the initiation of the study (t=48). MP numbers of each subset characterised are displayed in table 5.3, with corresponding *p*-values for individual group comparisons described in table 5.4. MP numbers are reported as median (interquartile range).

Due to small plasma volumes, the number of TF positive monocytic MPs were too few within the gate to be included in these results.

	Healthy Controls	HIV + Treatment-naïve Week 0	HIV + Treatment-naïve Week 48	HIV + Treatment-experienced (ART>2years) Week 0	HIV + Treatment-experienced (ART>2years) Week 48
Total MPs					
Annexin V+	538,538 (24,637-1,082,439)	1,330,219 (315,461-1,225,816)	483,947 (36,777-880,043)	555,499 (193,550-911,608)	406,384 (182,999-816,932)
T lymphocyte MPS					
CD3+	8,942 (1,672-13,272)	46,279 (18,741-58,753)	34,789 (22,861-52,349)	17,944 (4,685-27,677)	13,967 (4,770-26,490)
CD3+ CD4+	310 (0-1,634)	3,442 (764-4,352)	0 (0-4,970)	1,530 (95-2,602)	1,631 (642-3,612)
CD3+ CD8+	0 (0-476)	4,590 (764-18,241)	331 (0-1,657)	155 (0-1,052)	321 (0-662)
Monocyte MPs					
CD14+	12,927 (4,321-23,346)	36,480 (27,200-57,711)	34,291 (22,309-69,171)	26,429 (17,670-39,815)	19,146 (15,083-25,216)
Platelet MPs					
CD42a+	13,885 (2,487-170,429)	77,932 (12,430-102,960)	30,316 (30,486-133,291)	85,679 (30,486-133,291)	28,898 (14,850-129,203)
CD42a+ CD62p+	7,305 (0-37,294)	2,450 (846-6,534)	927 (387-3,865)	12,048 (4,494-20,271)	4,175 (309-9,476)
CD42a+ CD142+	13,833 (77-32,718)	1,234 (693-20,611)	5,798 (489-16,732)	15,108 (5,163-28,590)	1,554 (963-7,706)
Endothelial MPs					
CD144+	14,702 (1,642-26,695)	46,661 (20,653-51,216)	25,512 (18,223-59,081)	19,315 (5,710-35,422)	20,871 (8,991-37,166)
CD144+ CD54+	2,507 (1,108-4,122)	11,608 (3,347-16,579)	13,033 (5,027-19,879)	3,954 (860-6,235)	9,954 (4,548-24,818)
CD144+ CD62e+	5,990 (816-10,565)	7,150 (1,554-11,857)	7,952 (4,705-12,717)	8,414 (2,462-10,709)	5,780 (2,683-8,348)
CD144 CD105+	1,497 (563-1,906)	956 (286-5,741)	5,964 (2,408-13,004)	611 (95-2,881)	4,992 (1,365-11,800)
CD144+ CD31+	8,487 (272-6,534)	8,906 (2,863-12,342)	8,117 (2,863-17,726)	2,798 (1,147-4,590)	2,569 (1,865-2,890)
CD144+ CD106+	1,302 (544-2,108)	3,933 (1,962-7,237)	6,672 (3,360-12,590)	1,530 (382-3,371)	6,261 (3,496-11,961)

Table 5.3: MP counts in paediatric HIV infected patients treatment-naïve and treatment-experienced (on ART for >2 years), and age-matched healthy controls.

Isolated MPs from the plasma of treatment-experienced, uncontrolled HIV infected children, and healthy controls were analysed by flow cytometry. After ART initiation in the naïve cohort, follow up plasma samples taken at week 48 were also analysed, along with those in the ART-experienced treatment group. Counts are displayed as median (IQ range).

	HIV + Treatment-naïve t=0 vs t=48	HIV + Treatment-experienced (ART>2years) t=0 vs t=48	Healthy Controls vs HIV + Treatment-naïve t=0	Healthy Controls vs HIV + Treatment-naïve t=48	Healthy Controls vs HIV + Treatment-experienced (ART>2years) t=0	Healthy Controls vs HIV + Treatment-experienced (ART>2years) t=48	HIV + Treatment-naïve t=0 vs HIV + Treatment-experienced t=0	HIV + Treatment-naïve t=48 vs HIV + Treatment-experienced t=0	HIV + Treatment-naïve t=48 vs HIV + Treatment-experienced t=48
Total MPs									
Annexin V+	0.1016	0.3755	0.1477	0.9035	0.7804	0.9556	0.1477	0.5437	0.5118
T lymphocyte MPS									
CD3+	0.9658	0.6685	**0.0018**	**0.0008**	0.1404	0.2502	0.0501	**0.0198**	**0.0082**
CD3+ CD4+	0.6377	0.413	**0.005**	0.8090	0.1447	0.0542	0.0762	0.7360	0.2725
CD3+ CD8+	0.083	0.7334	**0.002**	0.2897	0.4415	0.3569	**0.0129**	0.7670	0.5999
Monocyte MPs									
CD14+	0.7002	0.0637	**0.0036**	**0.0008**	**0.0023**	**0.0494**	0.1446	0.1786	**0.0026**
Platelet MPs									
CD42a+	**0.0322**	0.5282	0.3769	0.6738	0.2127	0.4880	0.4221	**0.0331**	0.7319
CD42a+ CD62p+	0.3811	0.2958	0.5728	0.4969	0.7974	0.4722	0.0505	**0.0094**	0.3397
CD42a+ CD142+	0.7910	**0.0203**	0.8541	0.5979	0.7499	0.5127	0.2339	0.1210	0.6054
Endothelial MPs									
CD144+	0.6377	0.7910	**0.0014**	**0.0141**	0.2361	0.1239	**0.0225**	0.0999	0.1639
CD144+ CD54+	0.4316	**0.0052**	**0.0205**	**0.0026**	0.4732	**0.0006**	**0.0189**	**0.0048**	0.7462
CD144+ CD62e+	0.4961	0.5171	0.6057	0.2355	0.7146	0.9925	0.9999	0.5873	0.2571
CD144+ CD105+	0.0645	**0.0017**	0.9276	**0.0069**	0.3257	**0.0052**	0.4709	**0.0047**	0.7462
CD144+ CD31+	0.8501	0.6788	**0.0481**	0.0646	0.8701	0.9429	**0.0142**	**0.0071**	**0.0070**
CD144+ CD106+	0.2661	**0.0013**	**0.0017**	**0.0001**	0.8450	**0.0001**	**0.0165**	**0.0003**	0.7928

Table 5.4: P values comparing differences in MP counts between treatment groups and time points

Differences in MP counts were assessed by Wilcoxon matched-pairs signed rank test for the treatment-naïve and ART-experienced patient cohorts to compare week 0 and week 48, and a Mann-Whitney U test compared differences between groups at each time point. Differences that reached significance are highlighted.

5.4.3.1 Total MP number

Overall, there was no difference between the total number of annexin V positive MPs in both HIV positive patient groups and the healthy control population at week 0 (538,538 (IQR: 24,637-1,082,439), 1,330,219 (IQR: 315,461-1,225,816), 555,499 (IQR: 193,550-911,608); healthy control, treatment-naïve and treatment-experienced respectively, p>0.05 for comparisons between all groups). Moreover, following 48 weeks of ART in the treatment-naïve group, MP number decreased from 1,330,219 (IQR: 315,461-1,225,816) to 483,947 (IQR: 36,777-880,043) however this failed to reach statistical significance (p=0.1016 figure 5.7). In a similar fashion, the total MP number was not altered in those individuals who had been on therapy for >2 years (555,499 (IQR: 193,550-911,608) versus 406,348 (IQR: 182,999-816,932), t=0 and t=48 respectively p= 0.3755). Following this, MPs were further characterised according to their surface marker expression and consequently their parental cell type.

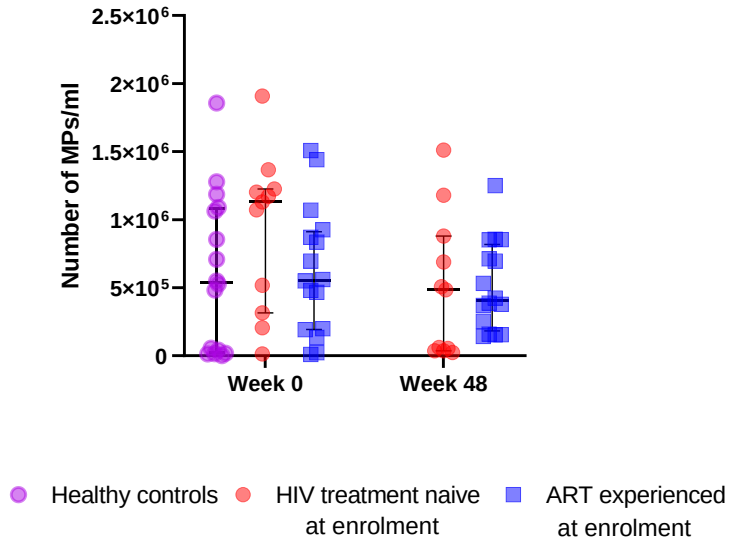

Figure 5.7: Number of circulating MPs in Paediatric HIV patients with controlled and uncontrolled viremia compared to healthy paediatric controls

Number of MPs (size <1µm and Annexin V+), were quantified by flow cytometry from plasma of HIV infected patients who were treatment-experienced (on ART for more than 2 years n= 16), or treatment-naïve (n=11) and compared to healthy age-matched controls (n=15). Samples were taken from each patient group at week 0, after which an additional sample was taken at week 48 for the ART-experienced patients, in addition to the treatment-naïve children who were initiated onto ART at the beginning of the study. Data is displayed as median with interquartile ranges. Statistical differences assessed by Wilcoxon matched-pairs signed rank test for the treatment-naïve and ART-experienced patient cohorts to compare week 0 and week 48, and a Mann-Whitney U test compared differences between groups at each time point.

5.4.3.2 Platelet MPs

Platelet MPs were primarily defined by their expression of glycoprotein IX (CD42a), then further characterised for those that were p-selectin (CD62p) positive indicative of platelet activation, and TF positive (CD142). Similar to total MP number, few differences were observed within the platelet MP subsets between groups or between time points (table 5.3 and 5.4, figure 5.8).

At week 0, the total PMP population was the same between both HIV positive patient groups and the healthy control population (13,885 (IQR: 2,487-170,429), 77,932 (IQR: 12,430-102,960), 85,679 (IQR: 30,486-133,291); healthy control, treatment-naïve and treatment-experienced respectively, $p>0.05$ for comparisons between all groups).

Following the induction of therapy in the treatment-naïve cohort, total platelet MPs decreased from 77,932 (IQR: 12,430-102,960) to 30,316 (IQR: 30,486-133,291) ($p=0.032$) by 48 weeks of therapy (Figure 5.8A), although it did not significantly alter total platelet MP number in the treatment-experienced group (85,679 (IQR: 30,486-133,291) versus 28,898 (IQR: 14,850-129,203), t=0 and t=48 respectively $p= 0.528$).

At baseline, P-selectin positive platelet MPs were lower in the treatment-naïve group when compared to HIV infected children on ART for more than 2 years at t=0 (2,450 (IQR: 846-6,534) versus 12,048 (IQR: 4,494-20,271), treatment-naïve and treatment-experienced respectively, $p=0.009$), although this did not reach significance when compared to healthy controls (2,450 (IQR: 846-6,534) versus 7,305 (IQR: 0-37,294) treatment-naïve and healthy controls respectively; $p=0.572$) (Figure 5.8B).

After 48 weeks of treatment, p-selectin positive MPs were reduced in both the treatment-naïve cohort (2,450 (IQR: 846-6,534) versus 927 (IQR: 387-3,865), t=0 and t=48 respectively *p*= 0.3811) and the treatment-experienced group compared to week 0 (12,048 (IQR: 4,494-20,271) versus 4,175 (IQR: 309-94,76), t=0 and t=48 respectively *p*= 0.2958), however these reductions failed to reach significance (Figure 5.8B).

TF positive platelet MP numbers were similar at the time of recruitment (t=0) between healthy control and ART-experienced patient groups (13,833 (IQR: 77-32,718) versus 15,108 (IQR: 5,163-28,590); healthy control and treatment-experienced respectively, *p*>0.05) (Figure 5.8C). Moreover, at baseline, there was no significant difference between TF MPs in the untreated cohort compared to the other patient populations.

TF MPs did not significantly alter after 48 weeks of therapy intervention (*p*=0.791), although CD42a+/CD142+ MPs did significantly decrease within the treatment-experienced cohort from 15,108 (IQR: 5,163-28,590) to 1,554 (IQR: 963-7,706) (*p*=0.02).

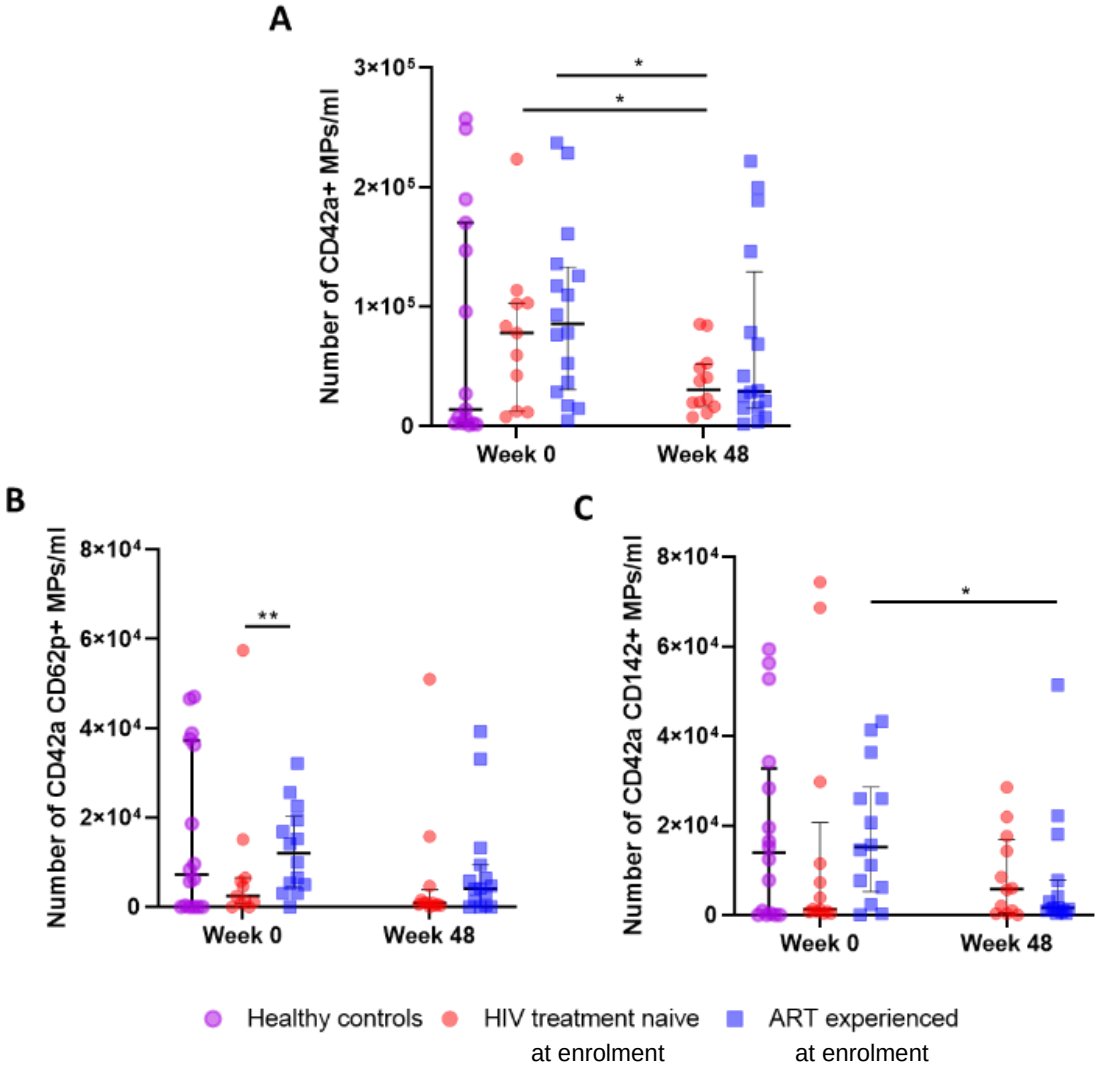

Figure 5.8: Number of circulating platelet MPs in Paediatric HIV patients with controlled and uncontrolled viremia compared to healthy paediatric controls

*Platelet MPs (size <1µm, Annexin V+ and CD42a+), were quantified by flow cytometry from plasma of HIV infected patients who were treatment-experienced (on ART for more than 2 years n=16), or treatment-naïve (n=11) and compared to healthy age-matched controls (n=15). Samples were taken from each patient group at week 0, after which an additional sample was taken at week 48 for the ART-experienced patients, in addition to the treatment-naïve children who were initiated onto ART at the beginning of the study. A) Total platelet MPs, B) Total P-selectin+ (CD62p) platelet MPs, C) Total Tissue Factor+ (CD142) platelet MPs. Data is displayed as median with interquartile ranges. Statistical differences assessed by Wilcoxon matched-pairs signed rank test for the treatment-naïve and ART-experienced patient cohorts to compare week 0 and week 48, and a Mann-Whitney U test compared differences between groups at each time point. * p<0.05, ** p<0.01, *** p<0.001, **** p<0.0001.*

5.4.3.3 T lymphocyte MPs

At week 0, T cell MPs, as defined by their CD3 expression, were greater in the treatment-naïve cohort compared to healthy controls (8,942 (IQR: 1,672-13,272) versus 46,279 (IQR: 18,741-58,753), healthy control and treatment-naïve respectively; p=0.0018), and the HIV treatment-experienced (46,279 (IQR: 18,741-58,753) versus 17,944 (IQR: 4,685-27,677), treatment-naïve versus treatment-experienced; p=0.050) (Figure 5.9A).

After 48 weeks, CD3+ MPs remained elevated in the plasma from patients initiated on ART (46,279 (IQR: 18,741-58,753) versus 34,789 (IQR: 22,861-52,349), t=0 and t=48 respectively; p=0.96) and unaltered in the ART-experienced cohort (17,944 (IQR: 4,685-27,677) versus 13,967 (IQR: 4,770-26,490) t=0 and t=48 respectively; p=0.66). The elevated MP number in the treatment-naïve patient group remained significantly elevated when compared to both healthy control patients (p=0.0008), and the treatment-experienced cohort at t=0 and t=48 despite treatment intervention (p=0.019 and p=0.0082 respectively).

TMPs were further classified according to their expression of both CD3 and CD4 (figure 5.9B and 5.9C). At baseline CD3+/CD4+ MPs were higher in the treatment-naïve patient group when compared to age-matched healthy controls (310 (IQR: 0-1,634) versus 3,442 (IQR: 746-4,352), healthy controls and treatment-naïve respectively; p=0.005), but failed to reach significance when compared to treatment-experienced patients at week 0 (3,442 (746-4,352) versus 1,530 (IQR: 95-2,602), treatment-naïve and treatment-experienced respectively; p=0.076). CD3+/CD4+ MPs were also greater in the ART-experienced cohort compared to healthy controls, although this did not reach

significance (310 (IQR: 0-1,634) versus 1,530 (IQR: 95-2,602), healthy controls and treatment-experienced respectively; *p*=0.14).

At 48 weeks, CD3+/CD4+ MPs decreased following treatment initiation in the naïve population from 3,442 (IQR: 746-4,352) to 0 (IQR: 0-4,970) (*p*=0.64 t=0 versus t=48), to within the range observed in healthy controls and children on ART.

CD3+/CD8+ also displayed a similar trend, where at baseline numbers were elevated in treatment-naïve patients compared to healthy control children (0 (IQR: 0-476) versus 4,590 (IQR: 764-18,241), healthy control children and treatment-naïve respectively; *p*=0.002), and ART-experienced children (4,590 (IQR: 764-18,241) versus 155 (IQR: 0-1052) treatment-naïve and treatment-experienced respectively; *p*=0.013) (figure 5.9C).

CD3+/CD8+ TMPs decreased after therapy initiation within the naïve cohort at week 48, although this change was not significant (4,590 (IQR: 764-18,241) versus 331 (IQR: 0-1,657), t=0 and t=48 respectively; *p*=0.083), levels did decrease to within the range of MPs found in the plasma of healthy controls and treatment-experienced children.

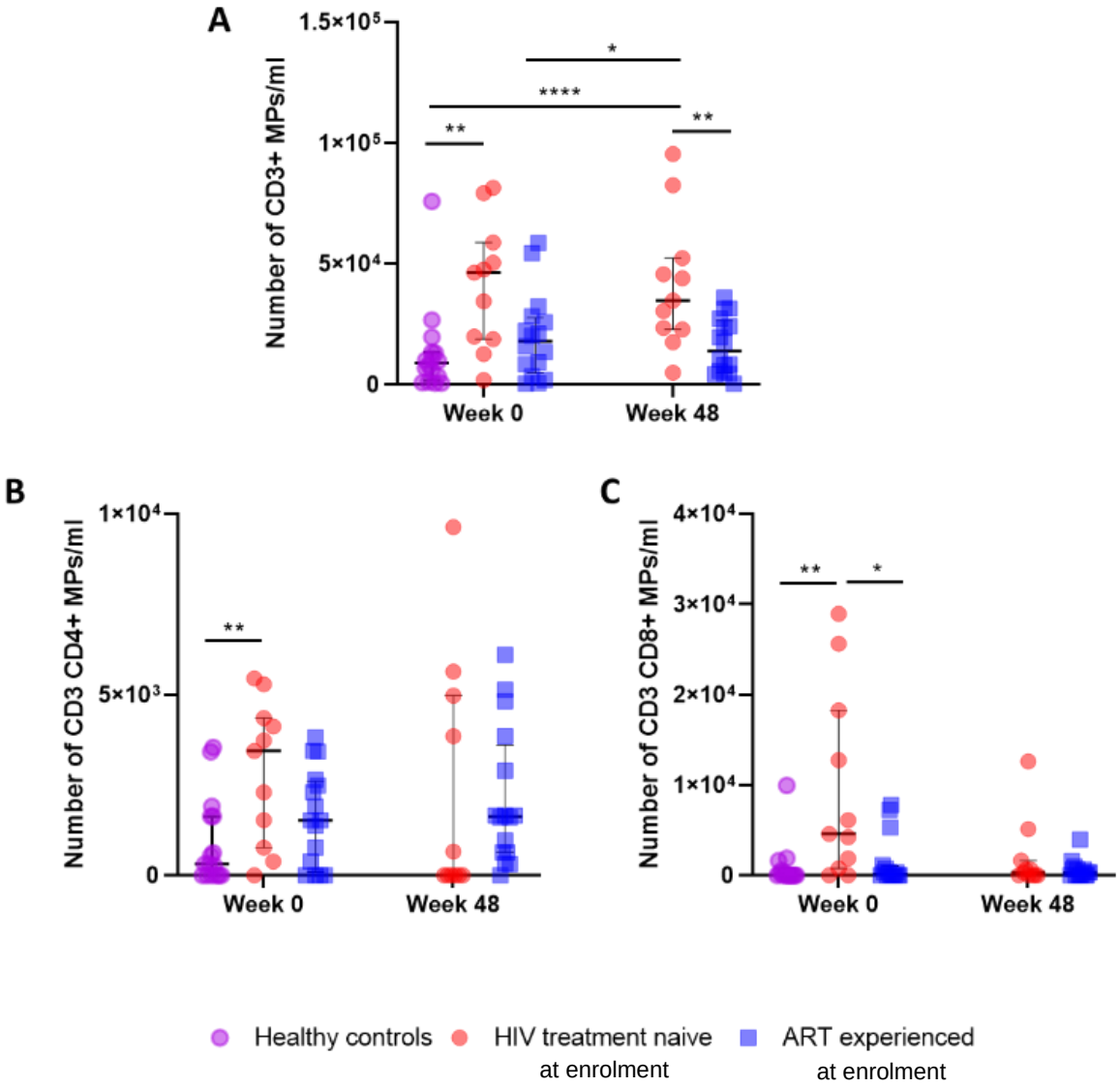

Figure 5.9: Number of circulating T lymphocyte MPs in Paediatric HIV patients with controlled and uncontrolled viremia compared to healthy paediatric controls

*T cell MPs (size <1µm, Annexin V+ and CD3+), were quantified by flow cytometry from plasma of HIV infected patients who were treatment-experienced (on ART for more than 2 years n=16), or treatment-naïve (n=11) and compared to healthy age-matched controls (n=15). Samples were taken from each patient group at week 0, after which an additional sample was taken at week 48 for the ART-experienced patients, in addition to the treatment-naïve children who were initiated onto ART at the beginning of the study. A) Total T cell MPs, B) Total T helper cell (CD4+) MPs, C) Total Cytotoxic T cell (CD8+) MPs. Data is displayed as median with interquartile ranges. Statistical differences assessed by Wilcoxon matched-pairs signed rank test for the treatment-naïve and ART-experienced patient cohorts to compare week 0 and week 48, and a Mann-Whitney U test compared differences between groups at each time point. * p<0.05, ** p<0.01, *** p<0.001, **** p<0.0001.*

5.4.3.4 Monocytic MPs

MPs derived from monocytes were quantified through their expression of CD14 and Annexin V (figure 5.10). At baseline, MMPS were elevated within both the treatment-naïve group compared to healthy control patients (12,927 (IQR: 4,321-23,346) versus 36,480 (IQR: 27,200-57,711), healthy control and treatment-naïve respectively; *p*=0.0036) and experienced ART patients when compared to healthy controls at t=0 (12,927 (IQR: 4,321-23,346) versus 26,429 (IQR: 17,670-39,815), healthy control and treatment-experienced respectively; *p*=0.0023).

After 48 weeks of treatment, MMPS remained elevated in the treatment-naïve cohort (34,291 (IQR: 22,309-69,171), *p*= 0.7002; t=0 compared to t=48) and within the treatment-experienced patient group compared to baseline (19,146 (IQR: 15,803-25,216), *p*= 0.064; t=0 compared to t=48). This was reflected in increased monocyte-derived MPs in comparison to healthy controls (treatment-naïve: 34,291 (IQR: 22,309-69,171) versus 12,927 (IQR: 4,321-23,346), treatment-naïve t=48 and healthy controls respectively; *p*=0.0008, treatment-experienced: 19,146 (IQR: 15,803-25,216) versus 12,927 (IQR: 4,321-23,346), treatment-experienced t=48 and healthy controls respectively; *p*=0.049).

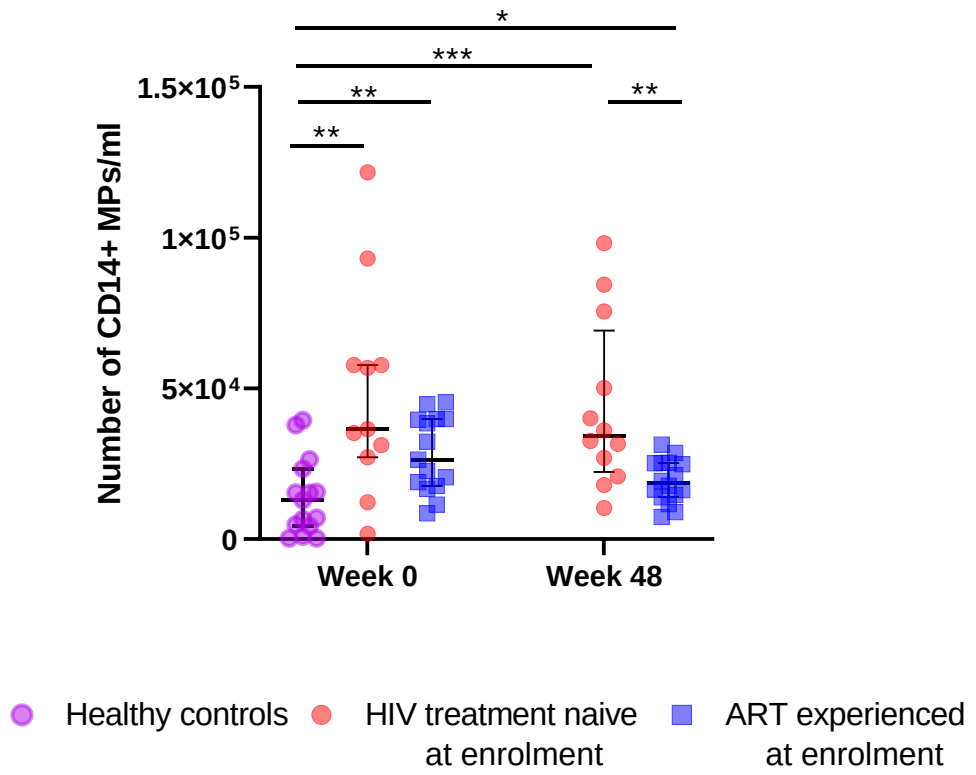

Figure 5.10: Number of circulating monocytic MPs in Paediatric HIV patients with controlled and uncontrolled viremia compared to healthy paediatric controls

*Total monocytic MPs (size <1µm, Annexin V+ and CD14+), were quantified by flow cytometry from plasma of HIV infected patients who were treatment-experienced (on ART for more than 2 years n=16), or treatment-naïve (n=11) and compared to healthy age-matched controls (n=15). Samples were taken from each patient group at week 0, after which an additional sample was taken at week 48 for the ART-experienced patients, in addition to the treatment-naïve children who were initiated onto ART at the beginning of the study. Data is displayed as median with interquartile ranges. Statistical differences assessed by Wilcoxon matched-pairs signed rank test for the treatment-naïve and ART-experienced patient cohorts to compare week 0 and week 48, and a Mann-Whitney U test compared differences between groups at each time point. * p<0.05, ** p<0.01, *** p<0.001, **** p<0.0001.*

5.4.3.5 Endothelial MPs

EMPs were characterised according to their CD144 and Annexin V expression, as CD144 is almost exclusively expressed on endothelial cells (figure 5.11). At baseline, the total number of CD144+ EMPs were significantly elevated in children with uncontrolled HIV compared to uninfected children (14,702 (IQR: 1,642-26,695) versus 46,661 (IQR: 20,653-51,216), healthy controls and treatment-naïve respectively; p=0.0014) and the HIV controlled cohort (19,315 (IQR: 5,710-35,422) versus 46,661 (IQR: 20,653-51,216), treatment-experienced and treatment-naïve respectively; p=0.023).

Following 48 weeks of ART treatment, EMP numbers reduced from 46,661 (IQR: 20,653-51,216) MPs per ml to 25,512 (IQR: 18,223-59,081) MPs per ml (p=0.64) in the treatment-naïve group, although these numbers remained significantly elevated compared to controls (25,512 (IQR: 18,223-59,081) versus 14,702 (IQR: 1,642-26,695), treatment-naïve week 48 and healthy controls respectively; p=0.014). No changes were observed in EMP numbers over the 48-week duration in the ART-experienced HIV infected children (19,315 (IQR: 5,710-35,422) versus 20,871 (IQR: 8,991-37,166), t=0 and t=48 respectively; p=0.79), which also fell within the EMP healthy control range.

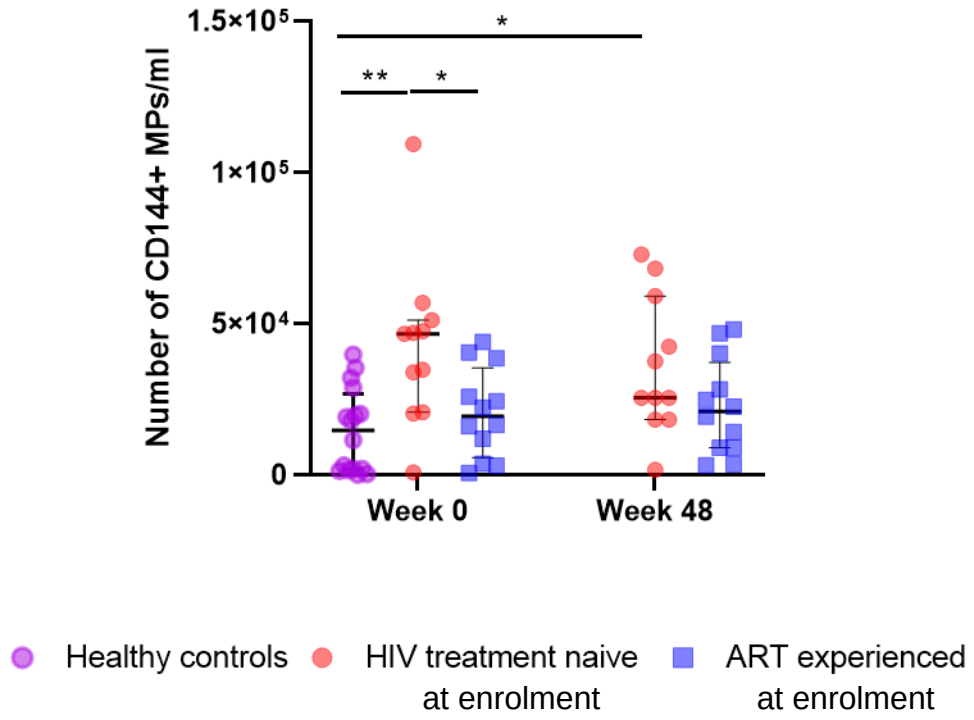

Figure 5.11: Number of circulating endothelial MPs in Paediatric HIV patients with controlled and uncontrolled viremia compared to healthy paediatric controls

*Endothelial cell derived MPs (size <1µm, Annexin V+ and CD144+), were quantified by flow cytometry from plasma of HIV infected patients who were treatment-experienced (on ART for more than 2 years n=16), or treatment-naïve (n=11) and compared to healthy age-matched controls (n=15). Samples were taken from each patient group at week 0, after which an additional sample was taken at week 48 for the ART-experienced patients, in addition to the treatment-naïve children who were initiated onto ART at the beginning of the study. Data is displayed as median with interquartile ranges. Statistical differences assessed by Wilcoxon matched-pairs signed rank test for the treatment-naïve and ART-experienced patient cohorts to compare week 0 and week 48, and a Mann-Whitney U test compared differences between groups at each time point. * p<0.05, ** p<0.01, *** p<0.001, **** p<0.0001.*

Further characterisation of EMPs by their expression of common markers found in the literature (CD54+ (ICAM-1), CD106+ (VCAM-1), CD105 (Endoglin), CD31 (PECAM-1)) was undertaken. At baseline, ICAM-1 positive endothelial MPs were higher in the naïve cohort than both healthy controls (2,507 (IQR: 1,108-4,122) versus 11,608 (IQR: 3,347-16,579), healthy control and treatment-naïve respectively; *p*=0.021) and treatment-experienced HIV infected children (11,608 (IQR: 3,347-16,579) versus 3,954 (IQR: 860-6,235), treatment-naïve and treatment-experienced respectively; *p*=0.0189) (figure 5.12A). Levels of ICAM-1+ EMPs were comparable between treatment-experienced children and healthy controls at baseline.

After 48 weeks of treatment in the naïve population, ICAM-1 positive EMPs remained elevated despite ART intervention (11,608 (IQR: 3,347-16,579) versus 13,033 (IQR: 5,027-19,879), t=0 and t=48 respectively; *p*=0.4316) and in the treatment-experienced population increased (3,954 (IQR: 860-6,235) versus 9,954 (IQR: 4,548-24,818), t=0 and t=48 respectively; *p*=0.0052) (figure 5.12A). These elevations in ICAM-1 EMPs in both HIV infected cohorts, were greater than EMP numbers in healthy controls (13,033 (IQR: 5,027-19,879) versus 2,507 (IQR: 1,108-4,122), treatment-naïve t=48 and healthy control respectively; *p*=0.0026 and 9,954 (IQR: 4,548-24,818) versus 2,507 (IQR: 1,108-4,122), treatment-experienced t=48 and healthy control respectively; *p*=0.0006), such that at 48 weeks there was no significant difference between both ART-treated cohorts.

At week 0, EMPs positive for both CD144 and endoglin (CD105) were similar in both HIV positive patient groups and the healthy control population (1,497 (IQR: 563-1,906), 956

(IQR: 286-5,741), 611 (IQR: 95-2,881); healthy control, treatment-naïve and treatment-experienced respectively, $p>0.05$ for comparisons between all groups) (figure 5.12B).

After 48 weeks of treatment from baseline, CD105 positive EMPs increased in both the HIV treatment-naïve patient group from 956 (IQR: 286-5,741) MPs per ml to 5,964 (IQR: 2,408-13,004) MPs per ml (t=0 and t=48 respectively; $p=0.064$) and in the treatment-experienced cohort from 611 (IQR: 95-2,881) MPs per ml to 4,992 (IQR: 1,365-11,800) MPs per ml (t=0 and t=48 respectively; $p=0.0017$). This elevation was significantly more than EMP levels found in healthy controls ($p=0.0069$ healthy control versus treatment-naïve, and $p=0.0052$ healthy control versus treatment-experienced).

This trend was also observed for EMPs co-stained with VCAM-1 (CD106), an adhesion molecule upregulated on endothelial cells following activation. At baseline, MP number was higher within the treatment-naïve patient group than healthy controls and treatment-experienced (1,302 (IQR: 544-2,108) versus 3,933 (IQR: 1,962-7,237), healthy control and treatment-naïve respectively; $p=0.0017$ and 3,933 (IQR: 1,962-7,237) versus 1,530 (IQR: 382-3,371), treatment-naïve and treatment-experienced respectively; $p=0.017$) (figure 5.12C).

After 48 weeks, this population of EMPs increased within the treatment-naïve population from 3,933 (IQR: 1,962-7,237) MPs per ml to 6,672 (IQR: 3,360-12,590) MPs per ml (t=0 and t=48 respectively), although this failed to reach significance ($p=0.26$), but did when compared to healthy control children ($p=0.0001$). A significant increase was however observed in the treatment-experienced cohort (1,530 (IQR: 382-3,371 versus

6,261 (IQR: 3,496-11,961), t=0 and t=48; *p*=0.0013), which remained significant when compared to healthy control children at baseline (*p*=0.0001).

Similarly, PECAM-1 (CD144+/CD31+) EMPs were higher in children with uncontrolled viremia compared to healthy children and treatment-experienced at week 0 (8,487 (IQR: 272-6,534) versus 8,906 (IQR: 2,863-12,342), healthy control and treatment-naïve respectively; *p*=0.048, and 2,798 (IQR: 1,147-4,590) versus 8,906 (IQR: 2,863-12,342), treatment-experienced and treatment-naïve respectively; *p*=0.014) (figure 5.12D).

No differences were observed in CD31+ EMP number following 48-weeks of ART treatment initiation in naïve patients (8,906 (IQR: 2,863-12,342) versus 8,117 (IQR: 2,863-17,726), t=0 and t=48 respectively; *p*=0.85), and treatment-experienced populations (2,798 (IQR: 1,147-4,590) versus 2,569 (IQR: 1,865-2,890), t=0 and t=48 respectively; *p*=0.68). A marked improvement in CD31+ EMP number was clearly seen in the controlled HIV cohort at each time point in the study, comparable to numbers found in healthy controls at week 0 (Figure 5.12D).

Finally, no significant alterations in E-selectin (CD62e+) EMPs were observed between patient groups at t=0 or following treatment initiation at week 48 for the treatment-naïve children and the treatment-experienced group (figure 5.12E).

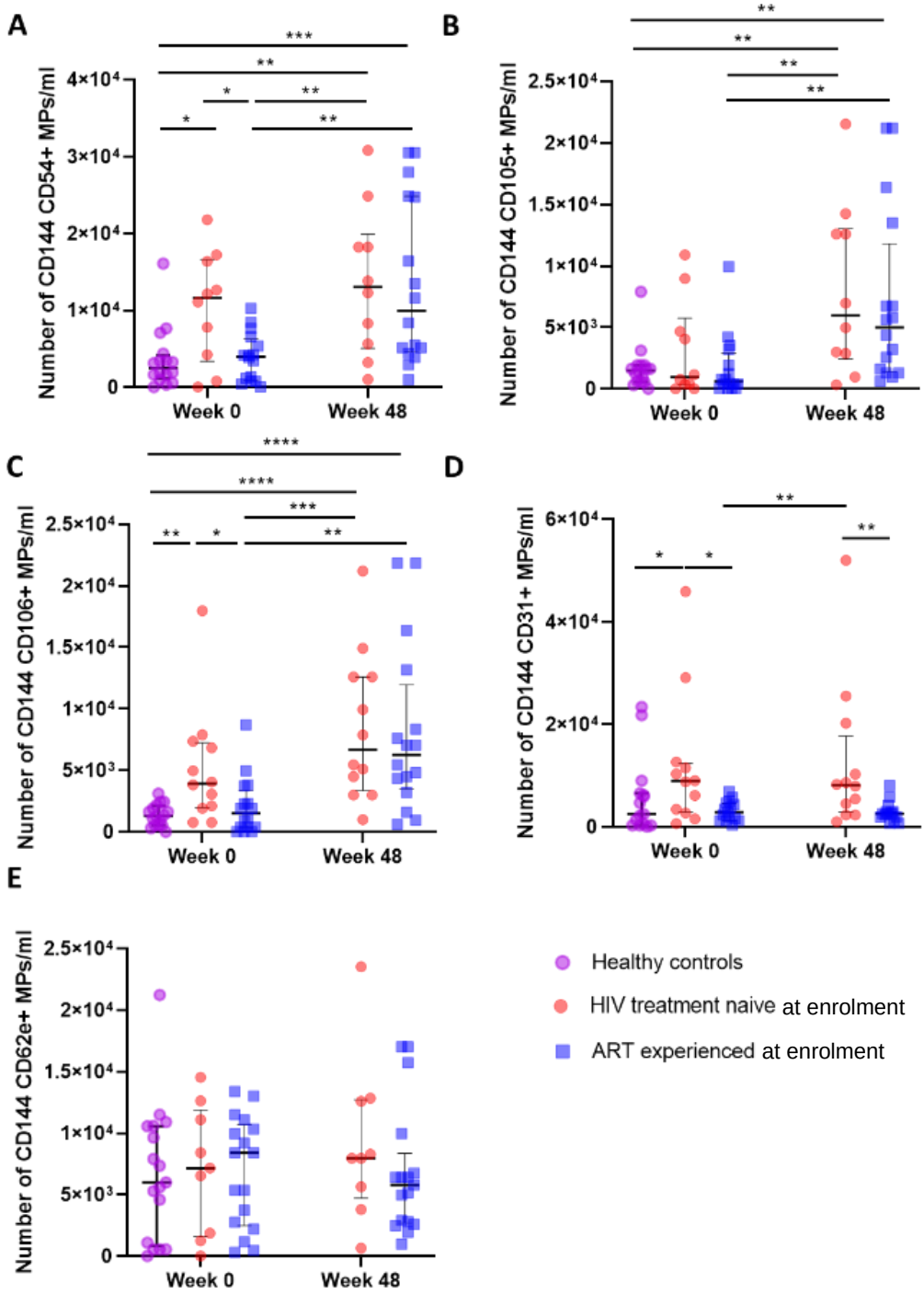

Figure 5.12: Number of circulating endothelial MPs phenotypes in Paediatric HIV patients with controlled and uncontrolled viremia compared to healthy paediatric controls

*Endothelial cell derived MPs (size <1µm, Annexin V+ and CD144+), were quantified by flow cytometry from plasma of HIV infected patients who were treatment-experienced (on ART for more than 2 years n=16), or treatment-naïve (n=11) and compared to healthy age-matched controls (n=15). Samples were taken from each patient group at week 0, after which an additional sample was taken at week 48 for the ART-experienced patients, in addition to the treatment-naïve children who were initiated onto ART at the beginning of the study. A) Total ICAM-1+ (CD54) endothelial MPs, B) Total Endoglin+ (CD105) endothelial MPs, C) Total VCAM-1+ (CD106) endothelial MPs, D) Total PECAM-1+ (CD31) endothelial MPs, E) Total e-selectin+ (CD62e) endothelial MPs. Data is displayed as median with interquartile ranges. Statistical differences assessed by Wilcoxon matched-pairs signed rank test for the treatment-naïve and ART-experienced patient cohorts to compare week 0 and week 48, and a Mann-Whitney U test compared differences between groups at each time point. * p<0.05, ** p<0.01, *** p<0.001, **** p<0.0001.*

5.5 Discussion

Initial experiments were performed in this chapter to optimise MP fixation, allowing the measurement of HIV infected plasma samples in containment level 2 facilities. For this aspect of method optimisation, a range of paraformaldehyde concentrations at 1%, 2% and 4% and BD Cell fix at 0.5x were tested. These followed institute safety guidelines allowing sample analysis in communal containment level 2 laboratories, as they have previously demonstrated the ability to effectively inactivate HIV particles (Martin.L, 1994).

From preliminary experiments, an obvious increase in annexin V positive staining was observed with paraformaldehyde at all concentrations, this resulted in BD cell fix 0.5x being tested as an alternative fixation step. No significant differences in annexin V staining were observed between unfixed and fixed samples, along with all MP markers of interest. Furthermore, the quantity of all fixed MP phenotypes were calculated to be within 95% confidence limits of corresponding unfixed samples, thus BD cell fix 0.5x was the selected method used the analysis of patient samples. This novel fixation method safely allows the characterisation of MPs from HIV infected samples in a containment level 2 facility.

5.5.1 MPs in children with HIV infection

MPs are found elevated in a number of inflammatory diseases including CVD (Berezin et al., 2015; Koga et al., 2005; Leroyer et al., 2007) and HIV (Corrales-Medina et al., 2010; Hijmans et al., 2019; Kelly, 2016; Mayne et al., 2012; Da Silva et al., 2011) when compared to healthy age-matched controls.

Initially, no differences in total MP number between either HIV infected cohorts and healthy controls were observed however, within each MP group, phenotypes fluctuated following treatment initiation. Therefore, we studied specific cell-derived MPs from T cell, platelet, endothelial and monocytic origin within an HIV-positive paediatric population receiving treatment, an HIV population following treatment initiation and healthy age-matched controls.

5.5.1.1 T cell MPs

T cell MPs were defined by their expression of CD3, and the co-expression of CD4 or CD8. Compared to healthy controls, overall T cell MPs (CD3+) increased in the treatment-naïve cohort and remained elevated at 48 weeks following the initiation of ART.

Within the CD3+ population, the numbers of T helper cell (CD4) and cytotoxic T cell (CD8) MPs were quantified. At week 0, CD3+/CD4+ MPs were elevated only in the treatment-naïve cohort compared to healthy controls and decreased with treatment initiation, falling within normal ranges.

As cellular MPs are released upon activation and apoptosis, elevations of these populations in treatment-naïve children are likely to be reflective of continued CD4+ T cell activation and T cell turnover. Following the initiation of ART in both adults and children, CD4+ T cell numbers recover, along with a reduction in their activation (Bosch et al., 2006; Funderburg et al., 2013).

CD3+/CD8+ MPs also displayed a similar trend whereby MPs were elevated within the naïve cohort compared to healthy controls and treatment-experienced; these levels also decreased at week 48. In treatment-naïve individuals CD4+ cell counts are decreased as a result of the viral infection, compared to healthy controls, followed by a marked expansion of CD8+ cells (resulting in a low CD4/CD8 ratio), and their activation (van den Dries et al., 2017; Masiá et al., 2016; Sainz et al., 2013). Therefore, this elevated MP phenotype within the uncontrolled individuals may be indicative of this activated and expanded population.

Moreover, in uncontrolled HIV infection, children who were treatment-naïve displayed higher counts of CD8+ TMPs compared to CD4+ TMPs. This is likely to be reflective of the imbalance of T helper cell and cytotoxic T cell cells that is observed in children with uncontrolled HIV infection (Sainz et al., 2013). Following therapy intervention and treatment experience, both T cell MP phenotypes normalise with healthy controls. This may be indicative of improved T cell subset ratio, as a result of increased CD4+ counts and the normalisation of CD8+ counts, and a decrease in activated T cell numbers following successful viral suppression (van den Dries et al., 2017; Guillé et al., 2019; Masiá et al., 2016; Sainz et al., 2013).

It is important to note however, that overall CD3+ MP counts do decrease following treatment initiation, but are still significantly increased when compared to healthy controls, unlike the individual CD4+ and CD8+ which normalise to controls. The CD3+ MPs do however normalise with controls following long term ART usage as with the individual CD4+ and CD8+ MPs.

These initial differences may be due to the smaller MP numbers of these individual CD4+ and CD8+ populations that are present in much lower numbers compared to total CD3+ MPs, along with the limitation of small plasma volumes. This means that MP numbers within these subsets, are nearing the limit of detection for this enumeration method using flow cytometry, presenting a limitation to this quantification method.

Furthermore, very little is currently known about individual T cell MP populations and their conditions under which they are released in vivo. Knowing that the surface markers which are present on the MP surface is not a regulated process it is unlikely that all CD4+ T cells would release MPs that displayed both CD3+ and CD4+, likewise with CD8+. Thus, in order to further understand the predictive nature of these individual populations, and their value as an indicator of T helper and cytotoxic T cell apoptosis, proliferation or activation, it would require further research into their mechanism of release, and their correlation with T cell clinical measures in these patients.

5.5.1.2 Platelet MPs

MPs of a platelet origin make up the largest proportion of total circulating MPs in the blood (Arraud et al., 2014). In this study, no significant differences were observed in total PMP counts, as defined by their CD42a expression, between any of the patient groups. This phenotype did significantly decrease in the naïve cohort following treatment intervention, which may reflect the effectiveness of ART to reduce immune activation especially within the first year of treatment initiation (van den Dries et al., 2017). Similarly, no differences were observed across each of the HIV infected groups

when compared to healthy controls, although CD62p+ platelet MPs were elevated in the treatment-experienced cohort when compared to treatment-naïve children.

In adults, it has been reported that overall PMP numbers are elevated when compared to healthy controls however, P-selectin+ PMP were similar among groups irrespective of treatment regime or treatment duration (Corrales-Medina et al., 2010). This finding that PMPs are elevated in HIV infected adults was supported by Hijmans., *et al* (2019) however, within this study CD62p was used alone to define MPs from a platelet origin, and Annexin V was not used to define the MP gate (Hijmans et al., 2019). CD62p is also expressed on the surface of activated endothelial cells thus, differences in these studies may be attributed to the non-specificity of this marker or the proportion of Annexin V negative MPs. Irrespective of these methodological differences both of these studies conclude that PMPs are elevated in adults with HIV infection receiving treatment.

Although no differences were observed between the treatment-experienced cohort and healthy controls for any of the platelet phenotypes in this case, there is a trend that with treatment these MPs are elevated.

5.5.1.3 Monocyte MPs

The finding that monocytic MPs were significantly elevated across all HIV infected patient groups in comparison to healthy control children is comparable to Hijmans., *et al's* (2019) study, where monocytic MPs were elevated in adults with HIV infection (Hijmans et al., 2019). The failure of these levels to normalise following treatment supports evidence that monocytes remain activated following ART initiation

demonstrated by higher sCD14 in plasma of children and adults following therapy intervention (Bi et al., 2016; Dysangco et al., 2017; Hattab et al., 2014; Sereti et al., 2017).

Although we were unable to evaluate levels of TF positive monocytic MPs in this study, these have been reported to increase in several CVDs (Chiva-Blanch et al., 2017; Christersson et al., 2017) with pro-coagulant properties aiding the initiation of the coagulation pathway (Del Conde et al., 2005; Falati et al., 2003).

5.5.1.4 Endothelial MPs

Elevations in MPs from an endothelial origin have been reported in adults with HIV infection (Hijmans et al., 2019; Kelly, 2016; Da Silva et al., 2011). Multiple surface markers have been reported in literature to describe endothelial MPs including CD144 (Leroyer et al., 2007), CD54 (Jimenez et al., 2003; Leroyer et al., 2007), CD62e (Abid Hussein et al., 2003; Gelderman and Simak, 2008; Jimenez et al., 2003), CD105 (Gelderman and Simak, 2008), CD106 (Abid Hussein et al., 2003; Jimenez et al., 2003) and CD31 (Jimenez et al., 2003; Leroyer et al., 2007). *In vitro* studies have suggested that endothelial cells release phenotypically different MPs upon activation and apoptosis, whereby constitutive markers (CD31, CD51 and CD105) are increased in cells undergoing apoptosis induced by serum starvation, and inducible markers (CD54, CD62e and CD106) are elevated following TNF-α activation (Jimenez et al., 2003).

Although a range of surface antigens have been used to describe EMPs, many of these markers are not exclusively expressed on endothelial cells, thus in this study, a

combination of Annexin V and CD144 were used to identify MPs exclusively from endothelial populations.

Total EMPs (CD144+) were elevated in treatment-naïve children, whereas EMP numbers were normalised to levels found in healthy control children following long term ART exposure. Within the uncontrolled HIV infected children, inducible markers of endothelial activation such as CD54 and CD106 present on MPs display a trend whereby numbers were elevated compared to healthy children; or increased in the case of CD106. These phenotypes normalised to healthy control values in the treatment-experienced group, demonstrating the improvement in endothelial function with longer-term ART use.

We found no differences in CD62e+/CD144+ MP numbers between HIV infected patient groups or healthy controls. Previous reports of CD62e+ EMPs elevated in HIV have only been demonstrated in adult patient groups, thus age, ART duration and regime may have influenced this phenotype in part explaining these differences (Hijmans et al., 2019; Kelly, 2016).

Furthermore, the constitutive marker CD105 was also increased on CD144+ EMPs following ART initiation, and significantly elevated compared to healthy controls. CD105 is expressed on proliferating and angiogenic endothelial cells (Kopczyńska and Makarewicz, 2012), thus the elevation of this phenotype following ART initiation may be indicative of a reparative phase of the endothelium following therapy intervention. This would also support the improvements in IMT and PWV reported within the treatment-

naïve cohort following therapy intervention in the original CHAPAS-3 CV sub-study (Kenny, 2016).

CD31 is also a constitutive endothelial marker found on apoptotic endothelial cells and their corresponding MPs *in vitro* (Jimenez et al., 2003). These MPs remained elevated in treatment-naïve children following treatment initiation, however normalised to healthy control levels following long-term ART. In uncontrolled HIV infection, systemic inflammation contributes to endothelial activation and damage, along with HIV encoded proteins that also directly interact with the endothelium promoting its dysfunction through; enhanced proliferation, apoptosis, cytokine secretion and upregulation of adhesion molecules (Anand et al., 2018). Thus, the elevation of this phenotype within the treatment-naïve cohort along with activated EMP markers may be indicative of enhanced endothelial activation and apoptosis following the interaction with viral proteins and inflammatory mediators.

Moreover, it has been suggested that the ratio between CD62e+ (Activated EMPs) and CD31+ (CD42a-) (Apoptotic EMPs) MPs may indicate an activated (≥10%) or apoptotic (≤1%) endothelial status *in vitro* (Jimenez et al., 2003). Unfortunately, in this study, the limitation in the number of flow cytometry antibody panels which could be designed for the small plasma volume failed to allow the quantification of CD42a-/CD31+ MPs.

Although the Immunophenotyping of EMPs allows us to speculate about the status of the endothelial cell from which it's derived, it is unclear if the process of surface antigen presentation during MP formation is random, or tightly regulated; thus, irrespective of

its marker expression it is evident that EMPs reflect the presence of endothelial dysfunction, proliferation and injury.

Taken together, this data suggests that MPs from an endothelial origin are increased in treatment-naïve HIV infected children, indicative of endothelial inflammation and damage. This supports literature whereby biomarkers of endothelial dysfunction are elevated compared to age-matched controls in both untreated adults, (Dysangco et al., 2017; Hileman et al., 2013; Kristoffersen et al., 2009; O'Halloran et al., 2015) and children (Kenny, 2016; Sainz et al., 2014) with HIV infection.

In this study CD54+, CD105+, CD31+ and CD106+ were still increased after 48 weeks of treatment however after longer exposure to therapy (median 3.77 years) levels were comparable to healthy controls. This is also reflected in literature whereby these markers of endothelial activation and clinical markers were also reduced following treatment initiation in children (Chanthong et al., 2014; Eckard et al., 2014; Ross et al., 2010) and adults (Gupta et al., 2012; Hileman et al., 2013; Kristoffersen et al., 2009; O'Halloran et al., 2015). In some cases, decreases in these markers were observed as early as four weeks (Padilla et al., 2011) following therapy intervention, however in other studies reductions were only reported after 24 months (Ticona et al., 2015). EMPs found in the treatment-experienced patient group were comparable to age-matched healthy controls suggesting that endothelial activation and damage is reduced with treatment.

This finding supports results from the primary CV sub-study from which this cohort of patients was selected. Within the sub-study, elevations in IMT were reduced in children receiving ART for a mean of 3.9 years and continued to improve over the 2-year duration of the study to return to within healthy ranges (Kenny, 2016).

5.5.2 Summary

In children infected with HIV receiving antiretroviral treatment for a median of 3.77 years, circulating levels of platelet, endothelial and T cell MPs were all found to return to ranges found in healthy controls.

Conversely, this study demonstrates that levels of circulating monocytic MPs (CD14) were elevated in children with untreated HIV infection and remained increased despite treatment intervention in this group. The increase in this MP phenotype was also observed within the treatment-experienced cohort following long term exposure to ART, compared to healthy control children.

In vitro data presented in this thesis, along with published literature has demonstrated the release of MMPS following their activation. Thus, elevated MP levels found within this patient cohort are likely to be reflective of their persistent activated status in both controlled and uncontrolled HIV (Ben-Hadj-Khalifa-Kechiche et al., 2010; Eyre et al., 2011; Wen et al., 2014).

Moreover, this MP phenotype (CD14+/Annexin V+) has demonstrated the functional ability to induce endothelial dysfunction *in vitro*, through the upregulation of adhesion molecules, cytokine secretion, and leukocyte activation (Cerri et al., 2006; Wang et al.,

2011; Wen et al., 2014). Data presented in this thesis also demonstrates that activated monocytes release MPs that play a functional role in further monocytic activation, though the induction of pro-inflammatory cytokine release, upregulation of adhesion molecules, elevating endothelial adhesion and subsequent transendothelial migration. Thus, an elevation in circulating MMPS in HIV is strongly suggestive of an environment that would promote monocyte activation and further MMP production.

The interaction between endothelial cells and monocytes with MMPS presents an additional mechanism through which endothelial dysfunction, atherogenesis and chronic inflammation may be enhanced within this population. The elevation of these MPs in children with HIV infection, despite the control of viral suppression, may therefore play a contributing role in accelerating atherosclerotic disease progression from a young age.

The increased numbers of MMPS indicates the persistent activation of circulating monocytes *in vivo*, supporting literature within which the observation of an inflammatory monocyte phenotypes (Han et al., 2009; Kim et al., 2010; McCausland et al., 2015; Tippett et al., 2011), elevations in biomarkers indicative of monocyte activation (Alvarez et al., 2017; Bi et al., 2016; Dysangco et al., 2017; Sereti et al., 2017) and circulating monocyte MPs (Hijmans et al., 2019) that have been reported in children and adults with HIV infection.

Therefore, the role that activated monocytes and their corresponding MPs play in atherosclerosis initiation, may be key mechanistic factors to accelerated disease pathogenesis and the increased risk of asymptomatic atherosclerosis found within the

paediatric population ((Idris et al., 2015; Miller et al., 2008; Werner et al., 2010). Furthermore, this persistent monocyte activation and functional impairment continues into adulthood, contributing to elevated CV risk and the development of clinical CVD.

5.5.3 Study limitations

Flow cytometry was the selected technique to analyse MPs in this study, as it provided the advantage of measuring multiple markers simultaneously in one sample with high throughput. However, using this method does introduce some limitations. MPs range in diameter from 0.1-1µm making smaller MPs difficult to distinguish from background noise and some of which may be below the limit of detection. To help improve the visualisation of MPs from background noise an Annexin V stain was used to bind to the exposed PS on their surface. Although this helped to confirm the MP population, in recent years it has been reported that a proportion of MPs are PS negative (Connor et al., 2010), however as Annexin V was used as the primary MP marker this Annexin V negative population was excluded from this analysis.

Alternative methods of MP identification and quantification have been described including fluorescent microscopy, dynamic light scattering, transmission electron microscopy, western blotting and ELISA assays (Gradziuk and Radziwon, 2017). Although each of these techniques have individual advantages and disadvantages associated with them, flow cytometry is the only method that allows the analysis of multiple markers and different MP subtypes at the same time. For this reason, in this clinical setting flow cytometry is most appropriate, however efforts should be focused on standardising this technique to allow for easier comparisons in future studies.

Chapter 6 – Conclusions

With the successful development of combination ART, HIV is no longer considered a fatal disease (Deeks et al., 2013), with patients receiving drug treatments expected to live a near-normal life expectancy (Palella et al., 1998). As HIV infected individuals are living longer, the rate of non-AIDS co-morbidities emerging, with CVD the leading cause of death within this population (Benjamin EJ et al., 2017; Shah et al., 2018; Smith et al., 2014). Through a number of complex interactions, people living with HIV infection show evidence of persistent immune activation leading to accelerated atherosclerosis disease progression (De Lima et al., 2018).

Biomarkers of immune activation and inflammation remain elevated in the plasma of both adults (Hsue et al., 2009; Hunt et al., 2008) and children (De Lima et al., 2018; Miller et al., 2010; Ross et al., 2010) with HIV infection despite successful viral suppression with ART. Furthermore, structural and functional changes of the endothelium provides evidence for asymptomatic atherosclerosis (Chanthong et al., 2014; Charakida et al., 2005, 2009; Hanna et al., 2016; Ross et al., 2010).

A biomarker is defined as a biological molecule which is indicative of normal or pathogenic processes used to identify an underlying condition or disease. One particular biomarker of interest explored in this thesis are MPs, as these circulating particles demonstrated predictive, functional and therapeutic properties in a number of disease states *in vitro* and *in vivo*. These extracellular vesicles may serve as novel biomarkers for the underlying pathophysiological processes of CVD, including thrombosis,

inflammation, endothelial dysfunction and angiogenesis, with the additional ability to provide information about the status of various cell types within a particular disorder (Dickhout and Koenen, 2018). Thus, MP enumeration may provide a more sensitive measure compared to current techniques including blood pressure and cholesterol with the growing potential to detect early stage CVD in clinical asymptomatic patients, allowing early intervention. Furthermore, the correlation between MP origin and numbers, with illness and disease may provide an additional powerful tool in disease progression and drug monitoring (Chen et al., 2018).

With respect to CVD pathogenesis, MPs have also demonstrated the ability to accelerate disease progression through disturbing endothelial homeostasis and enhancing endothelial dysfunction, as discussed in detail in Chapter 5. Circulating MPs quantified in the plasma of HIV infected adults have been shown to increase in MP number from an endothelial, platelet and leukocyte origin (Corrales-Medina et al., 2010; Hijmans et al., 2019; Kelly, 2016; Mayne et al., 2012; Da Silva et al., 2011), in addition to functional properties that may accelerate atherosclerosis pathogenesis through endothelial cell inflammation, oxidative stress, senescence and apoptosis (Hijmans et al., 2019).

Data presented in this thesis aimed to improve the understanding of the dynamics of circulating MPs in paediatric HIV infection following ART initiation, and in long term ART usage. In addition, MPs were isolated from a monocytic origin to allow the investigation of their function on monocytes isolated from healthy adults using a novel isolation method. By addressing the aims of this thesis, data presented here provides an insight as

to how this elevated MP phenotype may contribute to CVD pathogenesis in HIV infected individuals from a young age.

As monocytes play one of the key roles in atherosclerosis and display an activated phenotype in a number of inflammatory diseases including HIV, the first aim of this thesis was to optimise a novel isolation method of monocytes directly from whole blood; addressed in Chapter 3. Current isolation procedures either rely on binding to the CD14 receptor (FACS sorting and Positive isolation) providing potential impairments in functionality (Bhattacharjee et al., 2017; Kho et al., 2017), requiring prior PBMC purification that demonstrates alterations in surface marker expression (Mukherjee et al., 2015; Nieto et al., 2012; Tippett et al., 2011), or fully depletes CD16+ populations (negative selection).

A novel form of isolation was developed and optimised as part of an MTA agreement with StemCell™ Technologies, which provided an advantage over currently available methods through its ability to negatively isolate all three monocyte subsets directly from whole blood. The development of this method enabled the investigation of the potential influence of MMPS on monocyte behaviour in the following chapter. Optimised isolation conditions were established and outlined in Chapter 3 of this thesis.

Monocytic separation using two magnet strengths at 25°C and 8°C were initially assessed for their impact on isolated monocyte purity. At both temperatures, the Easy Eights™ magnet resulted in a low purity of the enriched monocyte fraction with significant red blood cell contamination meanwhile, isolation using the Big Easy™ magnet at both 25°C and 8°C resulted in a monocyte purity >90% proving to be the more

suitable magnet for this application. Following this, percentage subset recovery, activation and yield were determined within the enriched fraction following isolation at 25°C and 8°C using the Big Easy magnet. Neither temperature provided a significant advantage in any of these analyses, however purification at 8°C displayed a trend in increasing subset recovery, yield and a decrease in activation marker expression compared to those performed at room temperature.

Further changes in phenotype and function following this new isolation method were also assessed, and compared to a monocytic cell line (THP-1). An alteration in surface marker expression was found in both the intermediate and the non-classical populations following enrichment, however this is likely to reflect the sensitive nature of monocytic cells and the care that must be taken for experimentation *ex vivo*. Finally, enriched monocytes displayed the ability to secrete pro-inflammatory cytokines in response to increasing concentrations of LPS had phagocytic functionality, and migratory function to MCP-1.

Work presented in Chapter 3 defined isolation conditions to separate monocytes directly from whole blood, allowing their use in the subsequent chapter whereby MP influence on monocytic function and phenotype was investigated in a bid to gain further understanding of their biological function.

Chapter 4 explores the release and phenotype of monocytic MPs under different conditions and describes their effect on isolated human monocyte functionality *ex vivo*; addressing the second aim of this thesis. Monocytic MPs are elevated in disease states (Hijmans et al., 2019; Hoyer et al., 2012; Kanazawa et al., 2003) and have shown to

influence functionality of endothelial cells, epithelial cells, smooth muscle cells (Aharon et al., 2008; Cerri et al., 2006; Essayagh et al., 2007; Neri et al., 2011; Sarkar et al., 2009; Wang et al., 2011) and activate monocytic cells directly (Bardelli et al., 2012). Thus, this chapter provided an insight as to how functionality was altered to one that could promote atherosclerosis disease progression.

Initial data presented in this chapter supports the link between MP release and serum starvation-induced apoptosis (Koifman et al., 2017), with an increase in MP number compared to control conditions significant after 72 hours. Under stimulatory conditions, MP release from monocytes was much higher in comparison to serum starvation conditions. Furthermore, common monocytic inflammatory stimuli: LPS, TNF-α, IFN- γ and the calcium ionophore A23187, evoked a concentration-dependent release.

In addition, MP phenotype displayed a similar trend to that found on the parent cell on quiescent, apoptotic (serum starved) and activated THP-1 cells when generated with LPS and A23187. The percentage marker expression and mean fluorescent intensity of CD54 displayed a similar trend on both the parent cell and derived MPs across all conditions, with Annexin V MFI increased on activated MPs compared to quiescent cells and the highest being observed on apoptotic derived MPs. This is likely to be representative of surface expression on the outer membrane of the parent cell, as PS exposure occurs due to activation, apoptosis and necrosis (Bevers et al., 1982, 1983; Fadok et al., 1992).

The data presented here supports the data of Wen *et al.,* (2014), within which MPs derived from quiescent and LPS stimulated monocytic cell lines (MM6 and THP-1) displayed a similar trend in surface marker expression, with CD54 displaying the largest

increase (Wen et al., 2014). No other markers investigated here were altered on either the parent cell or the MPs which may present a limitation to using monocytic cell lines to investigate these changes. At present, it is unknown if *ex* vivo human monocyte-derived MPs mimic the phenotype of their parent cell under different conditions, and how these may change with disease. This provides a possible avenue for future work.

The effect of A23187 derived MPs on isolated human monocytes was also assessed to elucidate possible mechanisms through which these particles play a role in accelerated CVD pathogenesis. For these experiments, A23187 was selected as the stimulant due to the detection of LPS in the MP pellet determined by a positive endotoxin test in LPS derived MPs. In addition, the use of this compound for MP generation and assessment of functional influence has previously been described (Bardelli et al., 2012; Cerri et al., 2006; Neri et al., 2011; Satta et al., 1994).

The autocrine effect of A23187 derived monocytic MPs has previously been reported by Bardelli., *et al* (2011), within which MPs at pathophysiological conditions enhanced pro-inflammatory cytokine production of IL-6 and TNF-α via NFKB signalling (Bardelli et al., 2012). Data presented here support these findings, demonstrating that physiological conditions failed to induce an increase in IL-6 and TNF-α cytokine secretion however a significant increase was observed with pathophysiological concentrations. The secretion of IL-1β, IL-8 and IL10 was not significantly altered at any of the concentrations tested. The increase in IL-6 production was only significant compared to control after 24 hours in the initial cytokine secretion time-course demonstrating a potential feedback loop,

whereby activated monocytes leads to the production of MMPS, which in turn further enhances monocyte activation and MP release.

Further novel findings presented in this chapter demonstrate that pathophysiological concentrations of MMPS altered monocyte phenotype, upregulating CD11b expression, consequentially enhancing their adhesion to endothelial cells and transendothelial migration across an endothelial barrier. The adhesion of monocytes to the endothelium and their transmigration are one of the early initiating events of vascular inflammation, thus these findings present a mechanism through which CVD pathogenesis may be accelerated in patients with increased monocyte MP numbers. Further proteomic profiling of MPs derived under different conditions may provide insight into MP composition (Jin et al., 2005), and thus to the mechanism in which monocyte functionality and phenotyping is altered. Uncovering this information may provide a mechanism of interaction and possible therapeutic intervention.

Chapter 5 enumerates circulating MPs and their phenotypes in children with HIV infection, and the dynamic alteration of these during the first 48 weeks of treatment initiation; addressing the final aim of this thesis. To investigate this, a fixation protocol was first developed using plasma isolated from healthy control adults, to allow the analysis of circulating MPs derived from a T cell, endothelial, monocytic and platelet origin by 6 colour flow cytometry.

The plasma of 16 treatment-experienced and 11 treatment-naive HIV infected children were selected from samples collected as part of the CHAPAS-3 CV sub-study, along with 15 healthy control children. Circulating MPs were quantified in all three cohorts at

baseline (week 0), with additional analysis of MPs in blood samples taken at week 48 for both HIV infected groups; following ART initiation in the case of the treatment-naïve patients.

Total circulating MPs and those from a platelet origin were not significantly altered in treatment-naïve populations or treatment-experienced cohort compared to healthy controls. Following 48-week treatment initiation, these levels were not significantly altered and remained within the range of those found in healthy controls. Circulating T cell MPs, and those from CD4+ and CD8+ populations were elevated in treatment-naïve children at baseline, however these decreased following treatment initiation, likely to be reflective of the activated T cell phenotypes in untreated HIV infection (Douek et al., 2003; van den Dries et al., 2017).

Endothelial MPs showed a general trend whereby numbers were elevated in treatment-naïve populations compared to children with controlled HIV infection and healthy controls, which remained increased after 48 weeks of treatment initiation. However, children on long term ART showed a reduction in all endothelial MP phenotypes comparable to those found in healthy control children suggesting that endothelial activation and dysfunction is improved in this population long term. This is further supported by literature whereby these markers of endothelial activation and clinical markers were also reduced following treatment initiation in children (Chanthong et al., 2014; Eckard et al., 2014; Kenny, 2016; Ross et al., 2010).

Of particular significance, MPs from a monocytic origin were elevated in both HIV infected cohorts when compared to healthy controls and remained increased after 48

weeks despite ART initiation in the treatment-naïve cohort. This supports data provided by Hijmans *et al.,* (2019), whereby numbers of monocytic MPs were higher in adults with HIV infection with controlled viremia compared to healthy controls (Hijmans et al., 2019). In addition, the failure of these MPs to normalise with treatment provides additional evidence that persistent inflammation drives monocyte activation following ART initiation, also demonstrated through increased plasma sCD14 (Alvarez et al., 2017; Bi et al., 2016; Dysangco et al., 2017; Sereti et al., 2017) and an inflammatory phenotype (Han et al., 2009; Kim et al., 2010; McCausland et al., 2015; Tippett et al., 2011).

This is the first study that has examined longitudinal measures of MPs within a HIV positive paediatric cohort, and analysed how these changes compare to healthy age matched controls. One of the main limitations to this study is the access to only a small number of clinical parameters collected throughout the duration of the trial, meaning that we were unable to determine causality of elevated MP numbers. Despite this, from these observations and published literature, we can speculate that MPs from a monocytic origin are increased in these patients due to elevated monocyte activation as a result of enhanced immune activation, and translocation of microbial products from the GI tract (Ancuta et al., 2008; Brenchley et al., 2006).

To investigate this further and confirm this relationship, plasma markers of microbial translocation (LPS), immune activation and MMPs could be quantified alongside markers of activation on circulating monocytes and clinical measures of atherosclerosis over time. Within a larger cohort, this study would also allow the potential to further elucidate mechanisms related to activated monocytes as a driver of CVD that may be

observed with specific ART drug classes. Should an association be found between elevated microbial translocation, monocyte activation and MMPs with increased CVD risk within this patient cohort, the use of MMPs as a biomarker to monitor CV risk or to measure the response to treatment intervention may be beneficial.

In addition to this, the evaluation of MPs as novel predictive biomarkers of CVD progression is in its early stages within the field, with universal protocols yet to be established. Thus, to explore this potential further, future studies within this area should be focused on standardising storage, isolation and acquisition procedures of MP enumeration prior to evaluating their effectiveness as a biomarker within different disease states.

More recently, extracellular vesicle miRNA has gained considerable interest as a potential predictive biomarker of CVD, with alterations in miRNAs present in patients with cardiac damage, coronary artery disease and sub-clinical atherosclerosis (Corsten et al., 2010; Fichtlscherer et al., 2010; Huang et al., 2018). Circulating miRNAs have also been reported to play a role in HIV disease pathogenesis (Fowler and Saksena, 2013; Triboulet et al., 2007), with HIV infected patients expressing unique miRNAs compared to healthy controls (Narla et al., 2018). Evidence demonstrates the ability for these extracellular miRNAs to play a role in atherosclerotic pathogenesis (Koroleva et al., 2017), thus by analysing these markers in patients with HIV infection new pathways that promote the acceleration of HIV associated CVD may be discovered.

As discussed here, the aims of this thesis have been met. The findings presented contribute to the current understanding of monocytic MPs, and their potential alteration

in monocyte functionality *in vivo*. This work highlights the significance and importance of this subset elevated in paediatric HIV, and the possible mechanisms through which these may contribute to CVD pathogenesis. In addition, the development and optimisation of the negative isolation method provides an alternative platform to enrich all monocytic populations from whole blood, untouched and inactivated, facilitating the continued exploration of monocyte functionality in disease.

References

Abid Hussein, M.N., Meesters, E.W., Osmanovic, N., Romijn, F.P.H.T.M., Nieuwland, R., and Sturk, A. (2003). Antigenic characterization of endothelial cell-derived microparticles and their detection ex vivo. J. Thromb. Haemost. *1*, 2434–2443.

Abid Hussein, M.N., Böing, A.N., Sturk, A., Hau, C.M., and Nieuwland, R. (2007). Inhibition of microparticle release triggers endothelial cell apoptosis and detachment. J. Thromb. Haemost. *98*, 1096–1107.

Aharon, A., Tamari, T., and Brenner, B. (2008). Monocyte-derived microparticles and exosomes induce procoagulant and apoptotic effects on endothelial cells. Thromb. Haemost. *100*, 878–885.

Aldo, P.B., Craveiro, V., Guller, S., and Mor, G. (2013). Effect of culture conditions on the phenotype of THP-1 monocyte cell line. Am. J. Reprod. Immunol. *70*, 80–86.

Alkhatib, G., Combadiere, C., Broder, C.C., Feng, Y., Kennedy, P.E., Murphy, P.M., and Berger, E.A. (1996). CC CKR5: A RANTES, MIP-1α, MIP-1β receptor as a fusion cofactor for macrophage-tropic HIV-1. Science (80-.). *272*, 1955–1958.

Alvarez, P., Mwamzuka, M., Marshed, F., Kravietz, A., Ilmet, T., Ahmed, A., Borkowsky, W., and Khaitan, A. (2017). Immune activation despite preserved CD4 T cells in perinatally HIV-infected children and adolescents. PLoS One *12*, 1–15.

Amabile, N., Guérin, A.P., Leroyer, A., Mallat, Z., Nguyen, C., Boddaert, J., London, G.M., Tedgui, A., and Boulanger, C.M. (2005). Circulating endothelial microparticles are associated with vascular dysfunction in patients with end-stage renal failure. J. Am. Soc. Nephrol. *16*, 3381–3388.

Amabile, N., Heiss, C., Real, W.M., Minasi, P., McGlothlin, D., Rame, E.J., Grossman, W., De Marco, T., and Yeghiazarians, Y. (2008). Circulating endothelial microparticle levels predict hemodynamic severity of pulmonary hypertension. Am. J. Respir. Crit. Care Med. *177*, 1268–1275.

Amabile, N., Cheng, S., Renard, J.M., Larson, M.G., Ghorbani, A., McCabe, E., Griffin, G., Guerin, C., Ho, J.E., Shaw, S.Y., et al. (2014). Association of circulating endothelial microparticles with cardiometabolic risk factors in the Framingham Heart Study. Eur. Heart J. *35*, 2972–2979.

Amirayan-Chevillard, N., Tissot-Dupont, H., Capo, C., Brunet, C., Dignat-George, F., Obadia, Y., Gallais, H., and Mege, J.L. (2000). Impact of highly active anti-retroviral therapy (HAART) on cytokine production and monocyte subsets in HIV-infected patients. Clin. Exp. Immunol. *120*, 107–112.

Amoruso, A., Bardelli, C., Fresu, L.G., Poletti, E., Palma, A., Canova, D.F., Zeng, H.W., Ongini, E., and Brunelleschi, S. (2010). The nitric oxide-donating pravastatin, NCX 6550, inhibits cytokine release and NF-κB activation while enhancing PPARγ expression in human monocyte/macrophages. Pharmacol. Res. *62*, 391–399.

Anand, A.R., Rachel, G., and Parthasarathy, D. (2018). HIV Proteins and Endothelial Dysfunction: Implications in Cardiovascular Disease. Front. Cardiovasc. Med. *5*, 185.

Ancuta, P., Rao, R., Moses, A., Mehle, A., Shaw, S.K., Luscinskas, F.W., and Gabuzda, D. (2003). Fractalkine preferentially mediates arrest and migration of CD16 + monocytes. J. Exp. Med. *197*, 1701–1707.

Ancuta, P., Kamat, A., Kunstman, K.J., Kim, E.Y., Autissier, P., Wurcel, A., Zaman, T., Stone, D., Mefford, M., Morgello, S., et al. (2008). Microbial translocation is associated with increased monocyte activation and dementia in AIDS patients. PLoS One *3*, 10–20.

Antonello, V.S., Carlos Ferreira Antonello, I., Grossmann, T.K., Tovo, C.V., Brasil Dal Pupo, B., and De Quadros Winckler, L. (2015). Hypertension - An emerging cardiovascular risk factor in HIV infection. J. Am. Soc. Hypertens. *9*, 403–407.

Arraud, N., Linares, R., Tan, S., Gounou, C., Pasquet, J.M., Mornet, S., and Brisson, A.R. (2014). Extracellular vesicles from blood plasma: Determination of their morphology, size, phenotype and concentration. J. Thromb. Haemost. *12*, 614–627.

Auffray, C., Fogg, D., Garfa, M., Elain, G., Join-Lambert, O., Kayal, S., Sarnacki, S., Cumano, A., Lauvau, G., and Geissmann, F. (2007). Monitoring of blood vessels and tissues by a population of monocytes with patrolling behavior. Science (80-.). *317*, 666–670.

Auffray, C., Sieweke, M.H., and Geissmann, F. (2009). Blood Monocytes: Development, Heterogeneity, and Relationship with Dendritic Cells. Annu. Rev. Immunol. *27*, 669–692.

Badley, A.D., Algeciras-Schimnich, A., Belzacq-Casagrande, A.-S., Bren, G.D., Nie, Z., Taylor, J.A., Rizza, S.A., and Brenner, C. (2008). Analysis of HIV Protease Killing Through Caspase 8 Reveals a Novel Interaction Between Caspase 8 and Mitochondria. Open Virol. J. *1*, 39–46.

Baj-Krzyworzeka, M., Szatanek, R., Weglarczyk, K., Baran, J., and Zembala, M. (2007). Tumour-derived microvesicles modulate biological activity of human monocytes. Immunol. Lett. *113*, 76–82.

Baker, J. V., Hullsiek, K.H., Singh, A., Wilson, E., Henry, K., Lichtenstein, K., Onen, N., Kojic, E., Patel, P., Brooks, J.T., et al. (2014). Immunologic predictors of coronary artery calcium progression in a contemporary HIV cohort. AIDS *28*, 831–840.

Baker, J. V, Huppler Hullsiek, K., Bradford, R.L., Prosser, R., Tracy, R.P., and Key, N.S. (2013). Circulating levels of tissue factor microparticle procoagulant activity are reduced with antiretroviral therapy and are associated with persistent inflammation and coagulation activation among HIV-positive patients. J. Acquir. Immune Defic. Syndr. *63*, 367–371.

Bardelli, C., Gunella, G., Varsaldi, F., Balbo, P., Del Boca, E., Bernardone, I.S., Amoruso, A., and Brunelleschi, S. (2005). Expression of functional NK 1 receptors in human alveolar macrophages: Superoxide anion production, cytokine release and involvement of NF-κβ pathway. Br. J. Pharmacol. *145*, 385–396.

Bardelli, C., Amoruso, A., Federici Canova, D., Fresu, L.G., Balbo, P., Neri, T., Celi, A., and Brunelleschi, S. (2012). Autocrine activation of human monocyte/macrophages by monocyte-derived microparticles and modulation by PPARγ ligands. Br. J. Pharmacol. *165*, 716–728.

Barnett, C.F., Hsue, P.Y., and Machado, R.F. (2008). Pulmonary hypertension: An increasingly recognized complication of hereditary hemolytic anemias and HIV infection. JAMA - J. Am. Med.

Assoc. *299*, 324–331.

Barry, O.P., Pratico, D., Lawson, J.A., and FitzGerald, G.A. (1997). Transcellular activation of platelets and endothelial cells by bioactive lipids in platelet microparticles. J. Clin. Invest. *99*, 2118–2127.

Barry, O.P., Pratico, D., Savani, R.C., and FitzGerald, G.A. (1998). Modulation of monocyte-endothelial cell interactions by platelet microparticles. J. Clin. Invest. *102*, 136–144.

Basu, S., Campbell, H.M., Dittel, B.N., and Ray, A. (2010). Purification of specific cell population by fluorescence activated cell sorting (FACS). J. Vis. Exp. 1546.

Batool, S., Abbasian, N., Burton, J.O., and Stover, C. (2013). Microparticles and their roles in inflammation: A review. Open Immunol. J. *6*, 1–14.

Behrens, G.M.N., Grinspoon, S., and Carr, A. (2005). Cardiovascular risk and body-fat abnormalities in HIV-infected adults. N. Engl. J. Med. *352*, 1721–1722.

Beignon, A.S., McKenna, K., Skoberne, M., Manches, O., DaSilva, I., Kavanagh, D.G., Larsson, M., Gorelick, R.J., Lifson, J.D., and Bhardwaj, N. (2005). Endocytosis of HIV-1 activates plasmacytoid dendritic cells via Toll-like receptor-viral RNA interactions. J. Clin. Invest. *115*, 3265–3275.

Beliakova-Bethell, N., Massanella, M., White, C., Lada, S.M., Du, P., Vaida, F., Blanco, J., Spina, C.A., and Woelk, C.H. (2014). The effect of cell subset isolation method on gene expression in leukocytes. Cytom. Part A *85*, 94–104.

Ben-Hadj-Khalifa-Kechiche, S., Hezard, N., Poitevin, S., Remy, M.G., Florent, B., Mahjoub, T., and Nguyen, P. (2010). Differential inhibitory effect of fondaparinux on the procoagulant potential of intact monocytes and monocyte-derived microparticles. J. Thromb. Thrombolysis *30*, 412–418.

Benameur, T., Osman, A., Parray, A., Ait Hssain, A., Munusamy, S., and Agouni, A. (2019). Molecular Mechanisms Underpinning Microparticle-Mediated Cellular Injury in Cardiovascular Complications Associated with Diabetes. Oxid. Med. Cell. Longev. Article ID: 6475187.

Benjamin EJ, Blaha MJ, SE, C., Cushman M, Das SR, Deo R, de Ferranti SD, Floyd J, Fornage M, Gillespie C, et al. (2017). Heart Disease and Stroke Statistics-2017 Update: A Report From the American Heart Association. Circulation *135*, e146–e603.

Bentzon, J.F., Otsuka, F., Virmani, R., and Falk, E. (2014). Mechanisms of plaque formation and rupture. Circ. Res. *114*, 1852–1866.

Berckmans, R.J., Sturk, A., Van Tienen, L.M., Schaap, M.C.L., and Nieuwland, R. (2011). Cell-derived vesicles exposing coagulant tissue factor in saliva. Blood *117*, 3172–3180.

Berezin, A., Zulli, A., Kerrigan, S., Petrovic, D., and Kruzliak, P. (2015). Predictive role of circulating endothelial-derived microparticles in cardiovascular diseases. Clin. Biochem. *48*, 562–568.

Berezin, A.E., Kremzer, A., Berezina, T., and Martovitskaya, Y. (2016). The signature of circulating microparticles in heart failure patients with metabolic syndrome. J. Circ. Biomarkers *5*, 1–10.

Bernal-Mizrachi, L., Jy, W., Fierro, C., Macdonough, R., Velazques, H.A., Purow, J., Jimenez, J.J.,

Horstman, L.L., Ferreira, A., De Marchena, E., et al. (2004). Endothelial microparticles correlate with high-risk angiographic lesions in acute coronary syndromes. Int. J. Cardiol. *97*, 439–446.

Bernimoulin, M., Waters, E.K., Foy, M., Steele, B.M., Sullivan, M., Falet, H., Walsh, M.T., Barteneva, N., Geng, J.G., Hartwig, J.H., et al. (2009). Differential stimulation of monocytic cells results in distinct populations of microparticles. J. Thromb. Haemost. *7*, 1019–1028.

Bevers, E.M., Comfurius, P., Van Rijn, J.L.M.L., Hemker, H.C., and Robert, F.A.Z. (1982). Generation of Prothrombin-Converting Activity and the Exposure of Phosphatidylserine at the Outer Surface of Platelets. Eur. J. Biochem. *122*, 429–436.

Bevers, E.M., Comfurius, P., and Zwaal, R.F.A. (1983). Changes in membrane phospholipid distribution during platelet activation. BBA - Biomembr. *736*, 57–66.

Bhattacharjee, J., Das, B., Mishra, A., Sahay, P., and Upadhyay, P. (2017). Monocytes isolated by positive and negative magnetic sorting techniques show different molecular characteristics and immunophenotypic behaviour. F1000Research *6*, 2045.

Bi, X., Ishizaki, A., Van Nguyen, L., Matsuda, K., Pham, H.V., Phan, C.T.T., Ogata, K., Giang, T.T.T., Phung, T.T.B., Nguyen, T.T., et al. (2016). Impact of HIV infection and anti-retroviral therapy on the immune profile of and microbial translocation in HIV-infected children in Vietnam. Int. J. Mol. Sci. *17*, 1–13.

Bicker, H., Höflich, C., Wolk, K., Vogt, K., Volk, H.D., and Sabat, R. (2008). A simple assay to measure phagocytosis of live bacteria. Clin. Chem. *54*, 911–915.

Birx D.L, Redfield R.R, Tencer K, Fowler A, Burke D.S, Tosato, G. (1990). Induction of interleukin-6 during human immunodeficiency virus infection. Blood *76*, 2303–2310.

Bitbol, M., Fellmann, P., Zachowski, A., and Devaux, P.F. (1987). Ion regulation of phosphatidylserine and phosphatidylethanolamine outside-inside translocation in human erythrocytes. BBA - Biomembr. *904*, 268–282.

Bode, A.P., and Knupp, C.L. (1994). Effect of cold storage on platelet glycoprotein Ib and vesiculation. Transfusion *34*, 690–696.

Bonner, J. (2017). Elucidating the Mechanisms of Thromboembolism and Structural Arterial Disease in Children with Inflammatory Bowel Disease. (Unpublished PhD Thesis). Institute of Child Health, University College London, UK.

Bonnet, D., Aggoun, Y., Szezepanski, I., Bellal, N., and Blanche, S. (2004). Arterial stiffness and endothelial dysfunction in HIV-infected children. Aids *18*, 1037–1041.

Borrow, P., Lewicki, H., Hahn, B.H., Shaw, G.M., and Oldstone, M.B. (1994). Virus-specific CD8+ cytotoxic T-lymphocyte activity associated with control of viremia in primary human immunodeficiency virus type 1 infection. J. Virol. *68*, 6103–6110.

Bosch, R.J., Wang, R., Vaida, F., Lederman, M.M., and Albrecht, M.A. (2006). Changes in the slope of the CD4 cell count increase after initiation of potent antiretroviral treatment. J. Acquir. Immune Defic. Syndr. *43*, 433–435.

Bosshart, H., and Heinzelmann, M. (2004). Lipopolysaccharide-mediated cell activation without

rapid mobilization of cytosolic free calcium. Mol. Immunol. *41*, 1023–1028.

Brabazon, F., Bermudez, S., Shaughness, M., Khayrullina, G., and Byrnes, K.R. (2018). The effects of insulin on the inflammatory activity of BV2 microglia. PLoS One *13*, 1–13.

Brand, K., Fowler, B.J., Edgington, T.S., and Mackman, N. (1991). Tissue Factor mRNA in THP-1 Monocytic Cells Is Regulated at Both Transcriptional and Posttranscriptional Levels in Response to Lipopolysaccharide. Mol. Cell. Biol. *11*, 4732–4738.

Brekke, O.L., Waage, C., Christiansen, D., Fure, H., Qu, H., Lambris, J.D., Osterud, B., Nielsen, E.W., and Mollnes, T.E. (2013). The effects of selective complement and CD14 inhibition on the E. coli-induced tissue factor mRNA upregulation, monocyte tissue factor expression, and tissue factor functional activity in human whole blood. In Advances in Experimental Medicine and Biology, pp. 123–136.

Brenchley, J.M., Schacker, T.W., Ruff, L.E., Price, D.A., Taylor, J.H., Beilman, G.J., Nguyen, P.L., Khoruts, A., Larson, M., Haase, A.T., et al. (2004). CD4+ T cell depletion during all stages of HIV disease occurs predominantly in the gastrointestinal tract. J. Exp. Med. *200*, 749–759.

Brenchley, J.M., Price, D.A., Schacker, T.W., Asher, T.E., Silvestri, G., Rao, S., Kazzaz, Z., Bornstein, E., Lambotte, O., Altmann, D., et al. (2006). Microbial translocation is a cause of systemic immune activation in chronic HIV infection. Nat. Med. *12*, 1365–1371.

Brittain, E.L., Duncan, M.S., Chang, J., Patterson, O. V., DuVall, S.L., Brandt, C.A., So-Armah, K.A., Goetz, M., Akgun, K., Crothers, K., et al. (2018). Increased echocardiographic pulmonary pressure in HIV-infected and -uninfected individuals in the veterans aging cohort study. Am. J. Respir. Crit. Care Med. *197*, 923–932.

Brodsky, S. V., Zhang, F., Nasjletti, A., and Goligorsky, M.S. (2004). Endothelium-derived microparticles impair endothelial function in vitro. Am. J. Physiol. - Hear. Circ. Physiol. *286*, 1910–1915.

Brown, M.D., Feairheller, D.L., Thakkar, S., Veerabhadrappa, P., and Park, J.Y. (2011). Racial differences in tumor necrosis factor-α-induced endothelial microparticles and interleukin-6 production. Vasc. Health Risk Manag. *7*, 541–550.

Buonaguro, L., Barillari, G., Chang, H.K., Bohan, C.A., Kao, V., Morgan, R., Gallo, R.C., and Ensoli, B. (1992). Effects of the human immunodeficiency virus type 1 Tat protein on the expression of inflammatory cytokines. J. Virol. *66*, 7159–7167.

Burdo, T.H., Lentz, M.R., Autissier, P., Krishnan, A., Halpern, E., Letendre, S., Rosenberg, E.S., Ellis, R.J., and Williams, K.C. (2011a). Soluble CD163 made by monocyte/macrophages is a novel marker of HIV activity in early and chronic infection prior to and after antiretroviral therapy. J. Infect. Dis. *204*, 154–163.

Burdo, T.H., Lo, J., Abbara, S., Wei, J., DeLelys, M.E., Preffer, F., Rosenberg, E.S., Williams, K.C., and Grinspoon, S. (2011b). Soluble CD163, a novel marker of activated macrophages, is elevated and associated with noncalcified coronary plaque in HIV-infected patients. J. Infect. Dis. *204*, 1227–1236.

Butt, A.A., Chang, C.C., Kuller, L., Goetz, M.B., Leaf, D., Rimland, D., Gibert, C.L., Oursler, K.K.,

Rodriguez-Barradas, M.C., Lim, J., et al. (2011). Risk of heart failure with human immunodeficiency virus in the absence of prior diagnosis of coronary heart disease. Arch. Intern. Med. *171*, 737–743.

Calcaterra, S., Cappiello, G., Di Caro, A., Garbuglia, A.R., and Benedetto, A. (2001). Comparative analysis of total and integrated HIV-1 DNA in peripheral CD4 lymphocytes and monocytes after long treatment with HAART. J. Infect. *43*, 239–245.

Campbell-Yesufu, O.T., and Gandhi, R.T. (2011). Update on human immunodeficiency virus (HIV)-2 infection. Clin. Infect. Dis. *52*, 780–787.

Carlin, L.M., Stamatiades, E.G., Auffray, C., Hanna, R.N., Glover, L., Vizcay-Barrena, G., Hedrick, C.C., Cook, H.T., Diebold, S., and Geissmann, F. (2013). Nr4a1-dependent Ly6Clow monocytes monitor endothelial cells and orchestrate their disposal. Cell *153*, 362–375.

Carpintero, R., Gruaz, L., Brandt, K.J., Scanu, A., Faille, D., Combes, V., Grau, G.E., and Burger, D. (2010). HDL interfere with the binding of T cell microparticles to human monocytes to inhibit pro-inflammatory cytokine production. PLoS One *5*, 1–8.

Cerri, C., Chimenti, D., Conti, I., Neri, T., Paggiaro, P., and Celi, A. (2006). Monocyte/Macrophage-Derived Microparticles Up-Regulate Inflammatory Mediator Synthesis by Human Airway Epithelial Cells. J. Immunol. *177*, 1975–1980.

Chanthong, P., Lapphra, K., Saihongthong, S., Sricharoenchai, S., Wittawatmongkol, O., Phongsamart, W., Rungmaitree, S., Kongstan, N., and Chokephaibulkit, K. (2014). Echocardiography and carotid intima-media thickness among asymptomatic HIV-infected adolescents in Thailand. Aids *28*, 2071–2079.

Charakida, M., Donald, A.E., Green, H., Storry, C., Clapson, M., Caslake, M., Dunn, D.T., Halcox, J.P., Gibb, D.M., Klein, N.J., et al. (2005). Early structural and functional changes of the vasculature in HIV-infected children: Impact of disease and antiretroviral therapy. Circulation *112*, 103–109.

Charakida, M., Deanfield, J.E., and Halcox, J.P. (2007). Childhood origins of arterial disease. Curr. Opin. Pediatr. *19*, 538–545.

Charakida, M., Loukogeorgakis, S.P., Okorie, M.I., Masi, S., Halcox, J.P., Deanfield, J.E., and Klein, N.J. (2009). Increased arterial stiffness in HIV-infected children: Risk factors and antiretroviral therapy. Antivir. Ther. *14*, 1075–1079.

Chen, F., Wang, M., O'Connor, J.P., He, M., Tripathi, T., and Harrison, L.E. (2003). Phosphorylation of PPARγ via Active ERK1/2 Leads to its Physical Association with p65 and Inhibition of NF-κβ. J. Cell. Biochem. *90*, 732–744.

Chen, P., Su, B., Zhang, T., Zhu, X., Xia, W., Fu, Y., Zhao, G., Xia, H., Dai, L., Sun, L., et al. (2017). Perturbations of monocyte subsets and their association with T helper cell differentiation in acute and chronic HIV-1-infected patients. Front. Immunol. *8*, 272.

Chen, Y., Li, G., and Liu, M.L. (2018). Microvesicles as Emerging Biomarkers and Therapeutic Targets in Cardiometabolic Diseases. Genomics, Proteomics Bioinforma. *16*, 50–62.

Cheung, R., Ravyn, V., Wang, L., Ptasznik, A., and Collman, R.G. (2008). Signaling Mechanism of

HIV-1 gp120 and Virion-Induced IL-1β Release in Primary Human Macrophages. J. Immunol. *180*, 6675–6684.

Chironi, G., Simon, A., Hugel, B., Pino, M. Del, Gariepy, J., Freyssinet, J.M., and Tedgui, A. (2006). Circulating leukocyte-derived microparticles predict subclinical atherosclerosis burden in asymptomatic subjects. Arterioscler. Thromb. Vasc. Biol. *26*, 2775–2780.

Chiva-Blanch, G., Laake, K., Myhre, P., Bratseth, V., Arnesen, H., Solheim, S., Badimon, L., and Seljeflot, I. (2017). Platelet-, monocyte-derived & tissue factor carrying circulating microparticles are related to acute myocardial infarction severity. PLoS One *12*, 1–12.

Chou, J., Mackman, N., Merrill-Skoloff, G., Pedersen, B., Furie, B.C., and Furie, B. (2004). Hematopoietic cell-derived microparticle tissue factor contributes to fibrin formation during thrombus propagation. Blood *104*, 3190–3197.

Chow, F.C., Regan, S., Feske, S., Meigs, J.B., Grinspoon, S.K., and Triant, V.A. (2012). Comparison of ischemic stroke incidence in HIV-infected and non-HIV-infected patients in a US health care system. J. Acquir. Immune Defic. Syndr. *60*, 351–358.

Christensen-Quick, A., Vanpouille, C., Lisco, A., and Gianella, S. (2017). Cytomegalovirus and HIV Persistence: Pouring Gas on the Fire. AIDS Res. Hum. Retroviruses *33*, S23–S30.

Christersson, C., Lindahl, B., and Siegbahn, A. (2016). The composition and daily variation of microparticles in whole blood in stable coronary artery disease. Scand. J. Clin. Lab. Invest. *76*, 25–32.

Christersson, C., Thulin, Å., and Siegbahn, A. (2017). Microparticles during long-term follow-up after acute myocardial infarction. Thromb. Haemost. *117*, 1571–1581.

Clarke, L.A., Hong, Y., Eleftheriou, D., Shah, V., Arrigoni, F., Klein, N.J., and Brogan, P.A. (2010). Endothelial injury and repair in systemic vasculitis of the young. Arthritis Rheum. *62*, 1770–1780.

Clarkson, S.B., and Ory, P.A. (1988). CD16 developmentally regulated IgG Fc receptors on cultured human monocytes. J. Exp. Med. *167*, 408–420.

Coffelt, S.B., Tal, A.O., Scholz, A., De Palma, M., Patel, S., Urbich, C., Biswas, S.K., Murdoch, C., Plate, K.H., Reiss, Y., et al. (2010). Angiopoietin-2 regulates gene expression in TIE2-expressing monocytes and augments their inherent proangiogenic functions. Cancer Res. *70*, 5270–5280.

Coffin, J., and Swanstrom, R. (2013). HIV pathogenesis: dynamics and genetics of viral populations and infected cells. Cold Spring Harb. Perspect. Med. *3*, a012526.

Cohen, M.S., Chen, Y.Q., McCauley, M., Gamble, T., Hosseinipour, M.C., Kumarasamy, N., Hakim, J.G., Kumwenda, J., Grinsztejn, B., Pilotto, J.H.S., et al. (2016). Antiretroviral therapy for the prevention of HIV-1 transmission. In New England Journal of Medicine, (Massachussetts Medical Society), pp. 830–839.

Coleman, M.L., Sahai, E.A., Yeo, M., Bosch, M., Dewar, A., and Olson, M.F. (2001). Membrane blebbing during apoptosis results from caspase-mediated activation of ROCK I. Nat. Cell Biol. *3*, 339–345.

Collins, R.G., Velji, R., Guevara, N. V., Hicks, M.J., Chan, L., and Beaudet, A.L. (2000). P-selectin or

intercellular adhesion molecule (ICAM)-1 deficiency substantially protects against atherosclerosis in apolipoprotein E-deficient mice. J. Exp. Med. *191*, 189–194.

Combes, V., Dignat-George, F., Mutin, M., and Sampol, J. (1997). A new flow cytometry method of platelet-derived microvesicle quantitation in plasma. Thromb. Haemost. *77*, 220.

Del Conde, I., Shrimpton, C.N., Thiagarajan, P., and López, J.A. (2005). Tissue-factor-bearing microvesicles arise from lipid rafts and fuse with activated platelets to initiate coagulation. Blood *106*, 1604–1611.

Conklin, B.S., Fu, W., Lin, P.H., Lumsden, A.B., Yao, Q., and Chen, C. (2004). HIV protease inhibitor ritonavir decreases endothelium-dependent vasorelaxation and increases superoxide in porcine arteries. Cardiovasc. Res. *63*, 168–175.

Connor, D.E., Exner, T., Ma, D.D.F., and Joseph, J.E. (2010). The majority of circulating platelet-derived microparticles fail to bind annexin V, lack phospholipid-dependent procoagulant activity and demonstrate greater expression of glycoprotein Ib. Thromb. Haemost. *103*, 1044–1052.

Cooper, A., García, M., Petrovas, C., Yamamoto, T., Koup, R.A., and Nabel, G.J. (2013). HIV-1 causes CD4 cell death through DNA-dependent protein kinase during viral integration. Nature *498*, 376–379.

Corrales-Medina, V.F., Simkins, J., Chirinos, J.A., Serpa, J.A., Horstman, L.L., Jy, W., and Ahn, Y.S. (2010). Increased levels of platelet microparticles in HIV-infected patients with good response to highly active antiretroviral therapy. J. Acquir. Immune Defic. Syndr. *54*, 217–218.

Corsten, M.F., Dennert, R., Jochems, S., Kuznetsova, T., Devaux, Y., Hofstra, L., Wagner, D.R., Staessen, J.A., Heymans, S., and Schroen, B. (2010). Circulating MicroRNA-208b and MicroRNA-499 reflect myocardial damage in cardiovascular disease. Circ. Cardiovasc. Genet. *3*, 499–506.

Crescitelli, R., Lässer, C., Szabó, T.G., Kittel, A., Eldh, M., Dianzani, I., Buzás, E.I., and Lötvall, J. (2013). Distinct RNA profiles in subpopulations of extracellular vesicles: Apoptotic bodies, microvesicles and exosomes. J. Extracell. Vesicles *2*.

Cros, J., Cagnard, N., Woollard, K., Patey, N., Zhang, S.Y., Senechal, B., Puel, A., Biswas, S.K., Moshous, D., Picard, C., et al. (2010). Human CD14dim Monocytes Patrol and Sense Nucleic Acids and Viruses via TLR7 and TLR8 Receptors. Immunity *33*, 375–386.

Cummins, N.W., and Badley, A.D. (2014). Making sense of how HIV kills infected CD4 T cells: implications for HIV cure. Mol. Cell. Ther. *2*.

Currier, J.S., Taylor, A., Boyd, F., Dezii, C.M., Kawabata, H., Burtcel, B., Maa, J.F., and Hodder, S. (2003). Coronary heart disease in HIV-infected individuals. J. Acquir. Immune Defic. Syndr. *33*, 506–512.

Curtis, A.M., Wilkinson, P.F., Gui, M., Gales, T.L., Hu, E., and Edelberg, J.M. (2009). P38 Mitogen-Activated Protein Kinase Targets the Production of Proinflammatory Endothelial Microparticles. J. Thromb. Haemost. *7*, 701–709.

Cushing, S.D., Berliner, J.A., Valente, A.J., Territo, M.C., Navab, M., Parhami, F., Gerrity, R., Schwartz, C.J., and Fogelman, A.M. (1990). Minimally modified low density lipoprotein induces monocyte chemotactic protein 1 in human endothelial cells and smooth muscle cells. Proc. Natl.

Acad. Sci. U. S. A. *87*, 5134–5138.

Cybulsky, M.I., and Gimbrone, M.A. (1991). Endothelial expression of a mononuclear leukocyte adhesion molecule during atherogenesis. Science (80-.). *251*, 788–791.

d'Ettorre, G., Ceccarelli, G., Pavone, P., Vittozzi, P., De Girolamo, G., Schietroma, I., Serafino, S., Giustini, N., and Vullo, V. (2016). What happens to cardiovascular system behind the undetectable level of HIV viremia? AIDS Res. Ther. *13*, 1–17.

Daleke, D.L. (2003). Regulation of transbilayer plasma membrane phospholipid asymmetry. J. Lipid Res. *44*, 233–242.

Danesh, J., Wheeler, J.G., Hirschfield, G.M., Eda, S., Eiriksdottir, G., Rumley, A., Lowe, G.D.O., Pepys, M.B., and Gudnason, V. (2004). C-Reactive Protein and Other Circulating Markers of Inflammation in the Prediction of Coronary Heart Disease. N. Engl. J. Med. *350*, 1387–1397.

Data Collection on Adverse Events of Anti-HIV drugs (D:A:D) Study Group, Smith, C., Sabin, C. a, Lundgren, J.D., Thiebaut, R., Weber, R., Law, M., Monforte, A. d'Arminio, Kirk, O., Friis-Moller, N., et al. (2010). Factors associated with specific causes of death amongst HIV-positive individuals in the D:A:D Study. AIDS *24*, 1537–1548.

Deanfield, J.E., Halcox, J.P., and Rabelink, T.J. (2007). Endothelial function and dysfunction: Testing and clinical relevance. Circulation *115*, 1285–1295.

Deeks, S.G. (2011). HIV Infection, Inflammation, Immunosenescence, and Aging. Annu. Rev. Med. *62*, 141–155.

Deeks, S.G., Kitchen, C.M.R., Liu, L., Guo, H., Gascon, R., Narváez, A.B., Hunt, P., Martin, J.N., Kahn, J.O., Levy, J., et al. (2004). Immune activation set point during early HIV infection predicts subsequent CD4+ T-cell changes independent of viral load. Blood *104*, 942–947.

Deeks, S.G., Lewin, S.R., and Havlir, D. V. (2013). The end of AIDS: HIV infection as a chronic disease. Lancet *382*, 1525–1533.

Deng, H.K., Liu, R., Ellmeier, W., Choe, S., Unutmaz, D., Burkhart, M., Di Marzio, P., Marmon, S., Sutton, R.E., Mark Hill, C., et al. (1996). Identification of a major co-receptor for primary isolates of HIV-1. Nature *381*, 661–666.

Densmore, J.C., Signorino, P.R., Ou, J., Hatoum, O.A., Rowe, J.J., Shi, Y., Kaul, S., Jones, D.W., Sabina, R.E., Pritchard, K.A., et al. (2006). Endothelium-derived microparticles induce endothelial dysfunction and acute lung injury. Shock *26*, 464–471.

Devaraj, S., Kumaresan, P.R., and Jialal, I. (2011). C-reactive protein induces release of both endothelial microparticles and circulating endothelial cells in vitro and in vivo: Further evidence of endothelial dysfunction. Clin. Chem. *57*, 1757–1761.

Diamant, M., Nieuwland, R., Pablo, R.F., Sturk, A., Smit, J.W.A., and Radder, J.K. (2002). Elevated numbers of tissue-factor exposing microparticles correlate with components of the metabolic syndrome in uncomplicated type 2 diabetes mellitus. Circulation *106*, 2442–2447.

Dickhout, A., and Koenen, R.R. (2018). Extracellular Vesicles as Biomarkers in Cardiovascular Disease; Chances and Risks. Front. Cardiovasc. Med. *5*.

Dignat-George, F., and Boulanger, C.M. (2011). The many faces of endothelial microparticles. Arterioscler. Thromb. Vasc. Biol. *31*, 27–33.

Dillon, S.M., Lee, E.J., Kotter, C. V., Austin, G.L., Dong, Z., Hecht, D.K., Gianella, S., Siewe, B., Smith, D.M., Landay, A.L., et al. (2014). An altered intestinal mucosal microbiome in HIV-1 infection is associated with mucosal and systemic immune activation and endotoxemia. Mucosal Immunol. *7*, 983–994.

Dinh, D.M., Volpe, G.E., Duffalo, C., Bhalchandra, S., Tai, A.K., Kane, A. V., Wanke, C.A., and Ward, H.D. (2015). Intestinal Microbiota, microbial translocation, and systemic inflammation in chronic HIV infection. J. Infect. Dis. *211*, 19–27.

Dirajlal-Fargo, S., Sattar, A., Kulkarni, M., Funderburg, N., and McComsey, G.A. (2017). Soluble TWEAK may predict carotid atherosclerosis in treated HIV infection. HIV Clin. Trials *18*, 156–163.

Distler, J.H.W., Pisetsky, D.S., Huber, L.C., Kalden, J.R., Gay, S., and Distler, O. (2005a). Microparticles as regulators of inflammation: Novel players of cellular crosstalk in the rheumatic diseases. Arthritis Rheum. *52*, 3337–3348.

Distler, J.H.W., Huber, L.C., Hueber, A.J., Reich, C.F., Gay, S., Distler, O., and Pisetsky, D.S. (2005b). The release of microparticles by apoptotic cells and their effects on macrophages. Apoptosis *10*, 731–741.

Dixon, J.F.P., Law, J.L., and Favero, J.J. (1989). Activation of human T lymphocytes by crosslinking of anti-CD3 monoclonal antibodies. J. Leukoc. Biol. *46*, 214–220.

Doitsh, G., Cavrois, M., Lassen, K.G., Zepeda, O., Yang, Z., Santiago, M.L., Hebbeler, A.M., and Greene, W.C. (2010). Abortive HIV infection mediates CD4 T cell depletion and inflammation in human lymphoid tissue. Cell *143*, 789–801.

Doitsh, G., Galloway, N.L.K., Geng, X., Yang, Z., Monroe, K.M., Zepeda, O., Hunt, P.W., Hatano, H., Sowinski, S., Muñoz-Arias, I., et al. (2014). Cell death by pyroptosis drives CD4 T-cell depletion in HIV-1 infection. Nature *505*, 509–514.

Dong, Z.M., Chapman, S.M., Brown, A.A., Frenette, P.S., Hynes, R.O., and Wagner, D.D. (1998). The combined role of P- and E-selectins in atherosclerosis. J. Clin. Invest. *102*, 145–152.

Douek, D.C., Picker, L.J., and Koup, R.A. (2003). T cell dynamics in HIV-1 infection. Annu. Rev. Immunol. *21*, 265–304.

Dragic, T., Litwin, V., Allaway, G.P., Martin, S.R., Huang, Y., Nagashima, K.A., Cayanan, C., Maddon, P.J., Koup, R.A., Moore, J.P., et al. (1996). HIV-1 entry into CD4+ cells is mediated by the chemokine receptor CC-CKR-5. Nature *381*, 667–673.

van den Dries, L., Claassen, M.A.A., Groothuismink, Z.M.A., van Gorp, E., and Boonstra, A. (2017). Immune activation in prolonged cART-suppressed HIV patients is comparable to that of healthy controls. Virology *509*, 133–139.

Drozd, D.R., Kitahata, M.M., Althoff, K.N., Zhang, J., Gange, S.J., Napravnik, S., Burkholder, G.A., Mathews, W.C., Silverberg, M.J., Sterling, T.R., et al. (2017). Increased Risk of Myocardial Infarction in HIV-Infected Individuals in North America Compared with the General Population. J. Acquir. Immune Defic. Syndr. *75*, 568–576.

Duprez, D.A., Neuhaus, J., Kuller, L.H., Tracy, R., Belloso, W., De Wit, S., Drummond, F., Lane, H.C., Ledergerber, B., and Lundgren, J. (2012). Inflammation, coagulation and cardiovascular disease in HIV-infected individuals. PLoS One *7*, e44454.

Dysangco, A., Liu, Z., Stein, J.H., Dubé, M.P., and Gupta, S.K. (2017). HIV infection, antiretroviral therapy, and measures of endothelial function, inflammation, metabolism, and oxidative stress. PLoS One *12*, e0183511.

Eckard, A.R., O'Riordan, M.A., Storer, N., and McComsey, G.A. (2014). Long-term changes in carotid intima-media thickness among HIV-infected children and young. Antivir. Ther. *19*, 61–68.

Eckard, A.R., Raggi, P., Ruff, J.H., O'Riordan, M.A., Rosebush, J.C., Labbato, D., Daniels, J.E., Uribe-Leitz, M., Longenecker, C.T., and McComsey, G.A. (2017). Arterial stiffness in HIV-infected youth and associations with HIV-related variables. Virulence *8*, 1265–1273.

Egorina, E.M., Sovershaev, M.A., Bjørkøy, G., Gruber, F.X.E., Olsen, J.O., Parhami-Seren, B., Mann, K.G., and Østerud, B. (2005). Intracellular and surface distribution of monocyte tissue factor: Application to intersubject variability. Arterioscler. Thromb. Vasc. Biol. *25*, 1493–1498.

Ekong, N., Curtis, H., Ong, E., Sabin, C., Chadwick, D., Asboe, D., Balasubramaniam, V., Burns, F., Chadwick, D., Chaponda, M., et al. (2020). Monitoring of older HIV-1-positive adults by HIV clinics in the United Kingdom: a national quality improvement initiative. HIV Med.

El-Sadr, W.M., Lundgren, J.D., Neaton, J.D., Gordin, F., Abrams, D., Arduino, R.C., Babiker, A., Burman, W., Clumeck, N., Cohen, C.J., et al. (2006). CD4+ count-guided interruption of antiretroviral treatment. N. Engl. J. Med. *355*, 2283–2296.

Eleftheriou, D., Ganesan, V., Hong, Y., Klein, N.J., and Brogan, P.A. (2012). Endothelial injury in childhood stroke with cerebral arteriopathy. Neurology *79*, 2089–2096.

Elion, R.A., Althoff, K.N., Zhang, J., Moore, R.D., Gange, S.J., Kitahata, M.M., Crane, H.M., Drozd, D.R., Stein, J.H., Klein, M.B., et al. (2018). Recent abacavir use increases risk of type 1 and type 2 myocardial infarctions among adults with HIV. J. Acquir. Immune Defic. Syndr. *78*, 62–72.

Elkord, E., Williams, P.E., Kynaston, H., and Rowbottom, A.W. (2005). Human monocyte isolation methods influence cytokine production from in vitro generated dendritic cells. Immunology *114*, 204–212.

Ellery, P.J., Tippett, E., Chiu, Y.-L., Paukovics, G., Cameron, P.U., Solomon, A., Lewin, S.R., Gorry, P.R., Jaworowski, A., Greene, W.C., et al. (2007). The CD16+ monocyte subset is more permissive to infection and preferentially harbors HIV-1 in vivo. J. Immunol. *178*, 6581–6589.

Espíndola, M.S., Soares, L.S., Galvão-Lima, L.J., Zambuzi, F.A., Cacemiro, M.C., Brauer, V.S., Marzocchi-Machado, C.M., De Souza Gomes, M., Amaral, L.R., Martins-Filho, O.A., et al. (2018). Epigenetic alterations are associated with monocyte immune dysfunctions in HIV-1 infection. Sci. Rep. *8*, 1–14.

Essayagh, S., Xuereb, J.-M., Terrisse, A.-D., Tellier-Cirioni, L., Pipy, B., and Sié, P. (2007). Microparticles from apoptotic monocytes induce transient platelet recruitment and tissue factor expression by cultured human vascular endothelial cells via a redox-sensitive mechanism. Thromb. Haemost. *98*, 831–837.

Eyre, J., Burton, J.O., Saleem, M.A., Mathieson, P.W., Topham, P.S., and Brunskill, N.J. (2011). Monocyte-and endothelial-derived microparticles induce an inflammatory phenotype in human podocytes. Nephron - Exp. Nephrol. *119*.

Fabbri-Arrigoni, F.I., Clarke, L., Wang, G., Charakida, M., Ellins, E., Halliday, N., Brogan, P.A., Deanfield, J.E., Halcox, J.P., and Klein, N. (2012). Levels of circulating endothelial cells and colony-forming units are influenced by age and dyslipidemia. Pediatr. Res. *72*, 299–304.

Fadok, V.A., Voelker, D.R., Campbell, P.A., Cohen, J.J., Bratton, D.L., and Henson, P.M. (1992). Exposure of phosphatidylserine on the surface of apoptotic lymphocytes triggers specific recognition and removal by macrophages. J. Immunol. *148*, 2207–2216.

Falati, S., Liu, Q., Gross, P., Merrill-Skoloff, G., Chou, J., Vandendries, E., Celi, A., Croce, K., Furie, B.C., and Furie, B. (2003). Accumulation of tissue factor into developing thrombi in vivo is dependent upon microparticle P-selectin glycoprotein ligand 1 and platelet P-selectin. J. Exp. Med. *197*, 1585–1598.

Feinstein, M.J., Bahiru, E., Achenbach, C., Longenecker, C.T., Hsue, P., So-Armah, K., Freiberg, M.S., and Lloyd-Jones, D.M. (2016). Patterns of cardiovascular mortality for HIV-infected adults in the United States: 1999 to 2013. Am. J. Cardiol. *117*, 214–220.

Feng, Y., Broder, C.C., Kennedy, P.E., and Berger, E.A. (1996). HIV-1 entry cofactor: Functional cDNA cloning of a seven-transmembrane, G protein-coupled receptor. Science (80-.). *272*, 872–877.

Février, M., Dorgham, K., and Rebollo, A. (2011). CD4 T cell depletion in human immunodeficiency virus (HIV) infection: role of apoptosis. Viruses *3*, 586–612.

Fichtlscherer, S., De Rosa, S., Fox, H., Schwietz, T., Fischer, A., Liebetrau, C., Weber, M., Hamm, C.W., Röxe, T., Müller-Ardogan, M., et al. (2010). Circulating microRNAs in patients with coronary artery disease. Circ. Res. *107*, 677–684.

Fischer-Smith, T., Tedaldi, E.M., and Rappaport, J. (2008). CD163/CD16 coexpression by circulating monocytes/macrophages in HIV: Potential biomarkers for HIV infection and AIDS progression. AIDS Res. Hum. Retroviruses *24*, 417–421.

Fitch, K. V., Srinivasa, S., Abbara, S., Burdo, T.H., Williams, K.C., Eneh, P., Lo, J., and Grinspoon, S.K. (2013). Noncalcified coronary atherosclerotic plaque and immune activation in HIV-infected women. J. Infect. Dis. *208*, 1737–1746.

Forlow, S.B., McEver, R.P., and Nollert, M.U. (2000). Leukocyte-leukocyte interactions mediated by platelet microparticles under flow. Blood *95*, 1317–1323.

Forsyth, K.D., and Levinsky, R.J. (1990). Preparative procedures of cooling and re-warming increase leukocyte integrin expression and function on neutrophils. J. Immunol. Methods *128*, 159–163.

Fowler, L., and Saksena, N.K. (2013). Micro-RNA: New players in HIV-pathogenesis, diagnosis, prognosis and antiviral therapy. AIDS Rev. *15*, 3–14.

Fox, J.E.B., Austin, C.D., Reynolds, C.C., and Steffen, P.K. (1991). Evidence that agonist-induced activation of calpain causes the shedding of procoagulant-containing microvesicles from the

membrane of aggregating platelets. J. Biol. Chem. *266*, 13289–13295.

Freed, E.O. (2015). HIV-1 assembly, release and maturation. Nat. Rev. Microbiol. *13*, 484–496.

Freiberg, M.S., McGinnis, K.A., Kraemer, K., Samet, J.H., Conigliaro, J., Curtis Ellison, R., Bryant, K., Kuller, L.H., and Justice, A.C. (2010). The association between alcohol consumption and prevalent cardiovascular diseases among HIV-infected and HIV-uninfected men. J. Acquir. Immune Defic. Syndr. *53*, 247–253.

Freiberg, M.S., Chang, C.C.H., Kuller, L.H., Skanderson, M., Lowy, E., Kraemer, K.L., Butt, A.A., Goetz, M.B., Leaf, D., Oursler, K.A., et al. (2013). HIV infection and the risk of acute myocardial infarction. JAMA Intern. Med. *173*, 614–622.

Freiberg, M.S., Chang, C.H., Skanderson, M., Vasan, R.S., Oursler, K.A., and Gottdiener, J. (2017). Association Between HIV Infection and the Risk of Heart Failure With Reduced Ejection Fraction and Preserved Ejection Fraction in the Antiretroviral Therapy Era. JAMA Cardiol *2*, 536–546.

Friis-Moller, N., Reiss, P., Sabin, C.A., Weber, R., Monforte, A.D.A., El-Sadr, W., Thiebaut, R., De Wit, S., Kirk, O., Fontas, E., et al. (2007). Class of antiretroviral drugs and the risk of myocardial infarction. N. Engl. J. Med. *356*, 1723–1735.

Friis-Møller, N., Sabin, C.A., Weber, R., d'Arminio Monforte, A., El-Sadr, W.M., Reiss, P., Thiébaut, R., Morfeldt, L., De Wit, S., Pradier, C., et al. (2003). Combination Antiretroviral Therapy and the Risk of Myocardial Infarction: The Data Collection on Adverse Events of Anti-HIV Drugs (DAD) Study Group. N. Engl. J. Med. *349*, 1993–2003.

Funderburg, N.T., Andrade, A., Chan, E.S., Rosenkranz, S.L., Lu, D., Clagett, B., Pilch-Cooper, H.A., Rodriguez, B., Feinberg, J., Daar, E., et al. (2013). Dynamics of immune reconstitution and activation markers in HIV+ treatment-naïve patients treated with raltegravir, tenofovir disoproxil fumarate and emtricitabine. PLoS One *8*, e83514.

Gasser, O., and Schifferli, J.A. (2004). Activated polymorphonuclear neutrophils disseminate anti-inflammatory microparticles by ectocytosis. Blood *104*, 2543–2548.

Gelderman, M.P., and Simak, J. (2008). Flow cytometric analysis of cell membrane microparticles. Methods Mol. Biol. *484*, 79–93.

Gemmell, C.H., Sefton, M. V., and Yeo, E.L. (1993). Platelet-derived microparticle formation involves glycoprotein IIb-IIIa Inhibition by RGDS and a Glanzmann's thrombasthenia defect. J. Biol. Chem. *268*, 14586–14589.

Gianella, S., Massanella, M., Richman, D.D., Little, S.J., Spina, C.A., Vargas, M. V., Lada, S.M., Daar, E.S., Dube, M.P., Haubrich, R.H., et al. (2014). Cytomegalovirus Replication in Semen Is Associated with Higher Levels of Proviral HIV DNA and CD4 + T Cell Activation during Antiretroviral Treatment . J. Virol. *88*, 7818–7827.

Gianella, S., Anderson, C.M., Var, S.R., Oliveira, M.F., Lada, S.M., Vargas, M. V., Massanella, M., Little, S.J., Richman, D.D., Strain, M.C., et al. (2016). Replication of Human Herpesviruses Is Associated with Higher HIV DNA Levels during Antiretroviral Therapy Started at Early Phases of HIV Infection. J. Virol. *90*, 3944–3952.

Gibellini, D., Zauli, G., Re, M.C., Milani, D., Furlini, G., Caramelli, E., Capitani, S., and La Placa, M.

(1994). Recombinant human immunodeficiency virus type-1 (HIV-1) Tat protein sequentially up-regulates IL-6 and TGF-β1 mRNA expression and protein synthesis in peripheral blood monocytes. Br. J. Haematol. *88*, 261–267.

Gilbert, G.E., Sims, P.J., Wiedmer, T., Furie, B., Furie, B.C., and Shattil, S.J. (1991). Platelet-derived microparticles express high affinity receptors for factor VIII. J. Biol. Chem. *266*, 17261–17268.

Giorgi, J. V., Lyles, R.H., Matud, J.L., Yamashita, T.E., Mellors, J.W., Hultin, L.E., Jamieson, B.D., Margolick, J.B., Rinaldo, C.R., Phair, J.P., et al. (2002). Predictive value of immunologic and virologic markers after long or short duration of HIV-1 infection. J. Acquir. Immune Defic. Syndr. *29*, 346–355.

Giuliano, I.D.C.B., De Freitas, S.F.T., De Souza, M., and Caramelli, B. (2008). Subclinic atherosclerosis and cardiovascular risk factors in HIV-infected children: PERI study. Coron. Artery Dis. *19*, 167–172.

González, P., Alvarez, R., Batalla, A., Reguero, J.R., Alvarez, V., Astudillo, A., Cubero, G.I., Cortina, A., and Coto, E. (2001). Genetic variation at the chemokine receptors CCR5/CCR2 in myocardial infarction. Genes Immun. *2*, 191–195.

Gradziuk, M., and Radziwon, P. (2017). Methods for detection of microparticles derived from blood and endothelial cells. Acta Haematol. Pol. *48*, 316–329.

Grossman, Z., Feinberg, M.B., and Paul, W.E. (1998). Multiple modes of cellular activation and virus transmission in HIV infection: A role for chronically and latently infected cells in sustaining viral replication. Proc. Natl. Acad. Sci. U. S. A. *95*, 6314–6319.

Grund, B., Baker, J. V., Deeks, S.G., Wolfson, J., Wentworth, D., Cozzi-Lepri, A., Cohen, C.J., Phillips, A., Lundgren, J.D., and Neaton, J.D. (2016). Relevance of interleukin-6 and D-dimer for serious non-AIDS morbidity and death among HIV-positive adults on suppressive antiretroviral therapy. PLoS One *11*, 1–16.

Guadalupe, M., Reay, E., Sankaran, S., Prindiville, T., Flamm, J., McNeil, A., and Dandekar, S. (2003). Severe CD4+ T-Cell Depletion in Gut Lymphoid Tissue during Primary Human Immunodeficiency Virus Type 1 Infection and Substantial Delay in Restoration following Highly Active Antiretroviral Therapy. J. Virol. *77*, 11708–11717.

Guadalupe, M., Sankaran, S., George, M.D., Reay, E., Verhoeven, D., Shacklett, B.L., Flamm, J., Wegelin, J., Prindiville, T., and Dandekar, S. (2006). Viral Suppression and Immune Restoration in the Gastrointestinal Mucosa of Human Immunodeficiency Virus Type 1-Infected Patients Initiating Therapy during Primary or Chronic Infection. J. Virol. *80*, 8236–8247.

Guillé, S.I., Prieto, L., Jimé nez de Ory, S.I., Isabel Gonzá lez-Tomé, M., RojoID, P., Luisa Navarro, M., José Mellado, M., Escosa, L., Sainz, T., Francisco, L., et al. (2019). Prognostic factors of a lower CD4/CD8 ratio in long term viral suppression HIV infected children. *14*, e0220552.

Gupta-Wright, A., Tembo, D., Jambo, K.C., Chimbayo, E., Mvaya, L., Caldwell, S., Russell, D.G., and Mwandumba, H.C. (2017). Functional analysis of phagocyte activity in whole blood from HIV/tuberculosis-infected individuals using a novel flow cytometry-based assay. Front. Immunol. *8*, 1222.

Gupta, S.K., Shen, C., Moe, S.M., Kamendulis, L.M., Goldman, M., and Dubé, M.P. (2012). Worsening Endothelial Function with Efavirenz Compared to Protease Inhibitors: A 12-Month Prospective Study. PLoS One *7*, 5–10.

Han, J., Wang, B., Han, N., Zhao, Y., and Song, C. (2009). CD14 high CD16 + Rather Than CD14 low CD16 + Monocytes Correlate With Disease Progression in Chronic HIV-Infected Patients. J. Acquir. Immune Defic. Syndr. *52*, 553–559.

Hanna, D.B., Post, W.S., Deal, J.A., Hodis, H.N., Jacobson, L.P., Mack, W.J., Anastos, K., Gange, S.J., Landay, A.L., Lazar, J.M., et al. (2015). HIV Infection Is Associated with Progression of Subclinical Carotid Atherosclerosis. Clin. Infect. Dis. *61*, 640–650.

Hanna, D.B., Guo, M., Bůžková, P., Miller, T.L., Post, W.S., Stein, J.H., Currier, J.S., Kronmal, R.A., Freiberg, M.S., Bennett, S.N., et al. (2016). HIV Infection and Carotid Artery Intima-media Thickness: Pooled Analyses Across 5 Cohorts of the NHLBI HIV-CVD Collaborative. Clin. Infect. Dis. *63*, 249–256.

Hanna, D.B., Lin, J., Post, W.S., Hodis, H.N., Xue, X., Anastos, K., Cohen, M.H., Gange, S.J., Haberlen, S.A., Heath, S.L., et al. (2017). Association of macrophage inflammation biomarkers with progression of subclinical carotid artery atherosclerosis in HIV-infected women and men. J. Infect. Dis. *215*, 1352–1361.

Hansson, G.K. (2005). Mechanisms of disease: Inflammation, atherosclerosis, and coronary artery disease. N. Engl. J. Med. *352*, 1685–1695.

Hattab, S., Guihot, A., Guiguet, M., Fourati, S., Carcelain, G., Caby, F., Marcelin, A.G., Autran, B., Costagliola, D., and Katlama, C. (2014). Comparative impact of antiretroviral drugs on markers of inflammation and immune activation during the first two years of effective therapy for HIV-1 infection: An observational study. BMC Infect. Dis. *14*, 1–9.

Hattab, S., Guiguet, M., Carcelain, G., Fourati, S., Guihot, A., Autran, B., Caby, F., Marcelin, A.G., Costagliola, D., and Katlama, C. (2015). Soluble biomarkers of immune activation and inflammation in HIV infection: Impact of 2 years of effective first-line combination antiretroviral therapy. HIV Med. *16*, 553–562.

Hearps, A.C., Maisa, A., Cheng, W.J., Angelovich, T.A., Lichtfuss, G.F., Palmer, C.S., Landay, A.L., Jaworowski, A., and Crowe, S.M. (2012). HIV infection induces age-related changes to monocytes and innate immune activation in young men that persist despite combination antiretroviral therapy. AIDS *26*, 843–853.

El Hed, A., Khaitan, A., Kozhaya, L., Manel, N., Daskalakis, D., Borkowsky, W., Valentine, F., Littman, D.R., and Unutmaz, D. (2011). Human Th17 cells are susceptible to HIV and are perturbed during infection. J. Infect. Dis. *201*, 843–854.

Henrich, T.J., Hobbs, K.S., Hanhauser, E., Scully, E., Hogan, L.E., Robles, Y.P., Leadabrand, K.S., Marty, F.M., Palmer, C.D., Jost, S., et al. (2017). Human immunodeficiency virus type 1 persistence following systemic chemotherapy for malignancy. J. Infect. Dis. *216*, 254–262.

Hijdra, D., Vorselaars, A.D.M., Grutters, J.C., Claessen, A.M.E., and Rijkers, G.T. (2013). Phenotypic Characterization of Human Intermediate Monocytes. Front. Immunol. 4–6.

Hijmans, J.G., Stockelman, K.A., Garcia, V., Levy, M. V., Madden Brewster, L., Bammert, T.D., Greiner, J.J., Stauffer, B.L., Connick, E., and DeSouza, C.A. (2019). Circulating microparticles are elevated in treated HIV-1 infection and are deleterious to endothelial cell function. J. Am. Heart Assoc. *8*, 1–14.

Hileman, C.O., Carman, T.L., Longenecker, C.T., Labbato, D.E., Storer, N.J., White, C.A., and McComsey, G.A. (2013). Rate and predictors of carotid artery intima media thickness progression in antiretroviral-naive HIV-infected and uninfected adults: A 48-week matched prospective cohort study. Antivir. Ther. *18*, 921–929.

Hingorani, A.D., Cross, J., Kharbanda, R.K., Mullen, M.J., Bhagat, K., Taylor, M., Donald, A.E., Palacios, M., Griffin, G.E., Deanfield, J.E., et al. (2000). Acute systemic inflammation impairs endothelium-dependent dilatation in humans. Circulation *102*, 994–999.

Ho, J.E., and Hsue, P.Y. (2009). Cardiovascular manifestations of HIV infection. Heart *95*, 1193–1202.

Hoffman, M., Monroe, D.M., and Roberts, H.R. (1992). Coagulation factor IXa binding to activated platelets and platelet-derived microparticles. A flow cytometric study. Thromb. Haemost. *68*, 74–78.

Holme, P.A., Müller, F., Solum, N.O., Brosstad, F., FrØland, S.S., and Aukrust, P. (1998). Enhanced activation of platelets with abnormal release of RANTES in human immunodeficiency virus type 1 infection. FASEB J. *12*, 79–90.

Hoyer, F.F., Giesen, M.K., Nunes França, C., Lütjohann, D., Nickenig, G., and Werner, N. (2012). Monocytic microparticles promote atherogenesis by modulating inflammatory cells in mice. J. Cell. Mol. Med. *16*, 2777–2788.

Hsu, D.C., Ma, Y.F., Hur, S., Li, D., Rupert, A., Scherzer, R., Kalapus, S.C., Deeks, S., Sereti, I., and Hsue, P.Y. (2016). Plasma IL-6 levels are independently associated with atherosclerosis and mortality in HIV-infected individuals on suppressive antiretroviral therapy. Aids *30*, 2065–2074.

Hsue, P.Y., and Waters, D.D. (2018). Time to recognize HIV infection as a major cardiovascular risk factor. Circulation *138*, 1113–1115.

Hsue, P.Y., Hunt, P.W., Schnell, A., Kalapus, S.C., Hoh, R., Ganz, P., Martin, J.N., and Deeks, S.G. (2009). Role of viral replication, antiretroviral therapy, and immunodeficiency in HIV-associated atherosclerosis. Aids *23*, 1059–1067.

Hsue, P.Y., Ordovas, K., Lee, T., Reddy, G., Gotway, M., Schnell, A., Ho, J.E., Selby, V., Madden, E., Martin, J.N., et al. (2012). Carotid intima-media thickness among human immunodeficiency virus-infected patients without coronary calcium. Am. J. Cardiol. *109*, 742–747.

Hsue, Y., Lo, J.C., Franklin, A., Bolger, A.F., Martin, J.N., Deeks, S.G., and Waters, D.D. (2004). Progression of Atherosclerosis as Assessed by Carotid Intima-Media Thickness in Patients with HIV Infection. Circulation *109*, 1603–1608.

Huang, Y.Q., Li, J., Huang, C., and Feng, Y.Q. (2018). Plasma MicroRNA-29c Levels Are Associated with Carotid Intima-Media Thickness and is a Potential Biomarker for the Early Detection of Atherosclerosis. Cell. Physiol. Biochem. *50*, 452–459.

Hulten, E., Mitchell, J., Scally, J., Gibbs, B., and Villines, T.C. (2009). HIV positivity, protease inhibitor exposure and subclinical atherosclerosis: A systematic review and meta-analysis of observational studies. Heart *95*, 1826–1835.

Hunt, P.W., Martin, J.N., Sinclair, E., Bredt, B., Hagos, E., Lampiris, H., and Deeks, S.G. (2003). T Cell Activation Is Associated with Lower CD4 + T Cell Gains in Human Immunodeficiency Virus–Infected Patients with Sustained Viral Suppression during Antiretroviral Therapy . J. Infect. Dis. *187*, 1534–1543.

Hunt, P.W., Brenchley, J., Sinclair, E., McCune, J.M., Roland, M., Page-Shafer, K., Hsue, P., Emu, B., Krone, M., Lampiris, H., et al. (2008). Relationship between T Cell Activation and CD4 + T Cell Count in HIV-Seropositive Individuals with Undetectable Plasma HIV RNA Levels in the Absence of Therapy. J. Infect. Dis. *197*, 126–133.

Hunt, P.W., Landay, A.L., Sinclair, E., Martinson, J.A., Hatano, H., Emu, B., Norris, P.J., Busch, M.P., Martin, J.N., Brooks, C., et al. (2011). A low T regulatory cell response may contribute to both viral control and generalized immune activation in HIV controllers. PLoS One *6*, e15924.

Hunt, P.W., Sinclair, E., Rodriguez, B., Shive, C., Clagett, B., Funderburg, N., Robinson, J., Huang, Y., Epling, L., Martin, J.N., et al. (2014). Gut epithelial barrier dysfunction and innate immune activation predict mortality in treated HIV infection. J. Infect. Dis. *210*, 1228–1238.

Idris, N.S., Grobbee, D.E., Burgner, D., Cheung, M.M.H., Kurniati, N., Sastroasmoro, S., and Uiterwaal, C.S.P.M. (2015). Cardiovascular manifestations of HIV infection in children. Eur. J. Prev. Cardiol. *22*, 1452–1461.

Iii, A.P.O., and Mackman, N. (2012). Microparticles in hemostasis. *108*, 1284–1297.

Islam, F.M., Wu, J., Jansson, J., and Wilson, D.P. (2012). Relative risk of cardiovascular disease among people living with HIV: A systematic review and meta-analysis. HIV Med. *13*, 453–468.

Janeway Jr., C.A., and Medzhitov, R. (2002). Innate immune recognition. Annu Rev Immunol *20*, 197–216.

Jaworowski, A., Kamwendo, D.D., Ellery, P., Sonza, S., Mwapasa, V., Tadesse, E., Molyneux, M.E., Rogerson, S.J., Meshnick, S.R., and Crowe, S.M. (2007). CD16+ monocyte subset preferentially harbors HIV-1 and is expanded in pregnant Malawian women with Plasmodium falciparum malaria and HIV-1 infection. J. Infect. Dis. *196*, 38–42.

Jayachandran, M., Litwiller, R.D., Owen, W.G., Heit, J.A., Behrenbeck, T., Mulvagh, S.L., Araoz, P.A., Budoff, M.J., Harman, S.M., and Miller, V.M. (2008). Characterization of blood borne microparticles as markers of premature coronary calcification in newly menopausal women. Am. J. Physiol. - Hear. Circ. Physiol. *295*, 931–938.

Jayachandran, M., Miller, V.M., Heit, J.A., and Owen, W.G. (2012). Methodology for isolation, identification and characterization of microvesicles in peripheral blood. J. Immunol. Methods *375*, 207–214.

Ji, J., Sahu, G.K., Braciale, V.L., and Cloyd, M.W. (2005). HIV-1 induces IL-10 production in human monocytes via a CD4-independent pathway. Int. Immunol. *17*, 729–736.

Jiang, W., Lederman, M.M., Hunt, P., Sieg, S.F., Haley, K., Rodriguez, B., Landay, A., Martin, J.,

Sinclair, E., Asher, A.I., et al. (2009). Plasma Levels of Bacterial DNA Correlate with Immune Activation and the Magnitude of Immune Restoration in Persons with Antiretroviral-Treated HIV Infection. J. Infect. Dis. *199*, 1177–1185.

Jimenez, J.J., Jy, W., Mauro, L.M., Soderland, C., Horstman, L.L., and Ahn, Y.S. (2003). Endothelial cells release phenotypically and quantitatively distinct microparticles in activation and apoptosis. Thromb. Res. *109*, 175–180.

Jin, M., Drwal, G., Bourgeois, T., Saltz, J., and Wu, H.M. (2005). Distinct proteome features of plasma microparticles. Proteomics *5*, 1940–1952.

Jy, W., Minagar, A., Jimenez, J.J., Sheremata, W.A., Mauro, L.M., Horstman, L.L., Bidot, C., and Ahn, Y.S. (2004). Endothelial microparticles (EMP) bind and activate monocytes: elevated EMP-monocyte conjugates in multiple sclerosis. Front. Biosci. *9*, 3137–3144.

Kanazawa, S., Nomura, S., Kuwana, M., Muramatsu, M., Yamaguchi, K., and Fukuhara, S. (2003). Monocyte-derived microparticles may be a sign of vascular complication in patients with lung cancer. Lung Cancer *39*, 145–149.

Kawai, T., and Akira, S. (2010). The role of pattern-recognition receptors in innate immunity: Update on toll-like receptors. Nat. Immunol. *11*, 373–384.

Kelesidis, T., Kendall, M.A., Yang, O.O., Hodis, H.N., and Currier, J.S. (2012). Biomarkers of microbial translocation and macrophage activation: Association with progression of subclinical atherosclerosis in HIV-1 infection. J. Infect. Dis. *206*, 1558–1567.

Kelly, C. (2016). HIV, Immune activation and Endothelial Damage in Malawian Adults. (Unpublished PhD Thesis). University of Liverpool, UK.

Kenny, J. (2016). The Impact of HIV and Antiretroviral Therapy on the Cardiovascular System of HIV-infected Children. (Unpublished PhD Thesis). Institute of Child Health, University College London, UK.

Khaspekova, S.G., Antonova, O.A., Shustova, O.N., Yakushkin, V. V., Golubeva, N. V., Titaeva, E. V., Dobrovolsky, A.B., and Mazurov, A. V. (2016). Activity of tissue factor in microparticles produced in vitro by endothelial cells, monocytes, granulocytes, and platelets. Biochemistry *81*, 114–121.

Kho, D.T., Johnson, R., Robilliard, L., Mez, E. du, McIntosh, J., O'Carroll, S.J., Angel, C.E., and Scott Graham, E. (2017). ECIS technology reveals that monocytes isolated by CD14+ve selection mediate greater loss of BBB integrity than untouched monocytes, which occurs to a greater extent with IL-1β activated endothelium in comparison to TNFα. PLoS One *12*, 1–19.

Kim, W.-K., Sun, Y., Do, H., Autissier, P., Halpern, E.F., Piatak, M., Lifson, J.D., Burdo, T.H., McGrath, M.S., and Williams, K. (2010). Monocyte heterogeneity underlying phenotypic changes in monocytes according to SIV disease stage. J. Leukoc. Biol. *87*, 557–567.

Kingsley, L.A., Deal, J., Jacobson, L., Budoff, M., Witt, M., Palella, F., Calhoun, B., and Post, W.S. (2015). Incidence and progression of coronary artery calcium in HIV-infected and HIV-uninfected men. AIDS *29*, 2427–2434.

Kinlay, S., Libby, P., and Ganz, P. (2001). Endothelial function and coronary artery disease. Curr.

Opin. Lipidol. *12*, 383–389.

Koga, H., Sugiyama, S., Kugiyama, K., Watanabe, K., Fukushima, H., Tanaka, T., Sakamoto, T., Yoshimura, M., Jinnouchi, H., and Ogawa, H. (2005). Elevated levels of VE-cadherin-positive endothelial microparticles in patients with type 2 diabetes mellitus and coronary artery disease. J. Am. Coll. Cardiol. *45*, 1622–1630.

Koifman, N., Biran, I., Aharon, A., Brenner, B., and Talmon, Y. (2017). A direct-imaging cryo-EM study of shedding extracellular vesicles from leukemic monocytes. J. Struct. Biol. *198*, 177–185.

Kopczyńska, E., and Makarewicz, R. (2012). Endoglin - A marker of vascular endothelial cell proliferation in cancer. Contemp. Oncol. *16*, 68–71.

Koroleva, I.A., Nazarenko, M.S., and Kucher, A.N. (2017). Role of microRNA in development of instability of atherosclerotic plaques. Biochem. *82*, 1380–1390.

Koshiar, R.L., Somajo, S., Norström, E., and Dahlbäck, B. (2014). Erythrocyte-derived microparticles supporting activated protein C-mediated regulation of blood coagulation. PLoS One *9*, e104200.

Kreutter, G., Kassem, M., El Habhab, A., Baltzinger, P., Abbas, M., Boisrame-Helms, J., Amoura, L., Peluso, J., Yver, B., Fatiha, Z., et al. (2017). Endothelial microparticles released by activated protein C protect beta cells through EPCR/PAR1 and annexin A1/FPR2 pathways in islets. J. Cell. Mol. Med. *21*, 2759–2772.

Kristoffersen, U.S., Kofoed, K., Kronborg, G., Giger, A.K., Kjaer, A., and Lebech, A.M. (2009). Reduction in circulating markers of endothelial dysfunction in HIV-infected patients during antiretroviral therapy. HIV Med. *10*, 79–87.

Kuller, L.H., Tracy, R., Belloso, W., De Wit, S., Drummond, F., Lane, H.C., Ledergerber, B., Lundgren, J., Neuhaus, J., Nixon, D., et al. (2008). Inflammatory and coagulation biomarkers and mortality in patients with HIV infection. PLoS Med. *5*, 1496–1508.

Kunjathoor, V. V., Febbraio, M., Podrez, E.A., Moore, K.J., Andersson, L., Koehn, S., Rhee, J.S., Silverstein, R., Hoff, H.F., and Freeman, M.W. (2002). Scavenger receptors class A-I/II and CD36 are the principal receptors responsible for the uptake of modified low density lipoprotein leading to lipid loading in macrophages. J. Biol. Chem. *277*, 49982–49988.

Lambotte, O., Taoufik, Y., De Goër, M.G., Wallon, C., Goujard, C., and Delfraissy, J.F. (2000). Detection of infectious HIV in circulating monocytes from patients on prolonged highly active antiretroviral therapy. J. Acquir. Immune Defic. Syndr. *23*, 114–119.

Lee, S.-T., Chu, K., Jung, K.-H., Kim, J.-M., Moon, H.-J., Bahn, J.-J., Im, W.-S., Sunwoo, J., Moon, J., Kim, M., et al. (2012). Circulating CD62E+ microparticles and cardiovascular outcomes. PLoS One *7*, e35713.

Lefèvre, C., Auclair, M., Boccara, F., Bastard, J.P., Capeau, J., Vigouroux, C., and Caron-Debarle, M. (2010). Premature senescence of vascular cells is induced by HIV protease inhibitors: Implication of prelamin a and reversion by statin. Arterioscler. Thromb. Vasc. Biol. *30*, 2611–2620.

Leite Pereira, A., Tchitchek, N., Lambotte, O., Le Grand, R., and Cosma, A. (2019).

Characterization of Leukocytes From HIV-ART Patients Using Combined Cytometric Profiles of 72 Cell Markers. Front. Immunol. *10*, 1777.

Leonetti, D., Reimund, J.M., Tesse, A., Viennot, S., Martinez, M.C., Bretagne, A.L., and Andriantsitohaina, R. (2013). Circulating Microparticles from Crohn's Disease Patients Cause Endothelial and Vascular Dysfunctions. PLoS One *8*, e73088.

Leroyer, A.S., Isobe, H., Lesèche, G., Castier, Y., Wassef, M., Mallat, Z., Binder, B.R., Tedgui, A., and Boulanger, C.M. (2007). Cellular Origins and Thrombogenic Activity of Microparticles Isolated From Human Atherosclerotic Plaques. J. Am. Coll. Cardiol. *49*, 772–777.

Li, S., Wei, J., Zhang, C., Li, X., Meng, W., Mo, X., Zhang, Q., Liu, Q., Ren, K., Du, R., et al. (2016). Cell-Derived Microparticles in Patients with Type 2 Diabetes Mellitus: A Systematic Review and Meta-Analysis. Cell. Physiol. Biochem. *39*, 2439–2450.

Lien, E., Aukrust, P., Sundan, A., Muller, F., Froland, S.S., and Espevik, T. (1998). Elevated levels of serum-soluble CD14 in human immunodeficiency virus type 1 (HIV-1) infection: correlation to disease progression and clinical events. Blood *92*, 2084–2092.

De Lima, L.R.A., Petroski, E.L., Moreno, Y.M.F., Silva, D.A.S., De Moraes Santos Trindade, E.B., De Carvalho, A.P., and De Carlos Back, I. (2018). Dyslipidemia, chronic inflammation, and subclinical atherosclerosis in children and adolescents infected with HIV: The PositHIVe Health Study. PLoS One *13*, 1–17.

Longenecker, C.T., Jiang, Y., Orringer, C.E., Gilkeson, R.C., Debanne, S., Funderburg, N.T., Lederman, M.M., Storer, N., Labbato, D.E., and McComsey, G.A. (2014). Soluble CD14 is independently associated with coronary calcification and extent of subclinical vascular disease in treated HIV infection. Aids *28*, 969–977.

Lorenz, M.W., Polak, J.F., Kavousi, M., Mathiesen, E.B., Völzke, H., Tuomainen, T.P., Sander, D., Plichart, M., Catapano, A.L., Robertson, C.M., et al. (2012). Carotid intima-media thickness progression to predict cardiovascular events in the general population (the PROG-IMT collaborative project): A meta-analysis of individual participant data. Lancet *379*, 2053–2062.

De Luca, A., de Gaetano Donati, K., Colafigli, M., Cozzi-Lepri, A., De Curtis, A., Gori, A., Sighinolfi, L., Giacometti, A., Capobianchi, M.R., and D'Avino, A. (2013). The association of high-sensitivity c-reactive protein and other biomarkers with cardiovascular disease in patients treated for HIV: a nested case–control study. BMC Infect. Dis. *13*, 1.

Lund, H., Boysen, P., Åkesson, C.P., Lewandowska-Sabat, A.M., and Storset, A.K. (2016). Transient migration of large numbers of CD14++ CD16+ monocytes to the draining lymph node after onset of inflammation. Front. Immunol. *7*, 322.

Lynn, W.A., Liu, Y., and Golenbock, D.T. (1993). Neither CD14 nor serum is absolutely necessary for activation of mononuclear phagocytes by bacterial lipopolysaccharide. Infect. Immun. *61*, 4452–4461.

Macey, M.G., McCarthy, D.A., Vordermeier, S., Newland, A.C., and Brown, K.A. (1995). Effects of cell purification methods on CD11b and l-selectin expression as well as the adherence and activation of leucocytes. J. Immunol. Methods *181*, 211–219.

Mack, M., Kleinschmidt, A., Bruhl, H., Klier, C., Nelson, P.J., Cihak, J., Plachy, J., Stangassinger, M., Erfle, V., and Schlondorff, D. (2000). Transfer of the chemokine receptor CCR5 between cells by membrane-derived microparticles: a mechanism for cellular human immunodeficiency virus 1 infection. Nat Med *6*, 769–775.

Maidji, E., Somsouk, M., Rivera, J.M., Hunt, P.W., and Stoddart, C.A. (2017). Replication of CMV in the gut of HIV-infected individuals and epithelial barrier dysfunction. PLoS Pathog. *13*, e1006202.

Maisa, A., Hearps, A.C., Angelovich, T.A., Pereira, C.F., Zhou, J., Shi, M.D.Y., Palmer, C.S., Muller, W.A., Crowe, S.M., and Jaworowski, A. (2015). Monocytes from HIV-infected individuals show impaired cholesterol efflux and increased foam cell formation after transendothelial migration. AIDS *29*, 1445–1457.

Mallat, Z., Benamer, H., Hugel, B., Benessiano, J., Steg, P.G., Freyssinet, J.M., and Tedgui, A. (2000). Elevated levels of shed membrane microparticles with procoagulant potential in the peripheral circulating blood of patients with acute coronary syndromes. Circulation *101*, 841–843.

Marcos-Ramiro, B., Oliva Nacarino, P., Serrano-Pertierra, E., Blanco-Gelaz, M.T., Weksler, B.B., Romero, I.A., Couraud, P.O., Tuñón, A., López-Larrea, C., Millán, J., et al. (2014). Microparticles in multiple sclerosis and clinically isolated syndrome: Effect on endothelial barrier function. BMC Neurosci. *15*.

Marcus, J.L., Neugebauer, R.S., Leyden, W.A., Chao, C.R., Xu, L., Quesenberry, C.P., Klein, D.B., Towner, W.J., Horberg, M.A., and Silverberg, M.J. (2016). Use of abacavir and risk of cardiovascular disease among HIV-infected individuals. J. Acquir. Immune Defic. Syndr. *71*, 413–419.

Márquez, M., Romero-Cores, P., Montes-Oca, M., Martín-Aspas, A., Soto-Cárdenas, M.J., Guerrero, F., Fernández-Gutiérrez, C., and Girón-González, J.A. (2015). Immune activation response in chronic HIV-infected patients: Influence of hepatitis C virus coinfection. PLoS One *10*, e0119568.

Martin.L (1994). Inactivation and disinfection of HIV: A summary.

Martin, S., Tesse, A., Hugel, B., Martínez, M.C., Morel, O., Freyssinet, J.M., and Andriantsitohaina, R. (2004). Shed Membrane Particles from T Lymphocytes Impair Endothelial Function and Regulate Endothelial Protein Expression. Circulation *109*, 1653–1659.

Martinez-Skinner, A.L., Veerubhotla, R.S., Liu, H., Xiong, H., Yu, F., McMillan, J.M., and Gendelman, H.E. (2013). Functional proteome of macrophage carried nanoformulated antiretroviral therapy demonstrates enhanced particle carrying capacity. J. Proteome Res. *12*, 2282–2294.

Martinez, M.C., and Andriantsitohaina, R. (2011). Microparticles in angiogenesis: Therapeutic potential. Circ. Res. *109*, 110–119.

Maruyama, I. (1998). Biology of endothelium. Lupus *7*, 41–43.

Masiá, M., Padilla, S., Barber, X., Sanchis, M., Terol, G., Lidón, F., and Gutiérrez, F. (2016).

Comparative impact of suppressive antiretroviral regimens on the CD4/CD8 T-cell ratio: A cohort study. Medicine (Baltimore). *95*, e3108.

Mastronardi, M.L., Mostefai, H.A., Soleti, R., Agouni, A., Martínez, M.C., and Andriantsitohaina, R. (2011). Microparticles from apoptotic monocytes enhance nitrosative stress in human endothelial cells. Fundam. Clin. Pharmacol. *25*, 653–660.

Mattingly, A.S., Unsal, A.B., Purdy, J.B., Gharib, A.M., Rupert, A., Kovacs, J.A., McAreavey, D., Hazra, R., Abd-Elmoniem, K.Z., and Hadigan, C. (2017). T-cell Activation and E-selectin Are Associated with Coronary Plaque in HIV-infected Young Adults. Pediatr. Infect. Dis. J. *36*, 63–65.

Mause, S.F., Von Hundelshausen, P., Zernecke, A., Koenen, R.R., and Weber, C. (2005). Platelet microparticles: A transcellular delivery system for RANTES promoting monocyte recruitment on endothelium. Arterioscler. Thromb. Vasc. Biol. *25*, 1512–1518.

Mavigner, M., Cazabat, M., Dubois, M., L'Faqihi, F.E., Requena, M., Pasquier, C., Klopp, P., Amar, J., Alric, L., Barange, K., et al. (2012). Altered CD4 + T cell homing to the gut impairs mucosal immune reconstitution in treated HIV-infected individuals. J. Clin. Invest. *122*, 62–69.

Mayne, E., Funderburg, N.T., Sieg, S.F., Asaad, R., Kalinowska, M., Rodriguez, B., Schmaier, A.H., Stevens, W., and Lederman, M.M. (2012). Increased platelet and microparticle activation in HIV infection: upregulation of P-selectin and tissue factor expression. J. Acquir. Immune Defic. Syndr. *59*, 340–346.

McCausland, M.R., Juchnowski, S.M., Zidar, D.A., Kuritzkes, D.R., Andrade, A., Sieg, S.F., Lederman, M.M., and Funderburg, N.T. (2015). Altered Monocyte Phenotype in HIV-1 Infection Tends to Normalize with Integrase-Inhibitor-Based Antiretroviral Therapy. PLoS One *10*, e0139474.

McComsey, G.A., O'Riordan, M., Hazen, S.L., El-Bejjani, D., Bhatt, S., Brennan, M.L., Storer, N., Adell, J., Nakamoto, D.A., and Dogra, V. (2007). Increased carotid intima media thickness and cardiac biomarkers in HIV infected children. AIDS *21*, 921–927.

McCune, J.M. (2001). The dynamics of CD4 T-cell depletion in HIV disease. Nature *410*, 974–979.

Mcgettrick, P., Barco, E.A., and Mallon, P.W.G. (2018). Ageing with HIV. Healthcare *6*.

McKibben, R.A., Margolick, J.B., Grinspoon, S., Li, X., Palella Jr, F.J., Kingsley, L.A., Witt, M.D., George, R.T., Jacobson, L.P., Budoff, M., et al. (2015). Elevated levels of monocyte activation markers are associated with subclinical atherosclerosis in men with and those without HIV infection. J. Infect. Dis. *211*, 1219–1228.

Meaney, M.P., Nieman, D.C., Henson, D.A., Jiang, Q., and Wang, F.-Z. (2016). Measuring Granulocyte and Monocyte Phagocytosis and Oxidative Burst Activity in Human Blood. J. Vis. Exp. e54264.

Meerschaert, J., and Furie, M.B. (1995). The adhesion molecules used by monocytes for migration across endothelium include CD11a/CD18, CD11b/CD18, and VLA-4 on monocytes and ICAM-1, VCAM-1, and other ligands on endothelium. J. Immunol. *154*, 4099–4112.

Mehandru, S., Poles, M.A., Tenner-Racz, K., Jean-Pierre, P., Manuelli, V., Lopez, P., Shet, A., Low, A., Mohri, H., Boden, D., et al. (2006). Lack of mucosal immune reconstitution during prolonged

treatment of acute and early HIV-1 infection. PLoS Med. *3*, 2335–2348.

Méndez-Lagares, G., Romero-Sánchez, M.C., Ruiz-Mateos, E., Genebat, M., Ferrando-Martínez, S., Muñoz-Fernández, M.A., Pacheco, Y.M., and Leal, M. (2013). Long-term suppressive combined antiretroviral treatment does not normalize the serum level of soluble CD14. J. Infect. Dis. *207*, 1221–1225.

Merino, A., Buendia, P., Martin-Malo, A., Aljama, P., Ramirez, R., and Carracedo, J. (2011). Senescent CD14+CD16+ monocytes exhibit proinflammatory and proatherosclerotic activity. J. Immunol. *186*, 1809–1815.

Merlini, E., Luzi, K., Suardi, E., Barassi, A., Cerrone, M., Martínez, J.S., Bai, F., D'Eril, G.V.M., Monforte, A.D.A., and Marchetti, G. (2012). T-Cell Phenotypes, Apoptosis and Inflammation in HIV+ Patients on Virologically Effective cART with Early Atherosclerosis. PLoS One *7*, e46073.

Mezentsev, A., Merks, R.M.H., O'Riordan, E., Chen, J., Mendelev, N., Goligorsky, M.S., and Brodsky, S. V. (2005). Endothelial microparticles affect angiogenesis in vitro: Role of oxidative stress. Am. J. Physiol. - Hear. Circ. Physiol. *289*, 1106–1114.

Michailidis, C., Giannopoulos, G., Vigklis, V., Armenis, K., Tsakris, A., and Gargalianos, P. (2012). Impaired phagocytosis among patients infected by the human immunodeficiency virus: implication for a role of highly active anti-retroviral therapy. Clin. Exp. Immunol. *167*, 499–504.

Miguet, L., Pacaud, K., Felden, C., Hugel, B., Martinez, M.C., Freyssinet, J.M., Herbrecht, R., Potier, N., Van Dorsselaer, A., and Mauvieux, L. (2006). Proteomic analysis of malignant lymphocyte membrane microparticles using double ionization coverage optimization. Proteomics *6*, 153–171.

Mikhail, I.J., Purdy, J.B., Dimock, D.S., Thomas, V.M., Muldoon, N.A., Clauss, S.B., Cross, R.R., Pettigrew, R.I., Hazra, R., Hadigan, C., et al. (2011). High rate of coronary artery abnormalities in adolescents and young adults infected with human immunodeficiency virus early in life. Pediatr. Infect. Dis. J. *30*, 710–720.

Milei, J., Ottaviani, G., Lavezzi, A.M., Grana, D.R., Stella, I., and Matturri, L. (2008). Perinatal and infant early atherosclerotic coronary lesions. Can. J. Cardiol. *24*, 137–141.

Miller, P.E., Haberlen, S.A., Metkus, T., Rezaeian, P., Kingsley, L.A., Witt, M.D., George, R.T., Jacobson, L.P., Brown, T.T., Budoff, M., et al. (2015). Cohort Study (MACS) Miller , HIV and coronary artery remodeling. Atherosclerosis *241*, 716–722.

Miller, T.L., Orav, E.J., Lipshultz, S.E., Arheart, K.L., Duggan, C., Weinberg, G.A., Bechard, L., Furuta, L., Nicchita, J., Gorbach, S.L., et al. (2008). Risk Factors for Cardiovascular Disease in Children Infected with Human. J. Pediatr. *October*, 491–497.

Miller, T.L., Somarriba, G., Orav, E.J., Mendez, A.J., Neri, D., Schaefer, N., Forster, L., Goldberg, R., Scott, G.B., and Lipshultz, S.E. (2010). Biomarkers of vascular dysfunction in children infected with human immunodeficiency virus-1. J. Acquir. Immune Defic. Syndr. *55*, 182–188.

Miller, T.L., Borkowsky, W., Dimeglio, L.A., Dooley, L., Geffner, M.E., Hazra, R., McFarland, E.J., Mendez, A.J., Patel, K., Siberry, G.K., et al. (2012). Metabolic abnormalities and viral replication are associated with biomarkers of vascular dysfunction in HIV-infected children. HIV Med. *13*,

264–275.

Miyazaki, Y., Nomura, S., Miyake, T., Kagawa, H., Kitada, C., Taniguchi, H., Komiyama, Y., Fujimura, Y., Ikeda, Y., and Fukuhara, S. (1996). High shear stress can initiate both platelet aggregation and shedding of procoagulant containing microparticles. Blood *88*, 3456–3464.

Molina, J.M., Scadden, D.T., Byrn, R., Dinarello, C.A., and Groopman, J.E. (1989). Production of tumor necrosis factor α and interleukin 1β by monocytic cells infected with human immunodeficiency virus. J. Clin. Invest. *84*, 733–737.

Møller, H.J. (2012). Soluble CD163. Scand. J. Clin. Lab. Invest. *72*, 1–13.

Monaco, C.L., Gootenberg, D.B., Zhao, G., Handley, S.A., Musie, S., Lim, E.S., Lankowski, A., Baldridge, M.T., Wilen, C.B., Flagg, M., et al. (2017). Altered Virome and Bacterial Microbiome in Human Immuni. Cell Host Microbe *19*, 311–322.

Monroe, K.M., Yang, Z., Johnson, J.R., Geng, X., Doitsh, G., Krogan, N.J., and Greene, W.C. (2014). IFI16 DNA sensor is required for death of lymphoid CD4 T cells abortively infected with HIV. Science (80-.). *343*, 428–432.

Montoro-García, S., Shantsila, E., Wrigley, B.J., Tapp, L.D., Abellán Alemán, J., and Lip, G.Y.H. (2015). Small-size Microparticles as Indicators of Acute Decompensated State in Ischemic Heart Failure. Rev. Española Cardiol. (English Ed. *68*, 951–958.

Morel, O., Pereira, B., Averous, G., Faure, A., Jesel, L., Germain, P., Grunebaum, L., Ohlmann, P., Freyssinet, J.M., Bareiss, P., et al. (2009). Increased levels of procoagulant tissue factor-bearing microparticles within the occluded coronary artery of patients with ST-segment elevation myocardial infarction: Role of endothelial damage and leukocyte activation. Atherosclerosis *204*, 636–641.

Mostefai, H.A., Agouni, A., Carusio, N., Mastronardi, M.L., Heymes, C., Henrion, D., Andriantsitohaina, R., and Martinez, M.C. (2008). Phosphatidylinositol 3-Kinase and Xanthine Oxidase Regulate Nitric Oxide and Reactive Oxygen Species Productions by Apoptotic Lymphocyte Microparticles in Endothelial Cells. J. Immunol. *180*, 5028–5035.

Mukherjee, R., Kanti Barman, P., Kumar Thatoi, P., Tripathy, R., Kumar Das, B., and Ravindran, B. (2015). Non-Classical monocytes display inflammatory features: Validation in Sepsis and Systemic Lupus Erythematous. Sci. Rep. *5*, 13886.

Mulenga, V., Musiime, V., Kekitiinwa, A., Cook, A.D., Abongomera, G., Kenny, J., Chabala, C., Mirembe, G., Asiimwe, A., Owen-Powell, E., et al. (2016). Abacavir, zidovudine, or stavudine as paediatric tablets for African HIV-infected children (CHAPAS-3): An open-label, parallel-group, randomised controlled trial. Lancet Infect. Dis. *16*, 169–179.

Muller, W.A. (2013). Getting Leukocytes to the Site of Inflammation. Vet. Pathol. *50*, 7–22.

Muntinghe, F.L.H., Verduijn, M., Zuurman, M.W., Grootendorst, D.C., Carrero, J.J., Qureshi, A.R., Luttropp, K., Nordfors, L., Lindholm, B., Brandenburg, V., et al. (2009). CCR5 deletion protects against inflammation-associated mortality in dialysis patients. J. Am. Soc. Nephrol. *20*, 1641–1649.

Murdoch, C., Tazzyman, S., Webster, S., and Lewis, C.E. (2007). Expression of Tie-2 by human

monocytes and their responses to angiopoietin-2. J. Immunol. (Baltimore, Md. 1950) *178*, 7405–7411.

Murooka, T.T., Deruaz, M., Marangoni, F., Vrbanac, V.D., Seung, E., Von Andrian, U.H., Tager, A.M., Luster, A.D., and Mempel, T.R. (2012). HIV-infected T cells are migratory vehicles for viral dissemination. Nature *490*, 283–287.

Mussbacher, M., Salzmann, M., Brostjan, C., Hoesel, B., Schoergenhofer, C., Datler, H., Hohensinner, P., Basílio, J., Petzelbauer, P., Assinger, A., et al. (2019). Cell type specific roles of nf-kb linking inflamation and thrombosis. Front. Immunol. *10*.

Nahrendorf, M., Swirski, F.K., Aikawa, E., Stangenberg, L., Wurdinger, T., Figueiredo, J.L., Libby, P., Weissleder, R., and Pittet, M.J. (2007). The healing myocardium sequentially mobilizes two monocyte subsets with divergent and complementary functions. J. Exp. Med. *204*, 3037–3047.

Nakagawa, F., May, M., and Phillips, A. (2013). Life expectancy living with HIV: recent estimates and future implications. Curr. Opin. Infect. Dis. *26*, 17–25.

Nakaoka, H., Hirono, K., Yamamoto, S., Takasaki, I., Takahashi, K., Kinoshita, K., Takasaki, A., Nishida, N., Okabe, M., Ce, W., et al. (2018). MicroRNA-145-5p and microRNA-320a encapsulated in endothelial microparticles contribute to the progression of vasculitis in acute Kawasaki Disease. Sci. Rep. *8*, 1–11.

Nakashima, Y., Raines, E.W., Plump, A.S., Breslow, J.L., and Ross, R. (1998). Atherosclerosis-Prone Sites on the Endothelium in the ApoE-Deficient Mouse. Arterioscler. Thromb. Vasc. Biol. *18*, 842–851.

Napoli, C., D'Armiento, F.P., Mancini, F.P., Postiglione, A., Witztum, J.L., Palumbo, G., and Palinski, W. (1997). Fatty streak formation occurs in human fetal aortas and is greatly enhanced maternal, hypercholesterolemia. Intimal accumulation of low density lipoprotein and its oxidation precede monocyte recruitment into early atheroeclerotic lesions. J. Clin. Invest. *100*, 2680–2690.

Narin, N., Yilmaz, E., Pamukcu, O., Baykan, A., Argun, M., Ozyurt, A., Onan, S., Sezer, S., and Uzum, K. (2014). Are endothelial microparticles early markers of pulmonary hypertension? Biomarkers *19*, 319–325.

Narla, V., Bhakta, N., Freedman, J.E., Tanriverdi, K., Maka, K., Deeks, S.G., Ganz, P., and Hsue, P. (2018). Unique circulating microRNA profiles in HIV infection. J. Acquir. Immune Defic. Syndr. *79*, 644–650.

Nash S, Desai S, Croxford S, Guerra L, Lowndes C, Connor N, G.O. (2018). Progress towards ending the HIV epidemic in the United Kingdom: 2018 report.

Neri, T., Armani, C., Pegoli, A., Cordazzo, C., Carmazzi, Y., Brunelleschi, S., Bardelli, C., Breschi, M.C., Paggiaro, P., and Celi, A. (2011). Role of NF-κB and PPAR-γ in lung inflammation induced by monocyte-derived microparticles. Eur. Respir. J. *37*, 1494–1502.

Neuhaus, J., Jacobs, D.R., Baker, J. V, Calmy, A., Duprez, D., Rosa, A. La, Kuller, L.H., Pett, S.L., Ristola, M., Ross, M.J., et al. (2010). Markers of Inflammation, Coagulation and Renal Function Are Elevated in Adults with HIV Infection for the INSIGHT SMART, MESA and CARDIA Research

Groups*. J. Infect. Dis. *201*, 1788–1795.

Nezu, T., Hosomi, N., Aoki, S., and Matsumoto, M. (2016). Carotid Intima-Media Thickness for Atherosclerosis. J Atheroscler Thromb *23*, 18–31.

Nie, Z., Phenix, B.N., Lum, J.J., Alam, A., Lynch, D.H., Beckett, B., Krammer, P.H., Sekaly, R.P., and Badley, A.D. (2002). HIV-1 protease processes procaspase 8 to cause mitochondrial release of cytochrome c, caspase cleavage and nuclear fragmentation. Cell Death Differ. *9*, 1172–1184.

Nie, Z., Bren, G.D., Vlahakis, S.R., Schimnich, A.A., Brenchley, J.M., Trushin, S.A., Warren, S., Schnepple, D.J., Kovacs, C.M., Loutfy, M.R., et al. (2007). Human Immunodeficiency Virus Type 1 Protease Cleaves Procaspase 8 In Vivo. J. Virol. *81*, 6947–6956.

Nielsen, C.T., Østergaard, O., Johnsen, C., Jacobsen, S., and Heegaard, N.H.H. (2011). Distinct features of circulating microparticles and their relationship to clinical manifestations in systemic lupus erythematosus. Arthritis Rheum. *63*, 3067–3077.

Nieto, J.C., Cantó, E., Zamora, C., Ortiz, M.A., Juárez, C., and Vidal, S. (2012). Selective loss of chemokine receptor expression on leukocytes after cell isolation. PLoS One *7*, 1–8.

Nix, L.M., and Tien, P.C. (2014). Metabolic syndrome, diabetes, and cardiovascular risk in HIV. Curr. HIV/AIDS Rep. *11*, 271–278.

Nomura, S., Tandon, N.N., Nakamura, T., Cone, J., Fukuhara, S., and Kambayashi, J. (2001). High-shear-stress-induced activation of platelets and microparticles enhances expression of cell adhesion molecules in THP-1 and endothelial cells. Atherosclerosis *158*, 277–287.

Nordell, A.D., McKenna, M., Borges, A.H., Duprez, D., Neuhaus, J., and Neaton, J.D. (2014). Severity of cardiovascular disease outcomes among patients with hiv is related to markers of inflammation and coagulation. J. Am. Heart Assoc. *3*, 1–10.

Nou, E., Lo, J., and Grinspoon, S.K. (2016). Inflammation, immune activation, and cardiovascular disease in HIV. AIDS *30*, 1495–1509.

Nyamweya, S., Hegedus, A., Jaye, A., Rowland-Jones, S., Flanagan, K.L., and Macallan, D.C. (2013). Comparing HIV-1 and HIV-2 infection: Lessons for viral immunopathogenesis. Rev. Med. Virol. *23*, 221–240.

O'Halloran, J.A., Dunne, E., Gurwith, M.M.P., Lambert, J.J.S., Sheehan, G.J., Feeney, E.R., Pozniak, A., Reiss, P., Kenny, D., and Mallon, P.W.G. (2015). The effect of initiation of antiretroviral therapy on monocyte, endothelial and platelet function in HIV-1 infection. HIV Med. *16*, 608–619.

O'Leary, D.H., Polak, J.F., Kronmal, R.A., Manolio, T.A., Burke, G.L., and Wolfson, S.K. (1999). Carotid-artery intima and media thickness as a risk factor for myocardial infarction and stroke in older adults. N. Engl. J. Med. *340*, 14–22.

Obregon, C., Rothen-Rutishauser, B., Gitahi, S.K., Gehr, P., and Nicod, L.P. (2006). Exovesicles from human activated dendritic cells fuse with resting dendritic cells, allowing them to present alloantigens. Am. J. Pathol. *169*, 2127–2136.

Ou, Z.J., Chang, F.J., Luo, D., Liao, X.L., Wang, Z.P., Zhang, X., Xu, Y.Q., and Ou, J.S. (2011).

Endothelium-derived microparticles inhibit angiogenesis in the heart and enhance the inhibitory effects of hypercholesterolemia on angiogenesis. Am. J. Physiol. - Endocrinol. Metab. *300*, 661–668.

Padilla, S.S., Masiá, M., García, N., Jarrin, I., Tormo, C., and Gutiérrez, F. (2011). Early changes in inflammatory and pro-thrombotic biomarkers in patients initiating antiretroviral therapy with abacavir or tenofovir. BMC Infect. Dis. *11*, 40.

Palella, F.J., Delaney, K.M., Moorman, A.C., Loveless, M.O., Fuhrer, J., Satten, G.A., Aschman, D.J., and Holmberg, S.D. (1998). Declining morbidity and mortality among patients with advanced human immunodeficiency virus infection. N. Engl. J. Med. *338*, 853–860.

Palella, F.J., Baker, R.K., Moorman, A.C., Chmiel, J.S., Wood, K.C., Brooks, J.T., and Holmberg, S.D. (2006). Mortality in the highly active antiretroviral therapy era: Changing causes of death and disease in the HIV outpatient study. J. Acquir. Immune Defic. Syndr. *43*, 27–34.

Passlick, B., Flieger, D., and Loms Ziegler-Heitbrock, H.W. (1989). Identification and characterization of a novel monocyte subpopulation in human peripheral blood. Blood *74*, 2527–2534.

Patel, A. (2014). Does the Role of Angiogenesis Play a Role in Atherosclerosis and Plaque Instability? Anat. Physiol. Curr. Res. *4*, 147.

Patz, S., Trattnig, C., Grünbacher, G., Ebner, B., Gülly, C., Novak, A., Rinner, B., Leitinger, G., Absenger, M., Tomescu, O.A., et al. (2013). More than cell dust: Microparticles isolated from cerebrospinal fluid of brain injured patients are messengers carrying mRNAs, miRNAs, and proteins. J. Neurotrauma *30*, 1232–1242.

Penton-Rol, G., Polentarutti, N., Luini, W., Borsatti, A., Mancinelli, R., Sica, A., Sozzani, S., and Mantovani, A. (1998). Selective inhibition of expression of the chemokine receptor CCR2 in human monocytes by IFN-γ. J. Immunol. *160*, 3869–3873.

Pérez-Casal, M., Downey, C., Cutillas-Moreno, B., Zuzel, M., Fukudome, K., and Ton, C.H. (2009). Microparticle-associated endothelial protein C receptor and the induction of cytoprotective and anti-inflammatory effects. Haematologica *94*, 387–394.

Philippova, M., Suter, Y., Toggweiler, S., Schoenenberger, A.W., Joshi, M.B., Kyriakakis, E., Erne, P., and Resink, T.J. (2011). T-cadherin is present on endothelial microparticles and is elevated in plasma in early atherosclerosis. Eur. Heart J. *32*, 760–771.

Pirro, M., Schillaci, G., Paltriccia, R., Bagaglia, F., Menecali, C., Mannarino, M.R., Capanni, M., Velardi, A., and Mannarino, E. (2006). Increased ratio of CD31+/CD42- microparticles to endothelial progenitors as a novel marker of atherosclerosis in hypercholesterolemia. Arterioscler. Thromb. Vasc. Biol. *26*, 2530–2535.

Post, W.S., Budoff, M., Kingsley, L., Palella, F.J., Witt, M.D., Li, X., George, R.T., Brown, T., and Jacobson, L.P. (2014). Associations between HIV Infection and Subclinical Coronary Atherosclerosis: The Multicenter AIDS Cohort Study (MACS). Ann Intern Med *160*, 458–467.

Povero, D., and Feldstein, A.E. (2016). Novel molecular mechanisms in the development of non-alcoholic steatohepatitis. Diabetes Metab. J. *40*, 1–11.

Preston, R.A., Jy, W., Jimenez, J.J., Mauro, L.M., Horstman, L.L., Valle, M., Aime, G., and Ahn, Y.S. (2003). Effects of severe hypertension on endothelial and platelet microparticles. Hypertension *41*, 211–217.

Pulliam, L., Gascon, R., Stubblebine, M., McGuire, D., and McGrath, M.S. (1997). Unique monocyte subset in patients with AIDS dementia. Lancet *349*, 692–695.

Qin, Z. (2012). The use of THP-1 cells as a model for mimicking the function and regulation of monocytes and macrophages in the vasculature. Atherosclerosis *221*, 2–11.

Quinn, M.T., Parthasarathy, S., Fong, L.G., and Steinberg, D. (1987). Oxidatively modified low density lipoproteins: A potential role in recruitment and retention of monocyte/macrophages during atherogenesis. Proc. Natl. Acad. Sci. U. S. A. *84*, 2995–2998.

Ramendra, R., Isnard, S., Mehraj, V., Chen, J., Zhang, Y., Finkelman, M., and Routy, J.P. (2019). Circulating LPS and (1→3)-β-D-glucan: A folie à deux contributing to HIV-associated immune activation. Front. Immunol. *10*, 1–9.

Randolph, G.J., and Furie, M.B. (1996). Mononuclear phagocytes egress from an in vitro model of the vascular wall by migrating across endothelium in the basal to apical direction: Role of intercellular adhesion molecule 1 and the CD11/CD18 integrins. J. Exp. Med. *183*, 451–462.

Randolph, G.J., Sanchez-Schmitz, G., Liebman, R.M., and Schäkel, K. (2002). The CD16+ (FcγRIII+) subset of human monocytes preferentially becomes migratory dendritic cells in a model tissue setting. J. Exp. Med. *196*, 517–527.

Rasmussen, L.D., Helleberg, M., May, M.T., Afzal, S., Kronborg, G., Larsen, C.S., Pedersen, C., Gerstoft, J., Nordestgaard, B.G., and Obel, N. (2015). Myocardial infarction among danish HIV-infected individuals: Population-attributable fractions associated with smoking. Clin. Infect. Dis. *60*, 1415–1423.

Riddy, D.M., Goy, E., Delerive, P., Summers, R.J., Sexton, P.M., and Langmead, C.J. (2018). Comparative genotypic and phenotypic analysis of human peripheral blood monocytes and surrogate monocyte-like cell lines commonly used in metabolic disease research. PLoS One *13*, 1–19.

Ridker, P.M. (2003). Clinical application of C-reactive protein for cardiovascular disease detection and prevention. Circulation *107*, 363–369.

del Rio, C. (2017). The Global HIV epidemic: What the pathologist needs to know. Semin. Diagn. Pathol. *34*, 314–317.

Della Rocca, D.G., and Pepine, C.J. (2010). Endothelium as a predictor of adverse outcomes. Clin. Cardiol. *33*, 730–732.

Rodger, A.J., Lodwick, R., Schechter, M., Deeks, S., Amin, J., Gilson, R., Paredes, R., Bakowska, E., Engsig, F.N., and Phillips, A. (2013). Mortality in well controlled HIV in the continuous antiretroviral therapy arms of the SMART and ESPRIT trials compared with the general population. AIDS *27*, 973–979.

Rodger, A.J., Cambiano, V., Phillips, A.N., Bruun, T., Raben, D., Lundgren, J., Vernazza, P., Collins, S., Degen, O., Corbelli, G.M., et al. (2019). Risk of HIV transmission through condomless sex in

serodifferent gay couples with the HIV-positive partner taking suppressive antiretroviral therapy (PARTNER): final results of a multicentre, prospective, observational study. Lancet *393*, 2428–2438.

Rogacev, K.S., Zawada, A.M., Hundsdorfer, J., Achenbach, M., Held, G., Fliser, D., and Heine, G.H. (2015). Immunosuppression and monocyte subsets. Nephrol. Dial. Transplant. *30*, 143–153.

Rood, I.M., Deegens, J.K.J., Merchant, M.L., Tamboer, W.P.M., Wilkey, D.W., Wetzels, J.F.M., and Klein, J.B. (2010). Comparison of three methods for isolation of urinary microvesicles to identify biomarkers of nephrotic syndrome. Kidney Int. *78*, 810–816.

Ross, A.C., Storer, N., Ann O'Riordan, M., Dogra, V., and McComsey, G.A. (2010). Longitudinal changes in carotid intima-media thickness and cadiovascular risk factors in human immunodeficiency virus-infected children and young adults compared with healthy controls. Pediatr. Infect. Dis. J. *29*, 634–638.

Royce, R.A., Sena, A., Cates Jr, W., and Cohen, M.S. (1997). Sexual transmission of HIV. N. Engl. J. Med. *336*, 1072–1078.

Den Ruijter, H.M., Peters, S.A.E., Anderson, T.J., Britton, A.R., Dekker, J.M., Eijkemans, M.J., Engström, G., Evans, G.W., De Graaf, J., Grobbee, D.E., et al. (2012). Common carotid intima-media thickness measurements in cardiovascular risk prediction: A meta-analysis. JAMA - J. Am. Med. Assoc. *308*, 796–803.

Sabatier, F., Roux, V., Anfosso, F., Camoin, L., Sampol, J., and Dignat-George, F. (2002a). Interaction of endothelial microparticles with monocytic cells in vitro induces tissue factor-dependent procoagulant activity. Blood *99*, 3962–3970.

Sabatier, F., Darmon, P., Hugel, B., Combes, V., Sanmarco, M., Velut, J.G., Arnoux, D., Charpiot, P., Freyssinet, J.M., Oliver, C., et al. (2002b). Type 1 and type 2 diabetic patients display different patterns of cellular microparticles. Diabetes *51*, 2840–2845.

Sabbione, A.C., Luna-Vital, D., Scilingo, A., Añón, M.C., and González de Mejía, E. (2018). Amaranth peptides decreased the activity and expression of cellular tissue factor on LPS activated THP-1 human monocytes. Food Funct. *9*, 3823–3834.

Sabin, C.A., Worm, S.W., Weber, R., Reiss, P., El-Sadr, W., Dabis, F., De Wit, S., Law, M., D'Arminio Monforte, A., Friis-Møller, N., et al. (2008). Use of nucleoside reverse transcriptase inhibitors and risk of myocardial infarction in HIV-infected patients enrolled in the D:A:D study: A multi-cohort collaboration. Lancet *371*, 1417–1426.

Sáenz-Cuesta, M., Irizar, H., Castillo-Triviño, T., Muñoz-Culla, M., Osorio-Querejeta, I., Prada, A., Sepúlveda, L., López-Mato, M.P., De Munain, A.L., Comabella, M., et al. (2014). Circulating microparticles reflect treatment effects and clinical status in multiple sclerosis. Biomark. Med. *8*, 653–661.

Saha, P., and Geissmann, F. (2011). Toward a functional characterization of blood monocytes. Immunol. Cell Biol. *89*, 2–4.

Sainski, A.M., Natesampillai, S., Cummins, N.W., Bren, G.D., Taylor, J., Saenz, D.T., Poeschla, E.M., and Badley, A.D. (2011). The HIV-1-Specific Protein Casp8p41 Induces Death of Infected

Cells through Bax/Bak. J. Virol. *85*, 7965–7975.

Sainz, T., Serrano-Villar, S., Díaz, L., Tome, M.I.G., Gurbindo, M.D., De José, M.I., Mellado, M.J., Ramos, J.T., Zamora, J., Moreno, S., et al. (2013). The CD4/CD8 ratio as a marker T-cell activation, senescence and activation/exhaustion in treated HIV-infected children and young adults. AIDS *27*, 1513–1516.

Sainz, T., Álvarez-Fuente, M., Navarro, M.L., Díaz, L., Rojo, P., Blázquez, D., De José, M.I., Ramos, J.T., Serrano-Villar, S., Martínez, J., et al. (2014). Subclinical atherosclerosis and markers of immune activation in hiv-infected children and adolescents: The carovih study. J. Acquir. Immune Defic. Syndr. *65*, 42–49.

Salem, M.A.E.K., Adly, A.A.M., Ismail, E.A.R., Darwish, Y.W., and Kamel, H.A. (2015). Platelets microparticles as a link between micro- and macro-angiopathy in young patients with type 1 diabetes. Platelets *26*, 682–688.

Samji, H., Cescon, A., Hogg, R.S., Modur, S.P., Althoff, K.N., Buchacz, K., Burchell, A.N., Cohen, M., Gebo, K.A., Gill, M.J., et al. (2013). Closing the gap: Increases in life expectancy among treated HIV-positive individuals in the United States and Canada. PLoS One *8*, 6–13.

Sandler, N.G., Wand, H., Roque, A., Law, M., Nason, M.C., Nixon, D.E., Pedersen, C., Ruxrungtham, K., Lewin, S.R., Emery, S., et al. (2011). Plasma levels of soluble CD14 independently predict mortality in HIV infection. J. Infect. Dis. *203*, 780–790.

Sankaran, S., George, M.D., Reay, E., Guadalupe, M., Flamm, J., Prindiville, T., and Dandekar, S. (2008). Rapid Onset of Intestinal Epithelial Barrier Dysfunction in Primary Human Immunodeficiency Virus Infection Is Driven by an Imbalance between Immune Response and Mucosal Repair and Regeneration. J. Virol. *82*, 538–545.

Sarkar, A., Mitra, S., Mehta, S., Raices, R., and Wewers, M.D. (2009). Monocyte derived microvesicles deliver a cell death message via encapsulated caspase-1. PLoS One *4*, e7140.

Sarwar, N., Butterworth, A.S., Freitag, D.F., Gregson, J., Willeit, P., Gorman, D.N., Gao, P., Saleheen, D., Rendon, A., Nelson, C.P., et al. (2012). Interleukin-6 receptor pathways in coronary heart disease: A collaborative meta-analysis of 82 studies. Lancet *379*, 1205–1213.

Sassé, T., Wu, J., Zhou, L., and Saksena, N.K. (2012). Monocytes and their role in human immunodeficiency virus pathogenesis. Am. J. Infect. Dis. *8*, 92–105.

Satchell, C.S., O'Halloran, J.A., Cotter, A.G., Peace, A.J., O'Connor, E.F., Tedesco, A.F., Feeney, E.R., Lambert, J.S., Sheehan, G.J., Kenny, D., et al. (2011). Increased platelet reactivity in HIV-1-infected patients receiving abacavir-containing antiretroviral therapy. J. Infect. Dis. *204*, 1202–1210.

Sato, T.N., Tozawa, Y., Deutsch, U., Karen, W.B., Fujiwara, Y., Maureen, G.M., Gridley, T., Wolburg, H., Risau, W., and Qin, Y. (1995). Distinct roles of the receptor tyrosine kinases Tie-1 and Tie-2 in blood vessel formation. Nature *376*, 70–74.

Satta, N., Toti, F., Feugeas, O., Bohbot, A., Dachary-Prigent, J., Eschwège, V., Hedman, H., and Freyssinet, J.M. (1994). Monocyte vesiculation is a possible mechanism for dissemination of membrane-associated procoagulant activities and adhesion molecules after stimulation by

lipopolysaccharide. J. Immunol. *153*, 3245–3255.

Scala, G., Ruocco, M.R., Ambrosino, C., Mallardo, M., Giordano, V., Baldassarre, F., Dragonetti, E., Quinto, I., and Venuta, S. (1994). The expression of the interleukin 6 gene is induced by the human immunodeficiency virus 1 tat protein. J. Exp. Med. *179*, 961–971.

Scanu, A., Molnarfi, N., Brandt, K.J., Gruaz, L., Dayer, J.-M., and Burger, D. (2008). Stimulated T cells generate microparticles, which mimic cellular contact activation of human monocytes: differential regulation of pro- and anti-inflammatory cytokine production by high-density lipoproteins. J. Leukoc. Biol. *83*, 921–927.

Schildberger, A., Rossmanith, E., Eichhorn, T., Strassl, K., and Weber, V. (2013). Monocytes, peripheral blood mononuclear cells, and THP-1 cells exhibit different cytokine expression patterns following stimulation with lipopolysaccharide. Mediators Inflamm. *2013*, Article ID 697972.

Schuetz, A., Deleage, C., Sereti, I., Rerknimitr, R., Phanuphak, N., Phuang-Ngern, Y., Estes, J.D., Sandler, N.G., Sukhumvittaya, S., Marovich, M., et al. (2014). Initiation of ART during Early Acute HIV Infection Preserves Mucosal Th17 Function and Reverses HIV-Related Immune Activation. PLoS Pathog. *10*.

Seigneuret, M., and Devauxt, P.F. (1984). ATP-dependent asymmetric distribution of spin-labeled phospholipids in the erythrocyte membrane: Relation to shape changes (phospholipid asymmetry/transverse diffusion/erythrocyte shape/bilayer couple/electron spin resonance). Cell Biol. *81*, 3751–3755.

Serbina, N. V., and Pamer, E.G. (2006). Monocyte emigration from bone marrow during bacterial infection requires signals mediated by chemokine receptor CCR2. Nat. Immunol. *7*, 311–317.

Sereti, I., Krebs, S.J., Phanuphak, N., Fletcher, J.L., Slike, B., Pinyakorn, S., O'Connell, R.J., Rupert, A., Chomont, N., Valcour, V., et al. (2017). Persistent, Albeit reduced, chronic inflammation in persons starting antiretroviral therapy in acute HIV infection. Clin. Infect. Dis. *64*, 124–131.

Shah, A.S.V., Stelzle, D., Ken Lee, K., Beck, E.J., Alam, S., Clifford, S., Longenecker, C.T., Strachan, F., Bagchi, S., Whiteley, W., et al. (2018). Global burden of atherosclerotic cardiovascular disease in people living with HIV systematic review and meta-analysis. Circulation *138*, 1100–1112.

Shankar, S.S., Dubé, M.P., Gorski, J.C., Klaunig, J.E., and Steinberg, H.O. (2005). Indinavir impairs endothelial function in healthy HIV-negative men. Am. Heart J. *150*, 933.e1-933.e7.

Shefler, I., Salamon, P., Reshef, T., Mor, A., and Mekori, Y.A. (2010). T Cell-Induced Mast Cell Activation: A Role for Microparticles Released from Activated T Cells. J. Immunol. *185*, 4206–4212.

Shih, P.T., Brennan, M.L., Vora, D.K., Territo, M.C., Strahl, D., Elices, M.J., Lusis, A.J., and Berliner, J.A. (1999). Blocking very late antigen-4 integrin decreases leukocyte entry and fatty streak formation in mice fed an atherogenic diet. Circ. Res. *84*, 345–351.

Sica, A., Saccani, A., Borsatti, A., Power, C.A., Wells, T.N.C., Luini, W., Polentarutti, N., Sozzani, S., and Mantovani, A. (1997). Bacterial lipopolysaccharide rapidly inhibits expression of C-C chemokine receptors in human monocytes. J. Exp. Med. *185*, 969–974.

Sico, J.J., Chang, C.C.H., So-Armah, K., Justice, A.C., Hylek, E., Skanderson, M., McGinnis, K., Kuller, L.H., Kraemer, K.L., Rimland, D., et al. (2015). HIV status and the risk of ischemic stroke among men. Neurology *84*, 1933–1940.

Da Silva, E.F.R., Fonseca, F.A.H., França, C.N., Ferreira, P.R.A., Izar, M.C.O., Salomão, R., Camargo, L.M., Tenore, S.B., and Lewi, D.S. (2011). Imbalance between endothelial progenitors cells and microparticles in HIV-infected patients naive for antiretroviral therapy. Aids *25*, 1595–1601.

Simak, J., and Gelderman, M.P. (2006). Cell membrane microparticles in blood and blood products: Potentially pathogenic agents and diagnostic markers. Transfus. Med. Rev. *20*, 1–26.

Skålén, K., Gustafsson, M., Knutsen Rydberg, E., Hultén, L.M., Wiklund, O., Innerarity, T.L., and Boren, J. (2002). Subendothelial retention of atherogenic lipoproteins in early atherosclerosis. Nature *417*, 750–754.

Smedman, C., Ernemar, T., Gudmundsdotter, L., Gille-Johnson, P., Somell, A., Nihlmark, K., Gårdlund, B., Andersson, J., and Paulie, S. (2012). FluoroSpot analysis of TLR-activated monocytes reveals several distinct cytokine-secreting subpopulations. Scand. J. Immunol. *75*, 249–258.

Smit, M., Brinkman, K., Geerlings, S., Smit, C., Thyagarajan, K., van Sighem, A. V., de Wolf, F., and Hallett, T.B. (2015). Future challenges for clinical care of an ageing population infected with HIV: A modelling study. Lancet Infect. Dis. *15*, 810–818.

Smith, C.J., Ryom, L., Weber, R., Morlat, P., Pradier, C., Reiss, P., Kowalska, J.D., De Wit, S., Law, M., Sadr, W., et al. (2014). Trends in underlying causes of death in people with HIV from 1999 to 2011 (D:A:D): A multicohort collaboration. Lancet *384*, 241–248.

Sonza, S., Mutimer, H.P., Oelrichs, R., Jardine, D., Harvey, K., Dunne, A., Purcell, D.F., Birch, C., and Crowe, S.M. (2001). Monocytes harbour replication-competent, non-latent HIV-1 in patients on highly active antiretroviral therapy. Aids *15*, 17–22.

Ståhl, A.L., Sartz, L., and Karpman, D. (2011). Complement activation on platelet-leukocyte complexes and microparticles in enterohemorrhagic Escherichia coli-induced hemolytic uremic syndrome. Blood *117*, 5503–5513.

Stanciu, L.A., Shute, J., Holgate, stephen T., and Djukanovic, R. (1996). Production of IL-8 and IL-4 by positively and negatively selected CD4 magnetic cell sorting (MACS). J. Immunol. Method *189*, 107–115.

Stec, M., Weglarczyk, K., Baran, J., Zuba, E., Mytar, B., Pryjma, J., and Zembala, M. (2007). Expansion and differentiation of CD14 + CD16 − and CD14 ++ CD16 + human monocyte subsets from cord blood CD34 + hematopoietic progenitors . J. Leukoc. Biol. *82*, 594–602.

Stent, G., and Crowe, S.M. (1997). Effects of monocyte purification and culture on integrin expression. APMIS *105*, 663–670.

Suades, R., Padró, T., Alonso, R., Mata, P., and Badimon, L. (2013). Lipid-lowering therapy with statins reduces microparticle shedding from endothelium, platelets and inflammatory cells. Thromb. Haemost. *110*, 366–377.

Suades, R., Padró, T., Alonso, R., Mata, P., and Badimon, L. (2015). High levels of TSP1+/CD142+

platelet-derived microparticles characterise young patients with high cardiovascular risk and subclinical atherosclerosis. Thromb. Haemost. *114*, 1310–1321.

Sunderkötter, C., Nikolic, T., Dillon, M.J., van Rooijen, N., Stehling, M., Drevets, D.A., and Leenen, P.J.M. (2004). Subpopulations of Mouse Blood Monocytes Differ in Maturation Stage and Inflammatory Response. J. Immunol. *172*, 4410–4417.

Suzuki, J., Fujii, T., Imao, T., Ishihara, K., Kuba, H., and Nagata, S. (2013). Calcium-dependent phospholipid scramblase activity of TMEM 16 protein family members. J. Biol. Chem. *288*, 13305–13316.

Swerdlow, D.I., Holmes, M. V., Kuchenbaecker, K.B., Engmann, J.E.L., Shah, T., Sofat, R., Guo, Y., Chung, C., Peasey, A., Pfister, R., et al. (2012). The interleukin-6 receptor as a target for prevention of coronary heart disease: A mendelian randomisation analysis. Lancet *379*, 1214–1224.

Tacke, F., Alvarez, D., Kaplan, T.J., Jakubzick, C., Spanbroek, R., Llodra, J., Garin, A., Liu, J., Mack, M., Rooijen, N. Van, et al. (2007). Monocyte subsets differentially employ CCR2, C... [J Clin Invest. 2007] - PubMed - NCBI. J. Clin. Invest. *117*, 185–194.

Tak, T., Drylewicz, J., Conemans, L., De Boer, R.J., Koenderman, L., Borghans, J.A.M., and Tesselaar, K. (2017). Circulatory and maturation kinetics of human monocyte subsets in vivo. Blood *130*, 1474–1477.

Tallone, T., Turconi, G., Soldati, G., Pedrazzini, G., Moccetti, T., and Vassalli, G. (2011). Heterogeneity of human monocytes: An optimized four-color flow cytometry protocol for analysis of monocyte subsets. J. Cardiovasc. Transl. Res. *4*, 211–219.

Taylor, J.A., Cummins, N.W., Bren, G.D., Rizza, S.A., Kolbert, C.P., Behrens, M.D., Knutson, K.L., Kahl, J.C., Asmann, Y.W., and Badley, A.D. (2010). Casp8p41 expression in primary T cells induces a proinflammatory response. AIDS *24*, 1251–1258.

Teichert-Kuliszewska, K., Maisonpierre, P.C., Jones, N., Campbell, A.I.M., Master, Z., Bendeck, M.P., Alitalo, K., Dumont, D.J., Yancopoulos, G.D., and Stewart, D.J. (2001). Biological action of angiopoietin-2 in a fibrin matrix model of angiogenesis is associated with activation of Tie2. Cardiovasc. Res. *49*, 659–670.

Terrisse, A.D., Puech, N., Allart, S., Gourdy, P., Xuereb, J.M., Payrastre, B., and Sié, P. (2010). Internalization of microparticles by endothelial cells promotes platelet/endothelial cell interaction under flow. J. Thromb. Haemost. *8*, 2810–2819.

Tesse, A., Martínez, M.C., Hugel, B., Chalupsky, K., Muller, C.D., Meziani, F., Mitolo-Chieppa, D., Freyssinet, J.M., and Andriantsitohaina, R. (2005). Upregulation of proinflammatory proteins through NF-κB pathway by shed membrane microparticles results in vascular hyporeactivity. Arterioscler. Thromb. Vasc. Biol. *25*, 2522–2527.

Théry, C., Ostrowski, M., and Segura, E. (2009). Membrane vesicles as conveyors of immune responses. Nat. Rev. Immunol. *9*, 581–593.

Thieblemont, N., Weiss, L., Sadeghi, H.M., Estcourt, C., and Haeffner-Cavaillon, N. (1995). CD14lowCD16high: A cytokine-producing monocyte subset which expands during human

immunodeficiency virus infection. Eur. J. Immunol. *25*, 3418–3424.

Ticona, E., Bull, M.E., Soria, J., Tapia, K., Legard, J., Styrchak, S.M., Williams, C., Mitchell, C., Rosa, A.L.A., and Coombs, R.W. (2015). Biomarkers of inflammation in HIV-infected Peruvian men and women before and during suppressive antiretroviral therapy. AIDS *29*, 1617–1622.

Tippett, E., Cheng, W.J., Westhorpe, C., Cameron, P.U., Brew, B.J., Lewin, S.R., Jaworowski, A., and Crowe, S.M. (2011). Differential Expression of CD163 on Monocyte Subsets in Healthy and HIV-1 Infected Individuals. PLoS One *6*, e19968.

Tomlinson, M.J., Tomlinson, S., Yang, X.B., and Kirkham, J. (2013). Cell separation: Terminology and practical considerations. J. Tissue Eng. *4*, 1–14.

Triant, V.A., Lee, H., Hadigan, C., and Grinspoon, S.K. (2007). Increased acute myocardial infarction rates and cardiovascular risk factors among patients with human immunodeficiency virus disease. J. Clin. Endocrinol. Metab. *92*, 2506–2512.

Triant, V.A., Meigs, J.B., and Grinspoon, S.K. (2009). Association of C-reactive protein and HIV infection with acute myocardial infarction. J. Acquir. Immune Defic. Syndr. *51*, 268–273.

Triboulet, R., Mari, B., Lin, Y.L., Chable-Bessia, C., Bennasser, Y., Lebrigand, K., Cardinaud, B., Maurin, T., Barbry, P., Baillat, V., et al. (2007). Suppression of MicroRNA-silencing pathway by HIV-1 during virus replication. Science (80-.). *315*, 1579–1582.

Tsou, C.L., Peters, W., Si, Y., Slaymaker, S., Aslanian, A.M., Weisberg, S.P., Mack, M., and Charo, I.F. (2007). Critical roles for CCR2 and MCP-3 in monocyte mobilization from bone marrow and recruitment to inflammatory sites. J. Clin. Invest. *117*, 902–909.

Tsuchiya, S., Yamaguchi, Y., and Kobayashi, Y. (1980). Tsuchiya S, Yamabe M, Yamaguchi Y, et al. Establishment and characterization of a human acute monocytic leukemia cell line (THP-1). Int J Cancer. 1980; 26:171–176. DOI: 10.1002/ijc.2910260208. *176*, 171–176.

Tulkens, J., Vergauwen, G., Van Deun, J., Geeurickx, E., Dhondt, B., Lippens, L., De Scheerder, M.A., Miinalainen, I., Rappu, P., De Geest, B.G., et al. (2018). Increased levels of systemic LPS-positive bacterial extracellular vesicles in patients with intestinal barrier dysfunction. Gut *0*, 4–6.

Del Turco, S., Basta, G., Lazzerini, G., Evangelista, M., Rainaldi, G., Tanganelli, P., Camera, M., Tremoli, E., and De Caterina, R. (2007). Parallel decrease of tissue factor surface exposure and increase of tissue factor microparticle release by the n-3 fatty acid docosahexaenoate in endothelial cells. Thromb. Haemost. *98*, 210–219.

Ullal, A.J., and Pisetsky, D.S. (2010). The release of microparticles by Jurkat leukemia T cells treated with staurosporine and related kinase inhibitors to induce apoptosis. Apoptosis *15*, 586–596.

Vachiat, A., McCutcheon, K., Tsabedze, N., Zachariah, D., and Manga, P. (2017). HIV and Ischemic Heart Disease. J. Am. Coll. Cardiol. *69*, 73–82.

Venneri, M.A., De Palma, M., Ponzoni, M., Pucci, F., Scielzo, C., Zonari, E., Mazzieri, R., Doglioni, C., and Naldini, L. (2007). Identification of proangiogenic TIE2-expressing monocytes (TEMs) in human peripheral blood and cancer. Blood *109*, 5276–5285.

Ventoso, I., Navarro, J., Muñoz, M.A., and Carrasco, L. (2005). Involvement of HIV-1 protease in virus-induced cell killing. Antiviral Res. *66*, 47–55.

Viñuela-Berni, V., Doníz-Padilla, L., Figueroa-Vega, N., Portillo-Salazar, H., Abud-Mendoza, C., Baranda, L., and González-Amaro, R. (2015). Proportions of several types of plasma and urine microparticles are increased in patients with rheumatoid arthritis with active disease. Clin. Exp. Immunol. *180*, 442–451.

Voudoukis, E., Vetsika, E.K., Giannakopoulou, K., Karmiris, K., Theodoropoulou, A., Sfiridaki, A., Georgoulias, V., Paspatis, G.A., and Koutroubakis, I.E. (2016). Distinct features of circulating microparticles and their relationship with disease activity in inflammatory bowel disease. Ann. Gastroenterol. *29*, 180–187.

Wang, J.G., Williams, J.C., Davis, B.K., Jacobson, K., Doerschuk, C.M., Ting, J.P., and Mackman, N. (2011). Monocytic microparticles activate endothelial cells in an IL-1beta-dependent manner. Blood *118*, 2366–2374.

Wang, J.M., Wang, Y., Huang, J.Y., Yang, Z., Chen, L., Wang, L.C., Tang, A.L., Lou, Z.F., and Tao, J. (2007). C-reactive protein-induced endothelial microparticle generation in HUVECs is related to BH 4 -dependent NO formation. J. Vasc. Res. *44*, 241–248.

Waters, D.D., and Hsue, P.Y. (2019). Lipid Abnormalities in Persons Living With HIV Infection. Can. J. Cardiol. *35*, 249–259.

Weber, C., Belge, K.U., Von Hundelshausen, P., Draude, G., Steppich, B., Mack, M., Frankenberger, M., Weber, K.S.C., and Ziegler-Heitbrock, H.W.L. (2000). Differential chemokine receptor expression and function in human monocyte subpopulations. J. Leukoc. Biol. *67*, 699–704.

Wen, B., Combes, V., Bonhoure, A., Weksler, B.B., Couraud, P.O., and Grau, G.E.R. (2014). Endotoxin-induced monocytic microparticles have contrasting effects on endothelial inflammatory responses. PLoS One *9*, e91597.

Werner, M.L.F., Pone, M.V.D.S., Fonseca, V.M., and Chaves, C.R.M.D.M. (2010). Lipodystrophy syndrome and cardiovascular risk factors in children and adolescents infected with HIV/AIDS receiving highly active antiretroviral therapy. J. Pediatr. (Rio. J). *86*, 27–32.

Westhorpe, C.L. V, Maisa, A., Spelman, T., Hoy, J.F., Dewar, E.M., Karapanagiotidis, S., Hearps, A.C., Cheng, W.-J., Trevillyan, J., and Lewin, S.R. (2014). Associations between surface markers on blood monocytes and carotid atherosclerosis in HIV-positive individuals. Immunol. Cell Biol. *92*, 133–138.

Whale, T.A. (2006). Passively acquired membrane proteins alter the functional capacity of bovine polymorphonuclear cells. J. Leukoc. Biol. *80*, 481–491.

WHO (2019). WHO | Data and statistics (World Health Organization).

Williams, K.J., and Tabas, I. (1995). The response-to-retention hypothesis of early atherogenesis. Arterioscler. Thromb. Vasc. Biol. *15*, 551–562.

Wilson, E.M.P., Singh, A., Hullsiek, K.H., Gibson, D., Henry, W.K., Lichtenstein, K., Önen, N.F., Kojic, E., Patel, P., Brooks, J.T., et al. (2014). Monocyte-Activation Phenotypes Are Associated

With Biomarkers of Inflammation and Coagulation in Chronic HIV Infection. J. Infect. Dis. *210*, 1396–1406.

Wong, K.L., Tai, J.J.-Y., Wong, W.-C., Han, H., Sem, X., Yeap, W.-H., Kourilsky, P., and Wong, S.-C. (2011). Gene expression profiling reveals the defining features of the classical, intermediate, and nonclassical human monocyte subsets. Blood *118*, e16-31.

Wong, K.L., Yeap, W.H., Tai, J.J.Y., Ong, S.M., Dang, T.M., and Wong, S.C. (2012). The three human monocyte subsets: implications for health and disease. Immunol. Res. *53*, 41–57.

Woywodt, A. (2002). Circulating endothelial cells: life, death, detachment and repair of the endothelial cell layer. Nephrol. Dial. Transplant. *17*, 1728–1730.

Wright, S.D., Ramos, R.A., Tobias, P.S., Ulevitch, R.J., and Mathison, J.C. (1990). CD14, a receptor for complexes of lipopolysaccharide (LPS) and LPS binding protein. Science (80-.). *249*, 1431–1433.

Xu, H., Manivannan, A., Crane, I., Dawson, R., and Liversidge, J. (2008). Critical but divergent roles for CD62L and CD44 in directing blood monocyte trafficking in vivo during inflammation. Blood *112*, 1166–1174.

Yukl, S.A., Shergill, A.K., Girling, V., Li, Q., Killian, M., Epling, L., Li, P., Kaiser, P., Haase, A., Havlir, D. V., et al. (2015). Site-specific differences in T cell frequencies and phenotypes in the blood and gut of HIV-uninfected and ART-treated HIV+ adults. PLoS One *10*, 1–20.

Zachowski, A., Devaux, P.F., Seigneuret, M., and Hermann, A. (1984). Asymmetric Lipid Fluidity in Human Erythrocyte Membrane: New Spin-Label Evidence. Biochemistry *23*, 4271–4275.

Zahran, A.M., Mohamed, I.L., El Asheer, O.M., Tamer, D.M., Abo-ELela, M.G.M., Abdel-Rahim, M.H., El-Badawy, O.H.B., and Elsayh, K.I. (2019). Circulating Endothelial Cells, Circulating Endothelial Progenitor Cells, and Circulating Microparticles in Type 1 Diabetes Mellitus. Clin. Appl. Thromb. *25*, 1–7.

Zanni, M. V, Schouten, J., Grinspoon, S.K., and Reiss, P. (2014). Risk of coronary heart disease in patients with HIV infection. Nat. Rev. Cardiol. *11*, 728–741.

Zawada, A.M., Rogacev, K.S., Rotter, B., Winter, P., Marell, R.R., Fliser, D., and Heine, G.H. (2011). SuperSAGE evidence for CD14 ++CD16 + monocytes as a third monocyte subset. Blood *118*, e50-61.

Zhang, G., and Ghosh, S. (2001). Toll-like receptor-mediated NF-κB activation: A phylogenetically conserved paradigm in innate immunity. J. Clin. Invest. *107*, 13–19.

Zhang, Q., Raoof, M., Chen, Y., Sumi, Y., Sursal, T., Junger, W., Brohi, K., Itagaki, K., and Hauser, C.J. (2010). Circulating mitochondrial DAMPs cause inflammatory responses to injury. Nature *464*, 104–107.

Zhang, Y., Zhao, C., Wei, Y., Yang, S., Cui, C., Yang, J., Zhang, J., and Qiao, R. (2018). Increased circulating microparticles in women with preeclampsia. Int. J. Lab. Hematol. *40*, 352–358.

Zhao, J., Zhou, Q., Wiedmer, T., and Sims, P.J. (1998). Level of expression of phospholipid scramblase regulates induced movement of phosphatidylserine to the cell surface. J. Biol. Chem.

273, 6603–6606.

Zhou, L., Somasundaram, R., Nederhof, R.F., Dijkstra, G., Faber, K.N., Peppelenbosch, M.P., and Fuhler, G.M. (2012). Impact of human granulocyte and monocyte isolation procedures on functional studies. Clin. Vaccine Immunol. *19*, 1065–1074.

Zhu, T., Muthui, D., Holte, S., Nickle, D., Feng, F., Brodie, S., Hwangbo, Y., Mullins, J.I., and Corey, L. (2002). Evidence for human immunodeficiency virus type 1 replication in vivo in CD14(+) monocytes and its potential role as a source of virus in patients on highly active antiretroviral therapy. J. Virol. *76*, 707–716.

Ziegler-Heitbrock, L., Ancuta, P., Crowe, S., Dalod, M., Grau, V., Hart, D.N., Leenen, P.J.M., Liu, Y.J., MacPherson, G., Randolph, G.J., et al. (2010). Nomenclature of monocytes and dendritic cells in blood. Blood *116*, 5–7.

Ziegler-Heitbrock, H.W.L., Fingerle, G., Ströbel, M., Schraut, W., Stelter, F., Schütt, C., Passlick, B., and Pforte, A. (1993). The novel subset of CD14+/CD16+ blood monocytes exhibits features of tissue macrophages. Eur. J. Immunol. *23*, 2053–2058.

Appendix 1

MATERIAL TRANSFER AGREEMENT

STEMCELL TECHNOLOGIES

STEMCELL Technologies Canada Inc. a Canadian corporation with an office at 1618 Station Street, Vancouver, British Columbia V6A 1B6, Canada (the "Provider") agrees to provide the **Kingston University**, with an address at Penrhyn Road, Kingston KT1 2EE, United Kingdom (the "Recipient") with certain research material: **EasySep Direct Pan Monocyte Isolation Kit** (the "Material") which has been requested by **Dr. Fran Arrigoni** (the "Scientist") for performance testing (the "Evaluation"), subject to the terms and conditions set forth in this Material Transfer Agreement (the "Agreement").

1. Derivative Materials. "Derivative Materials" means any substance constituting a functional or structural subunit, or product expressed by or isolated from the Material. The Recipient agrees that no Derivative Materials may be produced without the express written permission of the Provider. Examples of Derivative Materials include (but are not limited to): cell lines, recombinant constructs, cultures, or subcultures. To avoid doubt, the Recipient agrees that any Derivative Materials will become the property of the Provider and will be subject to this Agreement. The Recipient agrees to supply samples of any Derivative Materials to the Provider upon request.

2. Improvements. The Recipient shall not make any improvement, modification, enhancement or adaptation to or of Material (collectively "Improvements"). If in the event that the Recipient creates Improvements, such Improvements and all intellectual property rights pertaining to Improvements, whether patentable or not, will remain the property of the Provider. The Recipient shall not reverse engineer, reverse compile, disassemble or otherwise attempt to derive the composition or underlying information, structure or ideas of the Material, including, but not limited to, analyzing the Material by physical, chemical or biochemical means.

3. Legal Title. The transfer of the Material constitutes a non-exclusive license to use the Material solely for Evaluation. Legal title to the Material shall be unaffected by this Agreement or the transfer made hereunder. The Provider retains the ownership of the Material and all intellectual property rights pertaining to the Material, including, but not limited to: media formulation, know-how, show how, trade secrets, protocols, and data.

4. Confidentiality. The Recipient and Scientist shall maintain the confidentiality of the Provider's proprietary information respecting the Material (except as otherwise provided in paragraph 8 of this Agreement) including but not limited to: experiment protocols, know-how, show-how, inventions, creations, designs, methods, software, techniques, processes and other intellectual property and technical information.

5. Evaluation Conditions. The Material is provided to the Recipient for the purpose of Evaluation only. The Material is provided to the Recipient for use in animals or in vitro. **The Material will not be used in humans, including for purposes of diagnostic testing.** The Scientist and the Recipient will use the Material in compliance with all laws, governmental regulations, and guidelines that may be applicable to the Material.

6. Control of the Material. Neither the Scientist, nor the Recipient, nor any other person authorized to use the Material under this Agreement shall make available any portion of the Material to any person or entity other than laboratory personnel under the Scientist's immediate and direct control. No person authorized to use the Material shall be allowed to take or send the Material to any location other than the Scientist's laboratory without the Provider's prior written consent.

7. Warranty. The Material is experimental in nature and shall be used by the Recipient with prudence and appropriate caution. THE MATERIAL IS PROVIDED WITHOUT WARRANTY

   OF MERCHANTABILITY OR FITNESS FOR A PARTICULAR PURPOSE OR ANY OTHER WARRANTY, EXPRESS OR IMPLIED.

8. Results and Publications. The Recipient agrees to provide a summary of the results of the Evaluation to the Provider within sixty (60) days of completing the Evaluation. In addition, the Recipient agrees to send the Provider abstracts or manuscripts describing the results of the Evaluation at least thirty (30) days prior to the submission of the publication, thereby allowing the Provider the opportunity to protect proprietary or intellectual property relating to the Material that might be contained in the disclosure. The Recipient and Scientist agree not to publish results without the Provider's prior written consent. The Provider may use results for marketing, or other purposes at its sole discretion.

9. Effective Date and Duration of the Agreement. This Agreement is effective as of the latest date of signature and shall remain in effect for one (1) year thereafter. The Evaluation shall be conducted and completed during this one (1) year period, unless the duration of the agreement is extended by written agreement of both parties. Section 1, 2, 3, 4, 8, 9, 10, 11, 12 and 15 shall survive the expiration or termination of the Agreement.

10. Further Agreements and Return of Material. Nothing contained in this Agreement shall be construed, by implication or otherwise, as an obligation for any party to enter into any further agreement with the other, or as a grant of a license to use the Materials other than for the purposes of this Agreement. The Recipient shall, at the request of the Provider, return or destroy all unused Material.

11. Liability. In no event shall the Provider, or the Provider's trustees, officers, agents and employees be liable for any use by the Scientist or the Recipient of the Material or for any claim, liability, cost, expense, damage, deficiency, loss or obligation, of any kind or nature that may arise from or in connection with this Agreement or the use, handling, storage, or disposition of the Material by the Scientist, the Recipient or others who

possess the Material through a chain of possession leading back, directly or indirectly, to the Recipient or Scientist (collectively, "Claims"). The Recipient agrees to indemnify and hold harmless the Provider and the Provider's trustees, officers, agents, and employees from any and all Claims. The Recipient shall have no obligation to indemnify, defend or hold harmless a person or entity identified in the foregoing sentence if it is determined with finality by a court of competent jurisdiction that the relevant Claim resulted solely from such person's or entities' own gross negligence or willful misconduct. This paragraph 11 shall survive termination of the Agreement.

12. Assignments. This Agreement is not assignable.

13. Execution. This Agreement may be executed in counterparts, each of which together constitute one and the same instrument, binding on the parties, and each of which will together be deemed to be an original.

14. Governance. This Agreement shall be governed by the laws of the party against which a legal or administrative proceeding (for example, litigation, arbitration or mediation) is brought. For clarity, in a proceeding brought against the Recipient, the governing law shall be the laws of England, and in a proceeding brought against the Provider, the governing law shall be the laws of the Province of British Columbia, and where applicable, the laws of Canada.

15. Entire Agreement. This Agreement contains the entire agreement between the parties concerning the subject matter herein. No modification or waiver of any provision of this Agreement will be binding unless approved in writing by the parties.

[SIGNATURES TO FOLLOW]

FOR AND BEHALF OF PROVIDER:

STEMCELL Technologies Canada Inc.

FOR AND BEHALF OF RECIPIENT:

Kingston University

By:	By:
Name:	Name:
Title:	Title:
Date:	Date:

Appendix 2

Isotype controls		
Fluorochrome conjugate	**Isotype**	**Source**
AF700	IgG1, κ	Biolegend
PE-Cy7	IgG1, κ	Biolegend
PE	IgG2a, κ	Biolegend
PE	IgG1, κ	BD Bioscience
PerCp-Cy5.5	IgG1, κ	BD Bioscience
PerCp-Cy5.5	IgG2a, κ	Biolegend
FITC	IgM, κ	BD Bioscience
FITC	IgG1, κ	BD Bioscience
APC	IgG1, κ	Biolegend
APC	IgG2a, κ	Biolegend
Pacific Blue	IgG2a, κ	Biolegend

Table 7.1: Details of isotype controls used in flow cytometry experiments

Appendix 3

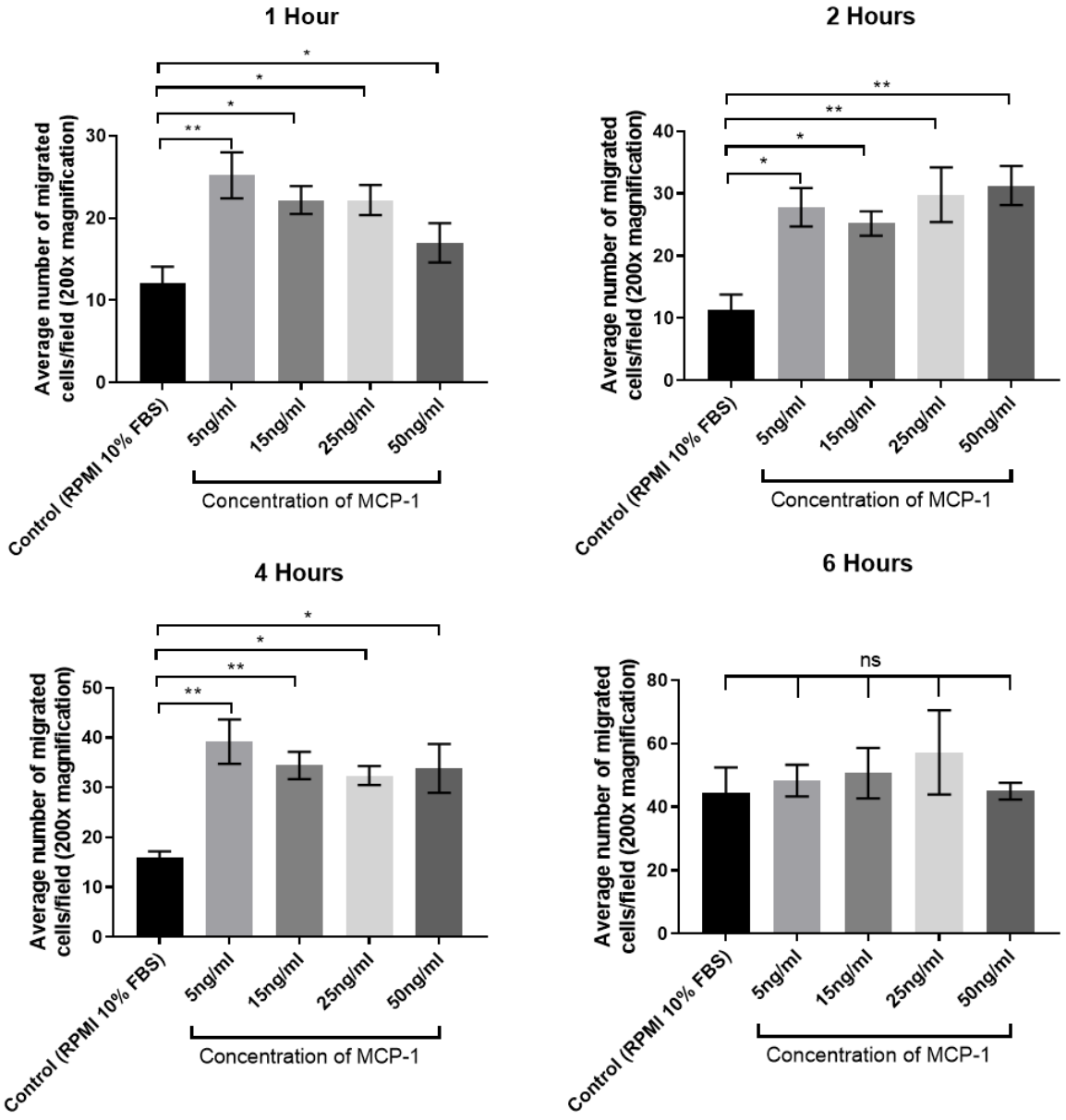

Figure 7.1: The effect of increasing concentrations of MCP-1 on human monocyte migration after 1, 2, 4 and 6 hours

*To find the optimum time point for monocyte migration towards MCP-1, Isolated monocytes ($5x10^4$), using the Big Easy magnet at 8˚C (n=3 5ng/ml MCP-1, n=1 for all other concentrations) were added to the top chamber of the 5.0μM pore inserts, and left to freely migrate to the lower compartment of the well containing increasing concentrations of Monocyte chemoattractant protein -1 (MCP-1) for 1, 2, 4 and 6 hours. Images were taken at 5 random fields, at 200x magnification. Results are displayed as the average number of migrated cells per field. * denotes p=<0.05, ** denotes p=<0.01, ns=non-significant determined by a ONE-WAY ANOVA with a Tukey's post hoc test.*

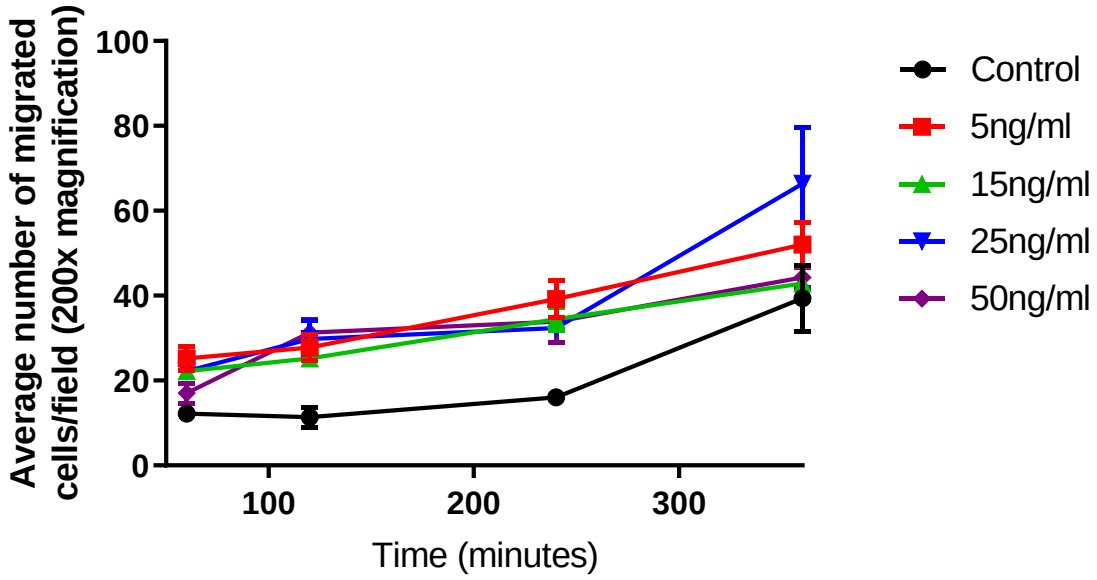

Figure 7.2: A timecourse of monocyte migration towards increasing concentrations of MCP-1 over 6 hours

A timecourse displaying the combined data presented in Figure 7.1, demonstrating the influence of increasing concentrations of MCP-1 (5ng/ml, 15ng/ml, 25ng/ml and 50ng/ml) on human monocyte migration ($5x10^4$, n=3 5ng/ml MCP-1, n=1 for all other concentrations) over the 6 hours timecourse.

To determine the optimal time to allow human monocytes to freely migrate MCP-1, a timecourse was performed over 6 hours. These results identified 4 hours as the optimum, as migration at each concentration of MCP-1 was statistically significant when compared to control. Furthermore, as 5ng/ml was the selected concentration for MCP-1 in further experiments, the largest difference in the number of migrated cells when using this concentration as a chemoattractant, in comparison to control conditions was observed after 4 hours.

Appendix 4

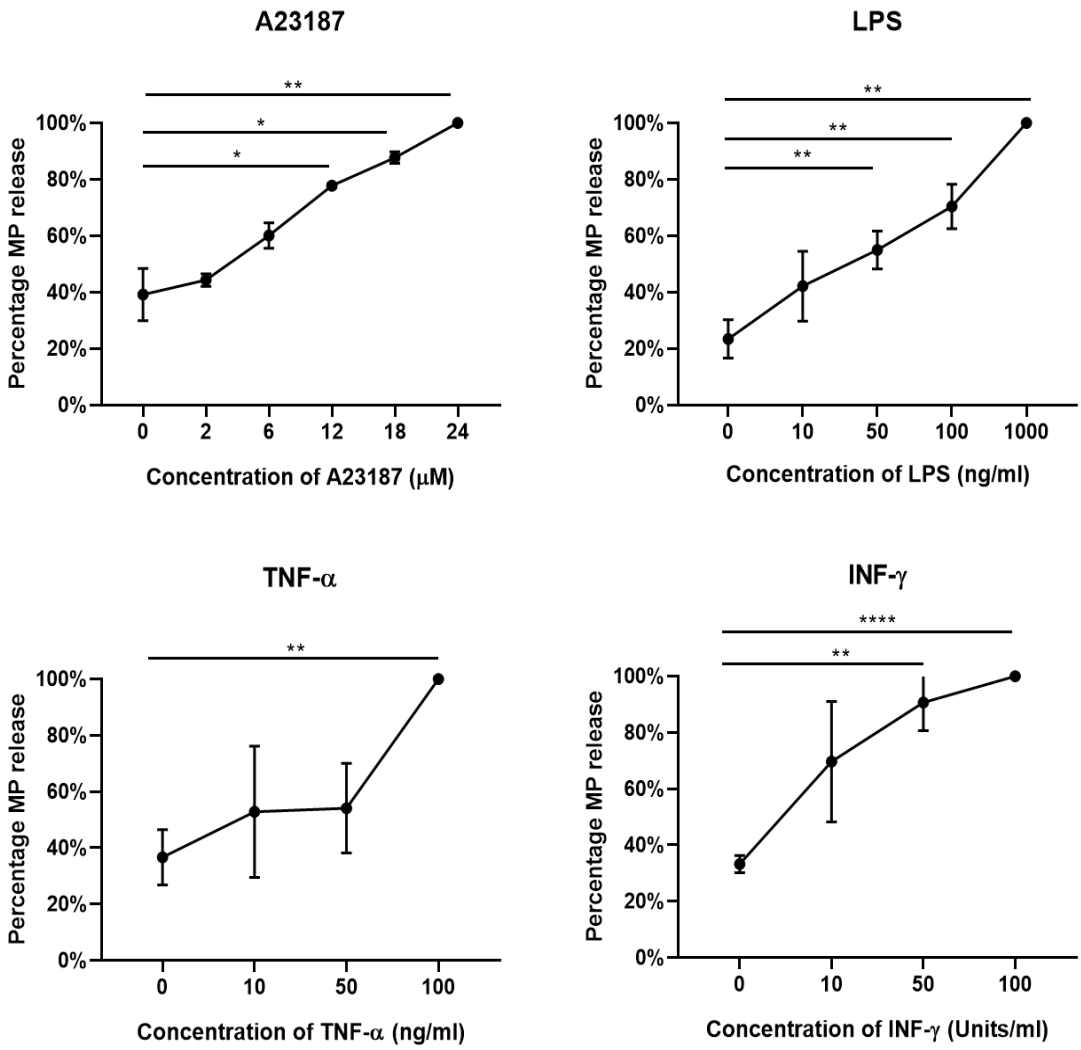

Figure 7.3: THP-1 cells release quantitatively different MPs following stimulation

*$1x10^6$ THP-1 cells/ml challenged with increasing concentrations of LPS (n=3), TNF-α (n=3) and IFN-γ (n=3) for 4 hours or 10 minutes for A23187 stimulation (n=3) in accordance with literature (Satta 1994, Cerri 2006, Nerri 2011, Baardelli 2011). Annexin V+ MPs were enumerated by flow cytometry, with data displayed percentage of maximum MP release±SEM. Differences for each treatment determined by ONE-WAY ANOVA, with a Tukey's post hoc test * p<0.05, ** p<0.01, *** p<0.001, **** p<0.0001.*

Appendix 5

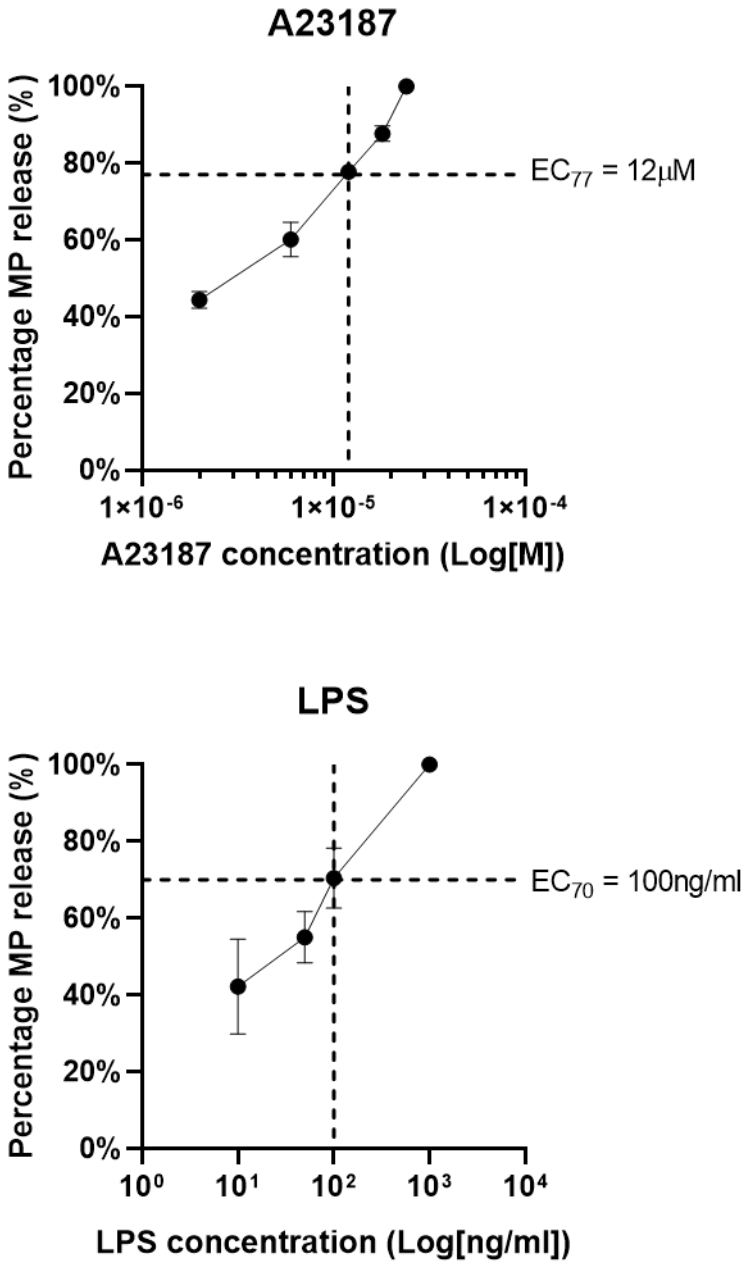

Figure 7.4: Determining the EC_{70}-EC_{80} MP release for A23187 and LPS

Graphs to demonstrate how the effective concentration that achieved 70-80% maximal response of MP release was determined for both A23187 and LPS. From these graphs, 12μM A23187 and 10ng/ml LPS were selected for further MP generation and analysis.

Appendix 6

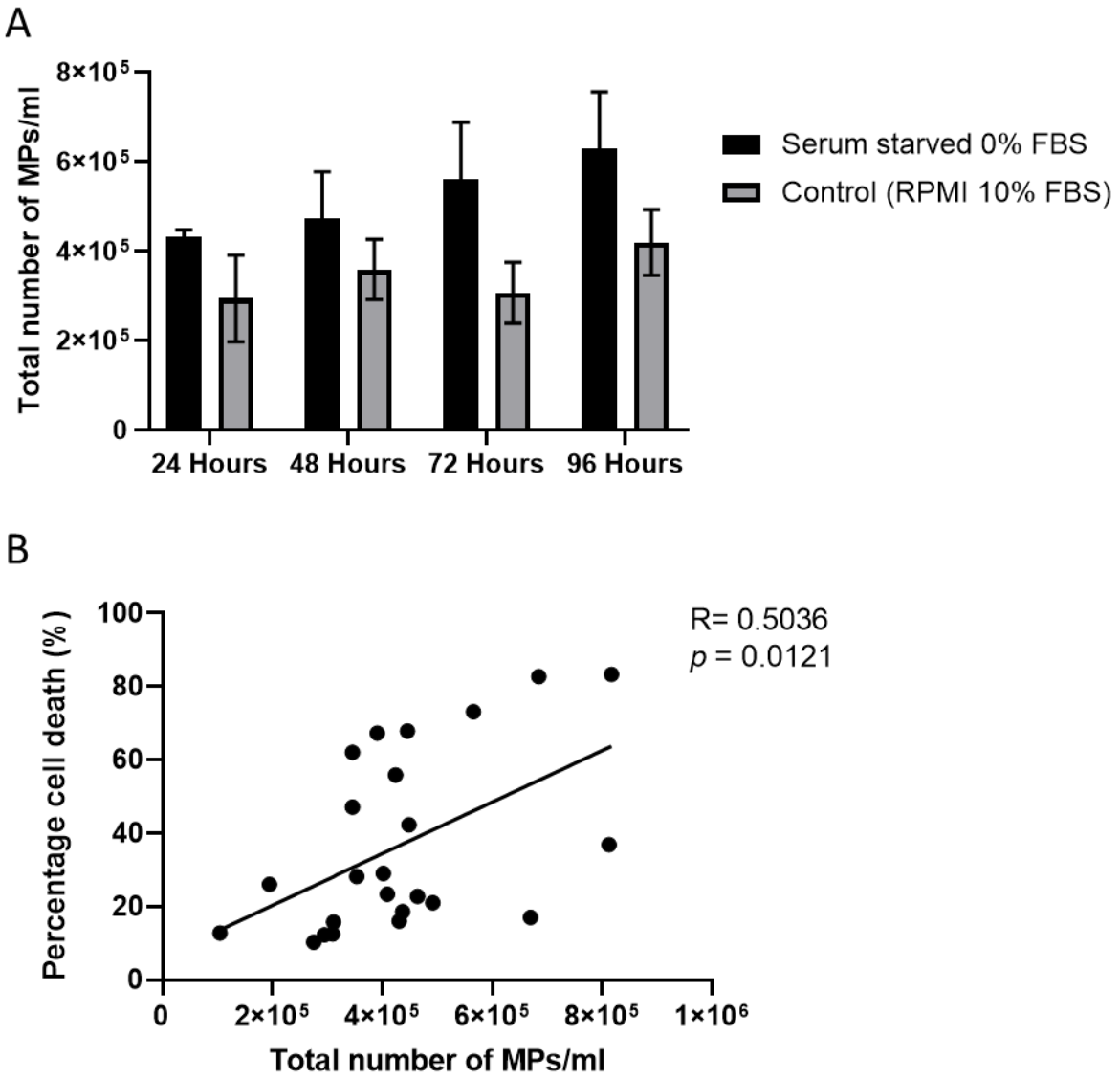

Figure 7.5: HUVECs release MPs in serum starvation conditions

1x10^5 HUVECs/ml were cultured to 80% confluence in Endothelial growth medium-2, and either serum-starved (n=3, black bars) to induce apoptosis or in control conditions with 10% FBS (n=3, grey bars) for 48, 72 and 96 hours. Annexin V+ MPs were enumerated by flow cytometry (A), along with parent cells stained with DAPI (B). A positive association was found between the number of MPs/ml and percentage of DAPI+ cells, Pearson's correlation coefficient R=0.503, p=0.0121. Data is displayed as mean ±SEM, with differences assessed by TWO-WAY ANOVA, with a Sidak's post hoc test.

Appendix 7

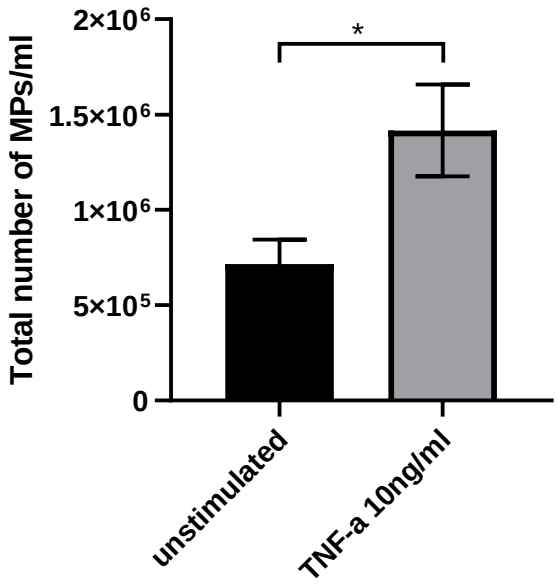

Figure 7.6: HUVECs release MPs following stimulation with TNF-α

1x10^5 HUVECs/ml grown to 80% confluence were challenged with 10ng/ml TNF-α (n=3), or Endothelial growth media-2 10% FBS (n=3) for 24 hours. Annexin V+ MPs were enumerated by flow cytometry, with data displayed as mean ±SEM. Differences for each treatment determined by an unpaired t-test p<0.05.*